

CHARACTERISATION OF DYSFUNCTIONAL WNT/ β -CATENIN SIGNALLING IN THE DOWN SYNDROME BRAIN

Doctoral Thesis
SIMONE GRANNO

CONDUCTED AT
University College London,
Gower Street, London WC1E 6BT
simone.granno.09@ucl.ac.uk
www.ucl.ac.uk

ACADEMIC SUPERVISORS
Professor Kirsten Harvey
Department of Pharmacology
UCL School of Pharmacy, Brunswick Square, London
Professor Elizabeth Fisher & Dr Frances Wiseman
Department of Neurodegenerative Disease
UCL Institute of Neurology, Queen Square, London

Table of contents

I.	Declaration	
II.	Acknowledgments	
III.	Abstract	
IV.	Impact statement	
V.	Glossary	
1	Chapter 1 - General Introduction	p. 15
1.1	Down syndrome	p. 15
1.1.1	Overview	p. 15
1.1.2	Hsa21 in DS pathology	p. 16
1.1.3	Dementia and Alzheimer's disease	p. 18
1.1.3.1	Overview	p. 18
1.1.3.2	Molecular pathology of AD	p. 19
1.1.4.	Alzheimer disease in Down syndrome (AD-DS)	p. 20
1.1.5	Mouse models of DS	p. 21
1.2	The Wnt signalling pathway	p. 23
1.2.1	Overview	p. 23
1.2.2	Wnt regulation of stem cell function	p. 25
1.2.3	Wnt signalling in neurodevelopment	p. 26
1.2.4	Wnt signalling in synaptogenesis and memory	p. 27
1.2.5	Wnt signalling in AD	p. 28
1.3	Wnt signalling in DS and AD-DS?	p. 31
1.4	Genes and proteins of DS: a literature overview	p. 33
1.4.1	The DS transcriptome	p. 33
1.4.1.1	The role of transcriptomics in the understanding of DS	p. 33
1.4.1.2	Gene expression profiling in DS mouse models	p. 34
1.4.1.3	Gene expression profiling in Human DS	p. 36
1.4.1.4	Overall considerations	p. 39
1.4.2.	The DS proteome and biochemical phenotypes	p. 40
1.4.2.1	Protein profiling in DS mouse models	p. 40
1.4.2.2	Protein profiling in human DS	p. 42
1.4.2.3	Overall considerations	p. 44
2	Chapter 2 - Aims and Objectives	p. 46

3	Chapter 3 - Materials and Methods	p. 50
3.1	RNA sequencing	p. 50
3.1.1	RNA extraction and sequencing	p. 50
3.1.2	Sequencing data analysis	p. 50
3.2	Cloning	p. 51
3.2.1	Polymerase chain reaction and DNA primer design	p. 51
3.2.2	Agarose gel electrophoresis and extraction	p. 52
3.2.3	Restriction digest and phenol-chloroform isoamyl (PCI) extraction	p. 54
3.2.4	DNA ligation	p. 55
3.2.5	<i>E. coli</i> transformation and culture	p. 55
3.2.6	Minipreparation of plasmid constructs (QIAGEN protocol)	p. 56
3.2.7	Diagnostic digest	p. 56
3.2.8	Quantification of DNA concentration	p. 57
3.2.9	DNA sequencing	p. 57
3.2.10	Maxipreparation of plasmid constructs (QIAGEN protocol)	p. 58
3.2.11	Summary of expression constructs employed	p. 58
3.3	DS mouse models	p. 59
3.3.1	Animal husbandry and general information	p. 59
3.3.2	Cortical and hippocampal dissection	p. 61
3.4	Quantitative real-time polymerase chain reaction - qPCR	p. 62
3.4.1	Tc1 expression cDNA generation via reverse transcription	p. 62
3.4.2	DNA primer and probe design	p. 63
3.4.3	qPCR	p. 65
3.5	Cell culture, luciferase assay and immunocytochemistry	p. 66
3.5.1	General cell line maintenance	p. 66
3.5.2	DYRK1A inhibition	p. 68
3.5.3	Lithium chloride and Wnt3a administration	p. 69
3.5.4	DNA transfection	p. 70
3.5.5	TCF/ β -Catenin TOPFLASH luciferase assay	p. 71
3.5.6	Generation of SH-SY5Y cells stably expressing the the TCF/LEF-Luciferase reporter	p. 72
3.5.7	Slide preparation for immunocytochemistry	p. 73
3.5.8	Airyscan and confocal microscopy	p. 73

3.6	Mouse, human and cell biochemistry	p. 74
3.6.1	Generation of mouse brain lysates	p. 74
3.6.2	Generation of human brain lysates from postmortem DS hippocampal samples	p. 74
3.6.3	Generation of human cell line lysates	p. 74
3.6.4	Co-immunoprecipitation	p. 75
3.6.5	SDS Polyacrylamide gel electrophoresis (SDS-PAGE)	p. 75
3.6.6	Western blotting	p. 76
3.7	Yeast two-hybrid screening	p. 78
3.7.1	The Jerome LeJeune Foundation interPP project	p. 78
3.7.2	ULTImate Y2H™ Analysis	p. 78
3.7.3	PBS scoring	p. 79
3.8	Bioinformatics	p. 80
3.8.1	Ingenuity Pathway Analysis	p. 80
3.8.2	STRING and Cytoscape protein interaction network analysis	p. 80
3.9	Data processing, quantification, statistical analysis and representation	p. 81
3.9.1	Image processing	p. 81
3.9.2	Western blot quantification	p. 81
3.9.3	Luciferase assay quantification	p. 81
3.9.4	Confocal imaging quantification	p. 82
3.9.5	Statistical analysis and graphs	p. 82
4	Chapter 4 - Experimental Results	p. 84
4.1	Chapter 4.1 - Analysis of the DS transcriptome	p. 88
4.1.1	Introduction	p. 88
4.1.1.1	Ingenuity Pathway Analysis (IPA): a reliable and validated approach	p. 88
4.1.2	Results	p. 90
4.1.2.1	Tc1 mouse	p. 90
4.1.2.1.1	DEX genes and Canonical Pathway analysis	p. 90
4.1.2.1.2	Diseases and functions	p. 95
4.1.2.2	DP1Tyb mouse	p. 96
4.1.2.2.1	DEX genes and Canonical Pathway analysis	p. 96

4.1.2.2.2	Diseases and functions	p. 101
4.1.3	Discussion	p. 102
4.1.3.1	Key conclusions on the aneuploid status of Tc1 and Dp1Tyb mice	p. 102
4.1.3.2	Comparative assessment of Tc1 and Dp1Tyb mice	p. 102
4.1.3.3	A putative Wnt contribution?	p. 104
4.2	Chapter 4.2 - Wnt signalling proteins in DS mouse models and humans	p. 110
4.2.1	Introduction	p. 110
4.2.1.1	Characterisation of the Wnt protein machinery	p. 111
4.2.2	Results	p. 114
4.2.2.1	Tc1 mouse	p. 114
4.2.2.1.1	qPCR validation of RNA sequencing data	p. 114
4.2.2.1.2	Canonical Wnt signalling in the Tc1 hippocampus	p. 119
4.2.2.1.3	Canonical Wnt signalling the Tc1 cortex	p. 120
4.2.2.2	DP1Tyb mouse	p. 122
4.2.2.2.1	Canonical Wnt signalling in the hippocampus	p. 122
4.2.2.2.2	Canonical Wnt signalling the cortex	p. 124
4.2.2.3	Additional segmental trisomy models	p. 124
4.2.2.3.1	Canonical Wnt signalling in the Ts1(10)Yey and Ts1(17)Yey hippocampus	p. 125
4.2.2.4	Human DS	p. 126
4.2.2.4.1	Canonical Wnt signalling in the human DS hippocampus	p. 127
4.2.3	Discussion	p. 128
4.2.3.1	Functional significance	p. 129
4.2.3.2	Implications	p. 131
4.3	Chapter 4.3 - DYRK1A-mediated Wnt signalling modulation	p. 135
4.3.1	Introduction	p. 135
4.3.1.1	DYRK1A: a multifaceted, dual-specificity kinase	p. 136
4.3.1.1.1	DYRK1A in health and disease	p. 137
4.3.1.1.2	The role of DYRK1A in DS and AD-DS	p. 140

4.3.1.1.3	Signalling pathway regulation by DYRK1A	p. 142
4.3.1.1.4	DYRK1A: a potential Wnt signalling regulator?	p. 143
4.3.1.1.5	Subcellular localisation: the master key to DYRK1A function?	p. 145
4.3.1.2	Luciferase quantification of Wnt signalling activity, an established approach	p. 146
4.3.2	Results	p. 148
4.3.2.1	DYRK1A-Wnt protein interaction networks	p. 149
4.3.2.1.1	STRING-based DYRK family interaction with Wnt components	p. 149
4.3.2.1.2	Yeast two-hybrid screening reveals several DYRK1A-Wnt interactions	p. 150
4.3.2.1.3	The poly-Histidine tail of DYRK1A interacts with DKK3	p. 151
4.3.2.1.4	DYRK1A precipitates with DKK3 and DVL1, but not β -catenin	p. 152
4.3.2.1.5	STRING/Cytoscape interaction network analysis	p. 155
4.3.2.2	DYRK1A is a bimodal Wnt signalling regulator	p. 158
4.3.2.2.1	DYRK1A inhibition and canonical Wnt signalling	p. 158
4.3.2.2.1.1	LiCl-mediated Wnt activation	p. 158
4.3.2.2.1.2	Wnt3a-mediated Wnt activation	p. 159
4.3.2.2.1.3	Investigation of a dose-dependent relationship for INDY	p. 161
4.3.2.2.1.4	DYRK1A inhibition in live cells	p. 162
4.3.2.2.2	DYRK1A overexpression and canonical Wnt signalling	p. 163
4.3.2.2.2.1	DVL1-mediated Wnt activation	p. 163
4.3.2.2.2.2	Combined effects of DYRK1A and DKK3 overexpression on Wnt signalling activity	p. 165
4.3.2.2.2.3	Effects of DYRK1A expression on GSK3 β	p. 166
4.3.2.3	Wnt signalling control over DYRK1A subcellular localisation	p. 167
4.3.2.3.1	Nuclear DYRK1A localises to the speckle compartment	p. 167
4.3.2.3.2	LiCl-mediated Wnt activation	p. 169
4.3.2.3.3	Wnt3a-mediated Wnt activation	p. 173
4.3.2.3.4	DVL1 treatment: DYRK1A co-localises with DVL1 in cytoplasmic phase transitions	p. 177
4.3.3	Discussion	p. 181
4.3.3.1	Bimodal DYRK1A regulation of Wnt signalling: potential mechanisms	p. 183
4.3.3.2	Limitations and future approaches	p. 185

5	Chapter 5 - General Discussion	p. 192
5.1	Summary of all results	p. 192
5.1.1	Wnt signalling is dysfunctional in DS	p. 193
5.1.2	DYRK1A regulates canonical Wnt signalling activity	p. 194
5.1.3.	Critical evaluation of experimental results	p. 195
5.1.3.1	Chapter 4.1 - Analysis of the DS transcriptome	p. 195
5.1.3.2	Chapter 4.2 - Wnt signalling proteins in DS mouse models and humans	p. 197
5.1.3.3	Chapter 4.3 - DYRK1A-mediated Wnt signalling modulation	p. 198
5.1.3.4	Overall considerations	p. 198
5.2	Wider implications of a DS-Wnt relationship	p. 199
5.2.1	Links between Wnt signalling and known DS phenotypes	p. 199
5.2.2	Potential therapeutic strategies: establishing Wnt signalling as a target pathway in DS	p. 203
5.2.2.1	Wnt-based therapies in AD and neurodegeneration	p. 203
5.2.2.2	Targeting DYRK1A in DS	p. 205
5.2.2.3	A Wnt-DYRK1A therapy for DS neurodevelopment and AD-DS?	p. 207
5.2.2.4	Beyond neurodegeneration and the DS brain	p. 210
5.2.2.5	Overall considerations	p. 210
6	Conclusions and future work: an avenue for the treatment of DS	p. 211
7	Bibliography	p. 215
7.1	Chapter 1 - General Introduction	p. 215
7.2	Chapter 2 - Materials and Methods	p. 228
7.3	Chapter 4.1 - Analysis of the DS transcriptome	p. 229
7.4	Chapter 4.2 - Wnt signalling proteins in DS mouse models and humans	p. 233
7.5	Chapter 4.3 - DYRK1A-mediated Wnt signalling modulation	p. 237
7.6	General Discussion	p. 246

I. Declaration

I, Simone Grannò^{1,2} confirm that the work presented in this thesis is my own. Where information has been derived from other sources, I confirm that this has been indicated. This thesis describes work conducted for the award of a UCL PhD degree in Neuroscience, from Oct 2013 to Jul 2017. The following is a list of those who additionally contributed essential data and/or intellectual input to this thesis:

Jonathon Nixon-Abell^{1,3}, Daniel C. Berwick^{1,4}, Justin Tosh², George Heaton¹, Sultan Almudimeegh¹, Zenisha Nagda¹, Jean-Cristophe Rain⁵, Manuela Zanda⁶, Vincent Plagnol⁶, Victor L.J. Tybulewicz^{7,8,9}, Karen Cleverley², Frances K. Wiseman^{2,9}, Elizabeth M.C. Fisher^{2,9} & Kirsten Harvey¹

Affiliations

¹Department of Pharmacology, UCL School of Pharmacy, University College London, 29-39 Brunswick Square, London WC1N 1AX, UK.

²Department of Neurodegenerative Disease, UCL Institute of Neurology, Queen Square, London WC1N 3BG, UK

³Cell Biology Section, Neurogenetics Branch, National Institute of Neurological Disorders and Stroke (NINDS), Bethesda, MD, USA.

⁴School of Health, Life and Chemical Sciences, The Open University, Walton Hall, Milton Keynes MK6 7AA, UK.

⁵Hybrigenics Services - Fondation Jérôme Lejeune, 3-5 Impasse Reille 75014 Paris, France

⁶UCL Genetics Institute, Darwin Building, Gower Street, London WC1E 6BT, UK

⁷The Francis Crick Institute, 1 Midland Rd, Kings Cross, London NW1 1AT, UK

⁸Department of Medicine, Imperial College, London W12 0NN, UK

⁹London Down Syndrome Consortium (LonDownS)

Statement of contributions

S.G., D.B and K.H. conceived and designed experiments. S.G. performed majority of experiments. S.G. and K.H. analysed all data and S.G. wrote the thesis. K.H. oversaw editing of the first draft. J. NA. performed imaging experiments and analysed the data. J.T., M.Z., V.P and F.W. designed and performed RNAseq experiments and analysed the primary data. S.G. analysed the RNAseq data with IPA®. F.W. provided training and supervision for qPCR experiments, performed and analysed by S.G. G.H., S.A. and Z.N. contributed to cell and luciferase experiments. S.G. and K.C. performed human sample experiments and S.G. analysed the data. J.C. R. designed and performed Y2H experiments and analysed the data. V.T. developed the Dp1Tyb mouse model. E.M.C.F. and V.T. developed the Tc1 mouse. K.H. and E.M.C.F. conceived and funded S.G.'s PhD project.

SIGNED AND DATED.....

II. Acknowledgements

First and foremost, I would like to extend my gratitude to the sixteen people who, in life, chose to bequeath their brains to scientific research. Their generosity made the key findings of this thesis possible. Likewise, I want to acknowledge all the mice who were euthanised to allow generation of the data presented here. Without them, this thesis could have not been produced, so thank you. I would also like to thank my primary supervisor, Prof. Kirsten Harvey, for her unrelenting support throughout my PhD. Kirsten, you welcomed me in your group when I was still just a medical student with little laboratory experience. You nevertheless trusted my potential, and personally oversaw my transformation into a research scientist. This has been a fundamental turning point in my clinical career, and I will be forever grateful to you for giving me this invaluable opportunity. I would also like to thank my secondary supervisors at the UCL Institute of Neurology, Prof. Elizabeth Fisher and Dr. Frances Wiseman. Thank you for your constant support, supervision and intellectual input, as well as for providing essential training in laboratory techniques. You also made it possible for me to obtain tissue samples from DS mouse models and postmortem humans, which greatly enhanced the impact of my research. Following, I would like to thank all lab members from both groups, and both institutions where I worked. These are the PhD students, postdocs and technicians who, through the years, offered their support and friendship in and out of the lab. Particularly, thank you to Dan, Jonny, Laura, George, Kayla, Phil, Andrea, Sultan, Zenisha, Stefania and Rand from the UCL School of Pharmacy. From the Institute of Neurology, thank you to Karen, Laura and Justin and all other Fisher-Isaacs lab members. I would also like to thank the UCL Medical School for granting me the opportunity to combine a PhD degree with my main medical training. Ultimately, I would like to thank UCL for supporting me since 2009, first as a medical student and then as a doctoral candidate. All this would have not been possible without you.

Ringraziamenti

E ora siamo giunti al momento in cui si ringraziano le persone più vicine. Questa parte è per voi. Grazie a te, Mamma, per tutta la fiducia, orgoglio e immenso supporto che mi hai sempre dato, fin da quando non sapevo parlare. Sei tu che, insieme a Riccardo - grazie anche a te! - mi hai spinto verso Londra, tu che mi hai sempre incoraggiato e aiutato anche quando decisi di estendere la durata dei miei studi di altri quattro anni. Grazie a te Papà, per aver sempre creduto in me, e per avermi supportato in ogni momento, bello o brutto, di questo viaggio. Spero di aver contribuito al tuo amore per la scienza, che fin da piccolo tu hai voluto stimolare. E ora veniamo a te, mia cara sorellina Biba. Questo viaggio l'abbiamo sempre fatto insieme, come dici tu, da fratelli e migliori amici. Grazie per avermi supportato quando mi lamentavo, e per aver gioito con me in ogni bel momento. Questi anni a Londra sarebbero stati molto più bui senza di te. Grazie anche a te, Edo, il mio fratellino intellettuale, per tutto il tuo supporto e affetto. Non vedo l'ora di averti di nuovo qui, per continuare insieme questa avventura. E ancora grazie ai miei amici, senza i quali non sarei mai arrivato dove sono. Siete voi, Didi, Bianca, Alessio, Benni e Livio. E infine ringrazio te, Bea, per essere entrata nella mia vita. La tua presenza nell'ultima fase è stata cruciale. Tu mi fai sentire figo e fiero di avere un PhD! Vi voglio bene!

III. Abstract

Down syndrome (DS) is the most common human aneuploidy. It results from the presence of three copies, or trisomy, of human chromosome 21 (Hsa21). DS is associated with a plethora of characteristic clinical features, most notably learning disability, altered body morphology, congenital heart disease and early-onset Alzheimer's disease (AD-DS). Despite knowledge of its primary cause, pathological mechanisms underlying DS are poorly understood, including potential deficits in essential signalling processes. This thesis investigates Wnt/ β -catenin signalling dysfunction in DS. The Wnt signalling pathway is a fundamental transduction cascade with key roles in development, cancer and neurodegeneration. Particularly, mounting evidence suggests that AD neuropathology may be underscored by critical dysfunction of canonical Wnt signalling. Given the close relationship between AD and DS, it is proposed in this thesis that Wnt abnormalities may also be present in the DS brain. This hypothesis is thus investigated, combining bioinformatics with RNA and protein analysis in DS mouse models and humans. The evidence gathered here suggests canonical Wnt signalling is dysfunctional in the DS brain. Most importantly, Wnt signalling activity is suppressed in the adult DS hippocampus. Furthermore, this thesis identifies the Hsa21-encoded kinase DYRK1A, an essential contributor to DS, as a novel, bimodal Wnt signalling regulator. DYRK1A may both suppress and enhance Wnt activity, depending on the activation state of the pathway. It is proposed that, in DS, dosage imbalance of *DYRK1A* may substantially affect Wnt signalling, with a complex array of resulting transcriptional changes to Wnt target genes. This mechanism may contribute to several developmental and adult features of DS, particularly learning disability and AD-DS. Overall, these findings may provide key evidence for the global understanding of this condition, and targeting Wnt signalling may open unexplored avenues for therapeutic development.

IV. Impact Statement

This thesis presents novel preclinical insight into a condition of great relevance to the wider scientific community, and to society in general. DS is the most common human aneuploidy and genetic cause of AD, and thus places a significant burden on multiple levels of healthcare worldwide. Moreover, the nearly universal development of AD-DS poses an ever greater challenge to the ageing DS population. Despite improvements in life expectancy for DS individuals, no pharmacological therapy is available. Additionally, this condition heavily impacts the quality of life of those affected and their families. Therapeutic development is thus urgently needed. The Wnt signalling pathway has been extensively characterised over three decades, mainly in the context of cancer and, recently, neurodegeneration. A wide variety of pharmacological agents modulating Wnt function is already under development. Future translation of this work into a viable therapeutic approach, aimed at normalising Wnt function in DS, would therefore build upon solid foundations. Ultimately, it is hoped that the findings of this thesis will help establish Wnt signalling modulation as a potential treatment for AD-DS and beyond.

V. Glossary

2-DE - Two-dimensional gel electrophoresis

ACh - Acetylcholine

AD - Alzheimer's disease

AICD - APP intracellular domain

AKT - Protein kinase B

APC - Adenomatous polyposis coli

APP - Amyloid precursor protein

ATP - Adenosine triphosphate

BACE2 - Beta-site APP-cleaving enzyme 2

CBR1 - Carbonyl reductase 1

CDK - Cyclin-dependent kinase

CDKL5 - Cyclin-dependent kinase-like protein 5

CHD - Congenital heart disease

CKI - Casein kinase 1

CLK - Cdc2-like kinase

CNS - Central nervous system

CRABP - Cellular retinoic acid-binding protein

CREB - Cyclic AMP-responsive element binding protein

CRY2 - Cryptochrome circadian clock 2

CSCs - Cancer stem cells

CSF - Cerebrospinal fluid

CTNNA1 - α -catenin

CTNNB1 - β -catenin

CTNND1 - p120/ δ -catenin

CTSB - Cathepsin B

CaMKII - Ca²⁺/calmodulin-dependent protein kinase-II

Cdh1 - Cadherin 1

Co-IP - Co-immunoprecipitation

DAPI - 4',6-diamidino-2-phenylindole

DEX - Differentially expressed

DKK - Dickkopf-related protein

DMEM - Dulbecco's modified Eagle medium

DMSO - Dimethylsulfoxide

DNA - Deoxyribonucleic acid

DS - Down syndrome

DSCR - DS critical region

DVL1 - Disheveled 1

DYRK1A - Dual-specificity Y-regulated kinase 1A

Dp - Chromosomal duplication

EGCG - Epigallocatechin gallate

EPSCs - Excitatory post-synaptic currents

FABP - Fatty acid-binding protein

FAD - Familial AD

FF - FopFlash luciferase

FGF - Fibroblast growth factor

FISH - Fluorescent *in situ* hybridisation

FP - Floor plate

FRAT1 - Frequently rearranged In advanced T-Cell lymphomas 1

Fam53C - Family with sequence similarity 53, member C

Fz - Frizzled

GABA - γ -aminobutyric acid

GAP43 - Growth associated protein 43

GAPDH - Glyceraldehyde-3-phosphate dehydrogenase

GFP - Green fluorescent protein

GO - Gene ontology

GSK3 β - Glycogen synthase kinase 3 β

GTP - Guanosine triphosphate

HA - Haemagglutinin

HAPLN1 - Hyaluronan and proteoglycan link protein 1

HBSS - Hank's balanced salt solution

HD - Huntington's disease

HMGN - High mobility group nucleosome binding domain 1

HRP - Horseradish peroxidase

Hh - Hedgehog

Hip-1 - Huntingtin-interacting protein 1

Hsa - *H. sapiens* chromosome

IB - Immunoblotting

ICC - Immunocytochemistry

IDO1 - indoleamine 2,3-dioxygenase

IFN - Interferon

IPA - Ingenuity® Pathway Analysis

ITSN1 - Intersectin 1

IVIS - *In vivo* imaging system

INDY - Inhibitor of DYRK

Int1 - Integration 1

JAK - Janus kinase

JNK - JUN N-terminal kinase

KEGG - Kyoto Encyclopaedia of Genes and Genomes

KIP1 - Cyclin-dependent kinase inhibitor 1B

KO - Knockout

LEF - Lymphoid enhancing factor

LGR4/5 - Leucine rich repeat G protein-coupled receptor 4

LRP - Low-density lipoprotein receptor-related protein

LRKK2 - Leucine-rich repeat kinase 2

LTD - Long-term depression

LTP - Long-term potentiation

LiCl - Lithium chloride

MAG - Myelin associated glycoprotein

MAP - Microtubule-associated protein

MAPK - MAP kinase

MBP - Myelin-binding protein

MECP2 - Methyl-CpG binding protein 2

MEFs - Modified embryonic fibroblasts

mESCs - Mouse embryonic stem cells

MMCT - Microcell-mediated chromosomal transfer

MMTV - Mammary tumour virus

Mbn - Minibrain

Mmu - *M. musculus* chromosome

NFAT - Nuclear factor of activated T-cells

NFT - Neurofibrillary tangle

NGS - Next-generation sequencing

NICD - Notch intracellular domain

NLS - Nuclear localisation signal

NP - Neuritic plaque

NRCAM - Neuronal cell adhesion molecule

NT-3 - Neurotrophin 3

NaCl - Sodium chloride

OFT - Outflow tract

PBS - Phosphate-buffered saline

PBS (2) - Predicted biological score

PCP - Planar cell polarity

PCR - Polymerase chain reaction

PD - Parkinson's disease

PEST - Proline, glutamate, serine and threonine-rich

PFA - Paraformaldehyde

PVDF - Polyvinylidene fluoride

Podxl - Podocalyxin-like protein

QPCT - Glutamyl-peptide cyclotransferase

RNA - Ribonucleic acid

ROI - Region of interest

RT - Room temperature

RTK - Receptor tyrosine kinase

Rspo1 - R-spondin 2

S100B - S100 Calcium-binding protein B

SAGE - Serial analysis of gene expression

SC35 - Serine/arginine-rich splicing factor 2

SD - Standard deviation

SDS-PAGE - SDS polyacrylamide gel electrophoresis

SEMA3F - Semaphorin 3F

SIM2 - Single-minded family BHLH transcription factor 2

SOD1 - Superoxide dismutase 1

STRING - Search tool for retrieval of interacting genes/proteins

TBST - Tris-buffered saline Tween 20

TCF - T-Cell factor

TF - TopFlash luciferase

TGFB2 - Transforming growth factor β 2

TIAM1 - T-Cell lymphoma invasion and metastasis 1

TMOD1 - Tropomodulin 1

TYK2 - Tyrosine kinase 2

Tc1 - Transchromosomal mouse 1

Tg - Transgenic

VEGF - Vascular endothelial growth factor

VTT - Variable trisomic transcriptome

WHO - World Health Organisation

WIF1 - Wnt-inhibitory factor 1

WNT - **W**ingless-**I**ntegration

WT - Wild-type

Wg2 - Wingless 2

Y2H - Yeast two-hybrid

cDNA - Complementary DNA

gDNA - Genomic DNA

hESCs - Human embryonic stem cells

mDA - Midbrain dopaminergic neurons

mESCs - Mouse embryonic stem cells

mRNA - Messenger RNA

miRNA - Micro RNA

poly-A - Poly-alanine

poly-H - Poly-histidine

qPCR - Quantitative real-time PCR

β -TRCP - Beta-transducin repeat E3 ubiquitin protein ligase

General
INTRODUCTION
1-2

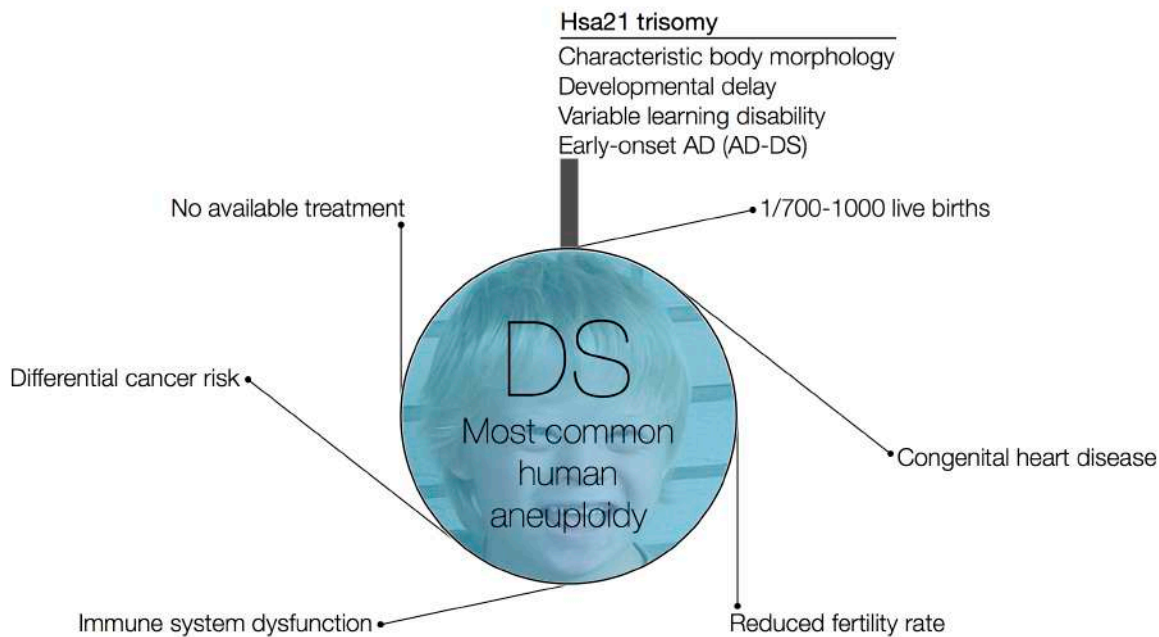


Fig. I.1 - Overview of characteristic features of DS.

Chapter 1 - General Introduction

The work conducted in this thesis generally bridges two overarching research themes: **1)** Down syndrome with its associated development of Alzheimer’s disease, and **2)** the functional relationship of these disease mechanisms with the Wnt signalling pathway. The associated scientific literature is broadly introduced here, and key aspects of both themes are further discussed in detail.

1.1 Down syndrome

1.1.1 Overview

Down syndrome (DS) is a genetic developmental disorder caused by the presence of an extra copy (trisomy) of human chromosome 21 (Hsa21) in the genome (1). First described by the UK physician John Langdon Down in 1866, DS is the most common human chromosomal abnormality, occurring in about 1/700-1000 live births in the United States (Centers for Disease Control and Prevention, 2006). In the vast majority of cases (95%), affected individuals possess a complete third copy of Hsa21, while a minority displays partial trisomy or mosaicism. The latter two result in a relatively milder variant. Although the severity of DS phenotypes varies widely amongst individuals affected, some specific features are invariably present. Learning disability and developmental delay are characteristic of all cases, albeit in a spectrum, with some individuals requiring significant care, and some able to lead a relatively independent life (2). Importantly, DS has long been associated with the nearly universal development of Alzheimer’s disease (AD) in adult life. One of the most striking features of this condition is in fact the invariable presence of AD-specific neuropathology from middle age (3, 4). Not all DS individuals develop clinical AD, but the risk is overall greatly increased (5).

Several craniofacial abnormalities are pathognomonic to DS, as is its associated growth pattern, for which adapted charts have been developed (6). In about 40% of cases, DS children are affected by congenital heart disease (CHD), mostly of ventricular septal or atrioventricular nature (7, 8). While the risk of solid neoplasms is reduced in DS (9), affected individuals are 10-15-fold more susceptible to haematological malignancies, particularly childhood leukaemias (6). Transient myeloproliferative disease, a malignancy identified as unique to DS, affects roughly 1 in 10 individuals (10). Additionally, DS is also characterised by endocrine, gastrointestinal and sexual dysfunction. While no treatment ameliorating the cognitive deficits of DS exists at present, associated disorders are treated based on clinical need and available therapies. Advancements in medical care and changes in societal attitudes towards mental disability have resulted in a significant extension of life expectancy. With appropriate care, DS individuals possess a 50 to 70 years life expectancy. Comparatively, median survival in the US was only 9 years as recently as 1949 (11).

1.1.2 Hsa21 in DS pathology

The two main aetiological hypotheses for DS propose that the phenotype may arise either as a direct pathological effect of increased Hsa21 gene dosage, or from non-specific genetic instability caused by the presence of an additional chromosome (6). Starting from the 1990s, the view that a putative “Down syndrome critical region” (DSCR) was responsible for most features of the DS phenotype gained wide prominence. It originated from multiple reports indicating the distal region of the Hsa21 long arm encoded key genes for DS pathology. Such evidence was produced in case studies on rare partial Hsa21 trisomies (12) and analysis of DS and non-DS relatives in selected families (13). Results suggested that the DSCR is necessary and sufficient for development of the signature features of DS.

A large amount of studies have provided structural and functional characterisation of Hsa21 in the last 2 decades. The complete sequence of the chromosome was produced for the first time in 2000 (14). The authors estimated Hsa21 to code for 225 functional proteins, with later studies suggesting the number might be as high as 364 (7). The latter have also provided a functional overview of Hsa21 genes employing comparative genomics and bioinformatics. Known Hsa21 proteins from the Swiss-Prot database were analysed with Gene Ontology Annotation, revealing the involvement of Hsa21 in 87 distinct biological processes. Interestingly, signal transduction pathways are the most common. Furthermore, Hsa21 proteins exert as many as 81 different molecular functions, the most frequent being DNA binding, transcription and transcription factor activity. Hsa21 proteins localise to 26 different subcellular components, mostly to the nucleus and plasma membrane, which is consistent with their prominent role in signal transduction. Upon the original description of trisomy 21 in 1959, it was hypothesised by LeJeune that all trisomic genes would undergo 1.5-fold overexpression relative to non-DS levels. It has been demonstrated, however, that only 37% of Hsa21 genes are overexpressed in the hypothesised fashion, while 45% are increased much less significantly, 18% are subject to even greater overexpression, and 9% are not significantly altered (7). The authors suggest that these data

favour the view of a candidate gene approach in describing DS phenotypes. Indeed, Hsa21 genes have been investigated in this respect. For instance, Chakrabarti and colleagues have shown that *Olig1* and *Olig2* triplication in the Ts65Dn mouse model of DS results in a developmental imbalance in excitatory and inhibitory neural populations of the forebrain, with an abnormal number of inhibitory neurons (15). Despite the available evidence, the DSCR view is being increasingly challenged. The advent of chromosome engineering techniques allowed for the development of mouse models carrying duplications of individual portions of Hsa21 ortholog regions (See 1.1.5). Through this method, it was shown by Olson and colleagues in *Science* that the DSCR alone is not sufficient for generation of DS craniofacial defects (16). Additionally, non gene-specific effects of Hsa21 trisomy have been described. Kuhn *et al.* have reported that Hsa21-associated microRNAs (miRNAs), small non-coding RNAs involved in post-transcriptional regulation, can modulate the expression of methyl CpG binding protein 2 (MECP2). This protein regulates the expression of target genes important for neuronal function, such as cAMP response element-binding protein (CREB) (17). The authors conclude that Hsa21 miRNAs might contribute to some of the neurochemical features of DS.

To date, the mechanistic role of Hsa21 in DS pathology remains elusive. While DS phenotypes cannot be simplistically linked to specific gene functions, a combination of gene-specific and non-specific effects is more likely than either alone. The phenotypic outcomes of Hsa21 trisomy are complex, and probably originate from an interplay between an overall imbalance of gene expression and specific effects of Hsa21 genes. Thus, the two hypotheses are not mutually exclusive and should be harmonised instead. The evidence on Hsa21 contribution to DS introduced here is further discussed and expanded in section 1.4.

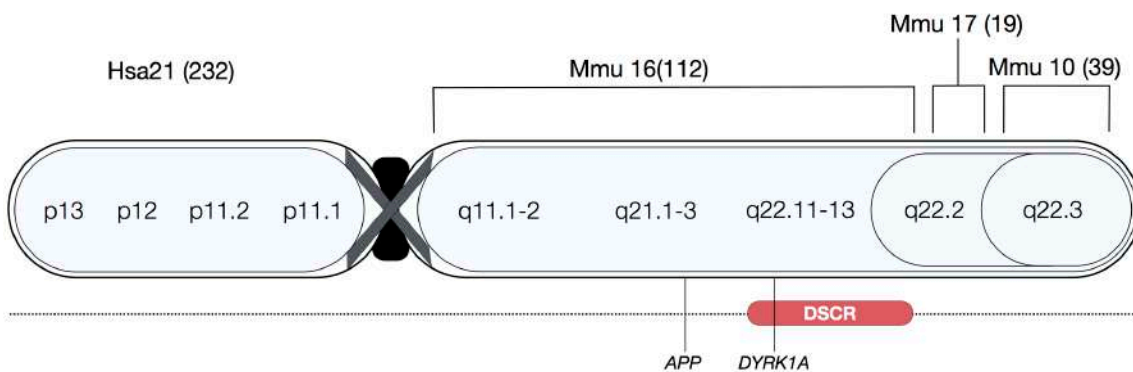


Fig. 1.2 - Known structure of Hsa21 and location of the DSCR on the distal long arm, which includes *DYRK1A*.

1.1.3 Dementia and Alzheimer's disease

As introduced, virtually all DS individuals may develop early AD neuropathology. To better contextualise the occurrence of this phenomenon, AD is briefly introduced here, discussing its best known features and associated pathological processes.

1.1.3.1 Overview

Dementia is a blanket term identifying a wide variety of neurodegenerative conditions generally affecting the ageing population. All forms of dementia share a degree of impairment in cognitive function, memory and behaviour. Cognitive deterioration is commonly associated with impairment in emotional control. It is important to differentiate dementia from the much milder, age-related cognitive decline observed in most of the population. Alzheimer disease (AD) is by far the most common form of dementia, accounting alone for about 60-70% of all cases (World Health Organisation - WHO, 2009). Currently, AD affects 20% of the worldwide population over age 80. Moreover, the latest WHO projections (Dementia Report, 2013) estimate a dramatic increase in the incidence of AD throughout the next 4 decades, with 135 million patients potentially affected in 2050. Most cases of AD are sporadic, although a small minority (0.1%) of earlier onset variants appear to be inherited in an autosomal dominant fashion (Familial Alzheimer disease - FAD).

As a form of dementia, AD is mainly characterised by a continuous decline in cognitive function, beginning around age 65 or over. Such decline is invariably associated with progressively widespread cortical atrophy. The traditional pathological hallmark of AD is deposition of neuritic plaques (NPs), composed of β -amyloid peptides ($A\beta$), and neurofibrillary tangles (NFTs), composed of hyperphosphorylated tau protein aggregates. Clinically, the earliest and most widely recognised symptom of AD is impairment and subsequent loss of short-term memory. Cognitive deterioration is accompanied, at later stages, by severe autonomic nervous system dysfunction. Death usually arises as a result of several secondary complications such as respiratory or cardiac failure. The clinical features of AD have been observed since the original description of the condition by Aloisius Alzheimer in 1906 (18). At present, no known therapeutic agent can arrest or reverse AD neurodegeneration, with acetylcholinesterase inhibitors such as donepezil only able to temporarily ameliorate symptoms by enhancing cholinergic neurotransmission (19). Although the term AD refers to the clinically overt disease, multiple lines of evidence suggest that the pathological process may commence years, if not decades, prior to clinical diagnosis (20, 21). This view established the preclinical stage of AD as an attractive target for therapeutic intervention.

1.1.3.2 Molecular pathology of AD

Accumulation of NPs and NFTs is an invariant feature of AD, and plays a key role in its pathogenesis. A β monomers are released from the proteolytic cleavage of amyloid precursor protein (APP), a trans-membrane protein of elusive neuronal function. Release of A β is catalysed by enzymatic complexes known as secretases, of which 3 isoforms are known (α , β , and γ). In physiological conditions, A β may act as a positive regulator of excitatory neurotransmission in rat hippocampal slices (22). Tau, an important microtubule-associated protein (MAP), is expressed primarily in the distal axon, where it interacts with tubulin, promoting its assembly into microtubules. When excessively phosphorylated, tau proteins form aggregates, disrupting microtubule organisation (23, 24). Although the specific mechanisms leading to neuronal death remain unclear, the neurotoxic properties of A β peptides and NFTs have long been recognised (25). Several studies suggest that aberrant accumulation of oligomeric forms of A β may impair excitatory neurotransmission at hippocampal synapses and in other cortical regions (26-28). In the context of memory formation, A β oligomers have been shown to antagonise induction of long-term potentiation (LTP) (29), promote *in vivo* long term depression (LTD) and alter dendritic spine morphology and density in the hippocampus (30). Consistently, these effects can be prevented by inhibiting A β oligomerisation (31). Moreover, recent studies in tau knockout mice have revealed that this protein is necessary for hippocampal LTD, the induction of which is accompanied by tau phosphorylation (32). The current understanding ascribes AD pathogenesis to extensive synaptic loss, and oligomeric A β has indeed been found to be a synaptotoxic species (33-35). Despite this toxicity, synaptic loss is increasingly understood to be a preclinical event in AD, preceding plaque and NFT deposition and cognitive decline.

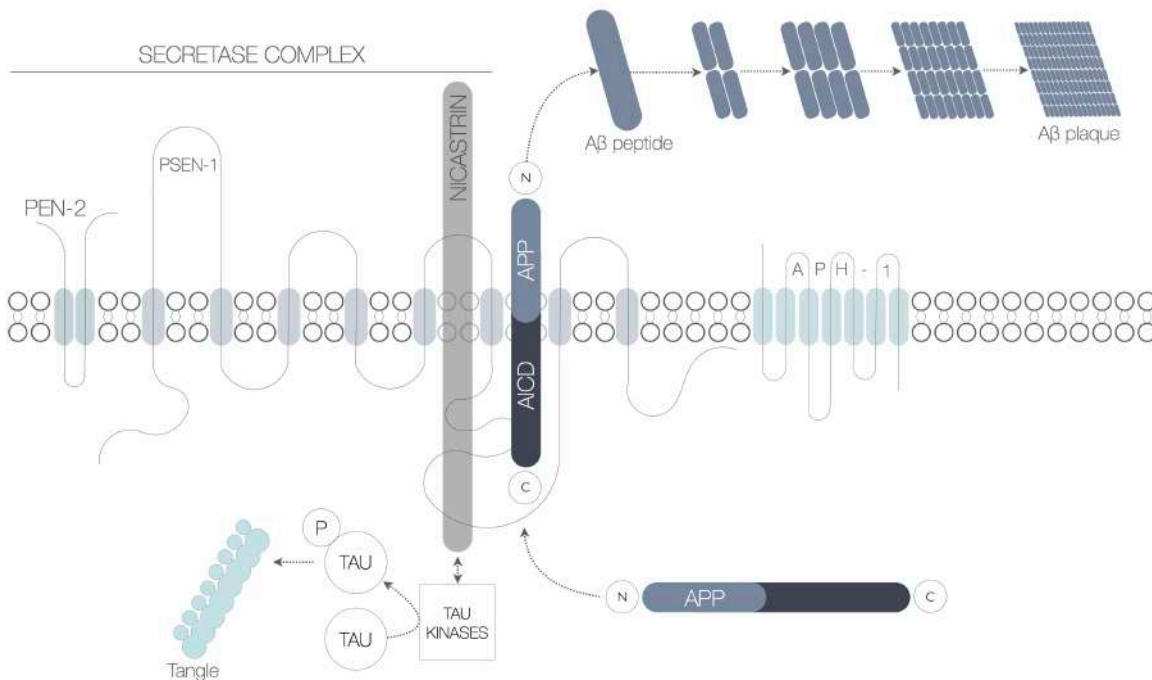


Fig. 1.3 - Classical model of AD neuropathology.

1.1.4 Alzheimer disease in Down syndrome (AD-DS)

In DS, clinical AD is diagnosed in roughly 60% of cases, starting at the fourth decade of life (5). A large amount of evidence supports this claim. Observations of this phenomenon even predate the 1906 description of AD itself: in a 1876 study, Fraser and Mitchell reported the occurrence of “premature ageing” in a group of DS individuals (36). Later case studies in the early 20th century suggested that DS individuals tend to develop AD pathology as well as clinical AD (37, 38). Compelling pathological evidence was definitively provided by Malamud *et al.*, who reported the invariable presence of A β plaques and NFTs in all DS people aged over 35 (3). In a later study, Schweber examined extensive autopsy data from DS brains, concluding that AD neuropathology is a universal finding in those aged 37 or more (39). Strikingly, DS individuals undergo accumulation of A β plaques starting as early as 8 years of age (40), with deposition rate increasing dramatically in an age-dependent manner (41).

Neuroimaging evidence, as reviewed by Teipel and Hampel, strongly indicates that an AD-like pattern of cortical atrophy and A β deposition is observed in DS via high-resolution MRI (42). A recent histological study also showed that while AD and AD-DS pathological specimens bear many similarities, there appears to be a significantly higher amount of NFTs in the latter (43). Because of the increased gene dosage characteristic of DS, research efforts have gone into establishing functional links between Hsa21 genes and AD pathology. To date, a few Hsa21-encoded proteins are interesting candidates for a mechanistic explanation of AD-DS, two of which are particularly worthy of mention:

APP - The *APP* gene is located on the long arm of Hsa21. Because A β levels correlate with its expression (5, 26), APP triplication could primarily account for the increased rate of plaque deposition observed in DS. Consistent with this view, APP locus duplication has been reported in multiple families with familial AD (44).

DYRK1A - dual-specificity tyrosine-(Y)-phosphorylation-regulated kinase 1A is a highly conserved protein kinase with a multitude of phosphorylation functions. It was first identified in 1995 as the *Drosophila* gene *minibrain* (*Mb*) encoding a kinase necessary for post-embryonic neurogenesis (45). In humans, the *DYRK1A* gene is located on the long arm of Hsa21 and, particularly, in the DSCR. It is well established that DYRK1A essentially contributes to several features of DS, particularly learning disability and central nervous system (CNS) abnormalities throughout embryonic development (46). DYRK1A is a favourable candidate for a mechanistic contribution of Hsa21 to AD pathology, given its well described functional relationships with tau metabolism, gamma-secretase function and A β itself. These lines of evidence are explored in detail in chapter 4.3.

1.1.5 Mouse models of DS

Since the advent of genetic engineering technology, several mouse models of DS have been developed. Historically, the most widely studied is the Ts65Dn, developed in 1990 by Davisson *et al.* (47). In the mouse, Hsa21 genes have their orthologs in portions of mouse chromosome 16 (Mmu16) and partly in Mmu10 and Mmu17. The Ts65Dn was developed via reciprocal translocation of mouse chromosomes 16 and 17 (Mmu16/17). As a result, the Ts65Dn is trisomic for most of Mmu16 regions of synteny to Hsa21. This model has been employed in a vast amount of DS studies, and key lines of evidence on its usage are discussed in further detail throughout section 1.4. Despite its wide use, the Ts65Dn mouse is not trisomic for Hsa21 in its entirety, and a considerable number of triplicated genes are not Hsa21 orthologs. Furthermore, not all genes on the translocation chromosome are significantly overexpressed (48). Therefore, recently developed mouse models, which more accurately recapitulate DS, are being increasingly used. With respect to this thesis, two classes of DS mouse models were employed.

The transchromosomal (Tc1) mouse was developed by Elizabeth Fisher and Victor Tybulewicz in 2005, and it is the first mouse model to contain a near-complete, freely-segregating copy of Hsa21 (49). The Tc1 mouse was generated through irradiation microcell-mediated chromosome transfer (MMCT). Via this approach, Hsa21 was harvested from human cells and subsequently inserted into mouse embryonic stem cells (mESCs). The original authors employed fluorescence in situ hybridisation (FISH) to show that the resultant Hsa21-trisomic mESCs contain approximately 90% of Hsa21, with intact code for 92% of known Hsa21 genes. The transchromosomal mESCs were then inserted into a murine blastocyst, thereby giving rise to an Hsa21 trisomic mouse chimera. Chimeras were then mated with wild-type (C57BL/6J) mice to achieve germline transmission of Hsa21 and generate Tc1 offspring. Subsequent backcrosses were then performed to homogenise the Tc1 genetic background, although this results in decrease of Hsa21 transmission as the generations progress. Even when fully retained, however, the presence of Hsa21 in the Tc1 CNS is not ubiquitous, with an average of 66% brain nuclei and 55% spinal cord nuclei screening positive for Hsa21 via interphase FISH and quantitative polymerase chain reaction (qPCR), respectively (49). Nevertheless, because mosaicism is a frequent finding in human DS (50), this Tc1 feature might be advantageous. Because the Tc1 contains a freely-segregating Hsa21, it is predicted to more accurately recapitulate the DS phenotype. Indeed, overexpression of several DS-related genes (*SOD1*, *SIM2*, *DYRK1A*, and *BACE2*) is observed in the Tc1 (49, 51). One prominent drawback of this model, however, is the known lack of functional overexpression of *APP*, which is reportedly deleted despite being originally introduced (51). This characteristic may hinder investigation of AD-DS phenotypes in the Tc1 mouse, which must therefore be crossed to *APP* transgenic models such as the J20 mouse (5). By contrast, *DYRK1A* activity has been found to be increased in Tc1 young and aged brains (52). This study also characterised the Tc1 phenotype further, describing several DS-like features. Tc1 embryos display a high frequency

of CHD, with 63% presenting ventricular septal or atrioventricular defects. Additionally, decreased cerebellar neuronal density is observed in adult mice, as seen in DS (53, 54). While basal synaptic transmission in the Tc1 hippocampus appears normal, LTP is significantly reduced. Consistently, Tc1 mice perform significantly worse than wild-type mice in the novel-object recognition task, a behavioural measure of hippocampal-dependent spatial learning. Similarly to human DS, T-cell activation is defective in the Tc1 model. The Tc1 does not however present with significant DS-like craniofacial abnormalities, with the exception of a smaller mandible. Since its development, the Tc1 has been extensively employed in DS research, revealing key aspects of DS pathology in cardiac development (55), haematopoiesis (56) and motor coordination (57), amongst others.

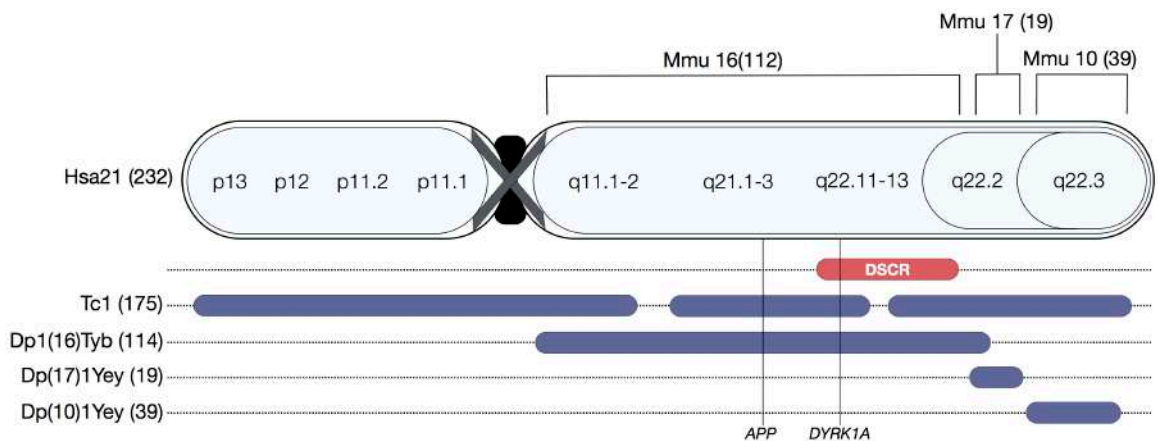


Fig. 1.4 - Genetic makeup overview of DS mouse models employed in this thesis, in relation to Hsa21.

The segmental trisomy/duplication (Ts/Dp) mice possess selected duplications of Mmu10/16/17 regions syntenic to Hsa21, similarly to the Ts65Dn, albeit with much greater specificity (58, 59). Generally, to achieve Mmu10/16/17 duplications, *loxP* sequences were targeted to the relevant chromosomal regions in mESCs, and subsequently duplicated via transfection of a Cre-expression vector. Subsequently, chimeras and the resulting constitutive mutants were generated in a similar manner to the Tc1. Backcrossing with wild-type (C57BL/6J) mice across five generations was then performed to homogenise the genetic background. The nomenclature of the strains follows a system whereby the last three letters are taken from the name of the main developer. For instance, Ts1Tyb mice have been generated by Victor Tybulewicz's laboratory. Dp1Tyb mice (59) - or the equivalent Ts1Yey (58) - are trisomic for Mmu16 regions of syntenicity to Hsa21, whilst the Dp1(10-17)Yey are trisomic for Mmu10-17 regions, respectively. Interestingly, these mice can be crossed to generate a compound mutant containing two duplications. The resulting mice can then be further crossed with the remaining strain, thereby resulting in a mutant trisomic for all Hsa21 syntenic regions. Yu *et al.* characterised these triple compound mutants, revealing an interesting phenotype (58, 60). Similarly to the Tc1, Dp mice displayed impairments in hippocampal LTP as well as altered performance in the Morris water maze test, a behavioural measure of hippocampal-dependent spatial learning. A consistent minority (~6.5%) presented congenital hydrocephalus. Although a rare occurrence, this has been observed in DS (61).

1.2 The Wnt signalling pathway

The principal aim of this thesis is to investigate a potential role the Wnt signalling pathway in DS. The structure and function of this pathway is introduced here, and later discussed in more detail (4.1-3.1).

1.2.1 Overview

The Wnt signalling pathway is one of the most highly conserved transmembrane signalling cascades in the kingdom Animalia. The earliest identification in 1982 by Roel Nusse and Harold Varmus described *integration1* (*Int1*) as a murine proto-oncogene for breast cancer (62). The same research group was able, in 1987, to homologise *Int1* to a well described *Drosophila Melanogaster* segmental polarity gene, *wingless2* (*Wg2*), the deletion of which induced the widely known wingless fly mutation. The term Wnt was coined as a portmanteau of **Wg2 and Int1**. After three decades since its discovery, research has partly unraveled the complexity of this signalling pathway. At present, three diverse Wnt signalling branches have been described: the **canonical/ β -catenin pathway** plays key roles in embryonal development, the cell cycle, cancer and neurodegeneration; the **non-canonical/planar cell polarity pathway (PCP)** controls cytoskeletal rearrangement in development through activation of Rho GTPases and Jun N-terminal kinase (JNK); the **Wnt Calcium pathway** modulates cytosolic Ca²⁺ levels, activating calcium/calmodulin-dependent protein kinase II (CaMKII). Although distinct in structure and function, all three interact and share sensitivity to the Wnt family of ligands, of which over 19 members have been identified. Furthermore, all pathways are activated via the same transmembrane receptor family, named frizzled (Fz, see below). At present, the main focus of this thesis is canonical/ β -catenin Wnt signalling. This pathway has its main effector in the transcriptionally active protein β -catenin. In the absence of Wnt ligands, cytoplasmic levels of β -catenin are maintained low via continuous proteasome-dependent degradation. This is achieved by a multi-protein complex known as the β -catenin destruction complex, which is composed of four proteins:

- i. **Adenomatous poliposis coli (APC)** was first identified as a tumour suppressor gene. Loss of APC is causative of familial adenomatous polyposis (63, 64).
- ii. **Axin** forms the backbone of the complex and possesses binding sites for the other components. In addition, its transcription is activated downstream of β -catenin, providing negative feedback for inactivation of the pathway. Axin was originally identified as an essential regulator of body axis formation during embryogenesis, hence its name (65).
- iii. **Glycogen synthase kinase 3 β (GSK3 β) and casein kinase I (CKI)** act in partnership to phosphorylate β -catenin at S45 (66, 67), allowing its interaction with β -transducin repeat-containing protein (β -TrCP), part of an E3 ubiquitin ligase complex (68). Additionally, GSK3 β phosphorylates axin (69), APC (70) and other components of the pathway. There are several described non-Wnt functions of GSK3 β such as NFAT phosphorylation, hedgehog and insulin signalling (71). Importantly GSK3 β has also been linked to tau phosphorylation (72, 73), an event mediated by a potential interplay with DYRK1A (see 4.3.1).

In the context of Wnt function, the frizzled family of receptors deserves further mention. Fz proteins are a subtype of G protein-coupled transmembrane receptors, and 10 distinct members (Fz1-10) are currently known (62). Their established biological function is the initiation of Wnt signalling cascades, and all three branches of the pathway are invariably sensitive to Fz activation (62, 74). These receptors are highly conserved in nature both structurally and functionally, and play well described, key developmental roles in *Drosophila*, *Xenopus*, zebrafish, mice and humans. Fz mutations are known to exert deleterious effects on organismal development, for instance by preventing efficient wing formation in flies. All Fz members possess a conserved, cysteine-rich extracellular domain implicated in ligand binding.

Functionally, Fz receptors associate with and are activated by Wnt ligands. These are also of key importance. The Wnt ligand family comprises a diverse array of lipid-modified secreted glycoproteins, with over 30 subtypes described (62). Whilst all Wnt ligands are capable of Fz binding and activation, individual members generally target different branches of the pathway. For example Wnt3a, later employed in this thesis, is specific to canonical Wnt signalling activation (75). Conversely, Wnt7a and Wnt16 are more closely associated with the Wnt PCP pathway (76). The existence of crosstalk and shared Wnt ligand sensitivity between such branches is however known (77). Similarly to Fz receptors, Wnt ligands are highly conserved across species, and play key roles in the development of virtually all eukaryotic multicellular organisms. Deletion of the *Drosophila* *Wg* gene, an ortholog of human Wnt genes, for instance, was shown to produce the famous wingless mutation in the original discovery of the pathway (62).

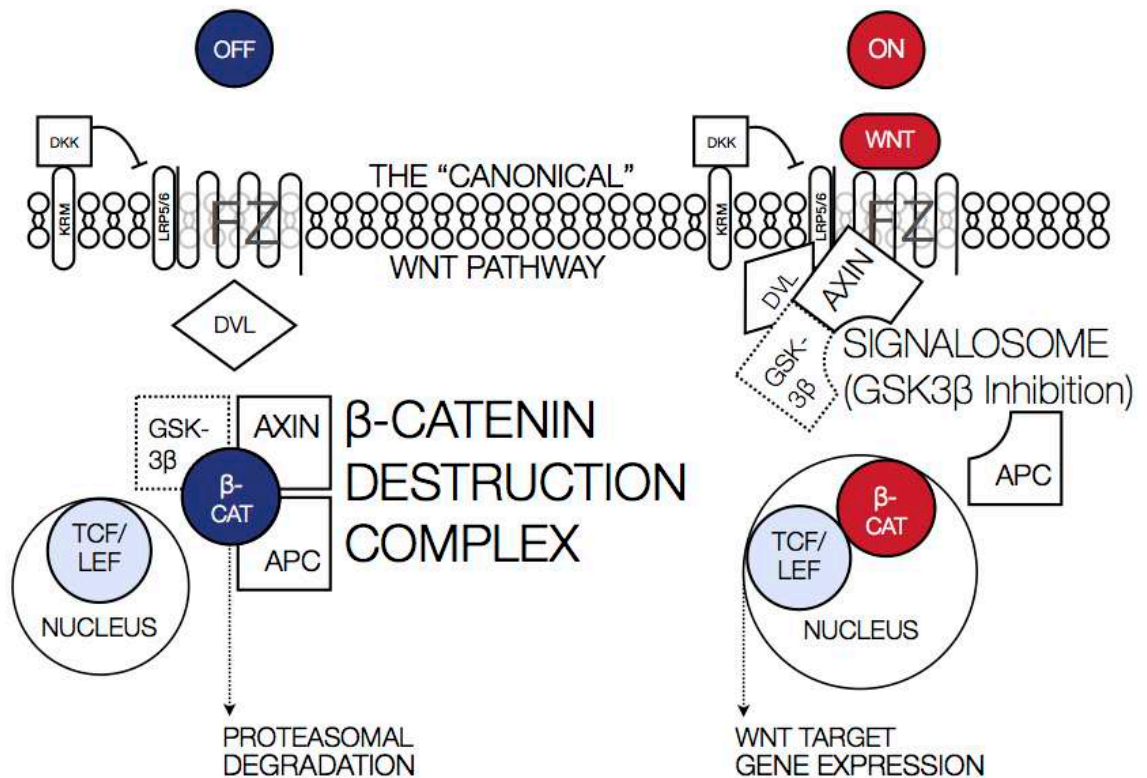


Fig. 1.5 - Visual overview of canonical Wnt signalling structure and activation mechanisms.

The basic functioning of canonical Wnt signalling, the main focus of this thesis, can be summarised as follows: transmembrane Fz receptors are coupled with LDL receptor related proteins 5 and 6 (LRP5/6). Fz activation by Wnt ligands induces translocation of the β -catenin destruction complex to the plasma membrane, primarily via recruitment of the second messenger dishevelled 1 (DVL1), which polymerises and interacts with Fz (78, 79). This, in turn, triggers LRP5/6 phosphorylation by GSK3 β and CKI. Such assembly results in functional sequestration of GSK3 β and CKI in a vesicular complex termed 'signalosome', effectively halting β -catenin phosphorylation and degradation. In this stabilised form, β -catenin undergoes nuclear translocation. Binding the T-cell and lymphoid enhancer 1 (TCF/LEF1) transcription factors therein activates expression of downstream target genes. This modality of action of β -catenin confers the Wnt pathway modulatory control over many biological processes. Wnt target genes ([The Wnt Homepage](#), 2017) have roles in cell proliferation [*Myelocytosis (MYC)*, *CYCLIND1*, *vascular endothelial growth factor (VEGF)*, *fibroblast growth factor (FGF)*], differentiation (*brachyury*, *siamosis*), and adhesion [*E-cadherin and neuronal cell-adhesion molecule (NRCAM)*]. Furthermore, several components of the pathway itself are also target genes, as introduced for axin. These include TCF/LEF, Fzs, LRPs and β -TrCP, demonstrating the existence of regulatory feedback mechanisms. Another important group of Wnt target genes are the *dickkopfs (DKKs)*. They encode DKK1-4, the secreted canonical Wnt antagonists. DKKs exert their inhibitory action by interacting with LRP5/6 co-receptors and causing their internalisation (80). Recent evidence has also shown that DKK1 may induce activity of the Wnt PCP pathway, suggesting that the two Wnt pathways may operate in an antagonistic fashion (81).

1.2.2 Wnt regulation of stem cell function

In recent years, roles for Wnt signalling have been identified in a variety of biological processes. One of the most well-characterised is the extensive involvement of Wnt signalling in stem cell function. In mouse embryonic stem cells (mESCs), canonical and non-canonical Wnt signalling promote self-renewal (82). Furthermore, Wnt signalling blockade may also prevent mESC expansion. Wray *et al.* reported that mESC expansion is mediated independently of β -catenin, while self-renewal is under control of the canonical pathway (83). In human embryonic stem cells (hESCs), partly conflicting reports indicate that canonical Wnt signalling may promote differentiation (84) and pluripotency (85). The current view is that temporal modulation of Wnt signalling activity during development might allow the pathway to control both aspects of stem cell function (86). Similar effects have also been observed in stem cells within several adult tissue subtypes. These include the haematopoietic system (87), the small intestine (88), the lung (89) and the heart, where canonical Wnt signalling mediates cardiomyocyte differentiation (90). Because of its ubiquitous role in controlling the rate of cell proliferation, aberrant Wnt signalling has been heavily implicated in the pathogenesis of several cancer types. An important example is breast cancer. Canonical Wnt signalling controls maintenance of mammary gland stem cells (MaSCs) during breast development (91). Excessive activation of the pathway induces mammary gland tumorigenesis, as demonstrated by Shackleton *et al.* using mouse mammary tumour virus (MMTV) transgenic mice (92). Furthermore, Wnt signals may also mediate distal metastasis by

cancer stem cells (CSCs). When infiltrating a distal tissue, CSCs locally recruit Wnt ligands via expression of the fibroblast-derived protein periostin (93). Aberrant Wnt signalling is also associated with the development of haematological, pulmonary and gastrointestinal malignancies (86). Because of its key role in tumorigenesis, canonical Wnt signalling is widely considered an appealing therapeutic target for the next generation of cancer treatments. Waaler *et al.*, for instance, showed that stabilisation of the β -catenin destruction complex with small molecule inhibitors may reduce tumour growth in mouse models of colonic carcinoma (94).

1.2.3 Wnt signalling in neurodevelopment

Given its cytoregulatory role in multiple tissue types, it is perhaps not surprising that Wnt signalling has also been linked to several cellular aspects of nervous system development. A historical finding in this context is the letter published in *Nature* by Thomas and Capecchi in 1990 (95). Employing chimeric mice homozygous for an *Int1* (*Wnt1*) disrupting mutation, the authors reported that ablation of this gene produced a phenotype of severe cerebral defects and ataxia. Specifically, they demonstrated that *Wnt1* is an essential requirement for normal development of the mesencephalon and metencephalon. Further studies led to the identification of specific Wnt signalling roles in dorsal patterning and neural tube development. In a 1997 milestone study published in *Nature*, Ikeya *et al.* demonstrated the importance of localised Wnt signalling for neural crest expansion and differentiation (96). Ablation of *Wnt1* and *Wnt3a* signalling resulted in a severe reduction of gliogenic and neurogenic neural crest derivatives, particularly in the hindbrain and spinal cord of mutant mice. Indeed, β -catenin is an absolute requirement for mouse embryogenesis, and its homozygous deletion is embryonically lethal (97, 98). The neurodevelopmental functions of canonical Wnt signalling have been further investigated in the context of midbrain dopaminergic neurons (mDA). This neural population originates from a ventral region of the neural tube, the floor plate (FP) (99). The FP also contributes to development of hindbrain and spinal cord non-mDA neural populations, albeit with very low neurogenicity. Differential levels of canonical Wnt signalling between these two regions appear to largely contribute to this discrepancy (100). Conditional ablation of β -catenin in murine embryos results in a significant decrease in mDA number (100). Particularly, loss of canonical Wnt signalling was associated with decreased expression of mDA progenitor markers *Lmx1a/b*, *Msx1* and *Otx2*. A severe reduction in progenitor proliferation was also observed, and expression of the proneural gene *Ngn2* was lost (100, 101). These results suggest that β -catenin is an important requirement in cell fate specification of mDA progenitors and consequently, neurogenesis. In gain-of-function studies employing a degradation-insensitive β -catenin mouse mutant, however, ectopic stabilisation of β -catenin also resulted in overall reduction of mDA neurons. Despite an increase in progenitor cell number, reduced cell cycle exit was observed, ultimately resulting in decreased neurogenicity (102). Joksimovic *et al.* also reported that, in the same mouse model, net levels of *Lmx1a/b* were reduced by sustained canonical Wnt signalling (103). Deletion of *Dkk1* in knock-out mouse embryos may also affect Wnt-mediated neurogenesis (104). Heterozygous mutants display a significantly lower number of differentiated mDA neurons, while very few

Dkk1 ^{-/-} embryos survive, suffering from severe abnormalities in morphogenesis and impaired fore-brain development. These somewhat counterintuitive findings offer insight into the complexity of neurodevelopmental Wnt signalling, demonstrating that tight control of β -catenin levels is required for mDA neurogenesis, with alterations in both directions exerting deleterious effects.

1.2.4 Wnt signalling in synaptogenesis and memory

Over the last decade, several studies have demonstrated that Wnt signalling is functionally indispensable for synaptic assembly and organisation (105). One of the earliest reports is a 2000 study by Hall *et al.* (106). The authors demonstrate that Wnt signalling is required for synapse formation at the presynaptic cerebellar input interface. Specifically, Wnt7a signalling modulates mossy fibre axon remodelling by decreasing axonal extension and stimulating growth cones in mouse cerebellar slices. Within the same anatomical system, deletion of Wnt7a resulted in altered distribution of presynaptic markers and morphological abnormalities in presynaptic axons (107). Moreover, DVL1 ablation enhanced this effect, with Wnt7a/DVL1 double mutant mice exhibiting impairments in neurotransmitter release at mossy fibre-granule cell synapses. Particularly, the frequency of miniature postsynaptic excitatory currents was reduced. In mossy fibres, administration of Wnt ligands resulted in increased synaptic vesicle recycling (107). The importance of Fz receptors in synaptic formation has also been elucidated. In hippocampal cultures, Fz1-mediated Wnt3a signalling acts to increase the number of presynaptic terminals (108), while Wnt7a may promote synaptogenesis via Fz5 stimulation (109). Through concomitant action of the non-canonical and calcium pathways, Wnts also control postsynaptic assembly. Wnt7a is an interesting example. In the hippocampus, it stimulates the presynaptic terminal via the canonical pathway (110), while also activating CaMKII in the postsynaptic terminal, promoting dendritic spine growth and resulting in increased synaptic strength (76). The non-canonical and calcium pathways are able to modulate several other aspects of synaptic transmission, such as amplitude of inhibitory currents and GABA-A receptor number (111). Beyond synapse formation, Wnt signalling has important roles in maintenance of synapse function in mature neurons. Several studies have documented the ubiquitous expression of Wnt signalling components in the adult brain (109, 112, 113). Purro *et al.* also showed that short-term exposure to DKK1 induces synaptic loss in mature neurons (114). Particularly, it appears to provoke changes in synaptic protein clustering, promoting dispersion from synaptic terminals whilst not altering overall protein levels. This effect is rescued by Wnt ligands, indicating that tight control of Wnt signalling is required for effective synaptic maintenance.

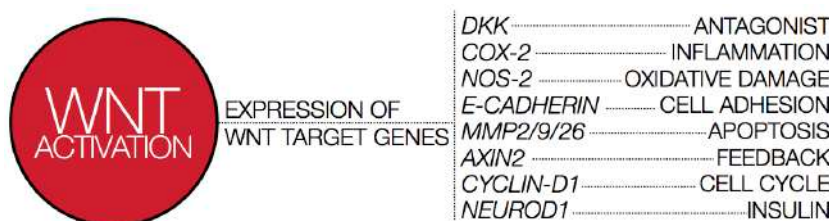


Fig. I.6 - Visual summary of some known Wnt signalling target genes.

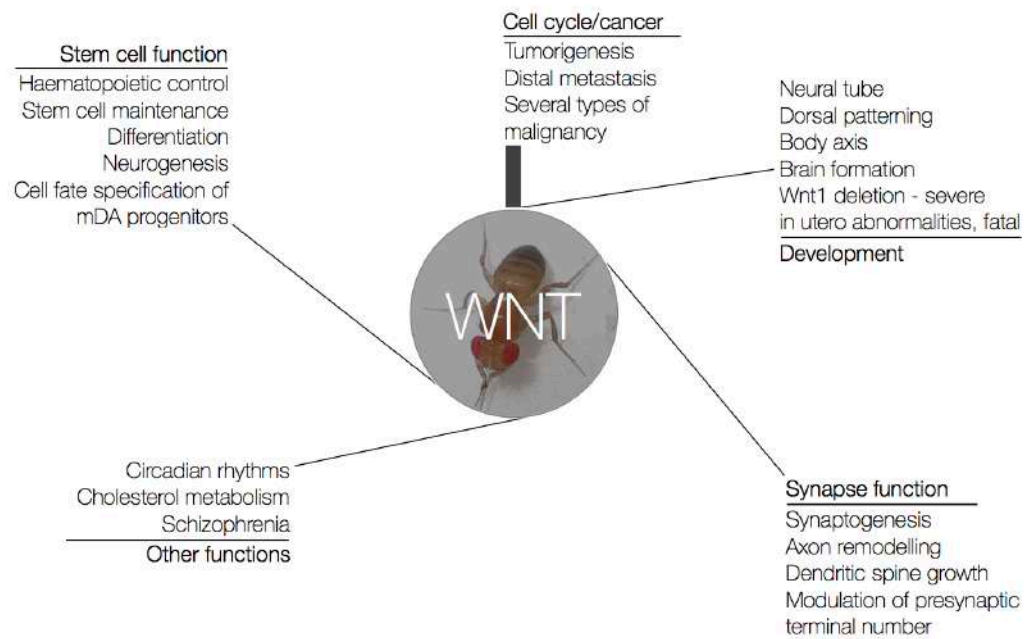


Fig. I.7 - Visual summary of known Wnt signalling functions.

1.2.5 Wnt signalling in AD

As introduced previously, clinical impairment in short term memory, accompanied by progressively widespread synaptic loss, is an early and invariant feature of AD. Thus, given the prominent role of Wnt components in synaptic assembly and maintenance, a functional relationship between AD and aberrant Wnt signalling is not unexpected. Indeed, multiple lines of evidence have described this relationship in recent years, revealing a complex network of interactions. At the population level, a genome-wide association study reported the existence of an LRP6 genetic variant with significant links to late onset, sporadic AD (115). Such polymorphism results in reduced expression of Wnt target genes. Additionally, post-mortem cortical samples of AD patients demonstrate increased levels of DKK1 (116), while clinical findings indicate that DKK3, closely related in structure and function to DKK1, is elevated in plasma and cerebrospinal fluid (CSF) samples of AD patients (117). Mutations in *presenilin-1* (*PSEN1*), an integral part of the γ -secretase complex, the enzymatic assembly responsible for APP cleavage into A β , have been linked to development of FAD. Earlier reports demonstrate that such mutations exert a modulatory effect on intracellular β -catenin levels, either decreasing (118), or increasing them (119). *PSEN1* has also been shown to associate with GSK3 β (120). Furthermore, inhibition of canonical Wnt signalling via GSK3 β overexpression significantly increases the rate of tau phosphorylation (121, 122). Conversely Rosso *et al.* showed that GSK3 β inhibition is a protective factor against A β -mediated synaptotoxicity (123). Consistently, evidence suggests that Wnt3a signalling activation in mice can prevent A β toxicity, decrease tau phosphorylation (124) and reduce the amount of several AD neuropathological markers (125). It is now clearly understood from *in vitro* evidence that A β may interact with multiple components of the Wnt pathway. For instance, it was shown to associate with the Fz receptor family (126), while the APP intracellular domain, a cytosolic counterpart of

A β , promotes neurite outgrowth via canonical Wnt signalling inhibition (127). Particular effort has gone into examining the relationship between A β and DKK1. Following administration of exogenous A β , synaptic disassembly was induced concurrently with increased expression of DKK1 in murine brain slices (114). In the same study, a DKK1 neutralising antibody was able to prevent A β -mediated synaptotoxicity. Consistent with this evidence, Killick *et al.* revealed an interesting relationship between the canonical and PCP pathways (81). It appears that clusterin, a canonical Wnt target gene (128), is required for the mutual interaction of A β and DKK1. While intracellular levels of clusterin increased following A β treatment, knockdown of clusterin reduced the A β -mediated increase in DKK1 expression. Examined against whole-genome protein expression levels in mouse primary neurons, this A β /clusterin/DKK1 pathway was then shown to drive the expression of several PCP target genes (81). Thus, the synaptotoxic effects of A β might be underlined by an altered balance between activity of the canonical and PCP Wnt signalling pathways.

More recent studies increasingly support the notion of suppressed Wnt activity in AD, as well as the interesting possibility of therapeutic targeting of this pathway. A literature review by Cisternas and Inestrosa (129) discussed the importance of cerebral glucose metabolism as a crucial contributor to AD. This phenomenon is well known. Decreased neuronal glucose uptake and impaired metabolism is in fact observed in AD and other neurodegenerative diseases, and is regarded as an early mediator of cellular pathology. The authors argue that current evidence implicates Wnt signalling in the regulation of neuronal energy metabolism, with particular relevance to AD. This proposal strengthens the notion that therapeutic normalisation of Wnt activity in AD might constitute an effective strategy. In parallel, Machhi *et al.* recently reported on the neuroprotective effects of multi-targeted isoalloxazine derivatives in rodent models of AD (130). These compounds display dual anticholinesterase and anti-A β aggregatory activity. The former is a known protective factor in AD, and constitutes the basis for currently available therapies (19). Importantly, the authors demonstrated a significant association of isoalloxazine treatment with Wnt signalling stimulation. AD-beneficial effects were in fact observed concomitantly to enhanced β -catenin and neuroD1 levels in a rat model. The latter is a well known Wnt target gene. These findings suggest that amelioration of AD pathology is functionally accompanied by Wnt signalling activation, thus providing further support to the disease relevance of this pathway. A similar correlation was also identified with an alternative treatment strategy for AD. In a recent study by Jin *et al.*, administration of sodium selenate therapy significantly reduced AD pathology in a triple transgenic mouse model (131). Similarly to the Machhi *et al.* report, concurrent Wnt signalling activation was detected in selenium-treated mice, with increased levels of β -catenin and target genes as well as GSK3 β inhibition. Data from these two studies therefore suggest that distinct AD treatment approaches invariably correlate with enhanced Wnt activity markers. It follows that regardless of which method is chosen to reduce AD pathology, canonical Wnt signalling appears to be stimulated in correlation. This line of reasoning indicates a potentially critical Wnt contribution to AD.

Taken together, these lines of evidence indicate that alterations in Wnt signalling and AD are likely interrelated. As well as interacting with APP/A β on multiple levels, Wnt signalling is implicated in neurogenesis, synaptic formation and viability, all of which are essential aspects of neuronal homeostasis. In parallel to recent developments in cancer biology, Wnt signalling is thus being increasingly perceived as a favourable candidate for therapeutic development in AD.

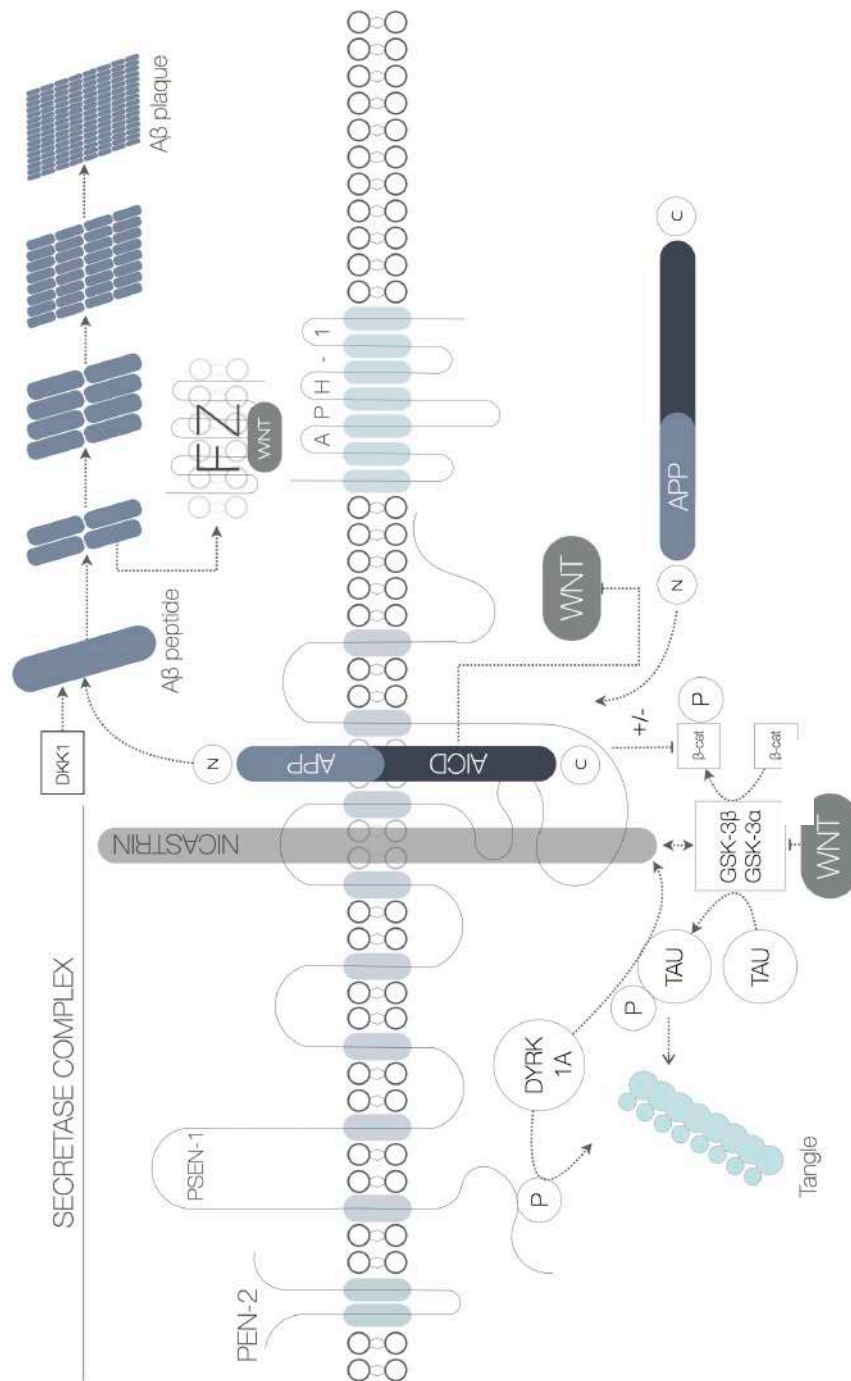


Fig. 1.8 - Classical model of AD neuropathology updated with currently known functional effects on/of Wnt signalling.

1.3 Wnt signalling in DS and AD-DS?

The essentials of AD, DS and AD-DS pathology have been considered. A vast amount of evidence suggests an accelerated process of AD-like pathogenesis in DS, supporting the idea that overexpressed Hsa21 genes exert a facilitatory effect on this phenomenon. Furthermore, an overview of the roles of Wnt signalling in several neuronal homeostatic processes suggests that altered Wnt activity influences AD pathology on multiple levels. Thus, provided that consistent AD-DS and AD-Wnt relationships exist, the possibility that altered Wnt signalling might also contribute to DS and AD-DS warrants investigation. This notion constitutes the primary hypothesis of this thesis.

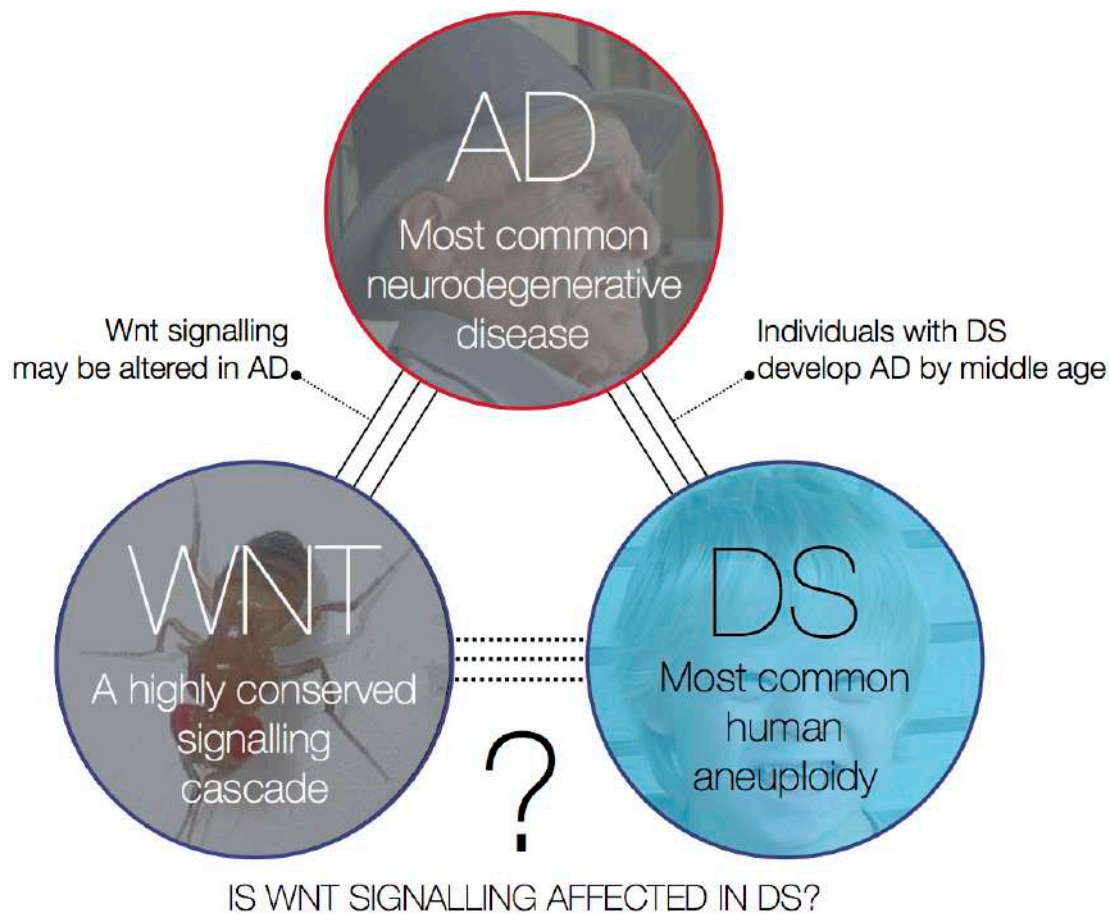


Fig. 1.9 - The primary hypothesis. Available evidence suggests dysfunctional Wnt signalling may be associated with DS.

In support of this idea a further line of evidence deserves mention, that is, **multiple Hsa21 genes have been found to interact with Wnt signalling**. As introduced above, the APP intracellular domain is a canonical Wnt signalling inhibitor which can modulate neurite morphology (127). As a favourable candidate for a functional AD-DS relationship, the interaction of APP with Wnt signalling raises the possibility that enhanced modulation of the pathway may result from enhanced *APP* gene dosage. Furthermore, the Hsa21 gene *TIAM1* has been identified as a Wnt target gene promoting intestinal tumour development in mouse models (132). Importantly, *DYRK1A* was recently shown to be a positive regulator of the δ -catenin/Kaiso pathway, increasing δ -catenin levels in *X.Laevi* embryos and mammalian cells (133). This is a ramification of canonical Wnt signalling, with δ and β -catenin sharing high similarity. δ -catenin binds to the Kaiso transcription factor, driving the expression of several target genes, some of which are in common with canonical genes (*siamosis*, *Wnt1*). Studies have also revealed an important relationship between *DYRK1A*, *GSK3 β* and tau. While *DYRK1A* phosphorylates tau at T212, this interaction has been shown to prime tau for further phosphorylation by *GSK3 β* at S208 and eventual degradation (72, 73). The *DYRK1A*-Wnt relationship is explored in more detail in the introduction to chapter 4.3.

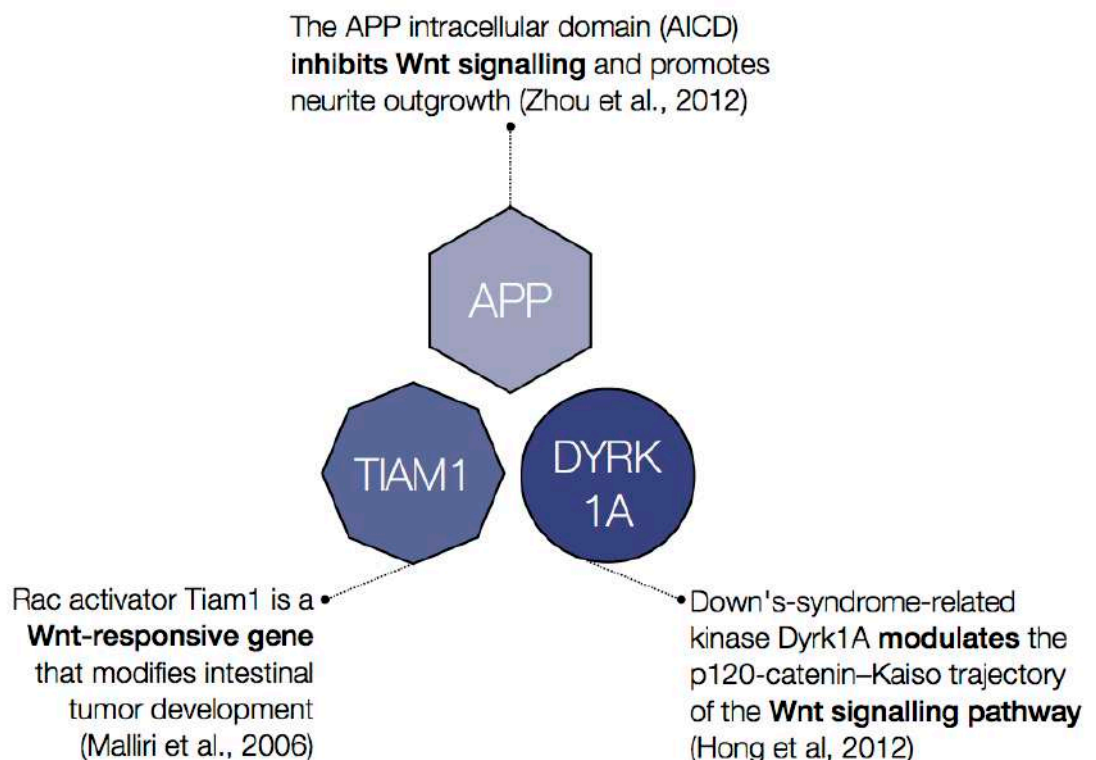


Fig. 1.10 - Preliminary evidence suggests multiple Hsa21-encoded proteins may function as Wnt signalling regulators, thus supporting the formulation of a candidate gene hypothesis for this thesis.

1.4 Genes and proteins of DS: a literature overview

The main hypothesis of this thesis was formulated in section 1.3. Before considering experimental results, however, it is essential to discuss the complex landscape of gene expression and protein abnormalities in DS. This section outlines current knowledge on these two fundamental aspects by critically assessing the available evidence. This also provides a theoretical framework to justify the experimental approaches undertaken in this thesis.

1.4.1 The DS transcriptome

Given the genetic origin of DS pathology, it follows that the defining characteristics of this condition are necessarily mediated by primary alterations in gene expression. Thus it is not surprising that this aspect of DS has been heavily investigated over the last few decades. In light of this, the main features of gene expression in DS, as well as key findings in the field, are discussed in the following sections.

1.4.1.1 The role of transcriptomics in the understanding of DS

Massively parallel complementary DNA (cDNA) sequencing, or RNA sequencing (RNAseq), is a well-established technique, which exploits the fundamental principle that the amount of transcript mRNA directly correlates with gene expression levels. This area of study is broadly known as transcriptomics. This relatively recent field has experienced great advances in the past decade (134), both for the fundamental understanding of the dynamic nature of the genome and for the investigation into a high number of diseases in which altered gene expression plays a key role. While the technique was originally based on microarray hybridisation technology, the advent of high-throughput next generation sequencing (NGS) has allowed analysis of the transcriptome to be performed on a much larger scale. Since the discovery of trisomy 21 as the primary cause of DS (1), investigation of the mechanisms mediating the phenotypic effects of this aneuploidy has proved challenging. The supernumerality of Hsa21 results in extremely complex, multi-layered effects on the transcriptome, the analysis of which can be hindered by several confounding factors. Gene expression variability, phenotypic heterogeneity and differential epigenetic stimuli are amongst the most important. As of today, no clear consensus exists still on whether features of DS are solely mediated by functional alteration of trisomic genes, or arise as a global effect of aneuploidy, notwithstanding the genetic repertoire of Hsa21 (135). Both mechanisms likely contribute to DS. However, the inherent difficulty in clarifying exactly if, and how the transcriptome is altered in this condition warrants the need for approaches which minimise confounding factors. Experiments conducted so far have been mostly based on quantitative real-time PCR (qPCR), fluorescent in situ-hybridisation (FISH) microarray and NGS strategies. In the context of DS, these approaches have served three purposes: to confirm and characterise the aneuploid status of the mouse strains or human samples under examination, to investigate genome-wide alterations in expression signatures, and to extrapolate functional significance from such alterations. These principles were also exploited in the work described in chapter 4.1., and will serve as a conceptual basis for justifying the approach undertaken.

1.4.1.2 Gene expression profiling in DS mouse models

Beginning in the early 2000s, a considerable amount of literature has investigated the transcriptome of DS mouse models (see introduction 1.1.5. for an overview of models). A seminal example is a study by the Antonarakis group, published in 2000 (136). In the classical Ts65Dn segmental trisomy model, the authors employed serial analysis of gene expression (SAGE) to probe the brain transcriptome of this mouse strain. Results revealed 330 differentially expressed (DEX) genes spanning several mouse chromosomes, 14 of which encoding ribosomal proteins. Aside from considerations regarding ribosomal dysfunction in DS, this study first contributed to sequencing of the mouse brain transcriptome. Additionally, it demonstrated the general principle that aneuploid gene dosage imbalance is not limited to trisomic genes, but results in genome-wide changes in expression. Similarly, subsequent work by Saran *et al.* (137) investigated the cerebellar transcriptome of the same model, in an attempt to elucidate mechanisms underlying the well known cerebellar dysmorphology of DS. The study found that overexpression of the 124 genes duplicated in the Ts65Dn cerebellum resulted in the presence of thousands of DEX genes, which the authors termed 'variable trisomic transcriptome' (VTT - this fitting term is henceforth adopted to refer to variability in the DS transcriptome). Concurrently, Lyle *et al.* employed the same mouse model to investigate expression levels of Hsa21 orthologs in six tissue types (138). The notion that such genes would undergo 1.5-fold overexpression in DS was mostly theoretical at the time, and this study elucidated a very important principle. The authors in fact demonstrated that, whilst overall the mean overexpression was close to 1.5-fold, just over a third (37%) of duplicated genes were expressed at this ratio. The remainder was overexpressed either below 1.5, above, or not overexpressed at all (for about 9% of theoretically duplicated genes). This pioneering finding implies the existence of complex regulatory mechanisms determining the DS phenotype, which are not necessarily dependent on gene dosage only. Similarly, another study in the Ts65Dn mouse examined expression patterns of duplicated genes across nine tissue types (139). The majority demonstrated enhanced transcript levels, but several genes did not.

More recent work has helped identify molecular processes potentially altered in DS, by combining transcriptomics with gene ontology analysis. A microarray-based study of the Ts1Cje mouse brain (see 1.1.5.) identified 317 DEX genes (140), mostly associated with the cerebellum and hippocampus. In addition to supporting the VTT theory, these results also demonstrated a unique gene expression profile in the Ts1Cje mouse. Functional clustering analysis predicted significant dysregulation of the interferon signalling pathway, establishing potential target molecular networks and highlighting the complex effects of aneuploidy on signalling networks. Additional molecular pathways of potential interest were also identified by Guedj and colleagues (141). This study investigated gene expression in the adult Ts1Cje mouse hippocampus and cerebral cortex. DEX genes were significantly more conspicuous in the hippocampus than the cortex and, similarly to all other studies discussed, spanned several chromosomes. Functional analysis identified NFAT signalling and neuroinflammation as potentially affected processes. The same group also investigated the foetal brain transcriptome of the Ts1C-

je mouse (142). They identified 71 DEX genes in embryonic (E15.5) Ts1Cje brains. Interestingly, functional analysis demonstrated upregulation of cell cycle markers and dysregulation of processes such as apoptosis and inflammation. This study provided key insight on potentially altered mechanisms at a critical stage of brain development, and detailed prenatal manifestations of the DS phenotype. The clear differences in genetic signatures between embryonic and adult Ts1Cje mouse brains (141, 142) also exemplify that the VTT is extremely dynamic on the temporal scale. This suggests that, in DS, the effects of Hsa21 trisomy on the transcriptome likely vary considerably throughout life.

RNAseq in DS mouse models has also been very useful in characterising recently developed strains. The Tc1 mouse, employed in this thesis, is the first DS model expressing a near complete, freely segregating Hsa21 (49). In an effort to determine the weight of each dosage-sensitive Tc1 gene, Gribble, Wiseman *et al.* combined fluorescent in situ hybridisation (FISH) with NGS technology to investigate the architecture of the human chromosome in this mouse (51). Results indicated that a number of previously unknown structural alterations of Tc1-Hsa21 are present in this mouse. The irradiation-transferred chromosome displayed 25 *de novo* rearrangements, six duplications and one deletion. These data provided valuable knowledge to researchers employing the Tc1 mouse to investigate its DS phenotype. Overall, the authors identified 50 Tc1-Hsa21 genes as either disrupted or deleted, and thus not functionally trisomic. These included *APP* - already identified as disomic in the Tc1 mouse (49) - and the leukaemia-relevant *RUNX1* gene. The key implication of these findings is that DS-like phenotypes described in the Tc1 mouse are unlikely to be mediated by any of the deleted genes, some of which are heavily implicated in DS pathology. Thus, this study provided means to reduce confounding factors when assessing data generated in the Tc1 mouse, including several experiments carried out as part of this thesis. Additionally, the authors proposed a definitive structure for Tc1-Hsa21, and this study for the first time detailed the effects of irradiation on a human chromosome. Interestingly, the transcriptome-based approach has also aided investigation of strategies to ameliorate behavioural deficits of DS mouse models. One example is a recent study of the Ts65Dn cerebellar transcriptome (143). The authors investigated the effects of regular exercise on locomotor deficits of these mice, and probed the cerebellar transcriptome for gene expression changes. Strikingly, lifelong running was sufficient to alter the expression of 4,315 genes, a five-fold increase compared to euploid mice subjected to regular exercise. Functional annotation revealed alterations in a wide range of biological processes, most notably regulation of apoptosis and neurogenesis. In addition, several signalling pathways linked to the cell cycle were also found to be enhanced in activity. Therefore, in addition to demonstrating the beneficial effects of a behavioural intervention in the Ts65Dn mouse, the authors also linked said amelioration to clear gene expression patterns. Overall, the studies discussed detail the advancing knowledge on the DS mouse transcriptome, and demonstrate the fundamental principle of the VTT, its dynamic nature and genome-wide occurrence. Additionally, they provided the evidential basis for combining transcriptomics with functional analysis in the exploration of target molecular pathways in DS.

1.4.1.3 Gene expression profiling in human DS

Similarly to the work conducted in mice, several studies have characterised the transcriptome of human DS individuals, providing vital information on the complex genetic picture underlying this aneuploidy. Performing such studies on humans has the added benefit of generating more DS-relevant data, with gene expression patterns originating from endogenously trisomic Hsa21 genes. However, confounding factors arise more commonly than in mice, owing to difficulties in generating sample groups with homogenous genetic background, a task easily achievable in mice through backcrossing and employment of littermates. Nevertheless, several studies performed on the human DS transcriptome exist which partly overcome this limitation. The ideal approach, as outlined by Antonarakis (135), is to identify pairs of monozygotic twins discordant for DS. Due to the extreme rarity of this occurrence, only one report exists at present (144).

One of the first examples of gene expression profiling in human autosomal trisomy is a microarray-based study in cells derived from trisomies 21/13 embryos (145). Trisomic genes were found to be upregulated only modestly (<1.3), and high variability in expression profiles was observed amongst trisomic samples. However, the authors observed that the vast majority of overexpressed genes did not map to trisomic regions of the genome. Similarly to the work in mice discussed above, this study led to the novel observation of secondary, genome-wide effects of Hsa21 trisomy on the VTT. The authors argue that whilst primary transcriptional alterations may be modest, secondary effects on non-trisomic genes are likely much more pervasive. A subsequent investigation was performed in the heart and cerebellum of 11 DS fetuses during mid-gestation (146). Whilst the experimental design suffered from a mix of genders and a difference in ethnicity between DS individuals (caucasian) and euploid controls (African American), results clearly demonstrated enhanced transcript levels for most Hsa21 genes. This finding highlighted the presence of primary alterations of the foetal DS transcriptome. In addition, the analysis also revealed the presence of 19 non-Hsa21 DEX genes, yet again in support of the VTT theory. An important step in characterising gene-dosage effects of trisomy on Hsa21 transcript levels was made by investigating adult DS-derived lymphoblastoid cells (147). Interestingly, results demonstrated that only 29% of Hsa21 transcripts (22% genes, 7% open reading frames) were actually overexpressed in the trisomic group. The remainder was compensated and present at similar expression levels to euploid controls, with a smaller proportion (15%) displaying high variability amongst individual cases. Perhaps surprisingly, these data imply that dosage imbalance effects only apply to a minority of Hsa21 genes. The authors thus conclude that this minority gene set is more likely to be responsible for the DS phenotype. Additionally, they speculate that the highly variable genes might underpin the phenotypic heterogeneity of DS individuals. These data are in line with previous findings in the Ts65Dn mouse discussed in 4.1.1.2 (138), and expanded on the key principle that the contribution of individual Hsa21 genes to DS is far from homogenous. This notion allows subsequent work, including this thesis, to focus the aim on candidate Hsa21 genes more likely to contribute significantly to DS. In the context of brain development, another study investigated the frontal

cortical transcriptome of DS fetuses at mid-gestation (148). Examining neural progenitor cells, the authors demonstrated an average 1.5-fold transcriptional enhancement of the DSCR (see introduction 1.1.2 for overview). Additionally, they identified a global disturbance in gene expression profiles, with as many as 1902 DEX genes. Ingenuity pathway analysis (IPA - see 4.1.1.4) was then employed to probe the dataset for functional links with cellular mechanisms and signalling pathways. Most notably, they detected associations with the cell cycle, cell death and oxidative stress. The latter process is then linked to overexpression of the Hsa21 gene S100 calcium-binding protein B (*S100B*). These data imply that, in the developing DS brain, neural progenitor cells might sustain enhanced oxidative stress. Perhaps more importantly, however, this study lent support to the notion that Hsa21 trisomy indeed results in pervasive transcriptional alterations.

As introduced, substantial phenotypic heterogeneity is present in DS. It follows that investigation of gene expression patterns underlying such variability is critical to the understanding of this condition. A study of human DS-derived lymphoblastoid and fibroblast cell lines assessed the extent of this variability (149). qPCR was employed to measure the expression of 100 and 106 Hsa21 genes in the two tissue types, respectively. Similarly to Ait Yahya-Graison *et al.* (147), results found only a proportion of Hsa21 genes to be overexpressed in lymphoblastoid (39%) and fibroblast (62%) cell lines. Importantly, the authors compared gene expression variability between DS and euploid samples employing the Kolmogorov-Smirnov test. This is a standard statistical test used to determine whether a probability distribution significantly deviates from a reference distribution. The analysis resulted in three groups of gene expression distributions, ranked based on the degree of overlap with euploid distributions. The authors argue that the gene group with distinct non-overlapping distribution contains genes likely mediating the DS phenotype. By contrast, Hsa21 genes with expression variability comparable to euploid samples are not dosage-sensitive, and thus less involved in DS traits. This study is of fundamental importance. It highlighted that despite trisomy, a considerable proportion of Hsa21 genes displays normal expression variability. This notion is to be taken into consideration when selecting candidate genes for further study. Additional insight into the relative contribution of Hsa21 regions to the DS phenotype comes from the study of partial trisomy cases (150). These are a rarer occurrence, yet allowing for more detailed dissection of DS traits. The authors employed microarray hybridisation to investigate 19 cases of partial trisomy 21. They identified distinct susceptibility regions of trisomy for 25 DS clinical phenotypes mapping to several Hsa21 segments. Whilst these data imply that multiple Hsa21 portions contribute to different aspects of DS, the majority of susceptibility regions mapped to a ~10 Mb portion of the chromosome. This study provided key evidence on the contribution of Hsa21 to the DS phenotype, further highlighting how not all chromosomal regions might be essential for pathology.

Whilst microarray studies have provided key findings elucidating gene expression in DS, they suffer from the limitation of only probing for a small fraction of available RNA. A more recent study employed large-scale RNAseq to probe the transcriptome of DS endothelial progenitor cells (151). This approach foremost demonstrated the complexity of the VTT, providing evidence for intronic transcription and alternative splicing of overexpressed genes. In addition to these key findings, the authors also identified 1787 DEX genes spanning the entire genome. Of these, 956 and 831 were up- and down-regulated, respectively. Interestingly, only 55 of the 132 Hsa21 genes expressed in endothelial progenitors were elevated in DS cells. Thus, large-scale RNAseq provided evidence of previously undescribed genetic mechanisms in DS, whilst also supporting the VTT theory and the heterogeneous contribution of Hsa21 genes. Other studies have profiled gene expression in DS at finer resolution, leading to interesting findings. Sullivan *et al* recently made a key discovery on the immune response in DS (152). Employing large-scale RNAseq, the authors investigated the transcriptome of DS fibroblast and lymphoblastoid cell lines, monocytes and T cells. Functional IPA analysis of DEX genes (see 4.1.1.5) revealed a consistent activation of interferon signalling across all cell types induced by Hsa21 trisomy. Cell-based proliferation assays were then performed to demonstrate reduced cell division following interferon-mediated activation of the kinases JAK1 and TYK2. This effect was rescued via treatment with JAK inhibitors. The authors argue that, in light of four interferon receptors being encoded on Hsa21, the enhanced signalling is likely due to direct gene dosage effects. Thus, the interferon pathway may be established as a therapeutic target in future studies. Additionally, this finding is of particular relevance to this thesis, which investigates Wnt signalling in DS (see 1.2). Significant cross-talk between the two pathways has in fact been previously observed in multiple instances (153, 154).

Contextually to brain development and pathology, RNAseq was recently performed on 11 DS brain regions (155), at time points spanning 14 weeks of gestation to 42 years old. This very extensive study was aimed at investigating spatiotemporal variations in the VTT of the DS brain throughout life. RNA was isolated from multiple regions of the neocortex, hippocampus and cerebellar cortex. Interestingly, while global expression profiles segregated the DS group from controls, age and brain regions were more significant contributors to variability than aneuploidy. This, the authors suggest, implies that the brain transcriptome is extremely variable in spatiotemporal nature. Overall, 1413 DEX genes were identified, spanning the entire genome. Whilst Hsa21 had the highest percentage of DEX genes compared to all other chromosomes, these made up only a fraction (76) of the overall transcriptional dysregulation. Additionally, only about 15-20% (depending on tissue) of Hsa21 genes were DEX. The authors also observed that whilst all Hsa21 DEX genes were upregulated, expression changes for all other DEX genes were roughly divided in half between up and downregulation. This result suggests that gene dosage imbalance in DS induces diverse alterations to the transcriptome, and a high number of genes actually undergoes downregulation. Amongst these, functional analysis of the DEX genes then identified key processes in neuronal development and maintenance as affected. It appears that gene clusters involved in oligodendrocyte maturation and myelination undergo

age-dependent downregulation in DS samples. This finding was then validated in human and Ts65Dn cortical samples via digital droplet PCR and immunoblotting. Results demonstrated significant decreases in myelination markers MAG and MBP. Overall, this comprehensive study provided important knowledge on the human DS VTT and its phenotypic consequences on neuronal function. As with other evidence discussed, yet more support was provided to the notion that Hsa21 genes contribute unequally to the DS phenotype. Additionally, it confirmed that Hsa21 trisomy is sufficient to induce complex transcriptional alterations with spatiotemporal variability throughout the DS brain.

In summary, the studies considered here have provided great improvements in the understanding of the human DS transcriptome. They demonstrated the importance of gene expression variability, the differential contribution of Hsa21 genes to the DS phenotypes, and the pervasiveness of genome-wide effects of aneuploidy.

1.4.1.4 Overall considerations

Before discussing results, a few key conclusions can be drawn from the reviewed literature on gene expression in DS mouse models and humans. First and foremost, it is now clear that the prediction of 1.5-fold overexpression need not apply to all Hsa21 genes. Second, that extensive variability in gene expression dysregulation exists. This implies that the differential contribution of trisomic genes to the DS phenotype is age and tissue-dependent, in addition to also varying amongst individuals. Third, the gene-dosage imbalance of a limited number of genes on Hsa21 triggers genome-wide alterations of extreme complexity, given the variability of results discussed above. Finally, the evidence considered demonstrates that combination of transcriptomics with bioinformatic analysis is a useful approach to investigate the intricate genetic landscape of DS.

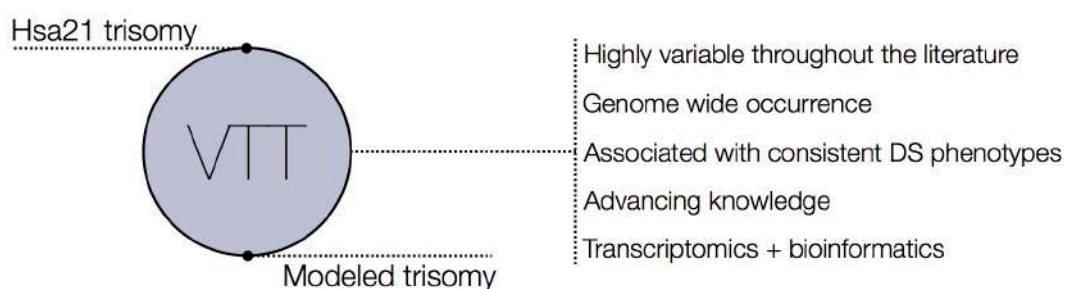


Fig. 1.11 - Features of the variable trisomic transcriptome (VTT).

1.4.2 The DS proteome and biochemical phenotypes

In light of the central dogma of molecular biology, which states that gene expression (ie mRNA) linearly correlates with protein levels, a general prediction follows for DS: given the supernumerary Hsa21, a theoretical 1.5-fold increase in Hsa21-encoded proteins would be expected. However, building on knowledge of the DS transcriptome (1.4.1), this is likely to be the case only for a minority of genes, with associated substantial variation amongst individuals, genders and age. Thus, investigation of protein profiles has been crucial for the understanding of DS, and generally addresses three key necessities. First, determining the extent to which aneuploidy actually affects overall protein levels in a given tissue. This applies both to Hsa21-encoded and secondarily affected proteins, and allows for refined characterisation of the DS phenotype. Second, assessing mechanistic dysfunction of the DS cellular protein machinery, particularly in the context of protein folding, degradation and trafficking. Third, weighing the individual contribution of Hsa21-encoded proteins to DS. This last point is particularly important, given that identification of candidate genes is the fundamental first step in the design of therapeutic strategies in DS. A great deal of research effort has gone into characterising protein profiles in DS models and humans, mostly combining standard quantitative Western blot approaches with large-scale proteomics. The available literature must be taken into consideration, in order to provide a theoretical framework justifying the approach undertaken in results chapter 4.2.

1.4.2.1 Protein profiling in DS mouse models

As for gene expression profiling, the majority of protein studies in DS models have been conducted in segmental trisomy models, particularly the Ts65Dn (see introduction 1.1.5). A great proportion of the available evidence has focused on proteins involved in DS neuropathology, given that intellectual disability and neurodegeneration are the two most prominent features of this condition.

One of the seminal examples of this approach is a 1987 study by Epstein *et al.*, which demonstrated an important principle (156). The authors sought to determine protein-level consequences of superoxide dismutase 1 (*Sod1*) triplication in the brain of *Sod1* transgenic mice. In human DS, SOD1 is an Hsa21-encoded enzyme thought to be important in oxidative stress. In addition to detecting enhanced mouse *Sod1* RNA levels, results in the same study indicated 1.6-6-fold elevations in *Sod1* enzymatic activity, detected via Western blot assessment of subunit composition of this enzyme. Overall, this study demonstrated that genetic triplication of an Hsa21 ortholog does indeed result in comparable alterations of the encoded protein. In the context of neuronal development in DS, a later study combined two-dimensional polyacrylamide gel electrophoresis (2-DE) and mass spectrometry to probe the proteome of mouse embryonic stem cells (ES) containing an additional Hsa21 (157). Two distinct sets of up- and downregulated proteins were identified. This finding suggests that, akin to the variable trisomic transcriptome (4.1.1.1), the DS proteome is also characterised by the presence of bidirectional changes. Several altered proteins were associated with cytoskeletal function, protein degradation and trafficking, mechanisms essential in neuronal homeostasis. Only two out of 225

known Hsa21-encoded proteins were upregulated (SOD1 and CCT8). The authors argue that this result is possibly caused by the limited scope of 2-DE. However, this also suggests that a minority of Hsa21-encoded proteins are more likely to be significantly upregulated in DS, thus contributing more heavily to observed phenotypes. A concomitant study investigated neuropathological protein profiles in the brain of Ts1Cje mice (158). The Ts1Cj3 is a model possessing duplications of Mmu16 regions syntenic to Hsa21, but not including *App* or *Sod1* (see introduction 1.1.5). Whilst A β metabolism was normal, tau phosphorylation was increased at S400, but neurofibrillary tangle (NFT) aggregation was not present. Interestingly, a significant enhancement in levels of active glycogen synthase kinase 3 β (GSK3 β), phosphorylated at Y216, were detected in brain lysates. Given that GSK3 β is the main inhibitor of β -catenin activation, this result is of particular relevance to this thesis, as it suggests potential downstream suppression of Wnt signalling. This study importantly showed that Hsa21 orthologs other than *App* and *Sod1* may also contribute to neuropathological features of DS.

It is worth noting that the Mmu ortholog of the Hsa21 gene *DYRK1A*, one of the later focuses of this thesis (see 4.3.2), is present in the Ts1Cje duplicated region. Several studies have indeed identified DYRK1A as a key contributor to tau pathology in DS models and humans. For example, Liu *et al.* employed the Ts65Dn mouse to demonstrate that *Dyrk1a* duplication produces elevated DYRK1A protein and activity levels in the murine brain (159). Accordingly, the authors also detected enhanced, DYRK1A-dependent tau phosphorylation, and hypothesised that this mechanism may contribute to NFT formation *in vivo*. In the hippocampus of the same model, another study investigated proteins critical for long-term synaptic plasticity (160). A significant decrease in levels of synaptophysin, a protein associated with synaptic density, was observed in the adult Ts65Dn hippocampus. This was accompanied by compensatory elevation of neuronal developmental proteins neurotrophin 3 (NT-3) and Cyclin-dependent kinase 5 (CDK5). Interestingly, CDK5 was previously shown to function antagonistically to DYRK1A in the context of tau phosphorylation (159). This study elucidates another principle of the DS proteome: overexpression of Hsa21 genes results in pathological phenotypes compounded by primary alterations of key proteins as well as secondary, compensatory effects. This implies that complex, multi-layered protein alterations are likely to underpin neuropathological features of DS.

More recent studies investigated the DS proteome in newly-developed models. Wang *et al.* employed isobaric tags for relative and absolute quantification (iTRAQ) to assess protein profiles in transchromosomal mouse ES cells containing a freely-segregating Hsa21 (161). These cells are also used to generate the Tc1 mouse model employed throughout this thesis (49). Interestingly, only three Hsa21-encoded human proteins were detected as elevated in Tc1 ES cells (cystatin B - CTSB, HMGN and CBR1). Overall, 37 proteins were significantly elevated, whilst 15 were decreased. These were mostly associated with cytoskeletal function and A β clearance. The low density lipoprotein-related proteins LRP2 and LRPAP1 were both found to be elevated. These belong to the same family as LRP5/6 co-receptors important in canonical Wnt signalling (62). Consistently, LRP2 is reportedly required for Shh

and Wnt signalling-mediated telencephalic patterning in developing mice (162). This finding implies the possibility of altered Wnt developmental processes in the Tc1 mouse. An interesting correlation with this idea is found in a recent proteomic study of the embryonic Ts1Cje mouse brain (163). The authors demonstrated a protein profile consistent with enhanced cell proliferative processes, also corroborated *in vivo*. This finding suggests that dysregulated cell proliferation might constitute an early event in the DS embryonic brain. Similarly to findings in the Ts1Cje brain (158), protein analysis of the Tc1 mouse brain found increased tau phosphorylation at T212 (52). This residue was hyperphosphorylated in the cerebral cortex and hippocampus of old (20 months) but not young (2 months) Tc1 mice. T212 is a known target of DYRK1A activity (46), and DYRK1A protein levels were elevated across all tissue types and ages. Additionally, GSK3 β was hyperphosphorylated at the inhibitory S9 residue. This site is thought to mediate functional segregation of GSK3 β between AKT- and Wnt signalling-associated pools (164). Whilst no differences were observed in GSK3 β activity (Y216) the S9 enhancement may imply an underlying shift of GSK3 β activity in favour of the Wnt signalling pool. This would result in downregulation of Wnt signalling activity.

Overall, the studies discussed here demonstrate the presence of complex proteomic alteration in the brain of DS mouse models at various developmental stages. This evidence highlights the occurrence of substantial heterogeneity in protein-level effects, which vary mostly according to age. Additionally, it is clear that the contribution of mouse proteins encoded on Hsa21 in humans is limited to a small number of candidates, at least in the brain. These so far include APP, SOD1 and DYRK1A, given their roles in A β deposition, oxidative stress and tau phosphorylation, respectively.

1.4.2.2 Protein profiling in human DS

Indeed, several lines of evidence also suggests substantial alterations in the human DS proteome. Similarly to transcriptomic approaches, human protein studies recapitulate features of DS more faithfully, but are also hindered by increased genetic variability. An early study in the brain of DS individuals presenting AD pathology identified an interesting phenotype (165). The authors showed alterations associated with glial cell proliferation, employing immunohistochemistry. A 30-fold increase in cells positively staining for the astrogliosis markers interleukin-1 (IL-1) and S100 was observed. A significant increase in these proteins was also detected in brain lysates. Over the last two decades, several studies have investigated the proteome of fetal DS brains. The first comprehensive proteomic profile in this context was produced in 2000 by Opperman *et al.* employing 2-DE (166). Results showed that the vast majority of protein levels were similar to control samples, but alterations were detected in key cytoskeletal components, including actin and tubulin. Following, a series of five consecutive studies by the Lubec research group provided key findings. Proteomic analysis of fetal DS brains first demonstrated abnormalities in multiple components of intermediate metabolism (e.g. pyruvate kinase) (167). The group later identified eight Hsa21-encoded proteins as significantly elevated, most importantly SOD1, CSTB and CBR1, which were also altered in DS mouse models (168). Interestingly, SOD1 has

been shown to antagonise canonical Wnt signalling activation induced by reactive oxygen species in human cells (169). In a further study (170), DS fetal brains also displayed decreased levels of α -tubulin and α -interneixin, proteins associated with the neuronal cytoskeleton. Tropomodulin 1 (TMOD1) and fatty acid binding protein (FABP) were on the other hand found to be elevated. This finding is particularly relevant to this thesis, in that evidence exists linking both *TMOD1* and *FABP* to Wnt signalling. TMOD1 is an actin-capping protein, and has been identified as a non-canonical Wnt target gene, being upregulated by Wnt5a (171). The activation of this pathway is known to antagonise and suppress canonical Wnt signalling activation (62). FABPs are considered markers of adipogenesis, and *FABP4* expression has been shown to be reduced by epigallocatechin gallate (EGCG) treatment via enhanced canonical Wnt signalling (172). Considering these links, increased levels of TMOD1 and FABP in the DS fetal brain identified by Lubec *et al.* could possibly reflect suppressed canonical Wnt signalling. Another recent proteomic study focused on oxidative stress pathways in the DS brain (173), identifying abnormal carbonylation of proteins associated with the intracellular quality control/autophagy system, such as cathepsin D. The authors further characterised this phenotype functionally, observing decreased activity of the proteasome and autophagosome. This led to the hypothesis that dysfunctional protein degradation in DS may contribute to abnormal A β deposition in later life. The same authors also conducted a thorough review of proteomic evidence in the DS brain (174), arguing that abnormal oxidative stress is likely to contribute to neurodegeneration in this syndrome.

In 2004, a protein study in post-mortem human DS and AD brains identified significantly elevated tau phosphorylation, at residues targeted by microtubule associated protein kinase (MAPK) (175). Accordingly, MAPK activity was also found to be elevated. By contrast, GSK3 β activity was reduced. The discussed Liu *et al.* study (4.2.1) also employed a cohort of human DS adults (159). Significantly elevated DYRK1A levels were observed, in association with hyperphosphorylated tau at DYRK1A-targeted residues. *In vitro* assays also showed that such phosphorylation could induce tau aggregation. It is worth noting that DYRK1A protein levels are ubiquitously elevated in virtually all DS brain structures, spanning infancy to adulthood, and across gender and ethnicity (176). This finding places DYRK1A in a key position with respect to brain pathology in DS. DYRK1A function in euploidy and DS is further discussed in chapter 4.3.1. The Sullivan *et al.* study (152) demonstrated interferon (IFN) pathway dysregulation in the transcriptome of DS-derived cell lines. The authors also employed immunoblotting to probe for protein level evidence of IFN dysregulation in the same cell models, particularly looking at components and targets of the pathway. The analysis, conducted in DS fibroblasts, demonstrated significant elevation of multiple IFN receptors, and enhanced phosphorylation of the cascade component STAT1. Moreover, the elevated IFN response was functionally assessed, suggesting that DS cells respond more pronouncedly to 24-hour IFN- α treatment. Overall, this study presented consistent genetic and biochemical data in support of altered IFN function in DS. A similar approach has been the broadly overarching theme of the work presented here.

1.4.2.3 Overall considerations

In summary, protein investigations in DS models and humans suggest widespread imbalances in protein homeostasis. Some of the more prominently affected processes include oxidative stress, cell proliferation, proteostasis, neuronal cytoskeletal components and proteins involved in tau metabolism. In both DS mice and humans, several Hsa21-encoded proteins are altered, most importantly DYRK1A and APP, given their roles in neurodegeneration (see 4.3.1 for more info on DYRK1A). However, substantial variability and age dependence exist, arguably to a greater extent than for transcriptomic data. Even in the case of consecutive investigations in humans, performed by the Lubec group (167, 168, 170, 177) and based on similar groups, results differed widely between studies. This variability applies to both Hsa21-encoded and secondarily affected proteins. One of the more reliably altered proteins is indeed DYRK1A, found to be affected in the vast majority of DS cases, and, in the context of the DS brain, consistently driving altered tau phosphorylation. Based upon literature evidence, DYRK1A levels were therefore selected as a reference marker to further confirm the aneuploid status of murine and human samples analysed in 4.2.

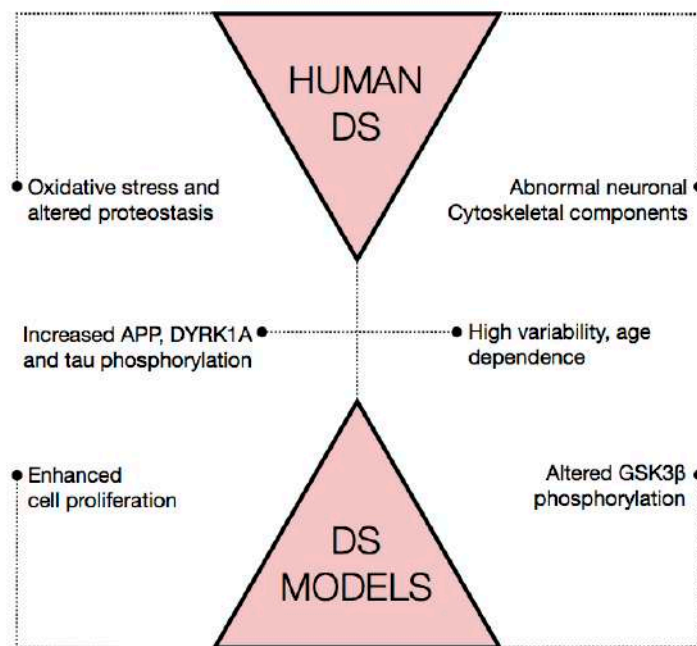


Figure I.12 - Proteomic changes in DS are highly variable between mouse models and humans, and span several biological processes.

Chapter 2 - Aims and Objectives

Despite the likelihood of Wnt signalling involvement in DS neuropathology, no evidence directly linking these two phenomena exists. Thus, the studies presented here sought to clarify and characterise this potential relationship, combining data from DS mouse models, human brain tissue and cell lines.

The primary hypothesis of this thesis was addressed in three logical phases, through a variety of experimental techniques:

- I. Investigation of transcriptional alterations in DS: Chapter 4.1 - Analysis of the DS transcriptome:**
 - A. RNA sequencing of the Tc1 and Dp1Tyb mouse hippocampus and DS fibroblasts.
 - B. Functional pathway analysis of RNA sequencing data via Qiagen IPA®.

- II. Investigation of protein-level Wnt signalling alterations in DS: Chapter 4.2 - Wnt signalling proteins in DS mouse models and humans:**
 - A. Assessment of Wnt signalling activity and components in Tc1 and Dp1Tyb mouse hippocampus and cerebral cortex.
 - B. Assessment of Wnt signalling activity and components in the human DS hippocampus.

- III. Characterisation of a candidate Hsa21 gene for Wnt-DS phenotypes: Chapter 4.3 - DYRK1A-mediated Wnt signalling modulation:**
 - A. Investigation of DYRK1A-Wnt protein interaction networks.
 - B. Investigation of DYRK1A-mediated modulation of Wnt signalling activity in human cells.
 - C. Investigation of DYRK1A subcellular localisation under differential Wnt activation states.

Each experimental phase is discussed in its relative results chapter (4.1-3), whilst the overall implications and future aims are integrated and considered in the general discussion section (5.1-2).

Materials &
METHODS
3

Chapter 3 - Materials and Methods

In this section, all techniques and tissues employed to generate experimental data for this thesis are outlined. In order to ease accessibility of this thesis to future readers from a wide variety of backgrounds, methods are briefly introduced conceptually before describing their application for experimental purposes. Therefore, in contrast to the manner in which methods are published in research articles, this section assumes no prior knowledge of the techniques on the reader's part. A generic cell biology, biochemistry and genetics background is however presumed.

3.1 RNA sequencing

Massively parallel complementary DNA (cDNA) sequencing, or RNA sequencing (RNAseq), is a well-established technique which exploits the fundamental principle that the amount of transcript mRNA directly correlates with gene expression levels. Thus, RNAseq is employed to quantify genome-wide expression signatures with high reliability (see, 4.1.1, for a literature overview of the technique). In this thesis, RNA sequencing was performed on hippocampal RNA derived from Tc1 and Dp1Tyb mice (see 3.3 and 4.1.1 for further info on mice), in order to probe for transcriptional profiles associated with Wnt signalling dysregulation (4.1.2). RNA sequencing and primary data analysis were conducted by the Elizabeth Fisher laboratory at the UCL Institute of Neurology, as detailed in the statement of contributions made at the beginning of the thesis.

3.1.1 RNA extraction and sequencing

Total hippocampal RNA from Tc1 ($n=3$, 3 months old) and Dp1Tyb ($n=3$, 5 months old) mice was extracted using the miRNeasy mini kit (Qiagen). Tissue was disrupted mechanically using a Tissue-Rupter, as per manufacturer's instructions and resuspended in DNase- and RNase-free water. Total hippocampal RNA sample quality was confirmed by Bioanalyzer (Agilent) and libraries were prepared with the TruSeq RNA v2 LS Kit (Illumina). RNAseq was then performed employing the HiSeq system (Illumina).

3.1.2 Sequencing data analysis

Due to the presence of human genes in the Tc1 mouse, a custom reference genome was assembled in order to assess expression levels of Hsa21 genes. A standard mouse genome (NCBI build 37.2) was combined with the Hsa21 sequence (NCBI build 37.2). The RNAseq data was then aligned to this custom genome employing Bowtie (v2.1.0) as part of the Tophat pipeline. Overall count data were then generated, employing the dexseq_count.py script, before combining counts for Hsa21 genes and mouse orthologs. The resulting data, also including non-Hsa21 genes, was then analysed by De-seq to generate adjusted P values.

3.2 Cloning

In this thesis, cloning was employed to generate DYRK1A expression constructs. The cloned sequences, or inserts, were directly amplified from genomic complementary DNA (cDNA), or sub-cloned from a previous construct. The process of cloning entails a variety of standard molecular biology techniques which are described in 3.2.1-10.

3.2.1 Polymerase chain reaction and DNA primer design

The polymerase chain reaction (PCR) involves the use of thermal cycling and a recombinant DNA polymerase to exponentially amplify a DNA sequence of interest. PCR represents the initial stage of the cloning process, generating the insert to be cloned into a specific plasmid vector. For this thesis, human brain cDNA (Clontech) was employed as a template for amplification of DYRK1A, human isoform 1 (NCBI reference sequence NM_001396.3).

Primer design - To ensure specificity of a PCR product, the sequence of interest must be primed for DNA polymerase binding via the action of specifically designed complementary oligonucleotides, termed primers. Primers are designed in pairs, forward and reverse, signalling polymerase binding at the 5' and 3' ends of the template, respectively. In the context of cloning, primers are designed to also introduce specific oligonucleotide sequences compatible with the cut sites of restriction endonucleases employed at later stages (see 3.2.3-4). All primers were designed with a standard word processor (Apple Pages) and the NCBI reference sequence for DYRK1A human isoform 1. The oligonucleotides were synthesised by Eurofins. Upon delivery, each primer was solubilised in ddH₂O to a stock concentration of 100 μM and stored at -20°C according to manufacturer instructions. The following table details primer sequence and cut sites introduced.

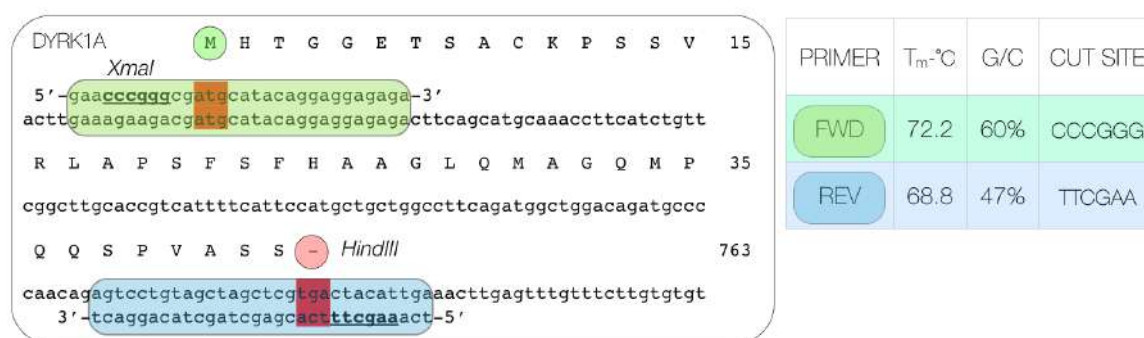


Fig. M.1 - Overview of representative primer design for DYRK1A cloning.

PCR - For PCR usage, each primer was further diluted to a working concentration of 10 μ M. As well as primers and template, a standard PCR reaction also requires a heat-resistant DNA polymerase, deoxynucleotide triphosphates (dNTPs) for template replication and a suitable buffer solution. All these were provided pre-mixed in the AccuPrime™ Pfx SuperMix (22 U/ml Thermococcus species KOD thermostable, anti-KOD antibodies, 66 mM Tris-SO₄ (pH 8.4), 30.8 mM (NH₄)₂SO₄, 11 mM KCl, 1.1 mM MgSO₄, 330 μ M dNTPs, AccuPrime™ proteins, stabilisers - Life Technologies). All reactions were performed employing a Veriti 96-well thermal cycler (Applied Biosystems) with specifically programmed cycles. The table below details the steps and components of each standard 25 μ l reaction. Following PCR, all products were subsequently analysed via agarose gel electrophoresis.

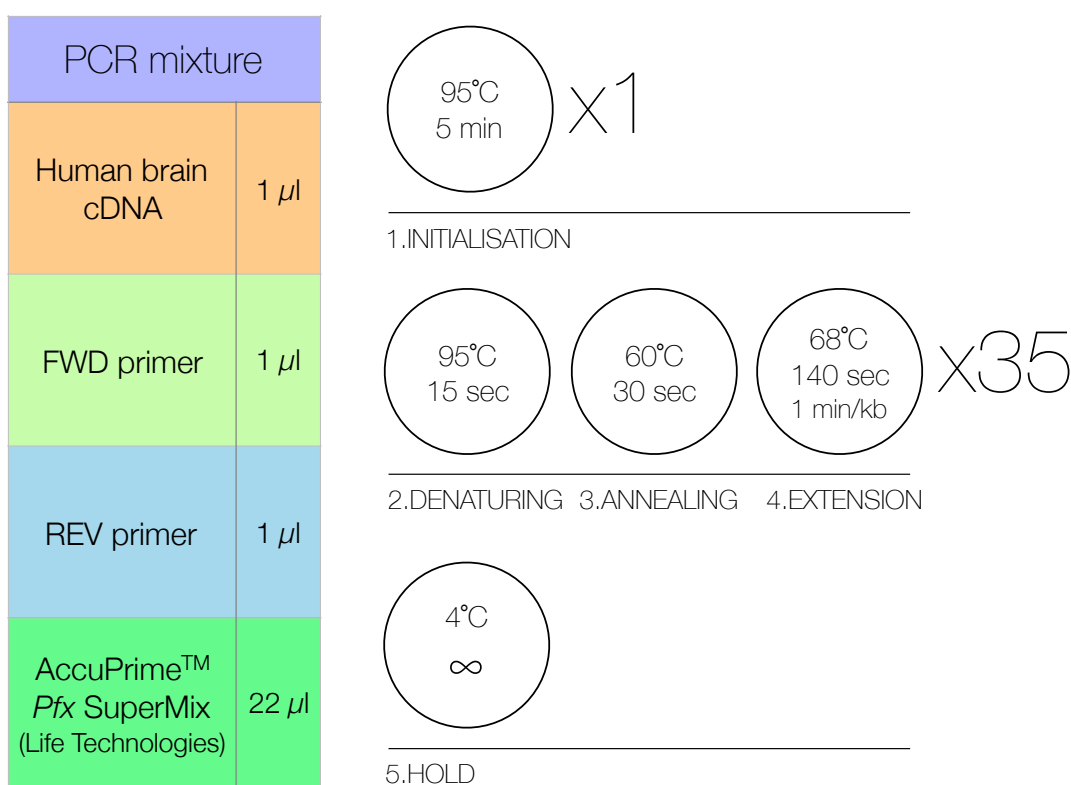


Fig. M.2 - Overview of a standard PCR protocol

3.2.2 Agarose gel electrophoresis and extraction

Electrophoresis - For a standard 10-lane, 1% DNA gel, 500mg of UltraPure™ Agarose (Life Technologies) were added to 50 ml of Tris-acetate EDTA (TAE) buffer (40mM Tris-base, 20mM acetic acid, 1mM EDTA at pH 8.0). Reagents were mixed thoroughly in a glass flask and subsequently heated in a microwave oven for 30 sec. The flask was then briefly allowed to cool under running tap water. The heating-cooling cycle was repeated 2-3 times, as required, until complete agarose dissolution. Thereafter, 5 μ l of SYBR® Safe DNA gel stain (Life Technologies) were added to the agarose solution to allow for DNA visualisation. The solution was then poured in a casting tray and a sample comb was inserted to generate 10 sample loading

lanes. After pouring, the gel was allowed to set for 30 min at room temperature. Once solidified, the gel was placed in a TAE-containing electrophoresis chamber connected to a Power Pac generator (Biorad). Prior to sample loading, 5 μ l of sample loading buffer were added to 25 μ l of each PCR product solution. Each gel lane was subsequently loaded with 30 μ l of buffered DNA sample. Additionally, two lanes were each loaded with 12 μ l of marker solution containing 10 μ l of 1Kb+ DNA ladder (NEB) and 2 μ l of sample loading buffer to ensure correct estimation of DNA size. Once loaded, the gel was ran for 30 min at a constant voltage of 100V and imaged under blue light employing a Safe Imager™ Transilluminator (Syngene). In positive results, DYRK1A DNA was observed as a single band migrating to ~2.3kb. Examples are shown below:



Fig. M.3 - Representative DNA agarose gel results, demonstrating DYRK1A migrating to 1.5 kb.

Gel extraction (QIAGEN protocol) - All extractions were performed employing the QIAquick® Gel Extraction Kit, which supplies all the required reagents. Bands corresponding to ~2.3 kb, the size of human DYRK1A isoform 1, were excised from the agarose gel using a clean surgical scalpel while being illuminated on a standalone blue light Safe Imager™ (Life Technologies). The excised gel slice was then weighted in a 1.5 ml microcentrifuge tube, and 3 volumes (100 mg~100 μ l) of Buffer QG (5.5 M guanidine thiocyanate, 20 mM Tris HCl pH 6.6) were added to the tube. The mixture was subsequently incubated at 50°C in a Eppendorf ThermoMixer® F1.5 for up to 10 minutes, as required, until complete dissolution of the gel slice. Thereafter, 1 gel volume of isopropanol was added. After brief vortexing on a Rotamixer (Hati) the solution was transferred to an 800 μ l QIAquick® spin column inserted into a provided 2 ml collection tube and centrifuged for 1 min at 14,680 rpm on a 5424 Tabletop Microcentrifuge (Eppendorf - "tabletop microcentrifuge"). The flow-through was consequently discarded, and 500 μ l of Buffer QG were added to the QIAquick® spin column. A further centrifugation-discarding cycle was performed. Thereafter, 750 μ l of Buffer PE (10 mM Tris-HCl pH 7.5, 80% Ethanol) were added to wash the column. Following centrifugation and discarding, the column was placed in a fresh 1.5 ml microcentrifuge tube. To elute DNA out of the QIAquick® spin column, 20 μ l of Buffer EB (10 mM Tris HCl, ph 8.5) were added to the centre of the column, which was allowed to stand for 1 min and then centrifuged for a further 1 min. The flow-through collected in the 1.5 ml microcentrifuge tube now contained the purified DNA sequence of interest.

3.2.3 Restriction digest and phenol-chloroform isoamyl (PCI) extraction

Restriction digest - For the PCR-amplified DYRK1A DNA, restriction sites for digestion by XbaI (cut sequence) and HindIII (cut sequence) were introduced by specifically designed oligonucleotide primers at the PCR stage (see 3.2.1). In commercially available plasmid vectors, several restriction sites are engineered into a “multiple cloning site” for immediate digestion. To ensure the correct introduction of compatible ends for ligation, both the DNA fragment and the vector backbone were digested with the same restriction enzymes. The restriction digest was performed on both the PCR-amplified DYRK1A DNA for ligation into the pRK5-FLAG vector (Addgene) and on a ready-made pCMV5-HA-DYRK1A construct (Addgene) for sub-cloning into the pEGFP-C1 vector. All enzymes and buffers were supplied by New England Biolabs. The tables below detail the components of each standard 20 μ l reaction. Each was incubated at 37°C in a Eppendorf ThermoMixer® F1.5 for 1 hr.

PCR-amplified DYRK1A		pRK5-FLAG (1 μ g/ μ l)		pCMV5-HA-DYRK1A (0.75 μ g/ μ l)		pEGFP-C1 (1 μ g/ μ l)	
DNA	15 μ l	DNA	1.5 μ l	DNA	2 μ l	DNA	1.5 μ l
<i>HindIII</i>	0.5 μ l	<i>HindIII</i>	0.5 μ l	<i>Sall</i>	0.5 μ l	<i>Sall</i>	0.5 μ l
<i>XbaI</i>	0.5 μ l	<i>XbaI</i>	0.5 μ l	H ₂ O	15.5 μ l	H ₂ O	16 μ l
H ₂ O	2 μ l	H ₂ O	15.5 μ l	Buffer 3.1	2 μ l	Buffer 3.1	2 μ l
Buffer Cut-Smart™	2 μ l	Buffer Cut-Smart™	2 μ l				

Fig. M.4 - Restriction digest reactions employed.

PCI extraction -. 80 μ l of distilled H₂O was added to Each 20 μ l reaction mixture. Thereafter, 100 μ l of phenol-chloroform isoamyl (PCI) were added to each reaction in a fume hood. All samples were subsequently centrifuged for 10 min at 14,680 rpm in a tabletop microcentrifuge. During centrifugation, a solution containing 10 μ l of 3M sodium acetate (C₂H₃NaO₂ - pH 5.2), 250 μ l of 96% (v/v) ethanol and 1 μ l of glycogen was prepared for each sample in clean 1.5 ml microcentrifuge tubes. Thereafter, the aqueous phase was removed from each centrifuged sample and added to the above mentioned sodium acetate/ethanol/ glycogen solution. Each reaction was subsequently incubated in dry ice for up to 10 min, as required, until complete solidification. Once frozen, each sample was centrifuged for 15 min at 14,680 rpm in a tabletop microcentrifuge. Following centrifugation, the sodium acetate/ethanol solution was carefully removed from each reaction, leaving only the DNA-containing glycogen pellet. Each tube was then left open for 10 min to allow for evaporation of any residual sodium acetate/ethanol. Once dried, each DNA pellet was re-suspended in Buffer EB. To account for the much higher DNA concentration of plasmid vectors, inserts were resuspended in 10 μ l EB, while vectors were resuspended in 50 μ l EB.

3.2.4 DNA ligation

Once purified, the digested inserts and plasmid vectors were ligated through their compatible ends to generate a desired construct. In this thesis, T4 DNA ligase (New England Biolabs® - NEB) was employed for all constructs. Each ligation reaction was incubated overnight at 4°C in ligation buffer (NEB). The table below details the components of each 10 µl standard reaction:

Ligation mixture	
Insert - DYRK1A	7 µl
Vector - pRK5-FLAG or pEGFP-C1	1 µl
Ligation Buffer	1 µl
T4 DNA ligase	1 µl

Fig. M.5 - Ligation reaction mix.

3.2.5 *E. coli* transformation and culture

All constructs were inserted into competent bacterial cells (*E. coli*) in order to achieve exponential replication. This step is essential to the efficient preparation of working stocks for later experimental use. Transformations were carried out for pRK5-FLAG-DYRK1A, pCMV5-HA-DYRK1A (at a prior stage following supply of the plasmid) and pEGFP-C1-DYRK1A. For this technique, a Bunsen burner flame was employed throughout to maintain a sterile environment around the bacterial cells and reagents. The microcentrifuge tubes containing the ligation reaction were maintained at ~4°C on ice while competent *E. coli* cells (stored at -80°C in solution - company) were being thawed on ice. Once defrosted, 100 µl of *E. coli* cells were added to the 10 µl ligation reaction in the same microcentrifuge tube. The solution was then incubated on ice for 10 min. Thereafter, the *E. coli* cells were subjected to a 45 sec heat-shock at 42°C in a JB Aqua 2s water bath (Grant) in order to temporarily permeabilise cell walls/plasma membranes, and allow uptake of the DNA construct. Following the heat-shock, the cells were incubated on ice for 2 min to recover, after which 250 µl of lysogeny broth (LB - Sigma Aldrich) were added to provide a growth medium. The *E. coli*/LB solution was then incubated at 37°C for 1 hr while being mixed at 1,500 rpm in an Eppendorf Thermo-Mixer® F1.5. During the incubation, bacteriological agar plates were warmed to 37°C. After 1 hr, the *E. coli*/LB solution was transferred and spread onto the plates. The agar had been previously enriched with antibiotic for positive selection. For pRK5-FLAG-/pCMV5-HA-DYRK1A, ampicillin was employed, while kanamycin was used for DYRK1A-pEGFP-C1. All plates were incubated at 37°C overnight. The following day, bacterial colonies could be observed growing on the agar surface. 5 colonies from each plate were gently removed from the agar plates with a 10 µl pipette tip. Each tip was ejected directly into a 15 ml centrifuge tube containing 10 ml of LB solution enriched with either kanamycin or ampicillin, depending on the construct, at a concentration of 1:1000. Each colony in solution was then allowed to further grow overnight at 37°C whilst being shaken.

3.2.6 Mini-preparation of plasmid constructs (QIAGEN protocol)

In order to confirm successful cloning, all DNA constructs amplified in bacterial cultures were extracted and purified on a small scale (mini-prep) prior to final preparation. This was achieved employing the QIAprep® Spin Miniprep Kit (QIAGEN), which supplies all required reagents. To pellet the bacterial cells, 1 ml of each overnight culture was transferred to a clean 1.5 ml tube and centrifuged for 3 min at 14,680 rpm in a tabletop microcentrifuge. The supernatant LB solution was then removed, the pellets were resuspended in 250 µl of Buffer P1 (50 mM Tris-HCl, 10 mM EDTA, 100 µg/ml RNaseA, pH 8.0), and 250 µl of Buffer P2 (200 mM NaOH, 1% SDS) were subsequently added to trigger a cell lysis reaction. The solutions were mixed thoroughly by inverting each tube 6 times. Thereafter, 350 µl of Buffer N3 (4.2 M Gu-HCl, 0.9 M potassium acetate, pH 4.8) were added to neutralise the lysis reaction and facilitate DNA binding to the spin columns at subsequent stages. Each tube was then centrifuged for 10 min at 14,680 rpm in a tabletop microcentrifuge to pellet the cell debris and large proteins released by the lysis reaction. Following, the supernatant was collected and transferred to a QIAprep® spin column inserted into a provided 2ml collection tube. Each column was then centrifuged for 1 min at 14,680 rpm to bind DNA to its membrane. The flow-through was discarded and the columns were washed with 750 µl Buffer PE, which was then removed by centrifuging each column twice for 1 min at 14,680 rpm. Thereafter, the columns were placed in clean 1.5 ml microcentrifuge tubes to collect the prepared DNA constructs, and 50 µl of Buffer EB were added to the membrane to elute DNA. After allowing elution for 1 min, each column was centrifuged for 1 min at 14,680 rpm.

3.2.7 Diagnostic digest

The DNA constructs prepared were then tested to ensure the presence of desired inserts. To this end, all constructs were digested as in 3.2.3. Only 5 µl of DNA preparation were added to the 20 µl reaction mixture, however, to account for higher concentration relative to a gel-purified PCR product. The digest products were subsequently analysed by agarose gel electrophoresis (See 3.2.2). In successfully ligated constructs, both the plasmid vector and insert were observed upon gel imaging, as two distinct bands of desired size. The figure below depicts representative examples.

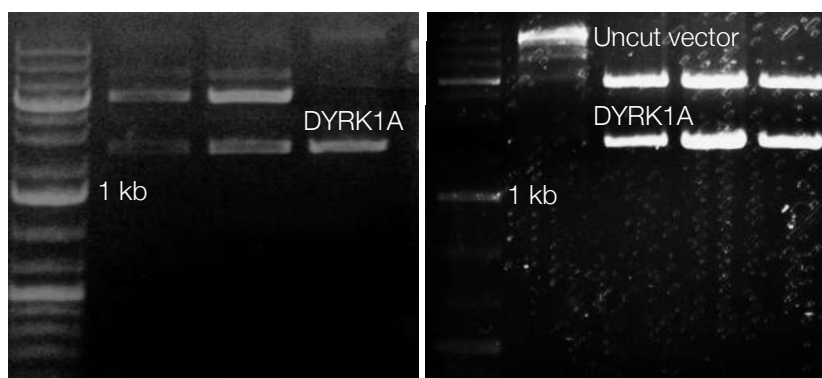


Fig. M.6 - Representative diagnostic digest results, demonstrating presence of vector and insert.

3.2.8 Quantification of DNA concentration

Prior to DNA sequencing, the concentration of each construct was measured employing a NanoDrop 2000 Spectrophotometer (Thermo Scientific), which determines micro-volume DNA concentration as a function of the sample's spectral absorbance. The NanoDrop's sample pedestal was first cleaned and subsequently initialised by measuring 1 µl of distilled H₂O. The instrument was then blanked with 1 µl of Buffer EB (used to elute DNA in 3.2.6) to exclude any interference from this buffer in the final measurements. Thereafter, 1 µl of each DNA preparation was added to the sample pedestal to determine concentration. Each measurement was repeated 3 times to account for instrument error. This technique was also performed on the final, large-scale DNA preparations (see 3.1.10) to determine the final stock concentration of each construct (see 3.5.4 for all concentrations).

3.2.9 DNA sequencing

All constructs employed in this thesis were validated via DNA sequencing. An external service was employed, namely the Dna Sequencing & Services™, University of Dundee, Dundee, Scotland. DNA sequencing was performed on both small and large scale (3.2.10) preparations of each construct, in order to ensure consistency. For each construct Each sequencing result was analysed in comparison to the DYRK1A reference sequence for human isoform 1 (NM_001396.3) employing the NCBI Basic Local Alignment Search Tool (BLAST) and the Sequencher software suite (Gene Codes). Vector maps were also consulted to ascertain the insert was in frame with the tag of interest (FLAG, EGFP, HA). All constructs and sequencing primers required were sent in solution according to the guidelines provided by the service, or otherwise selected from a list of primers in-house. (see <http://www.dnaseq.co.uk> for further details). The table below details each construct analysed, its sequencing primers and the results:

CONSTRUCT	FWD PRIMER	REV PRIMER	RESULT
pRK5-FLAG-DYRK1A	5'-acacatacgatntag-gtgacac-3'	5'-ggacaaaccacaac-tagaatgc-3'	Frameshift mutation at G340 (single nucleotide deletion)
pCMV5-HA-DYRK1A	Service's CMV Fwd	Service's CMV Rev	Correct insert supplied
pEGFPC1-DYRK1A	Service's pEGFPC1 Fwd	Service's pEGFPC1 Rev	Sub-cloning successful

Fig. M.7 - Sequencing primers employed.

3.2.10 Maxi-preparation of plasmid constructs (QIAGEN protocol)

All DNA constructs were then prepared on a large scale (maxi-prep) employing a HiSpeed® Plasmid Maxi Kit (QIAGEN), so as to achieve concentrations required for experimental use (See 3.5.4). To allow further exponential replication of the DNA constructs, 200 µl of each bacterial culture (see 3.2.5) were allowed to grow overnight in a 150 ml LB solution enriched with the antibiotic to which each construct displays resistance. Each sterilised flask was incubated overnight at 37°C whilst shaking. On the following day, all the 150 ml of overnight culture from each flask were aliquoted to 50 ml tubes and pelleted by centrifugation at top speed (14,000 rpm) and 4°C in an 5810 R centrifuge (Eppendorf - from here on samples will be referred to as “centrifuged” unless otherwise specified). The supernatant LB was then discarded and each pellet was sequentially resuspended in 10 ml Buffer P1. Following, 10 ml of Buffer P2 were added to each solution to start a lysis reaction, which was incubated at room temperature for 5 min then neutralised by addition 10 ml of Buffer P3 (3.0 M potassium acetate pH 5.5). The 30 ml lysate solution was then transferred to a QIAfilter Cartridge (essentially a large filtered syringe) and incubated for 10 min at room temperature. Thereafter, the lysate was filtered into and slowly through a HiSpeed Tip, a DNA sieve previously primed with buffer QBT (750 mM NaCl, 50 mM MOPS pH 7.0, 15% isopropanol, 0.15% triton X-100). Following the initial filtering, 60 ml of wash buffer QC (1.0M NaCl, 50 mM MOPS pH 7.0, 15% isopropanol) were allowed to slowly filter through the HiSpeed Tip from the attached QIAfilter Cartridge. 15 ml of Buffer QF (1.25M NaCl, 50 mM Tris-HCl pH 8.5, 15% isopropanol) were then filtered through to elute the DNA.

The eluate was collected in a 50 ml tube and 10.5 ml of isopropanol were added to precipitate DNA. The eluate/isopropanol mix was transferred to a 30 ml syringe attached to a QIAprecipitator module, an additional sieve for final collection of the purified DNA construct. The solution was first filtered through the QIAprecipitator and the flow-through was discarded. The module was then washed twice with 2 ml of 70% ethanol and subsequently dried by forcing air through the syringe twice more. To elute DNA, 1.5 ml of Buffer TE (Tris-EDTA) were added, filtered through the QIAprecipitator and collected in a 1.5 ml microcentrifuge tube. This step was repeated twice more with the same eluate to enhance the final concentration. Following the final preparation, each construct was sequenced for additional confirmation and thereby employed for experimental use.

3.2.11 Summary of expression constructs employed

pCMV5-HA-DYRK1A and pCS2-DKK3-FLAG were obtained from MRC PPU Reagents, while pCDNA3.1-FLAG-β-catenin was a gift from Eric Fearon (Addgene plasmid #16828). pRK5-FLAG-DVL1 was generated in-house as described previously (1), and pEGFP-DYRK1A was cloned as outlined above. These constructs were employed in luciferase assays, co-IPs and immunocytochemistry (see following sections). M50 Super 8X TOPflash and M51 Super 8X FOPflash were gifts from Randall Moon (Addgene plasmids #12456 and #12457) (2). pTK-Renilla (Renilla) was purchased from Promega. The latter three constructs were employed in luciferase assays to quantify Wnt signalling activity (see 3.5.5).

3.3 DS mouse models

This section describes maintenance of Tc1, Dp1Tyb, and Dp1(10-17)Yey mice, as well surgical dissection procedures employed to isolate target cerebral regions. These cohorts were employed for biochemical assessment of Wnt signalling and are distinct from those utilised for RNAseq and qPCR (see 3.1/4). Genetic material from the latter two was generated independently by the UCL Institute of Neurology.

3.3.1 Animal husbandry and general information

Tc(Hsa21)1TybEmcf (Tc1), Dp(16Lipi-Zbtb21)1TybEmcf (Dp1Tyb), Dp(17Abcg1-Rrp1b)1Yey (Dp(17)1Yey), and Dp(10Prmt2-Pdxk)1Yey (Dp(10)1Yey), mice (3-5) were bred at the Francis Crick Institute in specific pathogen free conditions, in a controlled environment and in accordance with the MRC Responsibility in the Use of Animals for Medical Research (1993) guidelines. Tc1 mice were maintained by crossing to (C57BL/6J x 129S8)F1 mice; all other strains were maintained by crossing with C57BL/6J mice. All animals were euthanised by cervical dislocation in accordance with the Animals (Scientific Procedures) Act 1986 and European Directive 2010/63/EU. Brains were collected from 160 ± 28 days old male Tc1 mice and 131 ± 7 days old male Dp1Tyb/Dp(17)1Yey/Dp(10)1Yey mice. The tables below detail the Tc1 and Dp1Tyb mice used to generate the experimental groups investigated in this thesis:

Tc1 MOUSE						
NAME	DOB	COLLECTED ON	SAMPLE AGE (d)	COHORT	EXPERIMENTAL BATCH	GENOTYPE - Hsa21
EF6/92.4f	03/09/13	21/03/14	199	1	A	+/-
EF6/91.3	05/09/13	20/03/14	196			+/-
EF6/91.3	05/09/13	20/03/14	196			-/-
EF6/91.3	05/09/13	20/03/14	196			-/-
EF6/91.8e	20/11/13	15/04/14	146	2		+/-
EF6/91.9f	24/11/13	14/04/14	141			+/-
EF6/91.8c	20/11/13	15/04/14	146			-/-
EF6/91.8d	20/11/13	15/04/14	146			-/-
EF6/89.6	22/09/13	20/03/14	179	3	B	+/-
EF6/96.1g	17/11/13	11/04/14	145			+/-
EF6/89.6	22/09/13	20/03/14	179			-/-
EF6/96.1f	17/11/13	11/04/14	145			-/-
EF6/96.1k	17/11/13	14/04/14	148	4		+/-
EF6/97.1d	17/11/13	22/03/14	125			+/-
EF6/96.1j	17/11/13	14/04/14	148			-/-
EF6/97.1c	17/11/13	22/03/14	125			-/-

Fig. M.8 - Overview of Tc1 mice employed for biochemical Wnt signalling study in this thesis.

Dp1Tyb MOUSE							
NAME	DOB	COLLECTED ON	SAMPLE AGE (d)	COHORT	EXPERIMENTAL BATCH	GENOTYPE	
TS1TYB/15.7b	11/01/14	04/06/2014	144	1	A	WT	
TS1TYB/15.7c	11/01/14	04/06/2014	144			WT	
TS1TYB/15.7d	11/01/14	04/06/2014	144			Ts1Tyb	
TS1TYB/18.3a	26/01/14	04/06/2014	129	2		Ts1Tyb	
TS1TYB/18.3b	26/01/14	04/06/2014	129			Ts1Tyb	
TS1TYB/18.3c	26/01/14	04/06/2014	129			WT	
TS1TYB/18.3d	26/01/14	04/06/2014	129			WT	
TS1TYB/18.3e	26/01/14	04/06/2014	129			WT	
TS1TYB/15.8d	01/02/14	04/06/2014	123	3		Ts1Tyb	
TS1TYB/15.8e	01/02/14	04/06/2014	123			WT	
TS1TYB/15.8f	01/02/14	04/06/2014	123			Ts1Tyb	
TS1TYB/33.2e	05/05/15	21/09/2015	139	4		B	Ts1Tyb
TS1TYB/33.2f	05/05/15	21/09/2015	139				Ts1Tyb
TS1TYB/35.1b	05/05/15	21/09/2015	139				WT
TS1TYB/31.3d	12/05/15	21/09/2015	132	5			WT
TS1TYB/31.3e	12/05/15	21/09/2015	132		WT		
TS1TYB/31.3f	12/05/15	21/09/2015	132		WT		
TS1TYB/31.3g	12/05/15	21/09/2015	132		Ts1Tyb		
TS1TYB/31.3h	12/05/15	21/09/2015	132		Ts1Tyb		
TS1TYB/32.3h	21/05/15	21/09/2015	123	6	Ts1Tyb		
TS1TYB/32.3i	21/05/15	21/09/2015	123		WT		

Fig. M.9 - Overview of Dp1Tyb mice employed for biochemical Wnt signalling study in this thesis.

3.3.2 Cortical and hippocampal dissection

All mouse brains were dissected in a safe cabinet with laminar air flow in the Wakefield Street Biological Services Unit, UCL ION, London. Full-body protective equipment was worn throughout, and all tools were thoroughly cleaned with 70% ethanol between each dissection. The technique was carried out with standard surgical tools and naked eye (see figure below). All mice were euthanised by neck dislocation, in accordance with Home Office regulations and The Humane Killing of Animals under Schedule 1 to the Animals (Scientific Procedures) Act 1986. To minimise stress, each mouse was culled away from its cage of origin. Following complete neck dislocation, death was ensured by assessing for complete disruption of the spinal cord at vertebral levels C1-3. The head was subsequently removed. Before discarding the body, a small tail clipping was collected for DNA extraction and future genotyping.

The cranial skin was then incised sagittally, beginning at the orbital midline, and separated laterally to expose the dorsal aspect of the cranium and reveal the foramen magnum. From this point, the cranial bone was carefully cut either side postero-anteriorly along the parietotemporal suture and then medially to the midline bregma. The frontal, parietal, inter parietal and occipital bones were then gently removed to reveal the brain, which was eased out of the cranial cavity (step 1) and transferred to a plastic dissection plate in 10 ml of phosphate-buffered saline (PBS) on ice. The whole brain was first washed in PBS by slowly swirling the plate to remove any residual blood. Thereafter, it was divided sagittally in left and right hemispheres (step 2) while the brain stem was removed, transferred to a 1.5 ml microcentrifuge tube, snap frozen at -196°C in liquid nitrogen and stored in dry ice at -80°C . The hippocampi were removed from each sagittal cortical section by gently separating the medial aspect of the cortex from the thalamus, striatum and other midbrain structures and by widening the lateral ventricles, thereby exposing the hippocampus (step 3). Following, the hippocampus was slowly eased out of the medial cortex (step 4). The resulting cortical and hippocampal samples were then snap frozen and stored in dry ice. After all dissections were carried out for one cage, the samples were transferred to a New Brunswick™ -86°C Ultra-low temperature U725 freezer for later use.

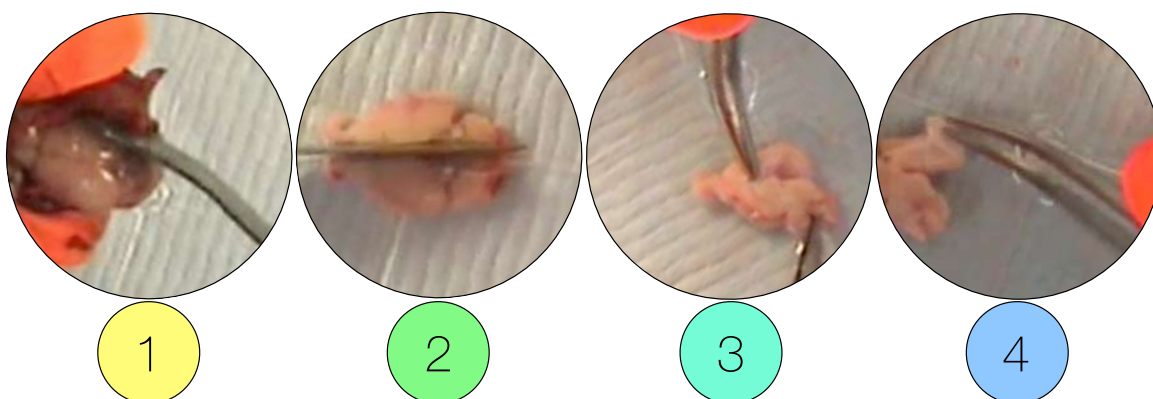


Fig. M.10 - Overview of cerebral dissection procedure performed on DS mouse models.

3.4 Quantitative real-time polymerase chain reaction - qPCR

In this thesis, qPCR was the technique of choice for quantification of DKK3 and AXIN2 expression in the Tc1 hippocampus. This study was undertaken to confirm preliminary RNA sequencing data (4.1.2). A total of 8 mice were analysed, comprising 4 Tc1 and 4 age-matched controls ($n=4$). The table below details the male mice from which the template genetic material was generated.

NUMBER	CODENAME	AGE AT COLLECTION (d)	SEX	GENOTYPE - Hsa21
483288	WT A	83	m	-/-
483554	WT B	95	m	-/-
483565	WT C	96	m	-/-
481897	WT D	95	m	-/-
483289	Tc1 A	83	m	-/+
509574	Tc1 B	87	m	-/+
509576	Tc1 C	87	m	-/+
509819	Tc1 D	77	m	-/+

Fig. M.11 - Tc1 hippocampal samples used as source of cDNA employed for qPCR.

3.4.1 Tc1 cDNA generation via reverse transcription

In order to generate stable templates for qPCR use, 1 μ g RNA preparations from each mouse were first reverse-transcribed to cDNA employing a QuantiTect[®] Reverse Transcription Kit (QIAGEN), which supplies all required reagents. All RNA preparations have been previously extracted by Elizabeth Fisher's laboratory. Prior to reverse transcription, all RNA preparations were cleared of genomic DNA contamination. Samples were thawed on ice and made up to a 12 μ l solution in RNase-free ddH₂O. 2 μ l of gDNA Wipeout Buffer (2.5-10% trometamol) were then added to each sample and incubated for 2 min at 42°C in an Eppendorf ThermoMixer[®] F1.5. Following, reverse transcription reaction mixtures were prepared as follows:

COMPONENT	VOLUME
QuantiScript [®] RT	1 μ l
QuantiScript [®] RT Buffer (dNTPs)	4 μ l
RT primer mix	1 μ l
Template RNA	14 μ l

Fig. M.12 - Reverse transcription reaction

Each reaction was incubated for 30 min at 42°C in an Eppendorf ThermoMixer® F1.5. Thereafter, the reverse transcriptase was inactivated by incubating at 95°C for 3 min. The ~1 µg (50 ng/µl) cDNA product was subsequently stored at -20°C for experimental use. For each sample, an identical reaction was performed alongside, substituting the reverse transcriptase with RNAse-free ddH₂O for usage as a negative control (-RT) to account for any non-specific amplification at the qPCR stage.

3.4.2 DNA primer and probe design

The qPCR technique requires the design of two primers, forward and reverse, and an additional oligonucleotide probe in between the two. The probe is a slightly longer oligonucleotide tagged with a fluorophore at its 5' end and a quencher at its 3' end. The latter withholds fluorescence unless the probe binds to its target DNA sequence and the fluorophore is cleaved via *Taq* polymerase exonuclease activity. The signal generated is directly proportional to the amount of probe amplified and consequently, to the amount of expression of a gene of interest. Importantly, qPCR primers must be able to recognise a template sequence representing an *expressed* gene, i.e. a sequence composed solely of joined exons. For this reason, primers must be designed so that at least one bridges between an exon-exon boundary, while the other and the intermediary probe may be designed identically to PCR primers.

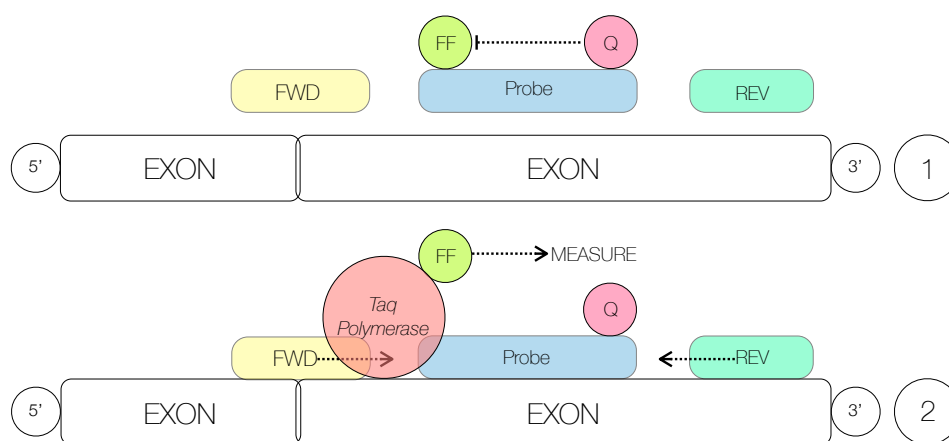


Fig. M.13 - Conceptual overview of qPCR primer-probe binding and fluorescence release.

Exon sequences for AXIN2 and DKK3 were obtained from the eEnsembl browser (<http://www.ensembl.org/index.html>) selecting for mouse genome. Primers and probes were designed employing Primer Express® Software (Life Technology) set on TAQman qPCR design. This program aids optimal primer design by providing instant information on primer G/C content, repeating patterns, secondary structures and T_m. Primers and probe were designed according to guidelines provided by Life Technology. Furthermore, each primer pair and probe was tested for specificity through the NCBI reverse ePCR web service (<http://www.ncbi.nlm.nih.gov/projects/e-pcr/forward.cgi>) by running a mouse transcriptome-based virtual PCR reaction to confirm correct amplification of the genes of interest. All primers and probes were synthesised by Eurofins. Upon delivery, primers were solubilised in ddH₂O while probes were dissolved in qPCR Probe Dilution Buffer (10 mM Tris-HCl, pH 8, 1mM EDTA) to a 100 μM stock concentration and stored at -20°C according to manufacturer instructions. The figures below detail primer sequence, characteristics and ePCR results for DKK3 and AXIN2.

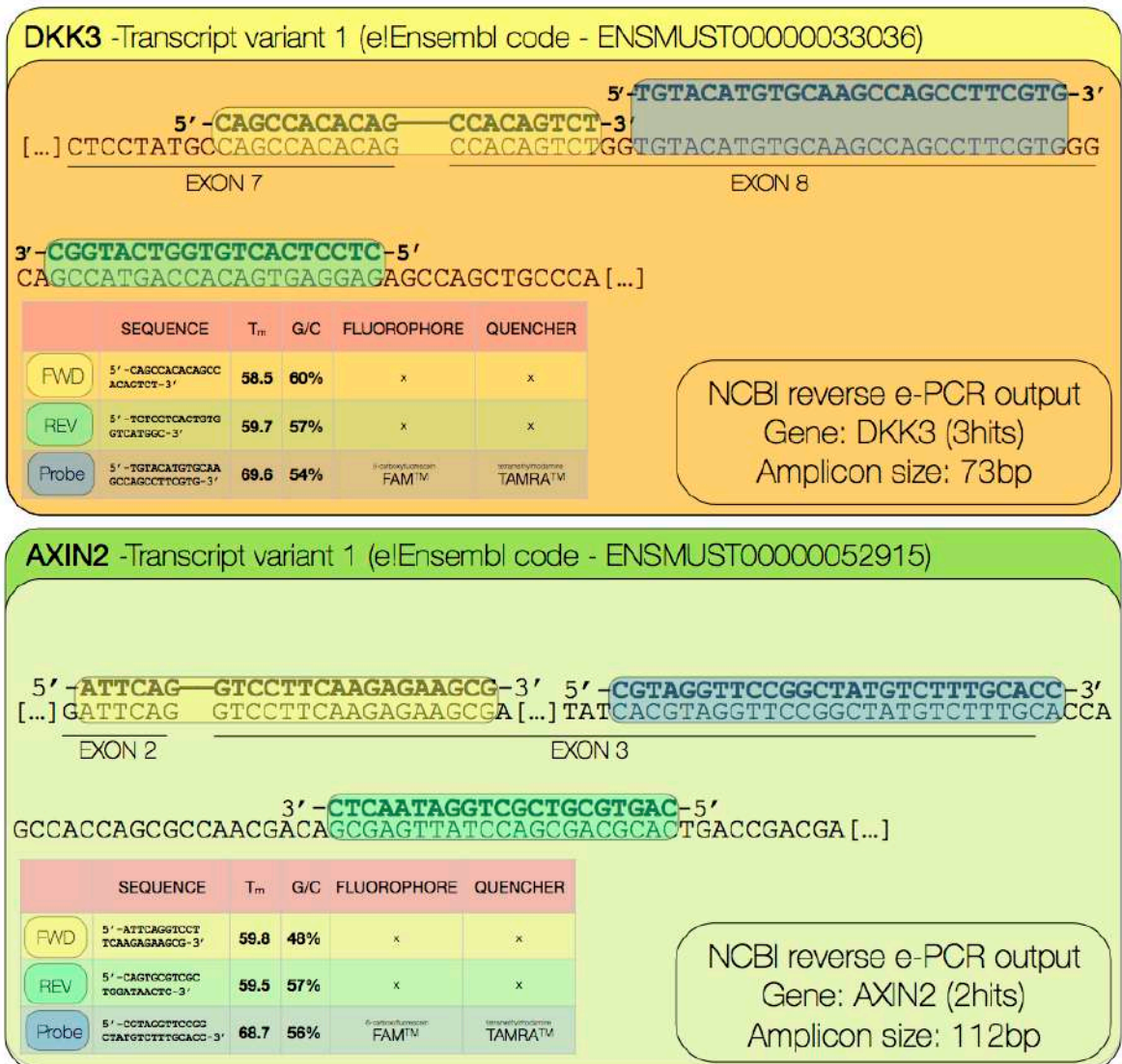


Fig. M.14 - qPCR primer sequence, characteristics and ePCR results for DKK3 and AXIN2

3.4.3 qPCR

For experimental use, primer and probe stocks were diluted to 40 μM (1:2.5) and 5 μM (1:20) in ddH₂O respectively. Furthermore, each 50 ng/ μl cDNA preparation was diluted 1:10 following routine laboratory practice for moderately-to-highly expressed genes. In addition to template cDNA, primers and probe, each qPCR reaction requires the amplification of a stably expressed gene to provide a reference for quantification. For this thesis, β -actin and glyceraldehyde 3-phosphate dehydrogenase (GAPDH) were employed. Both were supplied pre-mixed by Elizabeth Fisher's laboratory with primers and probe labeled with VIC[®] (Life Technology, composition not available publicly) and quenched by dihydrocyclopyrroloindole tripeptide minor groove binder (MGB). All reactions were incubated in TaqMan[®] Gene Expression Master Mix (AmpliTaq Gold[®] DNA Polymerase (Ultra Pure), Uracil-DNA glycosylase, dNTPs (with dUTP), ROX[™] Passive Reference, and optimized buffer components), which includes DNA polymerase and substrates as well as a passive reference signal providing constitutive fluorescence to control for sample loading. The following table details the components of each standard 15 μl reaction:

COMPONENT	VOLUME
TaqMan [®] Master Mix	7.5 μl
FWD primer	0.15 μl
REV primer	0.15 μl
Probe	0.45 μl
Reference gene	0.3 μl
ddH ₂ O	5.45 μl
cDNA template or -RT	1 μl

Fig. M.15 - Standard qPCR reaction mix.

Standards and plate setup - Each experiment was performed in a standard qPCR 96-well plate for each gene investigated and each reference gene considered. Prior to loading, the plate was inserted in an ice rack to maintain the samples at low temperature. All expression qPCR reactions require the generation of a standard curve quantifying gene expression in one reference sample as a function of its loaded concentration. This allows for reliable quantification of gene expression across all conditions under study. For all experiments performed in this thesis, sample *WT A* was selected as standard. The original 50 ng/ μl cDNA preparation obtained following 3.5.2 was diluted 1:5 (ie 2x experimental samples) and then 1:2 serially up to 1:80 relative to the original solution. All samples were loaded in technical triplicates to provide additional loading control (individual triplicates not included in final analysis).

Amplification reaction - For each sample analysed, the corresponding -RT control was loaded along side, also in triplicate. Once loaded, the 96-well plate was removed from the ice rack and thereby centrifuged at room temperature for 5 min at top speed. All experiments were performed employing a 7500 Fast Real-Time PCR System (Life Technologies) controlled by homonymous software. The qPCR was set to run under the Quantification protocol for a standard duration of approximately 90 min.

3.5 Cell culture, luciferase assay and immunocytochemistry

This section details human cell lines employed, routine aspects of tissue culture, pharmacological treatment and DNA transfection, novel development of a reporter human cell line and preparation of cultures for imaging experiments. The associated results are discussed in chapter 3 (4.3.2).

3.5.1 General cell line maintenance

All work with cell lines was conducted in a MSC-Advantage™ Class II Biological Safety Cabinet with laminar air flow, unless otherwise specified. All cell lines were grown, stored and treated at 37°C and 5% CO₂ in an MCO-18AC Panasonic CO₂ incubator. Four human cell lines were employed:

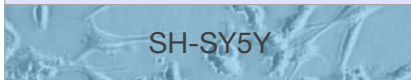
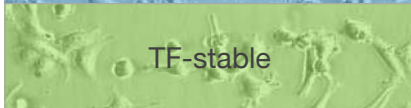
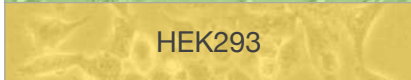
NAME	DESCRIPTION
 SH-SY5Y	Neuroblastoma cells. Employed in luciferase assays and DYRK1A overexpression experiments.
 TF-stable	Modified SH-SY5Y line, employed in all DYRK1A inhibition luciferase experiments. (see 3.5.6 for info on development of this line)
 HEK293	Human embryonic kidney cells. Employed in DYRK1A overexpression and imaging experiments.
 HeLa	Human cervical cancer-derived, oldest cell line in existence. Employed in Airyscan imaging experiments.

Fig. M.16 - Cell lines employed.

Each cell line was grown and maintained in a 100 ml sterile cell culture flask, the surface of which is readily optimised for cell attachment. Generally, these stocks were cultured at $\sim 10^6$ cells/ml in order to guarantee a high number of available cells, whilst preventing damaging over-confluent growth. This target concentration was measured regularly via fluorescence-mediated cell counting, employing a Muse® Cell Analyzer and Muse® Count & Viability Kit (Merck Millipore), following manufacturer's protocols. For each cell line, 10 ml of Dulbecco's Modified Eagle Medium (DMEM, Gibco) were employed as a maintenance growth medium. Moreover, all DMEM solutions were enriched with 100 µg/ml streptomycin and 100 U/ml penicillin to protect the cells against bacterial contamination. Foetal Bovine Serum (FBS) was also added to the medium, in order to provide nutrients essential for cell survival.

DMEM enriched with the above antibiotics and nutrients will henceforth be referred to solely as DMEM. Additionally, the growth medium for TF-stable cells was conditioned with 1:1000 G418 (Geneticin), an aminoglycoside antibiotic active against both prokaryotic and eukaryotic organisms. Because the TOPFLASH construct expressed in the TF-stable cell line (see 3.5.6) also encodes a G418 resistance gene, administration of this agent provides additional positive selective pressure, only allowing cells expressing the luciferase reporter to grow.

Cell passaging - The growth of each cell line was monitored daily by direct observation under a Nikon inverted optical microscope, to assess health status and growth confluence. All cells were passaged every 48-72 hrs. Via this technique, a fraction of the cells is removed and transferred to a new flask, ensuring continuous growth while maintaining cell number and density below the flask's surface area limit. To first dispose of accumulated debris and cell metabolites, all DMEM was removed from each flask. The cells were subsequently washed with 10 ml of Hank's Balanced Salt Solution (HBSS, Gibco - Composition) and by gently swirling each flask for 10 sec. Following, the HBSS was removed and each cell line was treated with 1 ml of 1mg/ml trypsin. The proteolytic action of trypsin, a serine protease of pancreatic production normally found in the vertebrate digestive tract, disrupts cell attachment to the flasks, allowing for re-suspension in solution for removal. The trypsin reaction was allowed to proceed for 1-3 min, as required, until cells were visibly detached. Thereafter, 9 ml of DMEM were added to each flask to re-suspend the cells and make the total volume up to 10 ml for ease of subsequent dilution. Each cell line was passaged as a fraction of the previous flask. SH-SY5Y cells were passaged 1:5 at 48 hrs, and 1:10 at 72 hrs. Differently, HEK293 cells were passaged 1:3 at 48 hrs, and 1:5 at 72 hrs. Each of the new flasks were prepared with as much DMEM as required for a total volume of 10 ml with respect to the amount of cells taken from the re-suspended solution. As an example, for a 1:5 passage, 2/10 ml of re-suspended SH-SY5Y cells were added to 8 ml of fresh DMEM in the new flask. Each cell line was passaged up to 20 times before being discarded and substituted with an equivalent clone.

Cell plating for experimental use - When required for study, cells were transferred to plates specifically designed for experimental use. The plating technique is essentially identical to passaging, differing only in the re-suspended cells being transferred to a different plate at a specific dilution, rather than to a new flask. For this reason, cells were always plated upon passaging.

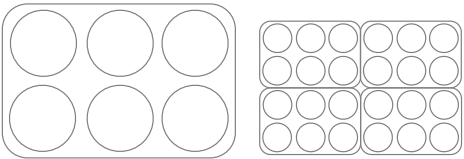
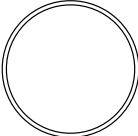
Experiment	Plate type	Cell dilution
Luciferase assay and immunocytochemistry	 6/24-well plate 2-0.5ml/well	$\sim 2 \cdot 10^4$ /ml
Biochemical analysis and co-IPs	 10 ml culture plate (company)	$\sim 10^5$ /ml

Fig. M.17 - Plates and dilutions employed for each experiment type.

3.5.2 DYRK1A inhibition

For all DYRK1A inhibition experiments (4.3.2.2.1), three commercially available inhibitors with diverse mechanisms of action were investigated: EGCG (Epigallocatechin-3-gallate), INDY ((1Z)-1-(3-Ethyl-5-hydroxy-2(3H)-benzothiazolylidene)-2-propanone), and Harmine (7-MeO-1-Me-9H-pyrido(3,4-b)-indole). Upon delivery, all inhibitors were solubilised according to manufacturer instructions and stored at -20°C in a spark-free freezer. Each stock solution was prepared as 1000x the concentration required experimentally. The table below details the properties and experimental dose of each inhibitor:

NAME	MANUFACTURER	REFERENCE	MECHANISM OF ACTION	<i>IN VITRO</i> IC ₅₀	DOSE	SOLVENT
EGCG	SIGMA-ALDRICH	Guedj et al. (2009) - Green Tea Polyphenols Rescue of Brain Defects Induced by Overexpression of DYRK1A.	ATP-noncompetitive	0.33 μ M	25 μ M	Ethanol
INDY	TOCRIS bioscience	Ogawa, et al. (2010) - Development of a novel selective inhibitor of the Down syndrome-related kinase Dyrk1A	ATP-competitive	0.24 μ M	25 μ M	Dimethylsulfoxide DMSO
HARMINE	TOCRIS bioscience	Adayev et al., 2011 - Harmine is an ATP-competitive inhibitor for dual-specificity tyrosine phosphorylation-regulated kinase 1A (Dyrk1A)	ATP-competitive	0.7 μ M	10 μ M	Dimethylsulfoxide DMSO

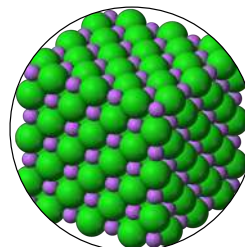
Fig. M.18 - Overview and features of DYRK1A inhibitors employed.

Characterisation of the above inhibitors has shown that INDY is both the most potent and specific inhibitor. While EGCG shows higher potency than Harmine, the latter as been shown to inhibit DYRK1A with increased specificity compared to EGCG. For all DYRK1A inhibition experiments, cells were administered treatment via DMEM solutions enriched with each inhibitor at a concentration of 1:1000 to achieve the required experimental dose. All treatments were performed for a duration of 6 hrs at 37°C.

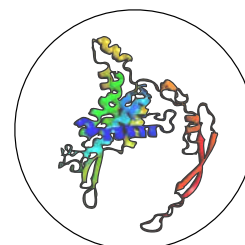
3.5.3 Lithium chloride and Wnt3a administration

For all experiments involving measurements of canonical Wnt signalling activity in human cell lines, treatment was required to artificially activate the pathway. For the studies described in 4.3.2, Lithium chloride and Wnt3a were employed.

Lithium chloride (LiCl) - LiCl is a potent activator of canonical Wnt signalling, an effect mediated by direct inhibition of the Wnt-inhibitory GSK3 β (6). For this thesis LiCl (Sigma) was provided as a solid salt and thereby solubilised in H₂O to achieve a 5 M stock concentration. In all experiments, LiCl treatment was administered to cells at a dose of 40 mM in accordance with previous publications (6) by enriching DMEM with LiCl at a 1:125 concentration. Equimolar solutions of Sodium chloride (NaCl - Sigma) were employed as a control treatment throughout. All treatments were administered for 6 hrs at 37°C.



Wnt3a - Wnt3a is a physiological ligand for canonical Wnt signalling. It exerts its effect by directly binding to and activating Fz receptors (7). Wnt3a was supplied by R&D Systems as 10 μ g in lyophilised form and solubilised in 200 μ l PBS to achieve a stock concentration of 50 μ g/ml. In all experiments, Wnt3a treatment was administered at a dose of 50 ng/ml in accordance with previous publications (6) by enriching DMEM with Wnt3a at a 1:1000 concentration. Equimolar amounts of PBS were employed as a control treatment throughout. For DYRK1A inhibition and overexpression experiments, Wnt3a treatment was administered for 6 hrs at 37°C.



3.5.4 DNA transfection

DNA transfection is a technique whereby a DNA construct can be temporarily integrated into a host cell for transient expression. This approach is widely adopted to investigate the effects of gene overexpression in a model system. In this thesis, DNA transfection was employed to investigate DYRK1A interaction with Wnt components, its effects on canonical Wnt signalling as well as its subcellular localisation under differential Wnt activation states.

All transfections were executed employing the FuGENE® HD Transfection Reagent (Promega) and carried out in SH-SY5Y, HeLa and HEK293 cells grown in 6-well or 10 cm plates (see 3.5.1). All transfection mixtures comprising the DNA to be inserted and the FuGENE® reagent were dissolved in 100/500 µl Opti-MEM® (Gibco) per transfected well or plate, respectively. In all cases, FuGENE® was administered at a 3:1 ratio relative to the µg/ml amount of DNA to be transfected. Following, the solution was incubated for 15 min at room temperature and subsequently administered to each well or plate. The transfected cultures were subsequently incubated at 37°C for 24 hrs before assaying. The table below details amounts constructs transfected:

TRANSFECTED CONSTRUCTS			
CONSTRUCT	STOCK	USE	EXP
pCMV5-HA-DYRK1A	0.751 µg/µl	Luciferase assay, DYRK1A expression, co-IP, ICC	0.25-5 µg/ml
pCMV5-Empty	1 µg/µl	Control vector for pCMV5-HA-DYRK1A	0.25-5 µg/ml
pEGFPC1-DYRK1A	0.827 µg/µl	ICC	0.25 µg/ml
pEGFPC1-Empty	1 µg/µl	Control vector for pEGFPC1-DYRK1A	0.25 µg/ml
pRK5-FLAG-DVL1	1 µg/µl	Luciferase assay, co-IP, ICC	0.25-5 µg/ml
pRK5-FLAG	1 µg/µl	Control vector for pRK5-Myc-DVL1	0.25-5 µg/ml
pCS2-DKK3-FLAG	0.350 µg/µl	Luciferase assay, co-IP	0.25-5 µg/ml
pCDNA3.1-β-cat-FLAG	1 µg/µl	co-IP	5 µg/ml
pGL3-TOPFlash Luciferase	1 µg/µl	Luciferase reporter. Relates TCF/β-catenin to a bioluminescent signal.	0.25 µg/ml
pGL3-FOPFlash Luciferase	1 µg/µl	Control reporter. Contains a mutated TCF/LEF binding site. Used to control for any non-specific effect of transfection.	0.25 µg/ml
pRL-Renilla Luciferase	0.1 µg/µl	Constitutively active luciferase reporter. Acts as internal control to normalise experimental luciferase activity.	0.025 µg/ml

Fig. M.19 - Overview of transfected constructs, purpose and amount employed (EXP).

3.5.5 TCF/ β -Catenin TOPFLASH luciferase assay

The luciferase assay is a technique whereby the amount or activity of a protein of interest can be measured by relating it to the expression of a firefly (*P. pyralis*) luciferase gene (see 4.3.1 for a literature overview of the technique). Consequent administration of luciferase substrate generates a measurable bioluminescent signal directly proportional to the amount of protein of interest. In the context of this thesis, the luciferase signal was related to transcriptionally active, or monomeric β -catenin as a measure of canonical Wnt signalling activity. This was achieved via the pGL3-TOPFlash Firefly Luciferase construct, which encodes a TCF/LEF site for β -catenin binding upstream of a luciferase reporter.

All luciferase assays were performed with a Dual-Luciferase[®] Reporter Assay System (Promega). Two general approaches were undertaken. For DYRK1A inhibition experiments, the TF-stable cell line was employed (see 3.5.6). For DYRK1A overexpression experiments, however, to ensure all cells expressing DYRK1A would also concomitantly express the luciferase construct, unmodified SH-SY5Y and HEK293 cells were co-transfected with both the DYRK1A and luciferase constructs. Additionally, this approach requires an internal normalisation signal to account for differing transfection efficiencies across cell populations. This was achieved via concomitant transfection of the pRL-Renilla Luciferase construct, which provides a constitutively active renilla (*R. reniformis*) luciferase signal, thereby only reflecting transfection efficiency. (See 3.9.3 for further details on luciferase quantification). All cells were grown and assayed in 6-well plates following the treatment of interest (e.g.: DYRK1A inhibition/overexpression).

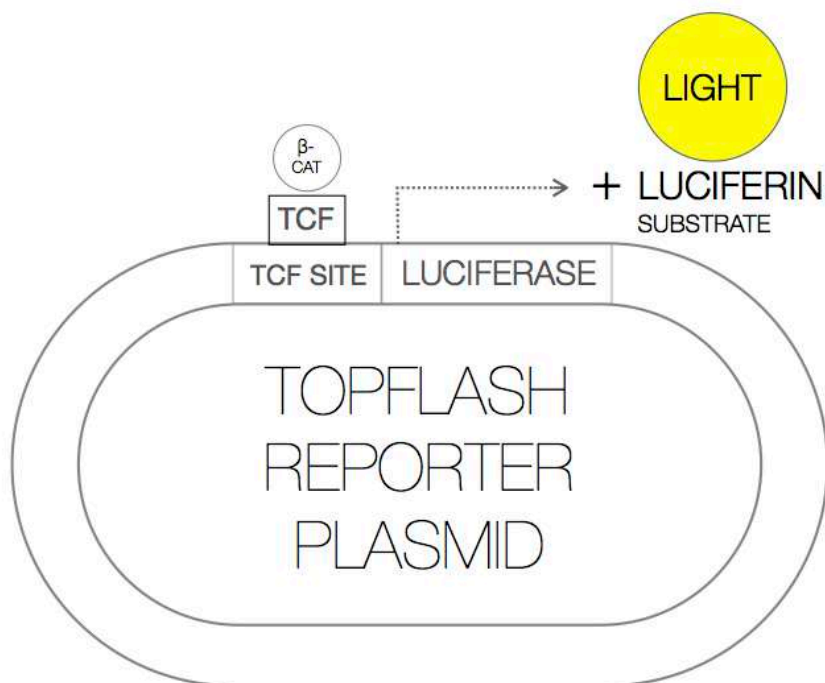


Fig. M.20 - General principle of the TCF/ β -Catenin TOPFLASH luciferase assay, which relies on a reporter plasmid.

Chapter 3 - Materials and Methods

The 6-well plates were removed from the incubator and the DMEM was subsequently discarded. Each well was washed twice with 10 ml of PBS. Thereafter, 250 μ l of Passive Lysis Buffer (50 μ l 5X Passive Lysis Buffer, 200 μ l dH₂O - Promega) were added to each well and incubated at room temperature for 10 min and 35 rpm rotation on a Stuart gyro-rocker SSL3 (from here on referred to as gyro-rocker). Once lysed, TF-stable cells were assayed by adding 10 μ l of lysate to 50 μ l of Luciferase Assay Reagent II (Promega - i.e. luciferase enzyme substrate) and thereby measuring the bioluminescent signal in a GLOMAX™ 20/20 luminometer (Promega), adopting the Steady-Glo® protocol with 10 sec integration. The luminescence value was expressed in Relative Light Units (RLU) and recorded. Each value was subsequently normalised to the average of each control condition (i.e.: no treatment).

Thereafter, the average value recorded for each condition was expressed as a ratio of the normalised averages. Unmodified SH-SY5Y and HEK293 cells were assayed employing the Dual-Glo® protocol with 10 sec integration. Following the firefly luciferase measurement described above, each 60 μ l reaction was treated with 50 μ l of Stop & Glo® Buffer (49 μ l buffer, 1 μ l renilla substrate - Promega), which quenches the firefly luciferase reaction and provides a substrate for the renilla luciferase. The renilla activity was subsequently measured as an internal control. The overall luciferase signal was expressed as a ratio of firefly/renilla and the values were then normalised as above.

For results in 4.3.2.2.1.4, luciferase activity was measured in live cells from the TF-stable line by enriching DMEM with 150 μ g/mL D-luciferin (Systems Biosciences) and employing the IVIS system (Perkin-Elmer) to image plates 20 min post-treatment.

3.5.6 Generation of SH-SY5Y cells stably expressing the the TCF/LEF-Luciferase reporter

The SH-SY5Y cell line was engineered to stably express the pGL3-TOPFlash Firefly Luciferase construct. Consequently, all cells within this line produce a canonical Wnt signalling/luciferase signal, and do not require additional transfections to be assayed. This also provides the advantage of greatly increased signal-to-noise ratio. Stable TOPflash SHSY5Y cells were made in a two-step process. Firstly, the TCF/LEF-responsive promoter and luciferase reporter from M50 Super 8x TOPflash (2) was cloned into a plasmid with suitable antibiotic resistance for selection in mammalian cells. To this end, the CMV promoter was removed from pcDNA3 by restriction digestion with BglII and NotI, and a NotI-BamHI fragment from M50 Super 8X TOPflash ligated into these sites. The responsiveness of the resultant plasmid to transient transfection with DVL1 was confirmed by luciferase assay and found to be approximately ~25% that of M50 Super 8x TOPflash. Secondly, this plasmid was stably transfected into SH-SY5Y cells. The plasmid was linearised by PvuI digestion and transfected into SH-SY5Y cells, with stably transfected cells selected for resistance to G418 (800 μ g/ml) following standard procedures. Twelve clonal cell lines were established and compared for basal luciferase expression and fold-induction in response to 30mM LiCl treatment. Clone #3 was chosen for experiments since the cell line displayed the greatest sensitivity to Wnt pathway activation. The cell line is referred to as 'TF-stable' throughout this thesis.

3.5.7 Slide preparation for immunocytochemistry

For this thesis, Immunocytochemistry (ICC) was adopted to assess the subcellular localisation and translocation of DYRK1A. All experiments were performed in the HeLa and HEK-293 human cell lines.

HeLa - Cells were seeded at ~60% confluency into No. 1.5 imaging chambers (Lab-Tek) coated with 400-600 µg/ml Matrigel (Corning) and transfected immediately using Lipofectamine 3000 (Thermo Fisher Scientific) according to the manufacturer's specifications. HA-DYRK1A was transfected at 250ng/well, or else co-transfected with FLAG-DVL1 at the same concentration. Wnt3a and LiCl treatment including the appropriate controls were conducted as detailed above 5 hours prior to fixation. After 18 hours cells were fixed with 4% (w/v) paraformaldehyde (PFA) for 20 min at room temperature (RT). Samples were then permeabilised with 0.2% (w/v) saponin (Sigma-Aldrich) for 30 min, and blocked in 5% (v/v) donkey serum (Sigma-Aldrich) doped with 0.05% (w/v) saponin for 1 hour at RT. FLAG and HA primary antibodies (Sigma-Aldrich) were diluted in block to 1:100, added to cells, and incubated overnight at 4°C. Secondary anti-mouse and anti-rabbit antibodies conjugated to Alexa 488 and Alexa 594 (1:1000; Life Technologies) were made in block and incubated with samples for 30 min at RT. A 1:5000 Hoescht 33258 and 1:1000 Phalloidin 647 (both ThermoFisher Scientific) dilution in PBS was incubated for 30 mins at RT to label the nucleus and F-actin respectively. Cells were thoroughly washed and Imaging was performed in fresh PBS.

HEK293 - Cells were seeded at ~60% confluency onto glass coverslips previously coated with 0.1mg/ml poly-D lysine and grown into 6-well plates. Transfection was performed as above but employing 3:1 fuGene HD (Promega) as transfection reagent. Treatment was also performed as above. After 18 hours cells were fixed with 4% (w/v) paraformaldehyde (PFA) for 20 min at RT. Samples were then permeabilised for 30 min in 0.5% (w/v) Triton-X 100, and blocked in 5% (w/v) FBS with 0.05% (w/v) Triton-X 100. The DYRK1A (Abcam) rabbit polyclonal primary antibody was incubated as above at 1:500 dilution. Secondary anti-rabbit Alexa 488 was incubated as above. A 1:1000 DAPI (ThermoFisher Scientific) dilution in block buffer was incubated for 30 mins at RT to label the nucleus.

3.5.8 Airyscan and confocal microscopy

Airyscan microscopy is a recently developed imaging technique which offers improvements in image resolution over traditional methods. Confocal microscopy is limited by the diffractive nature of light. Below a certain size, information is lost to light scattering, escaping detection. Confocal systems with Airyscan possess an additional detector which captures such diffracted light. Images are generated in combination by both detectors, thus enhancing spatial resolution. For this thesis, Airyscan imaging was performed using a Zeiss 880 outfitted with an Airyscan module. Data was collected using a 63x 1.4 NA objective and immersion oil optimised for 30°C (Carl Zeiss). Colours were collected sequentially by frame to minimise crosstalk, and Airyscan processing was performed using the Airyscan module in the commercial ZEN software package (Carl Zeiss). Confocal imaging was performed using a Zeiss 710, also using a 63x 1.4 NA objective and immersion oil.

3.6 Mouse, human and cell biochemistry

The biochemical techniques described in this section were employed to measure a variety of Wnt signalling proteins, as well as *DYRK1A*, in DS mouse model and human samples, SH-SY5Y and HEK-293 cells.

3.6.1 Generation of mouse brain lysates

All lysates were generated from samples outlined in 3.3.1. Experimental batches A and B were extracted on separate attempts, as were the hippocampal and cortical samples, amounting to 8 lysates/attempt. The dissected samples were allowed to thaw on ice. Thereafter, each sample was suspended in 1.5 ml (cortex) or 500 μ l (hippocampus) of brain extraction buffer (50 mM Tris, 5 mM $MgCl_2$, 150 mM NaCl, 1% NP-40, protease inhibitor (tab), 1:100 phosphatase inhibitor cocktail) in a microcentrifuge tube. Following, each sample was lysed by mechanical disruption with a tissue homogeniser and subsequently centrifuged for 10 min at 14,680 rpm and 4°C in a tabletop microcentrifuge to pellet debris. Thereafter, the supernatant was transferred into fresh 1.5 ml tubes and aliquoted for immediate analysis or storage at -20°C.

3.6.2 Generation of human brain lysates from post mortem DS hippocampal samples

All post-mortem human brain samples were processed in accordance with the Human Tissue Act 2004 and directives from the Human Tissue Authority (UK). The study was reviewed and approved by NHS Research Ethics committee, London-Queen Square. Samples were provided, anonymised, by the Newcastle brain bank, from 55 (\pm 11) and 56 (\pm 12) years old AD-DS individuals and age-matched euploid controls, respectively. All people involved had granted full research consent. 10 mg of frozen tissue from hippocampal and cortical samples was excised in a sterile environment and triturated with a plastic pestle in 130 μ l brain lysis buffer prior to snap-freezing in liquid nitrogen and storage at -20°C.

3.6.3 Generation of human cell line lysates

For *DYRK1A* overexpression experiments and co-IPs, proteins were extracted and purified from cells for subsequent biochemical analysis by SDS-PAGE and Western blotting (3.6.5-6). Following incubation in the desired experimental condition, DMEM was removed from each 10 ml culture plate, which was then washed twice with ice-cold PBS. Thereafter, each plate was treated with 1 ml of cell lysis buffer (150 mM NaCl, 50 mM Tris pH 7.5, 5mM EDTA and 0.25% nonyl-phenoxypolyethoxyethanol-40 (NP-40), protease inhibitor tab) which includes salts to preserve physiological cell acidity and osmolarity and a detergent to disrupt membrane structure. The lysis reaction was allowed to proceed for 2 min with gentle swirling of the plate on a Stuart gyro-rocker SSL3 at 10 rpm. The contents of the each plate were then detached using a cell scraper and the 1 ml buffer/lysate solution was subsequently transferred to a 1.5 ml centrifuge tube for a 5 min incubation on ice. Following, each lysate was centrifuged for 10 min at 4°C and 14,680 rpm in a tabletop micro-centrifuge to pellet cell debris. The supernatant was collected from each tube, transferred to a fresh 1.5 ml and either analysed directly, employed for co-IP or stored at -20°C,

3.6.4 Co-immunoprecipitation

Co-immunoprecipitation (co-IP) is a standard technique for the study direct protein-protein interactions. It relies on the fundamental principle of specific antibody-antigen binding (-immuno). Antibodies to endogenous or tagged peptides can be employed to extract individual proteins from lysate solutions (-precipitation) with the aid of an antibody-binding physical support, such as viscous gels or beads. The primarily 'pulled down' protein is termed bait. When such protein under study is pulled down, any secondary interactors (prey) physically bound to it also precipitate out of solution. The resultant fusion proteins can then be isolated and identified via SDS-PAGE and Western blotting (3.6.5-6). In this thesis, co-IP was employed to test overexpressed *DYRK1A* as prey for interaction with a number of key Wnt components. Baits were also overexpressed as FLAG-tagged constructs. FLAG peptides allow for robust precipitation of tagged proteins, and greatly improve signal-to-noise ratio. In all cases, the technique was carried out in HEK-293 cells cultured in 10 cm plates. HEK293 cells were co-transfected with 0.5 µg/ml HA-DYRK1A and 0.5 µg/ml FLAG-DVL1/β-catenin-FLAG/DKK3-FLAG or relative empty controls and lysed as described above. Thereafter, 40 µl of anti-FLAG M2 affinity gel (Sigma) were added to 1 ml of each lysate to bind potential fusion proteins. Following 1 hr of rotational incubation at 4 °C, the gel was washed five times by centrifugation and resuspension in cell lysis buffer. 150 ng 3xFLAG peptide (Sigma) were used to elute the fusion proteins. Eluates were then denatured and analysed as described below. Each co-IP was performed independently at least three times.

For each co-IP performed, four transfection conditions were employed (**Fig. R3.4-6**). Expression of empty vectors acted as negative control, so as to exclude non-specific pulldown of proteins by the FLAG affinity gel. Expression of FLAG-tagged bait constructs alone acted as positive control, confirming detectable pull-down at the appropriate molecular weight. Expression of the non-tagged *DYRK1A* prey construct alone was performed to exclude non-specific pulldown of overexpressed protein by the affinity gel. Expression of both bait and prey constructs constituted the experimental condition under investigation. Input lysates for the above conditions were also analysed alongside to confirm expression of the constructs under study.

3.6.5 SDS Polyacrylamide gel electrophoresis (SDS-PAGE)

In this thesis, SDS-PAGE was used to size-separate proteins in all samples employed for Western blot analysis. Prior to electrophoresis, 50 µl of NuPAGE® LDS Sample Buffer (Glycerin, LDS - Life Technologies) and 20 µl of NuPAGE® Sample Reducing Agent (500 mM dithiothreitol (DTT) - Life Technologies) were added to 130 µl of mouse/human brain and cell lysate or co-IP eluate. Each resultant 200 µl solution was subsequently incubated at 95°C for 5 min in an Eppendorf ThermoMixer® F1.5 to aid protein denaturing. Thereafter, 10 µl of each solution were loaded in a 10 or 20-lane NuPAGE® Bis-Tris Precast polyacrylamide gel (Life Technologies). The gel was inserted in an electrophoresis chamber (Biorad) and submerged in NuPAGE® MOPS SDS Running Buffer (50 mM MOPS, 50 mM Tris Base, 0.1% SDS, 1 mM EDTA, pH 7.7) enriched with 500 µl NuPAGE® Antioxidant (Life Technologies). The gel was then ran at a voltage of 90 V for 1 hr 45 min.

3.6.6 Western blotting

Western blotting was here employed to analyse DS mouse and human brain samples, as well as cell lysates from *DYRK1A* overexpression experiments and co-IPs. The technique is routinely performed in four stages: sample transfer, blocking, antibody treatment, and imaging. These are detailed below.

Transfer - Following, SDS-PAGE, all samples were transferred to a 0.45 μm pore Immobilon-P polyvinylidene fluoride (PVDF) membrane (Merck Millipore) in semi-dry conditions (i.e. minimal amounts of buffer solutions required). First, appropriately sized membranes were cut out of the roll stock and briefly soaked in methanol and dH_2O to reduce hydrophobicity. Each membrane was then submerged in sample transfer buffer (25 mM Tris, 192 mM glycine, 10% methanol) for 2 min, whilst 4 sheets of filter paper were briefly soaked in transfer buffer to provide additional solution and encapsulation during transfer. Thereafter, each protein gel was placed upon the membrane, with two sheets of filter paper stacked above and below. The transfer was then executed in a Trans-Blot[®] SD Semi-Dry Electrophoretic Transfer Cell (Biorad) connected to a Power Pac 3000 (Biorad) power supply at a voltage of 20 V for 1 hr.

Blocking - To prevent non-specific antibody binding at later stages, each transferred membrane was blocked via incubation in 10 ml of 5% bovine milk dissolved in Tris-buffered saline-Tween 20 (TBST - 50 mM Tris-HCl, pH 7.4, 150 mM NaCl, 0.1% Tween 20) for 1 hr at room temperature whilst rotating at 40 rpm in a gyro-rocker. Following blocking, the membrane was washed 3 times in 10 ml TBST for 5 min.

Antibody treatment - All primary and secondary antibodies employed in this thesis are detailed on the next page (**Fig. M.20**). All primary antibodies were administered at 4°C overnight in a 5% milk-TBST solution whilst rotating at 40 rpm on a gyro-rocker. All secondary antibodies were administered for 1 hr at room temperature also in a 5% milk-TBST solution whilst rotating. These were also pre-conjugated to horseradish peroxidase (HRP) for chemiluminescence detection. Following incubation, each membrane was washed 3 times in 10 ml TBST for 5 min and subsequently placed in 10 ml PBS for imaging and storage at 4°C. When probing for multiple Wnt signalling proteins, the membrane was cut according to predicted molecular weight and each section treated separately.

Imaging - Following antibody treatment, each membrane section was soaked in 500 μl of SuperSignal[®] West Femto Maximum Sensitivity Substrate (250 μl Proprietary luminol, 250 μl Stable Peroxide Buffer, Thermo Scientific) to generate a quantifiable HRP activity signal directly proportional to the amount of antibody bound and consequently, of the protein of interest. Immediately following application of the substrate, each membrane was wrapped in cling film and analysed in a GeneGnome[®] XRQ Chemiluminescence imager (High quantum efficiency (QE) camera - Syngene) controlled by GeneSnap[®] software under a 10s exposure with signal integration over 20 images. Thereafter, each membrane was also imaged with white light to ascertain protein size against the molecular weight marker (see 3.9 for details on signal quantification and statistical analysis).

PRIMARY ANTIBODIES				
ANTIBODY	TARGET SIZE	COMPANY	ORIGIN	DILUTION
Anti-DKK3	60 kDa	Abcam®	Goat	1:2000
Anti-DYRK1A	85 kDa	Abnova®	Mouse	1:2000
Anti-GSK3β	47 kDa	Cell Signalling®	Rabbit	1:2000
Anti-pGSK3α/β (S9)	47 kDa	Cell Signalling®	Rabbit	1:5000
Anti-β-catenin	92 kDa	Cell Signalling®	Rabbit	1:2000
Anti-active β-catenin	92 kDa	Merck Millipore®	Mouse	1:2000
Anti-β-actin	42 kDa	Abcam®	Mouse	1:5000
Anti-FLAG	Variable	Abcam®	Mouse	1:2000
Anti-SC35 (nuclear speckle)	90 kDa	Abcam®	Mouse	1:500

SECONDARY ANTIBODIES			
ANTIBODY / TARGET	COMPANY	ORIGIN	DILUTION
Anti-Mouse IgG	Santa Cruz®	Rabbit	1:2000
Anti-Rabbit IgG	Santa Cruz®	Donkey	1:2000
Anti-Goat IgG	Santa Cruz®	Donkey	1:2000

Fig. M.21 - Overview of primary and secondary antibodies employed in Western blotting.

3.7 Yeast two-hybrid screening

Yeast two-hybrid screening (Y2H) is a long established technique for the study of direct protein interactions in the artificial environment of yeast cell nuclei. In this thesis, collaboratively-generated Y2H data were consulted in order to search for Wnt-relevant protein interactions of the Hsa21-encoded kinase DYRK1A (see 4.3.2).

3.7.1 The Jerome LeJeune Foundation interPP project

The Jerome LeJeune Foundation (Paris, France) is a large research charity named after the homonymous pioneering scientist who first identified Hsa21 trisomy in DS. The foundation sponsors a wide variety of multi-disciplinary research aiming to further the understanding of DS and facilitate development of effective therapeutic interventions. One of the ongoing efforts by the foundation is the protein-protein interaction (Inter-PP) project. This decade-long endeavour aims to systematically identify and further characterise direct protein-protein interactions of Hsa21-encoded proteins. The InterPP database is vast, and currently includes hundreds of thousands of detected interactions. Such database is continuously being assembled on behalf of the foundation by a partner company, Hybrigenics Services (S.A.S., Paris, France - <http://www.hybrigenics-services.com>).

Employing Y2H library screening, a high-throughput variant of the original assay, all Hsa21-encoded proteins are tested for any interaction possible. Such interactions are integrated in growing protein networks, and classified according to binding strength and reliability. Overall, the Inter-PP project aims to generate DS-relevant, preliminary protein interaction data for later validation, and is thus heavily collaborative in nature. In this thesis, partnership with the Jerome LeJeune Foundation was established, with the particular aim of identifying the presence of any Wnt signalling-related protein interactors of the kinase DYRK1A. Additionally, the DYRK1A interaction with DKK3 was further characterised by Hybrigenics specifically for this thesis (see, 4.3.2). The techniques, materials and analysis protocols associated with Y2H screening in this thesis are outlined below.

3.7.2 ULTimate Y2H™ Analysis

Y2H screening was performed by Hybrigenics Services. The coding sequence for full length DYRK1A isoform 1 (NCBI reference (NM_001396.3) was PCR-amplified and cloned into pB27 as a C-terminal fusion to LexA (LexA-DYR1A), and into pB29 as an N-terminal fusion to LexA (DYR1A-LexA). The constructs were checked by sequencing and used as a bait to screen a random-primed Adult Brain cDNA library constructed into pP6. pB27 and pB29 derive from the original pBTM116 vector (91), and pP6 is based on the pGADGH plasmid (92). For the N-LexA-DYRK1A-C and the N-DYRK1A-LexA-C bait constructs, 65 million (6.5-fold the complexity of the library) and 115 million (11.5-fold the complexity of the library) clones were screened using a mating approach with YHGX13 (Y187 ade2-101::loxP-kanMX-loxP, mata) and L40ΔGal4 (mat a) yeast strains as previously described (93). 269 and 253 His⁺ colonies, respectively, were selected on a medium lacking tryptophan, leucine and

histidine and 2 mM 3-AT for N-LexA-DYRK1A-C and 5 mM 3-AT for N-DYRK1A-LexA-C to maintain a strong selectivity and manage the slight autoactivation. The prey fragments of the positive clones were amplified by PCR and sequenced at their 5' and 3' junctions. The resulting sequences were used to identify the corresponding interacting proteins in the GenBank database (NCBI) using a fully automated procedure.

3.7.3 PBS scoring

A confidence score (PBS, for Predicted Biological Score) was attributed to each interaction. The PBS relies on two different levels of analysis. Firstly, a local score takes into account the redundancy and independency of prey fragments, as well as the distribution of reading frames and stop codons in overlapping fragments. Secondly, a global score takes into account the interactions found in all the screens performed at Hybrigenics using the same library. This global score represents the probability of an interaction being nonspecific. For practical use, the scores were divided into four categories, from A (highest confidence) to D (lowest confidence). A fifth category (E) specifically flags interactions involving highly connected prey domains previously found several times in screens performed on libraries derived from the same organism. Finally, several of these highly connected domains have been confirmed as false-positives of the technique and are now tagged as F. The PBS scores have been shown by Hybrigenics to positively correlate with the biological significance of interactions.

3.8 Bioinformatics

This section details bioinformatics approaches undertaken for this thesis, namely pathway analysis of RNAseq, database-mediated protein interaction screening for DYRK1A, and assembly of protein interaction networks.

3.8.1 Ingenuity Pathway Analysis

The Qiagen Ingenuity® Pathway Analysis (IPA®) tool was employed to probe mouse and human RNAseq datasets for association with molecular pathways, and particularly Wnt signalling. Tc1 and Dp1Tyb RNAseq analysis was performed on datasets of non-Hsa21/Mmu16 DEX genes at adjusted $P < 0.05$ (Tc1) and $P < 0.01$ (Dp1Tyb). In all cases, IPA analysis parameters were left at default, searching only for direct relationships and for human, mouse and rat orthologs.

3.8.2 STRING and Cytoscape protein interaction network analysis

The protein interaction database and analysis tool STRING v10.0 (58) was employed to probe for DYRK family-Wnt interactions in 4.3.2.1.1, and to build the networks in 4.3.2.1.5. Protein interactions were identified from the human interactome in both cases. For 4.3.2.1.1, each DYRK (1A/B-4) was individually employed as a single starting node, and networks were thereby generated by enriching with the 50 or 100 best-scoring direct interactors. To isolate DYRK-relevant functional associations, networks were limited to primary DYRK interactions, without further enriching. For 4.3.2.1.5, the integrated literature/experimental basic DYRK1A network was enriched twice, with the 10 best-scoring primary and secondary interactors. The network was then imported into the Cytoscape analysis tool (<http://www.cytoscape.org>), and its visual properties were modified to distinguish amongst node types and visually aid description of the results. The network was displayed employing a spring-embedded layout, manually adjusted to reflect the known structure of canonical Wnt signalling.

3.9 Data processing, quantification, statistical analysis and representation

This section discusses data processing, quantification and analysis in all techniques for which this aspect was not otherwise specified in previous methods sections.

3.9.1 Image processing

In all western blots, only minimal image processing was performed, post-quantification, for illustrative purposes only. Raw .sgd files were converted to .tiff and colour-inverted to display background as white/grey. Average brightness was set so as to obtain a grey background and clearly visible, non-overexposed band. Minimum and maximum levels were adjusted slightly (no more than 5-10%) to improve visualisation of bands with a weaker signal, but never to values approaching, or corresponding to, the peak brightness levels. All processing described was performed in imageJ (Fiji version). Figures in 4.2.2.1-4 and 4.3.2.2.2.3 display horizontally cropped sections of representative blots, and black lines indicate where the image was occasionally cropped vertically. All co-IP gels in 4.3.2.1.4 are presented uncropped from 1 representative repeat. For IVIS luciferase experiments in 4.3.2.2.1.4, minimum and maximum display levels were automatically set by the system according to measured signal, independent of quantification.

3.9.2 Western blot quantification

Protein bands were quantified from non-processed, raw image files only, directly at the acquisition stage via the GeneTools® software analyser (Syngene GeneGnome system), by manually selecting an identical area around each gel lane. Automatic background subtraction was applied to all quantified bands, accounting for non-specific luminescence to enhance accuracy of the signal. The resultant values for all proteins of interest were then normalised to amounts of β -actin within the same gel, in order to provide a reliable loading control. For phospho/de-phosphoproteins analysed (active β catenin, pS9 GSK3 β) values were first normalised to β -actin and subsequently to total amounts of the relative protein, which were also normalised to β -actin. Values were further normalised to the mean of the control condition (WT for mice, euploid for human samples, empty vector control for cells) for each individual experimental repeat.

3.9.3 Luciferase assay quantification

For all luciferase experiments, TOP/FOPFLASH values quantified alone (4.3.2.2.1.1-3) or as a ratio to renilla luciferase activity (4.3.2.2.2.1-2) were normalised to the mean control condition signal (i.e. No Wnt stimulation) across all independent repeats. In 4.3.2.2.1.3, the mean normalised signal of treated cells with LiCl + 0.01% DMSO was assumed as maximum response and all other values expressed at percentages. For IVIS experiments in 4.3.2.2.1.4, preset circular regions of interest (ROIs) were applied to each well, and background was automatically corrected for by subtracting from an average background ROI. For all sample groups, mean, SD and SEM were calculated.

3.9.4 Confocal imaging quantification

Confocal data collected from the Zeiss 710 was used to quantify the nuclear to cytoplasmic ratio of HA-DYRK1A under Wnt stimulation and control conditions. Bitplane (IMARIS) was used to create masks to the nucleus and entire cellular volume. Alexa 488 conjugated HA-DYRK1A fluorescence intensity was integrated across both masks. The nuclear signal was subsequently subtracted from the signal of the entire cellular volume, providing cytoplasmic HA-DYRK1A fluorescence. Data is displayed as a ratio of nuclear to cytoplasmic fluorescence intensity.

3.9.5 Statistical analysis and graphs

RNAseq data was analysed by Deseq. All P values reported were adjusted for false discovery rate (FDR). IPA-generated P values reported for canonical pathway analysis and disease function analysis were produced by Fisher's exact test and thresholded at $P < 0.05$. STRING protein interaction networks for the DYRK family were analysed by STRING, correcting for FDR. All other statistical analyses were performed in GraphPad Prism 07a. For mouse biochemistry, qPCR and DYRK1A expression experiments, reported P values were calculated by two-tailed t-test. For all Luciferase experiments, one-way ANOVA with post-hoc Sidak's multiple comparisons test was employed. For dose-response curve experiments in 4.3.2.2.1.3, linear regression was calculated on % of maximum (LiCl + DMSO) values, throughout the entire dose range of 1-100 μM . All heat maps and box plots were created in GraphPad Prism 07. In all cases, box span represents first to third quartiles, bands represent the median of each sample group, and whiskers represent minimum/maximum values. Throughout this thesis, relative 'increases' were colour coded as red and 'decreases' as blue, in a combination of hues safe for all types of colour vision deficiency. See relevant sections of materials and methods for additional details on quantification and processing methods employed.

For all qPCR as well as mouse and human DS immunoblotting experiments, samples were quantified in technical triplicate (qPCR) or duplicate (others), and the resultant values were averaged. The reported n for these experiment thus represent the number of individual tissues employed. For example, $n=8$ Tc1 hippocampal samples indicates analysis of 16 total samples (including 8 WT controls) measured twice (total of 32 values quantified) in separate gels and averaged. For all cell-based experiments, a minimum of three independent repeats were performed on separate days. For each experimental condition under study, multiple biological replicates were employed in order to improve measurement accuracy. All signal values obtained from replicates were however averaged prior to analysis. In this case, therefore, all reported n represent the number of independent repeats, and the data were analysed accordingly.

Experimental RESULTS

4

RESULTS

Analysis of the DS transcriptome

4.1

Chapter 4.1 - Analysis of the DS transcriptome

4.1.1 Introduction

The importance of transcriptomic analysis in DS, along with the key findings in the field, were discussed in the main introduction (1.4.1). In this respect, two notions are crucial: **1)** Genome-wide transcriptional alterations beyond Hsa21 are invariably present in DS models and humans. **2)** The differential expression of both Hsa21 and secondarily affected genes is highly variable between individuals, and amongst individual studies. Such variability, akin to that observed in the euploid population, is thus a key feature of the DS transcriptome. This chapter discusses analysis of gene expression data generated from two murine models of DS, the Tc1 (1) and Dp1Tyb (2) (see 1.1.5), via RNA sequencing (RNAseq). The principal aim was to probe the hippocampal transcriptome of these models, in order to confirm their aneuploid status. RNA sequencing also served to investigate the presence of genome-wide transcriptional alterations beyond Hsa21 or Mmu16 genes in the hippocampus of the two models. Additionally, gene expression data was also employed to preliminarily determine the *presence* of any altered Wnt-relevant genes. A dual strategy was undertaken, combining RNA sequencing technology with bioinformatic pathway analysis tools.

4.1.1.1 Ingenuity Pathway Analysis: a reliable and validated approach

QIAGEN Ingenuity® Pathway Analysis (IPA®) is a powerful tool intended for the search and analysis of 'omics datasets. The software features a proprietary knowledge base, which employs text-mining of existing scientific literature to extrapolate significance from large datasets. The most common usage of IPA by far has been in the analysis of transcriptomics or proteomics data. The software can be supplied with large lists of DEX genes, along with their respective fold changes and statistical significance values. IPA can then determine the biological meaning of such data, by **1)** linking each gene to known biological functions and cellular compartments and **2)** Identifying significantly altered signalling pathways by pooling the expression values of associated genes together (4.1.2.1-3.1). **3)** Identifying which biological and diseases processes are significantly associated with observed expression patterns, and predict if they are enhanced or suppressed (4.1.2.1-2.3). Taken together, these features allow for meaningful and unbiased investigation of 'omics data.

Indeed, the usage of IPA has been established and validated throughout the last decade, with hundreds of studies employing this tool. Two examples in the context of DS have already been discussed (3, 4). Specialised literature to guide the appropriate usage of IPA also exists (5). Indeed, this strategy has already been adopted to investigate the Wnt signalling pathway in literature reports. A 2010 study (6) employed IPA to analyse the transcriptome of tumour-associated macrophages. The authors demonstrate that their known ability to facilitate tumour invasion is mediated by an enhancement of Wnt signalling activity. This was identified by IPA as a significant enrichment in Wnt-related DEX genes

in tumour-associated macrophages. Similarly, in the context of ischaemic heart disease, a recent study employed IPA to determine signalling pathways responsible for tissue factor-mediated thrombosis (7). The transcriptome of tissue factor-silenced human vascular smooth muscle cells was compared to wild-type tissue. The IPA analysis revealed significant dysregulation of Wnt signalling components. These studies provide proof of concept of the reliability and sensitivity of IPA in the analysis of gene expression datasets.

Overall, RNAseq and IPA were employed to answer three key experimental questions, addressed in the results section (4.1.2):

- I. Are DS-related Hsa21 and Mmu16 genes significantly overexpressed in the Tc1 and Dp1Tyb mouse hippocampus? Ie, are these true models of aneuploidy?
- II. Do any of the DEX genes in Tc and Dp1Tyb mice correlate with Wnt signalling at all?
- III. Which biological/disease functions are associated with expression patterns?

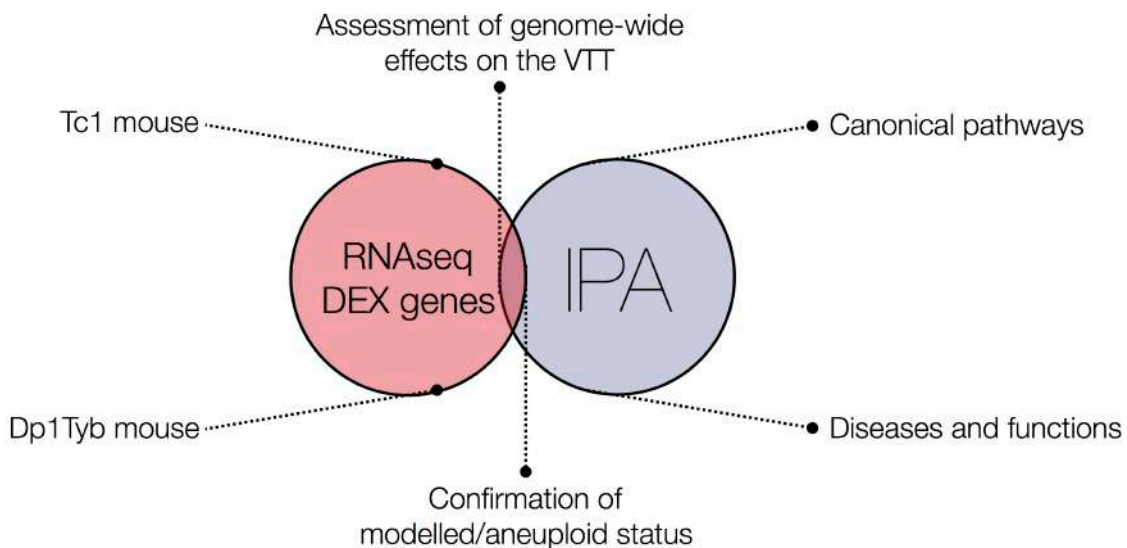


Fig. R1.a - Conceptual overview of strategy undertaken in results section 4.1.2, harmonising existing literature approaches discussed in introduction 4.1.1 with modern RNA sequencing and pathway analysis tools.

4.1.2 Results

4.1.2.1 Tc1 mouse

The Tc1 mouse model incorporates a near-complete Hsa21 (1) (see 1.2.5.2) and is functionally trisomic for about 75% of protein coding genes from Hsa21, spanning both arms of the chromosome. This mouse strain is genetically trisomic for both *DYRK1A* and *APP*, but the latter gene is not functionally overexpressed.

4.1.2.1.1 DEX genes and Canonical Pathway analysis

Following RNA isolation from $n=3$, age-matched Tc1 and WT mouse hippocampi at 3 months of age, the resultant material was reverse transcribed into cDNA (see 3.1) in order to obtain a stable template for subsequent use. RNAseq was then performed along with statistical testing to determine which genes were differentially expressed (DEX) in the Tc1 hippocampus. Since Hsa21 genes in the Tc1 mouse are human, they are not present in WT control RNA. In order to reliably assess their expression levels, all Hsa21 gene reads in the Tc1 group were summed to the amounts of each relevant Mmu ortholog, thus allowing for meaningful comparison with WT expression (see chapter 3).

Results revealed significantly elevated expression of 148 human genes from Hsa21 (**Fig. R1.1a-b**), in accordance with previous reports on the known Tc1 genetic makeup (8). Whilst a number of Hsa21 genes were found to be duplicated or deleted (*APP*), most of the key DS-related genes, including *DYRK1A*, were significantly overexpressed around 1.5-fold (**Fig. R1.1b**). Because the aim of this study was to determine genome-wide gene expression changes, these results were not included in the subsequent pathway analysis, in order to restrict the scope to non-Hsa21 genes secondarily affected by the additional chromosome. Setting the significance cutoff at $P<0.05$, RNAseq then identified 62 DEX genes in the Tc1 hippocampus (**Fig. R1.2**), spanning virtually all Mmu chromosomes (**Fig. R1.3**).

Taken together, these data demonstrate the presence of overexpressed Hsa21 genes in the Tc1 hippocampus, confirming its aneuploid status. Thus, this mouse can be considered a reliable DS model for subsequent use (see 4.2.2). Additionally, RNAseq also demonstrated the presence of genome-wide transcriptional alterations in the Tc1 hippocampus, beyond Hsa21. This is a well described phenomenon known to occur in both DS models and humans, as introduced (see 1.4).

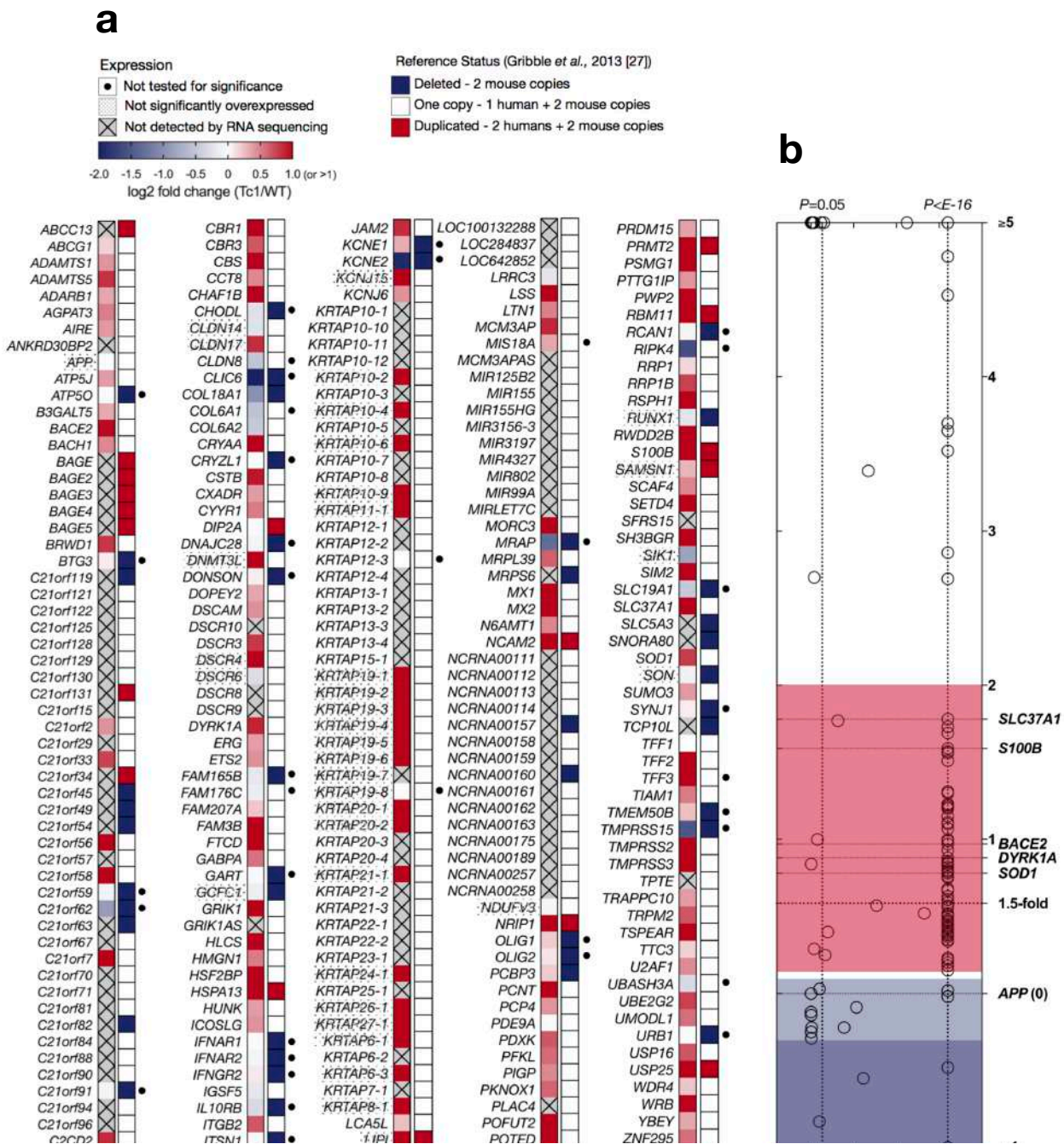


Fig. R1.1 - Overview of Hsa21 genes in the Tc1 mouse hippocampus ($n=3$, $P<0.05$), as detected by RNAseq. **a.** Expression levels of 148 Hsa21 genes which could reliably be measured and tested for significance, presented alphabetically and color-coded according to \log_2 fold change/WT. The known status of all genes, previously determined by Gribble *et al.* (2013), is shown alongside as reference. **b.** Expression levels plotted as a function of significance, highlighting AD-DS-relevant genes and demonstrating the presence of several genes not functionally trisomic (blue), including *APP*.

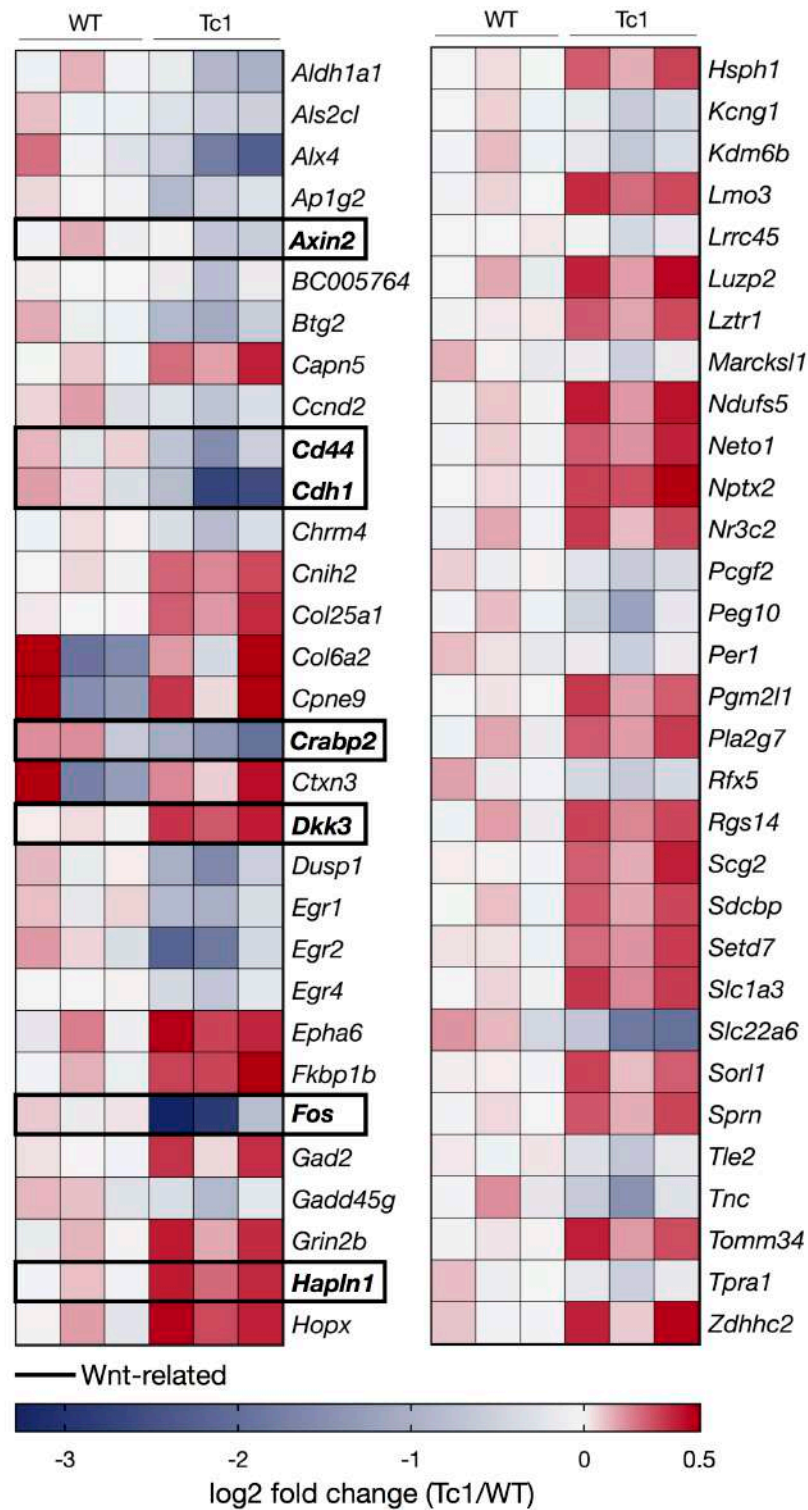


Fig. R1.2 - Mmu DEX genes in the Tc1 mouse hippocampus secondarily affected by Hsa21 trisomy. Heat map represent expression levels of 62 Tc1 DEX genes ($n=3$, $P<0.05$), demonstrating the occurrence of genome-wide, bidirectional transcriptional alterations. Wnt-related genes detected by IPA are highlighted in bold.

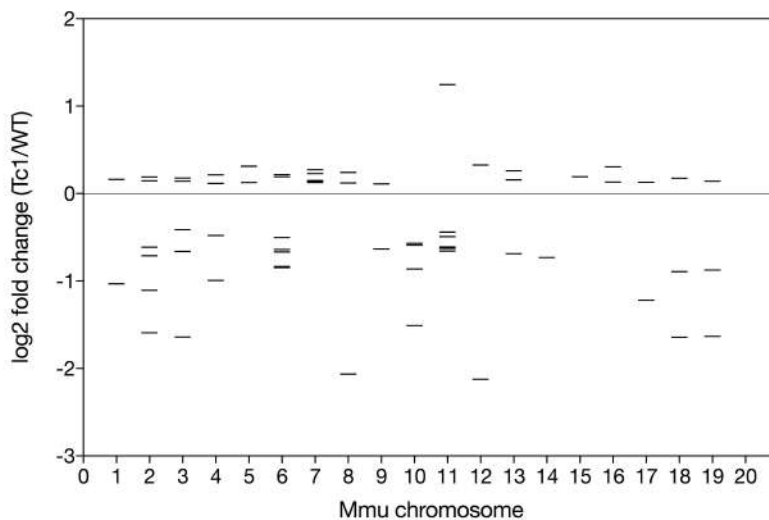


Fig. R1.3 - Mmu DEX genes in the Tc1 mouse hippocampus. The 62 Tc1 DEX genes ($n=3$, $P<0.05$) are displayed arranged by chromosomal number, demonstrating genome-wide, bidirectional transcriptional alterations.

Following, the non-Hsa21 DEX gene list, along with all associated fold changes relative to WT, was analysed employing IPA. The software was instructed to search for expression patterns associated with known signalling pathways. With preliminary relevance to this thesis, IPA detected a strong association of the dataset with canonical Wnt signalling ($P=0.00173$) for seven DEX genes (**FigR1.2, bold**). These were *Dkk3*, *Axin2*, *Cdh1*, *Cd44*, *Crabp2*, *Fos* and *Hapln1*.

As introduced previously, *dkk3* is a secreted Wnt modulator with both antagonistic and stimulating properties (9, 10), part of the dickkopf family of genes and possessing known associations with hippocampal development, neurogenesis and AD pathology. RNAseq revealed *dkk3* to be aberrantly overexpressed in the Tc1 hippocampus. *Axin2*, which was found to be decreased, is a Wnt target gene related to the beta-catenin destruction complex protein axin. It is thought to function as negative feedback modulator, being activated by beta-catenin itself and subsequently dampening Wnt signalling activation (11, 12). *Axin2*, similarly to *dkk3*, has also been shown to participate in hippocampal development. Both *cd44* and *cdh1* are known Wnt-associated genes with roles in immune system function and cancer development, respectively. The former is a known Wnt target gene, meaning its expression may correlate with pathway activity. Both were found to be significantly decreased by RNAseq. Another Wnt-associated DEX gene identified was *fos* (c-fos). This is a well described stress-responsive human proto-oncogene, which encodes the principal member of the fos family of transcription factors. It is also a recognised Wnt target, with multiple studies linking its expression to Wnt signalling activation (13-15). In the Tc1 hippocampus, *fos* levels were found to be significantly down-regulated. In fact, *fos* had the largest single decrease in the entire dataset, corresponding to approximately 7/8-fold. Additionally, the DEX gene cellular retinoic acid-binding protein II (*Crabp2*) is also associated with Wnt signalling, albeit the evidence is much weaker. This gene encodes a protein with demonstrated importance to neural axis anteroposterior patterning in *Xenopus*, and has been charac-

terised as an indirect target of Wnt signalling activation (16). Additionally, its human relative *CRAPB1* has been shown to participate in expansion on the neural crest in the developing CNS, a process tightly regulated by Wnt signalling (17). Similarly to *fos*, a significant decrease in *crabp2* expression was observed in the Tc1 mouse hippocampus. Finally, hyaluronan and proteoglycan link protein 1 (*Hapln1*) which was upregulated, has also been recently linked to Wnt signalling. Bioinformatics approaches have identified human *HAPLN1* as a downstream target of Wnt signalling activation (18). In the context of human cancer, *de novo* *HAPLN1* expression has been identified as marker of Wnt-induced development of aggressive hepatocellular carcinoma (19). However, little evidence exists investigating *HAPLN1* and Wnt signalling, and it is possible that the relationship between this gene and the pathway may be spurious. Overall, this first level of analysis preliminarily indicates that, in the Tc1 hippocampus, seven non-Hsa21 DEX genes may be associated with Wnt signalling (**Fig. R1.4**).

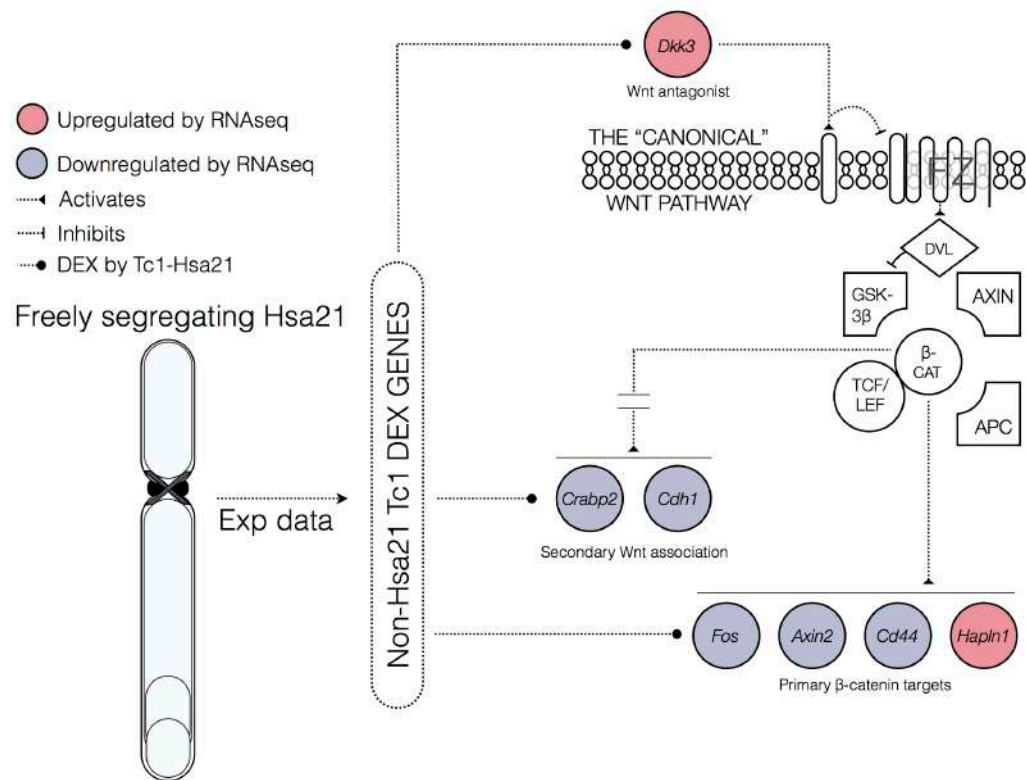


Fig. R1.4 - Contextualised overview of RNAseq-observed levels of Wnt-relevant DEX genes in the Tc1 mouse hippocampus. Genes are colour-coded according to observed up-/downregulation.

4.1.2.1.2 Diseases and functions

Following pathway analysis, the RNAseq data was probed for associations with known diseases or functions by IPA, employing its proprietary annotation database which is similar in intent and scope to Gene Ontology (GO) annotations. Results identified a number of processes potentially altered in the Tc1 hippocampus (**figure R1.5**). A z-score was also generated to predict the direction of change of each annotation. Several mechanisms associated with neurodegeneration were found to be enhanced (eg 'apoptosis of neurons'), whilst terms linked to cell proliferative mechanisms were suppressed (eg 'cell cycle progression'). Accordingly, the Tc1 hippocampus has reportedly lower synaptic density with dysfunctional dentate gyrus-CA3 connectivity (20) and learning deficits (1). The Tc1 mouse also displays increased spontaneous locomotion (21), and the term 'hyperactive behaviour' registered a positive z-score. Interestingly, several of the terms listed are also associated with canonical Wnt signalling. Two prominent examples include the term 'cell proliferation of tumour cell lines' and 'apoptosis of neurons'. The former process is a well known outcome of Wnt signalling dysregulation (22-24), with decades-long research efforts implicating the pathway in cell proliferation. The term was downregulated in the analysis. Neuronal apoptosis, on the other hand, was found to be enhanced. The role of Wnt signalling in this disease process has been substantiated in more recent years, particularly in the context of Alzheimer's disease (25, 26). Other significantly affected functions, such as 'invasion of tumour cell lines' and 'neuronal cell death' are also associated with Wnt signalling by the same lines of evidence. Overall, the disease and function analysis aided in demonstrating the reliability of the RNAseq and IPA analysis, by identifying altered neuronal mechanisms already reported in the Tc1 mouse.

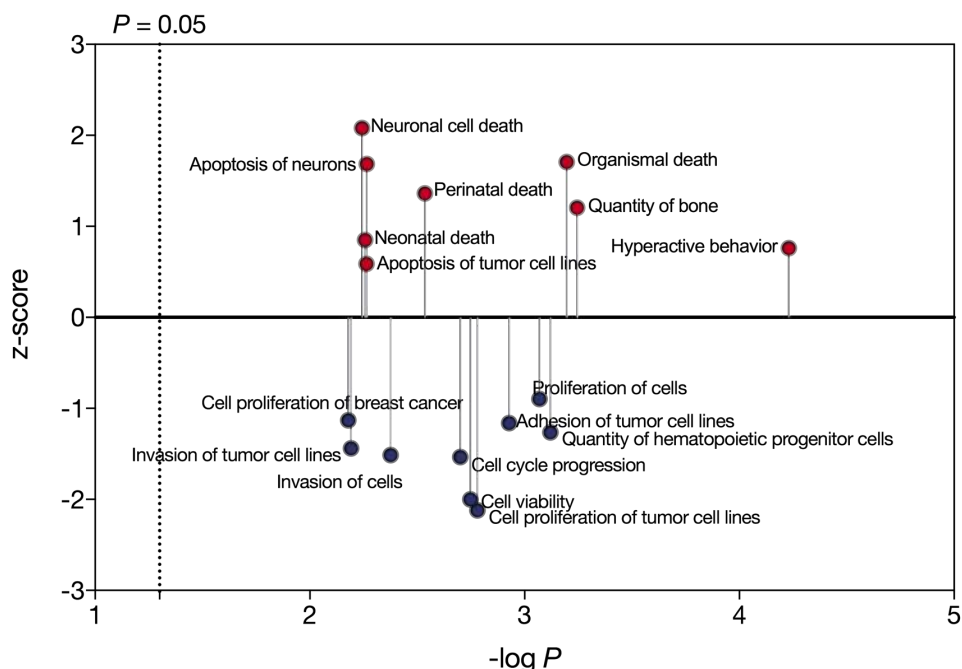


Fig. R1.5 - Diseases and functions analysis generated by IPA according to overall expression patterns of 62 Tc1 DEX genes, plotting activation z-scores as a function of significance. In accordance with known Tc1 phenotypes, the report indicates upregulation (red) of neurodegenerative processes and hyperactive behaviour. By contrast, mechanisms associated with cell proliferation are downregulated (blue).

4.1.2.2 Dp1Tyb mouse

The Dp1Tyb mouse model contains a duplication of the Mmu16 region syntenic to the proximal portion of the Hsa21 long arm, approximately spanning q11.2-q22.2 (2). This is by far the largest Hsa21 syntenic region, corresponding to 48% of protein-coding genes of the human chromosome (27, 28). As introduced (see 1.1.5), the Dp1Tyb mouse is essentially similar to the Ts1Yey model (29, 30), possessing a duplication of the same region. This strain functionally overexpresses both DYRK1A and APP. However, it must be stressed that the Dp1Tyb mouse, unlike the Tc1, should be considered as a partial model of DS, since only Mmu16 orthologs to Hsa21 are duplicated. This model is however useful to further dissect the differential contribution of Hsa21 genes to DS, given that overexpression is limited to a fraction of Hsa21 orthologs. These, importantly, include the DSCR (see 1.1.2). The RNAseq and subsequent analysis were performed in a similar manner to the Tc1 mouse.

4.1.2.2.1 DEX genes and Canonical Pathway analysis

Following RNA isolation from $n=5$, age-matched 4 months old Dp1Tyb and WT mouse hippocampi, the resultant material was reverse transcribed into cDNA, sequenced and analysed as in 4.1.2.1.1. Results demonstrated significantly elevated expression of 106 Mmu16 genes spanning the duplicated region (*Lipi-Zbtb21*) as previously described (**Fig. R1.6a-b**, (2)). Similarly to the Tc1 mouse, these results demonstrate the presence of overexpressed Mmu16-Hsa21 ortholog genes in the Dp1Tyb hippocampus, confirming their duplicated status. Thus, this mouse can also be considered a reliable partial DS model for subsequent use (see 4.2.2). Importantly, both *Dyrk1a* and *App*, essential in DS and AD-DS, were significantly overexpressed about 1.5-fold. These data were not included in the subsequent IPA analysis, as in 4.1.2.1.1. Following, RNAseq identified genome-wide transcriptional alterations beyond Mmu16, as observed in the Tc1 hippocampus. At a cutoff of $P<0.01$, 202 non-Hsa21-Mmu16 DEX genes were detected (**Fig. R1.7**), spanning all mouse chromosomes, (**Fig. R1.8**). This DEX gene list, however, did not display a significant Wnt association by IPA ($P=0.057$). Despite this, the dataset contained seven DEX genes linked to Wnt signalling (**Fig. R1.7, bold**). These were *Fzd2* (frizzled-2), *Axin2*, *Podxl* (Podocalyxin), *Rspo1* (R-spondin1), *Sox11/12* and *Hapln1*.

The protein Fzd2 is a transmembrane receptor essential for canonical Wnt signalling activation (1.2.1). In the Dp1Tyb hippocampus, it was found to be downregulated. The expression of this receptor is known to be altered in several human cancers (31, 32). *Podxl* is a known marker of embryonic stem cell pluripotency (33), and its expression levels have been shown to correlate with Wnt signalling activation (34). *Rspo1* is a particularly interesting DEX gene. It is a well described secreted regulator of Wnt signalling, and potently promotes activation of the pathway in the context of ovarian development (35) and angiogenesis (36). It is thought to antagonise the action of the Wnt inhibitor DKK1 (37) and to bind to receptors dedicated to Wnt signalling modulation, LGR4/5 (38). In the Dp1Tyb, *Rspo1* expression was found elevated. Similarly to the Tc1 mouse, *hapln1* expression was also increased in the Dp1Tyb line.

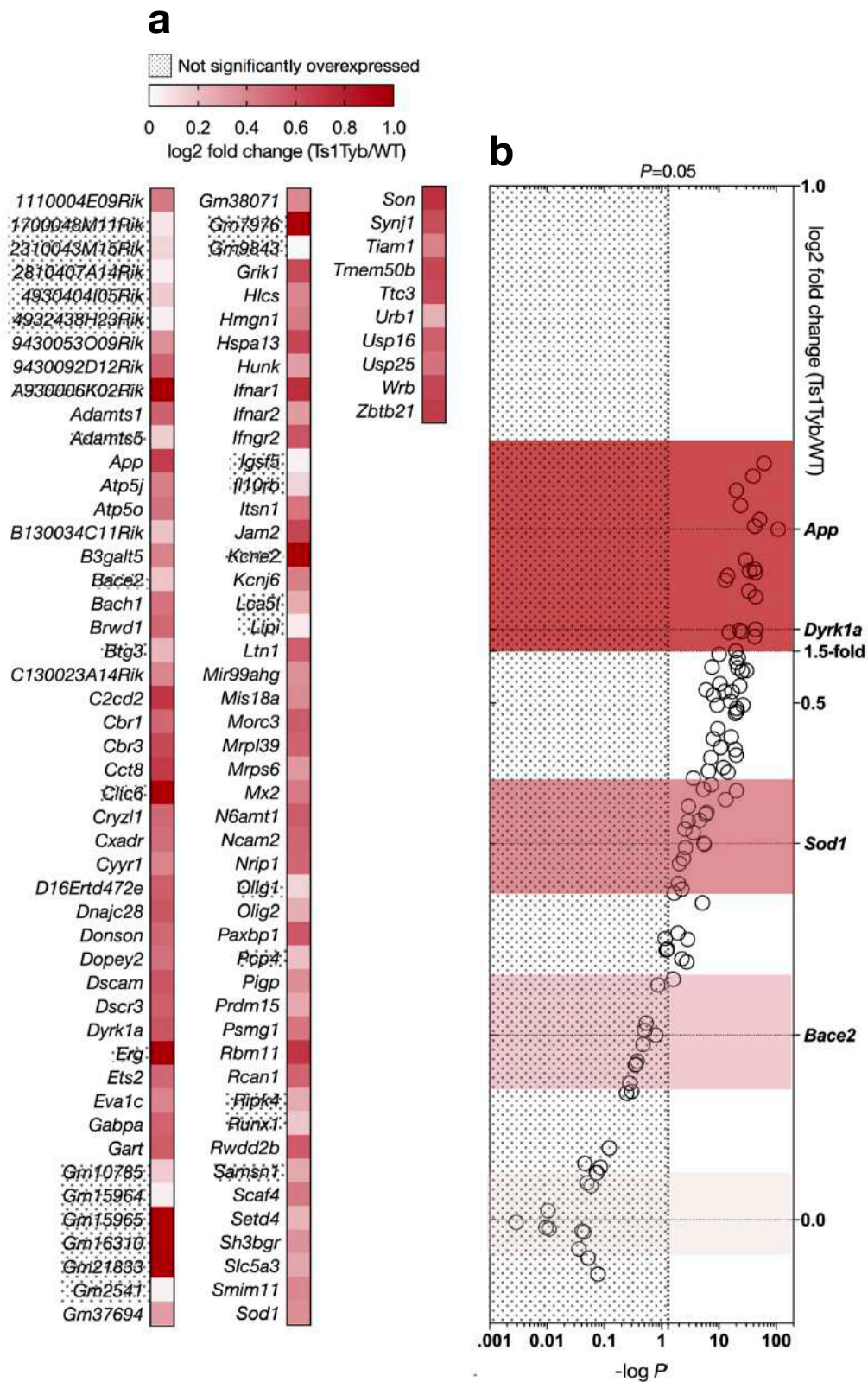


Fig. R1.6 - Overview of Mmu16 genes spanning the duplicated region (*Lipi-Zbtb21*, [2]) in the Dp1Tyb mouse hippocampus ($n=5$, $P<0.05$), as detected by RNAseq. **a**. Expression levels of 106 Mmu16 genes, presented as in **R1.1a**. **b**. Expression levels plotted as in **R1.1b**, highlighting AD-DS-relevant genes and demonstrating the presence of several genes not significantly duplicated (dot pattern in both panels). The theoretical 1.5-fold threshold is highlighted, indicating a minority of Mmu16 genes as more likely responsible for observed expression patterns and phenotypes.

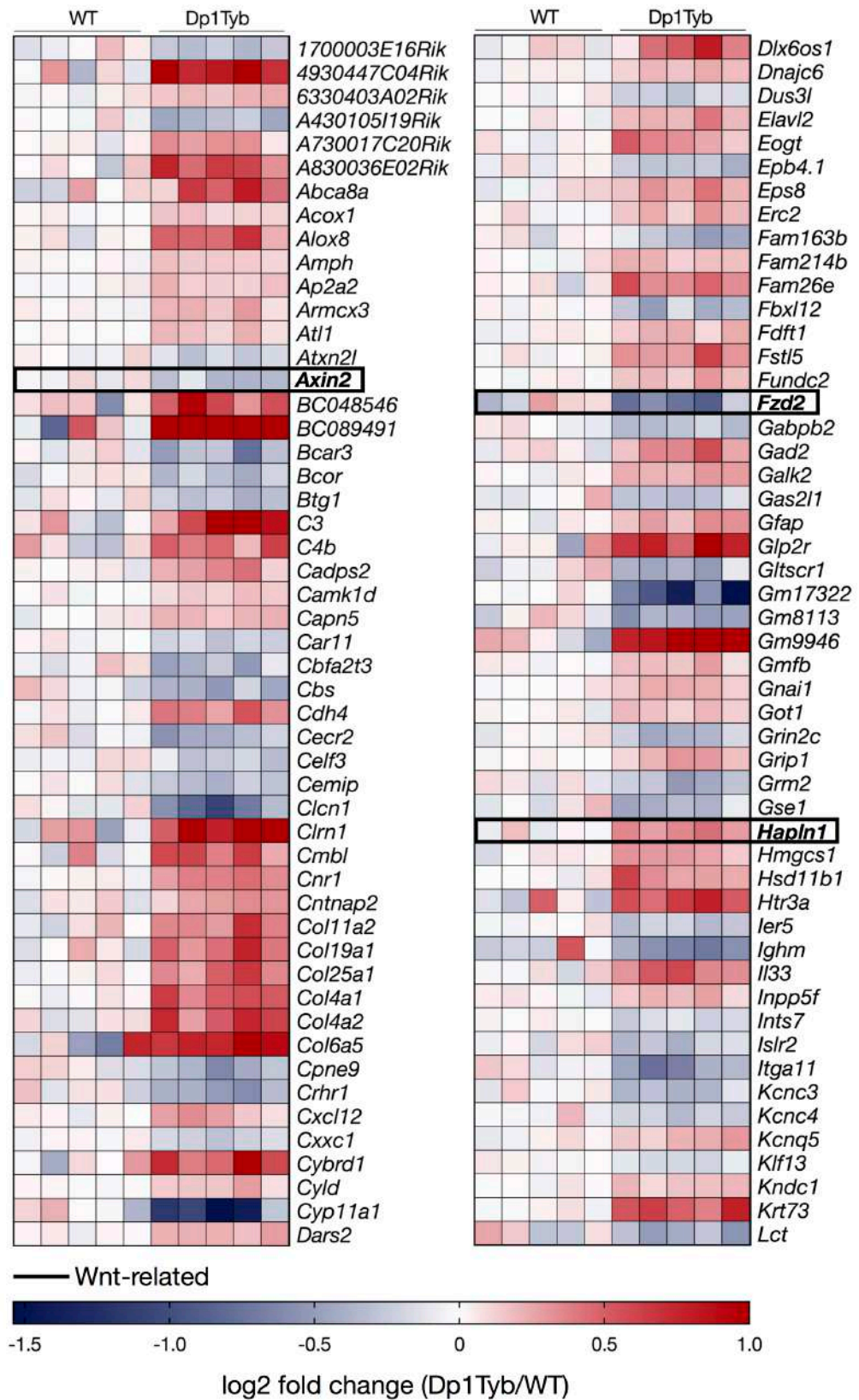


Fig. R1.7 - Mmu DEX genes in the Dp1Tyb mouse hippocampus secondarily affected by Mmu16 duplication. Heat map represent expression levels of 202 Dp1Tyb DEX genes ($n=5$, $P<0.01$), demonstrating the occurrence of genome-wide, bidirectional transcriptional alterations. Wnt-related genes detected by IPA are highlighted in bold.

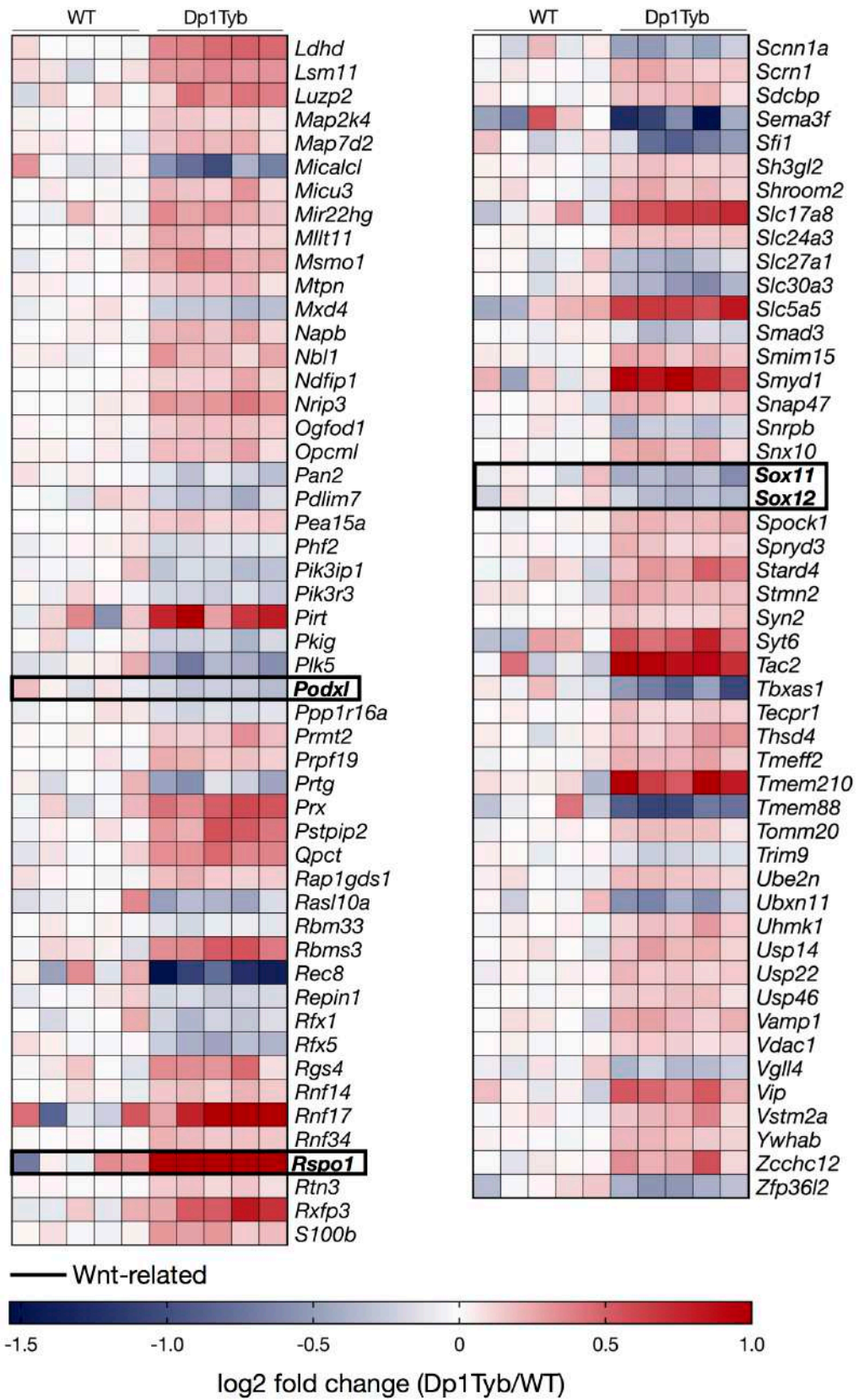


Fig. R1.7 (contd.) - Mmu DEX genes in the Dp1Tyb mouse hippocampus.

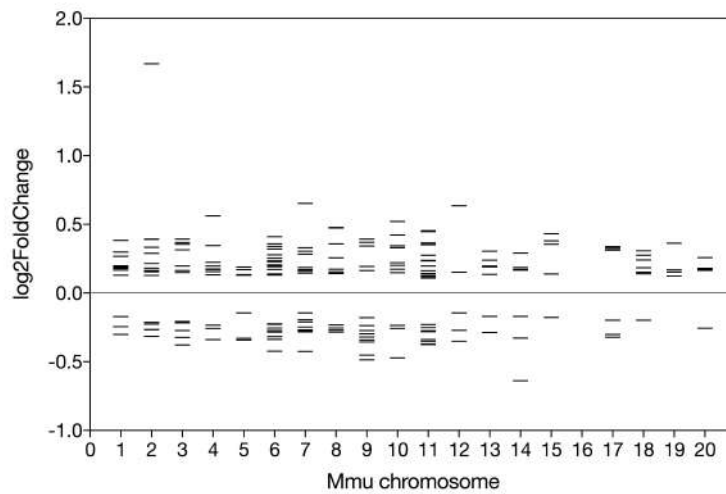


Fig. R1.8 - Mmu DEX genes in the Dp1Tyb mouse hippocampus. The 201 Dp1Tyb DEX genes ($n=5$, $P<0.01$) are displayed arranged by chromosomal number, demonstrating genome-wide, bidirectional transcriptional alterations.

Overall, IPA analysis did not indicate an association of Dp1Tyb hippocampal gene expression with Wnt signalling. Thus, these data are not sufficient to infer a functional link between the pathway and observed transcriptional changes. Nevertheless, it can be objectively stated that hippocampal Dp1Tyb RNAseq does indicate altered expression of seven genes related to Wnt signalling (**Fig. R1.9**).

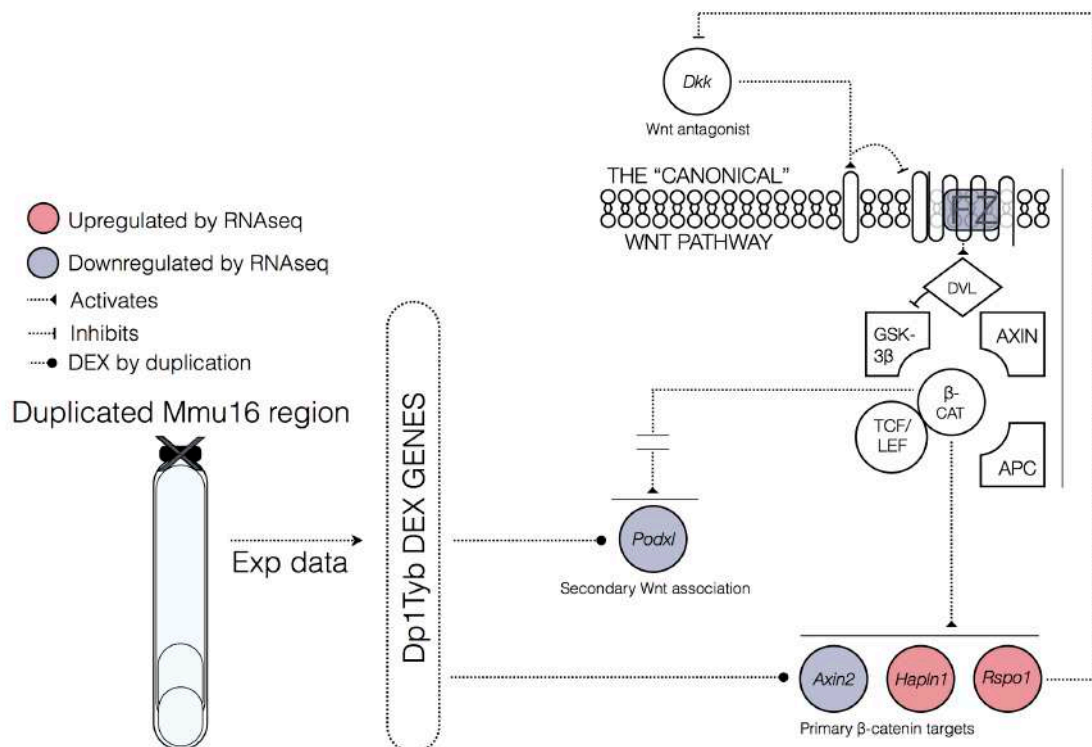


Fig. R1.9 - Contextualised overview of RNAseq-observed expression levels of Wnt-relevant genes in the Dp1Tyb mouse hippocampus. Genes are colour-coded according to observed up-/downregulation.

4.1.2.2.2 Diseases and functions

In the Dp1Tyb mouse, disease and function analysis was performed as in 4.1.2.1.3 (Fig. R1.10). The analysis revealed alterations in terms linked to enhanced proliferative and neuronal developmental processes (eg ‘sprouting’) and reduced long-term potentiation (LTP). The latter finding is in line with previous studies in mice with duplications in Mmu16 regions syntenic to Hsa21, which clearly demonstrated LTP deficits (30, 39, 40). Interestingly, several of the upregulated processes are known to be affected by Wnt signalling activity, similarly to the Tc1 mouse. Two important examples with relevance to hippocampal function include ‘branching of neurites’ and LTP. The former mechanism has been linked to Wnt signalling, particularly in the context of neuronal development (41, 42). Wnt activation has been consistently associated with positive regulation of neurite branching and axonal guidance. Here, this process was found to be upregulated, suggesting the potential presence of overactive Wnt signalling. Moreover, the key process in memory formation, LTP, has also been shown to be affected by Wnt signalling activity. Wnt ligand secretion is known to regulate hippocampal LTP in direct correlation with synaptic activity (43), and activity of the pathway is an established contributor to memory formation (44).

Overall, this analysis provided additional insight into the effects of altered gene expression in the Dp1-Tyb mouse hippocampus. Similarly to the Tc1 mouse, the presence of dysfunctional processes already described in the Dp1Tyb mouse strengthens the reliability of the RNAseq/IPA approach.

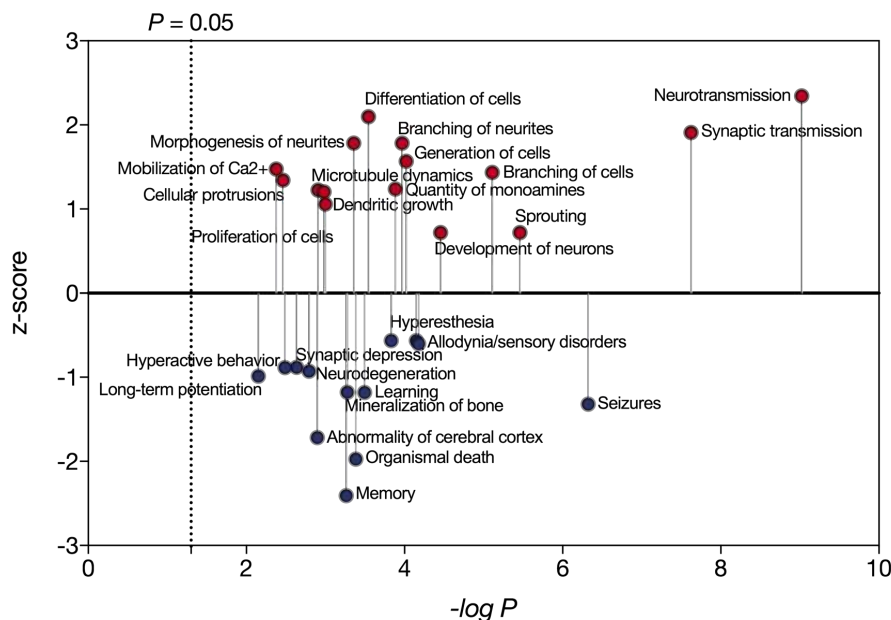


Fig. R1.10 - Diseases and functions analysis generated by IPA according to overall expression patterns of 202 Dp1Tyb DEX genes, plotting activation z-scores as a function of significance. In accordance with known Dp1Tyb phenotypes, the report indicates downregulated (blue) LTP. Mechanisms associated with cell differentiation and neuronal development are upregulated (red).

4.1.3 Discussion

4.1.3.1 Key conclusions on the aneuploid status of Tc1 and Dp1Tyb mice

The studies described in this chapter investigated the hippocampal transcriptome of 2 established DS mouse models via RNAseq. This primarily allowed for quantitative analysis of expression profiles in two gene groups: **1)** Primary DS-related genes, which undergo duplication in humans affected by trisomy 21 (**Fig. R1.1/6**), and **2)** Secondly affected genes beyond Hsa21/Mmu16, with transcriptional alterations spanning all mouse chromosomes (**Fig. R1.2-3/7-8**).

The former group is represented by detectable Hsa21 genes in the Tc1 mouse, and by Mmu16-Hsa21 orthologs in the Dp1Tyb. For both models, the majority of theoretically duplicated genes was overexpressed, with the notable exception of *APP* in the Tc1 mouse. Importantly, all other genes relevant to DS and AD-DS were detected at or around 1.5-fold overexpression (**Fig. R1.1/6**). Key examples include *DYRK1A* (see 4.3 for a detailed overview), *SOD1*, *BACE2*, and *S100B*. These data provided evidence on the aneuploid status of Tc1 and Dp1Tyb mice. In accordance with previous studies (1, 2, 8), the RNAseq performed here confirms the expected overexpression of key DS-related genes. Therefore, it can be stated that based on available data, these models at least partly recapitulate gene expression patterns observed in human DS, notwithstanding their limitations. Such conclusion is crucial to this thesis, as it supports the employment of Tc1 and Dp1Tyb mice in further studies (see 4.2.2). It is also worth noting that, with respect to the Tc1 mouse, the confirmed absence of *APP* overexpression allows for the prediction that any potential Wnt signalling phenotypes, investigated later, are unlikely to be mediated by said gene in this model.

Analysis of the latter gene group also demonstrated a key point. That is, modelled aneuploidy produced significant, genome-wide alterations in expression profiles for both mice investigated. It follows that overexpression of DS-related Hsa21-Mmu16 genes alone is sufficient to induce secondary transcriptional changes affecting a high number of genes. As discussed in the general introduction (see 1.4), the occurrence of this phenomenon in both DS models and humans is well described. A multitude of studies in fact indicates that, in DS, altered gene expression is not limited to Hsa21 genes, albeit with high variability. In this respect, the literature-consistent observations made here demonstrate the DS-like status of the mice employed, and further justify their use in later studies.

4.1.3.2 Comparative assessment of Tc1 and Dp1Tyb mice

To aid interpretation of the experimental data generated here, it is important to compare and contrast the two DS models employed. Whilst both mice essentially attempt to recapitulate trisomy 21, they indeed present significant differences. First and foremost, their genotypes differ extensively. The Tc1 mouse possesses a freely-segregating, near complete Hsa21 (1, 8). Germ line transmission of the human chromosome is somewhat inefficient, and these mice also display mosaicism. Furthermore,

some Hsa21 genes are deleted, whilst others are triplicated and thus present in four copies (**Fig. R1.1**). Despite these limitations, the Tc1 mouse does overexpress the vast majority of *human* genes altered in DS, and displays several phenotypes observed in humans. Compared to other available DS models, the Tc1 is perhaps one of the most accurate representation of the syndrome. The Dp1Tyb, on the other hand, can hardly be considered a true, full model of DS *per se*. It must be stressed that this mouse only displays *partial* trisomy, in the form of a selectively duplicated portion of Mmu16, containing several Hsa21 orthologs. Thus Dp1Tyb models overexpress *mouse* genes, which represent only a part of the DS genotype. Indeed the duplicated region includes the DSCR, along with genes known to be critical for the occurrence of DS and associated pathologies (e.g.: *Dyrk1a*, *App*, *Bace2*, *Sod1*, *Tiam1*). Importantly, The Dp1-3 models were originally developed with the purpose of isolating duplications of Hsa21 orthologs on Mmu10, 16 and 17, respectively (39, 45). Each model thus retains a fraction of Hsa21 trisomy. Only when triple-crossed do Dp mice truly possess full trisomy. Therefore, studies performed on the Dp1Tyb mouse alone should not be taken as investigations of a true DS-like phenotype. Rather, they should serve as a tool to dissect the contribution of Mmu16-Hsa21 orthologs to DS.

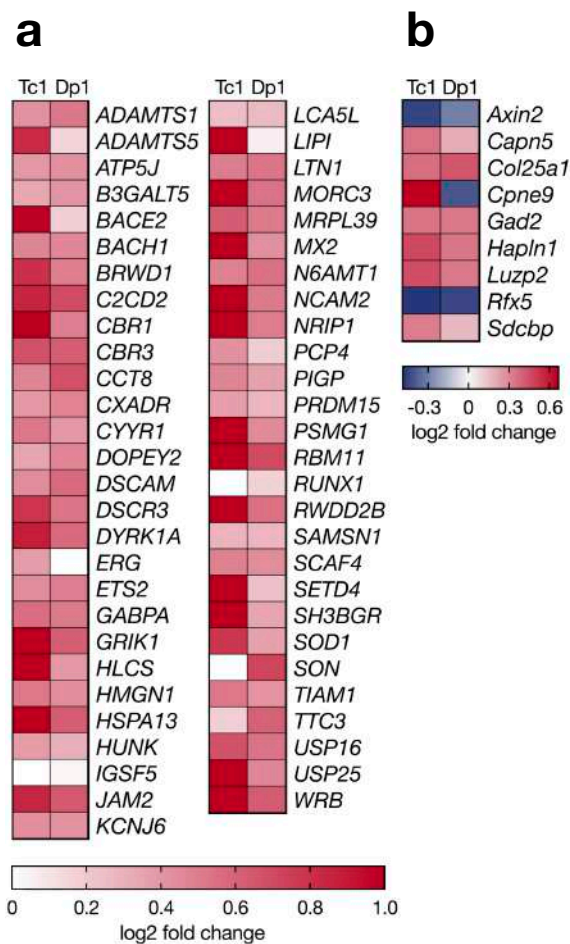


Fig. R1.11 - Comparative expression levels of overlapping DEX genes in Tc1 and Dp1Tyb mice. **a.** Hsa21-Mmu16 genes. **b.** Secondary DEX genes. In the vast majority of cases, expression levels correlated.

The marked differences between Tc1 and Dp1Tyb mice are clearly reflected by the RNAseq data presented here. Whilst both models overexpressed a high number of DS-related genes, only partial overlap was observed. Out of the 148 (Tc1) and 106 (Dp1Tyb) Hsa21-Mmu16 genes detected by RNAseq, just 55 actually overlapped and were overexpressed in both (**Fig. R1.11a**). Amongst these, however, featured a number of key players in DS (*DSCR3*, *DYRK1A*, *BACE2*, *SOD1*, *TIAM1*). The remaining 93 Hsa21 (Tc1) and 51 Mmu16 (Dp1Tyb) DEX genes did not match between the two. This clearly implies potentially significant differences in the phenotypic outcomes of Tc1 versus Dp1Tyb transcriptomes. It follows that direct comparison of the two models is not necessarily a reliable approach. Instead, the Dp1Tyb model should be seen as a means to isolate the effects of those Hsa-Mmu16 orthologs which do overlap with the Tc1 mouse. That is, the presence of a specific phenotype in both mice might be ascribed to the function of said genes. These differences are further highlighted

Chapter 4.1 - Analysis of the DS transcriptome

by comparative analysis of secondarily affected genes. Both models displayed genome-wide transcriptional alterations, as seen in human DS. However, out of the 62 (Tc1) and 202 (Dp1Tyb) non-Hsa21/Mmu16 DEX genes, only 9 overlapped (**Fig. R1.11b**). All overlapping genes excluding Cpne9 correlated in expression level. In the context of this thesis, it is worth specifying that out of these 9 genes, 2 were associated with Wnt signalling (*AXIN2* and *HAPLN1*).

Overall, whilst Tc1 and Dp1Tyb mice both partially model DS phenotypes, the genetic background of these organisms is markedly different. Therefore, results generated here and in later chapters of this thesis should be assessed in light of this notion. It need not be necessarily expected that observed phenotypes must present in an absolutely congruent fashion. The Tc1 and Dp1Tyb, along with additional segmental trisomy models, should be compared and contrasted to gain insight into which portions of Hsa21 are most likely responsible for observed phenotypes.

4.1.3.3 A putative Wnt contribution?

The principal aim of this thesis is to investigate a potential link between altered canonical Wnt signalling and DS. That is, the hypothetical notion that this complex pathway may, at the very least partly, contribute to cellular dysfunction in the DS brain. For this reason, the RNAseq datasets were probed for enrichment with components of known signalling pathways, including canonical Wnt signalling.

In the Tc1 hippocampus, a significant association was detected, suggesting that expression patterns might partly correlate with Wnt signalling function. This was supported by the presence of seven Tc1 DEX genes primarily involved in Wnt activity and regulation, according to literature knowledge. It could be speculated that, through the transcriptional targeting of several genes, Wnt signalling might effectively extend the gene dosage effects of Hsa21 trisomy to parts of the genome not primarily affected by the aneuploidy. However, the current analysis is not sufficient to make any further inferences. It cannot be stated that, simply because Wnt-associated DEX genes are present in the Tc1 mouse, the pathway itself is actually affected. Hippocampal RNA was derived from a cell-heterogenous sample, thus it is impossible to determine the cellular origin of individual gene expression patterns. This is crucial to establishing whether the Wnt-associated DEX genes belong to a single, uniform signalling pathway. Therefore, these data only allow for the preliminary conclusion that some Wnt-related genes are transcriptionally altered in the Tc1 hippocampus. Such conclusion is purely based on objective observation, and does not imply that the DEX genes produce, or result from, Wnt signalling dysfunction. Biochemical investigation of Wnt activity in this mouse is required to reliably establish a functional link, if any, with the pathway (see 4.2.2).

A similar line of reasoning applies to the Dp1Tyb mouse. Whilst a further seven Wnt-related DEX genes were detected, probing with IPA did not indicate a significant association with the pathway. Thus, no further conclusion can be drawn beyond the objective observation that a number of genes associated with Wnt signalling are abnormally expressed. The cell heterogeneity issue mentioned for

the Tc1 mouse also applies to the Dp1Tyb. Thus, biochemical investigation of Wnt activity in this model is also required to primarily establish a functional link, if any, with the pathway (see 4.2.2).

Granted that no inferences on the involvement of Wnt signalling in DS can be made based on the data discussed in this chapter, there is one finding worth of consideration. Whilst the Wnt-related DEX genes differed between Tc1 and Dp1Tyb datasets, two out of seven hits correlated. Specifically, *Axin2* and *Hapln1* were down- and upregulated, respectively, in both mice (**Fig. R1.11-12**). This seeming consistency, albeit a weak finding, might, at least partly, suggest an underlying common alteration in Wnt signalling activity. It should be particularly noted that *Axin2* is an established Wnt target gene, and its expression is known to correlate with activity of the pathway (11, 12). Overall, it may only be concluded that both DS models abnormally express a number of Wnt-related genes, amongst others. Such abnormal expression, additionally, does not even imply that the detected genes are altered *in relation* to Wnt signalling, despite their known links with the pathway. Several other mechanisms producing the observed transcriptional patterns may be envisioned. The seemingly Wnt-associated genes might be affected by the activation of unrelated pathways which function in parallel to Wnt signalling. On the other hand, non-specific aberrations in transcription factor activity, resulting from aneuploidy, might also contribute to abnormal gene expression. Furthermore, structural differences between control and DS model tissues might produce alterations which are only apparently related to gene expression, but instead reflect shifts in cellular composition and number. Positive pathway associations may ultimately well occur for several mechanisms other than Wnt, given the high number and heterogeneity of DEX genes detected in both mice. It is indeed possible that, by consulting IPA for enrichment in alternative pathways, multiple significant associations may be found. Given the *a priori* hypothesis of a Wnt-DS relationship made for this thesis, the IPA analysis cannot be considered to be unbiased. Its results, therefore, must not be taken as definitive transcriptomic evidence of said hypothesis, but rather as tangential findings which warrant further investigation. Importantly, it should be highlighted that the only objective, reliable conclusion to be drawn from this chapter is the following: both Tc1 and Dp1Tyb mice overexpress their duplicated Hsa21-Mmu16 genes, which secondarily result in genome-wide transcriptional changes, as seen in human DS.

For the purpose of this thesis it is however critical to establish whether alterations in Wnt signalling activity are present at the protein level in DS models and humans. This work is discussed in chapter 4.2. In light of the DSCR view of gene contributions to DS (2, 46, 47), it is likely that a small number of Hsa21 genes may contribute more significantly to any putative Wnt phenotype. Therefore, mechanistic investigation of potential Wnt abnormalities in DS must entail a candidate gene approach to determine which, if any, individual Hsa21 genes may be responsible. This work is described in chapter 4.3.

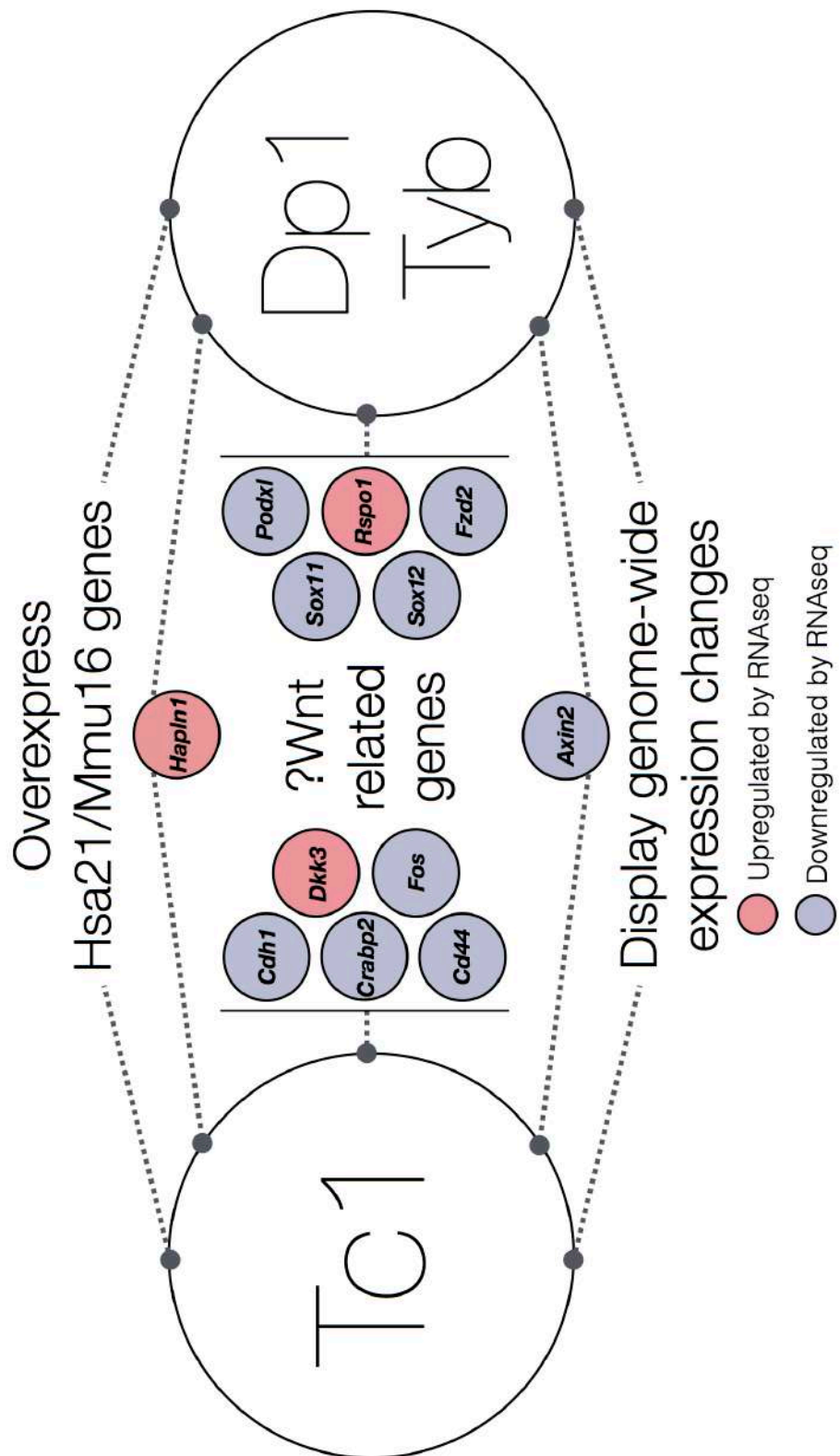


Fig. R1.12 - Visual summary of overall results obtained in this chapters. Further investigation is required to clarify the presence of these phenotypes, and is discussed in chapter 4.2.

RESULTS

Wnt signalling proteins in DS mouse models
and humans

4.2

Chapter 4.2 - Wnt signalling proteins in DS mouse models and humans

4.2.1 Introduction

In the studies described in chapter 4.1, the Tc1 and Dp1Tyb mouse hippocampus displayed altered expression of several non-Hsa21-Mmu16 genes. This suggests the presence of genome-wide transcriptional changes, as seen in human DS. Amongst these genes, a small subset was identified as functionally related to Wnt signalling (e.g.: *Axin2*, *Dkk3*). Preliminary bioinformatic investigation via IPA demonstrated a significant association with the Wnt pathway for the Tc1 mouse, but not the Dp1Tyb. The hippocampal transcriptome of both mice nevertheless included Wnt-related DEX genes. These findings are not sufficient to implicate Wnt dysfunction in DS. However, for the purpose of this thesis, they constituted a *preliminary* finding, and warranted investigation. Given the detected overexpression of several DS-relevant Hsa21-Mmu16 genes (4.1), the Tc1 and Dp1Tyb models were considered as suitable for further study.

In order to probe for a potential Wnt-DS relationship, the next logical step is to investigate whether the activity and components of this pathway are at all altered in this condition, at the protein level. The importance of proteomic studies in DS, as well as the key findings, were discussed in the main introduction (1.4). Similarly to the DS transcriptome, protein changes are highly variable amongst individuals, and suggest abnormalities of several biological mechanisms. It is currently unknown whether such alterations include components of Wnt signalling. This must be crucially established if a functional DS-Wnt relationship is to be proposed at all. As introduced (1.2), canonical Wnt signalling heavily relies on a complex protein machinery controlling degradation of β -catenin and finely regulating its nuclear translocation. Therefore, whilst the downstream effects of Wnt signalling are transcriptional, its activation is a primarily cytosolic event. This implies that a number of key Wnt signalling proteins can be utilised as markers of Wnt signalling activation states, and thus provide validation, or falsification, of the data collected so far. In the context of Wnt signalling, the chief protein to be taken into consideration is β -catenin itself. Whilst this protein is abundant intracellularly, only a small fraction of its total amount is transcriptionally active. As introduced (1.2), the biochemical correlate of active β -catenin is its S45 and T41-dephosphorylated form. It follows that assessment of the dephosphorylated β -catenin fraction provides reliable information on activity of the pathway in the tissue under examination. Additionally, the assessment of levels of other Wnt components can enrich the analysis with further insight into the overall state of the pathway.

This approach was undertaken for the work described here, and this chapter summarises biochemical investigation of Wnt signalling in *ex vivo* tissue sourced from the DS mouse model and human DS brain. Moreover, protein investigation is useful to confirm the aneuploid status of mouse or human tissues under investigation. Measurement of Hsa21-encoded proteins in fact provides a useful indicator of aneuploidy, as well as a practical mean of segregating samples into control and DS/model groups for analysis.

4.2.1.1 Characterisation of the Wnt protein machinery

As introduced, a number of key protein-level findings in the field of Wnt signalling deserve brief consideration in order to contextualise the approach undertaken in this chapter. In the basal state, the complex transmembrane and cytosolic machinery which composes the Wnt pathway continuously tags β -catenin for degradation by the proteasome. Activation of the pathway, on the other hand, halts this mechanism and permits nuclear translocation of β -catenin. It follows that levels of this protein constitute a very useful indicator of overall Wnt activity. Indeed, abundant evidence from multiple fields shows the reliability of quantifying active β -catenin levels to this end.

β -catenin was first identified in the context of cell adhesion, as a cytoplasmic E-cadherin binding protein (1) required for the formation of cell-cell junctions. However, the functional diversity of β -catenin soon came to light when it was identified as homologue to Armadillo, a *Drosophila* segmental polarity protein (2). The same group also implicated β -catenin in *Xenopus* axial patterning shortly after (3). This apparent duality in β -catenin function was finally clarified by Funayama *et al.* in 1995 (4). Employing *Xenopus* embryos, the authors demonstrated that β -catenin overexpression resulted in dual body axis formation. Interestingly, results indicated that the cell adhesion-mediating, N-terminal of β -catenin was not required for the induction of the above phenotype, which remained present upon deletion of said sequence. The internal, adenomatous polyposis coli (APC)-binding domain of β -catenin was shown to be necessary for dual axis formation instead. This key result suggested a cadherin-independent role for β -catenin, and the authors first proposed its role as an intracellular signalling molecule. This property of β -catenin was also linked to GSK3 β , which was shown to regulate its subcellular distribution and axis-inducing function (5). Shortly after, the signalling importance of β -catenin was functionally established in a 1996 study by Morin *et al.*, published in *Science* (6). The authors identified abnormal activation of this protein, driven by adenomatous polyposis coli (APC) inactivation, as a key event in the development of colorectal neoplasia. Furthermore, APC disruption is in some cases not necessary, with activating β -catenin mutations identified as sufficient to induce neoplasia. This key study, amongst others, helped firmly establish the idea that β -catenin activation plays a fundamental role in Wnt-mediated tumorigenesis. Since then, a vast amount of literature has confirmed the importance of β -catenin in a high number of Wnt-mediated processes, and a strong consensus on its centrality to Wnt function exists at present (7-11).

As introduced (see 1.2) the other essential facet of Wnt signalling is the β -catenin destruction complex, which finely regulates basal activity levels. Its chief components are GSK3 β , APC and axin. The first reports on this multi-protein complex were published independently by Behrens *et al.*, who demonstrated axin binding to β -catenin, GSK3 β , and APC (12), and Yost *et al.*, who showed the same interaction in the context of *Xenopus* axis formation (13). Reviewers now agree that the β -catenin destruction complex is fundamentally important in Wnt function, and that alterations in any of its components are likely to disrupt physiological Wnt function (14, 15). One further key implication is

that proteins projected to significantly regulate intracellular Wnt signalling are likely to interact with all components of the destruction complex. One prominent example is leucine-rich repeat kinase 2 (LRRK2), a multi-domain protein involved in familial Parkinson's disease and an established Wnt modulator. LRRK2 has been shown in several instances to directly interact with the β -catenin destruction complex (16, 17).

Finally, the dickkopf family (DKK) of secreted Wnt inhibitors is also an important protein marker of Wnt activity, particularly in the context of neurodegeneration. Their importance has been established in multiple lines of evidence. DKKs play central roles in Wnt-mediated craniofacial development (18). Additionally, *DKK1* is also a Wnt target gene itself implicated in the pathogenesis of several cancers (19) as well as development of midbrain dopaminergic neurons (20). Similarly, DKK3 is another important Wnt inhibitor, which is reportedly suppressed in cervical cancer (21) and induces apoptosis of human prostate cancer cells (22). Accordingly, DKK3 is also elevated in platelet progenitor cells in individuals affected by myeloproliferative neoplasia (23). In the context of neurodegeneration, both DKK3 and DKK1 are now known to be functionally important. Both are associated with hippocampal development and AD (24-26). In the context of DS, DKK3 was identified as a potentially altered Wnt component in the transcriptome of Tc1 mice .

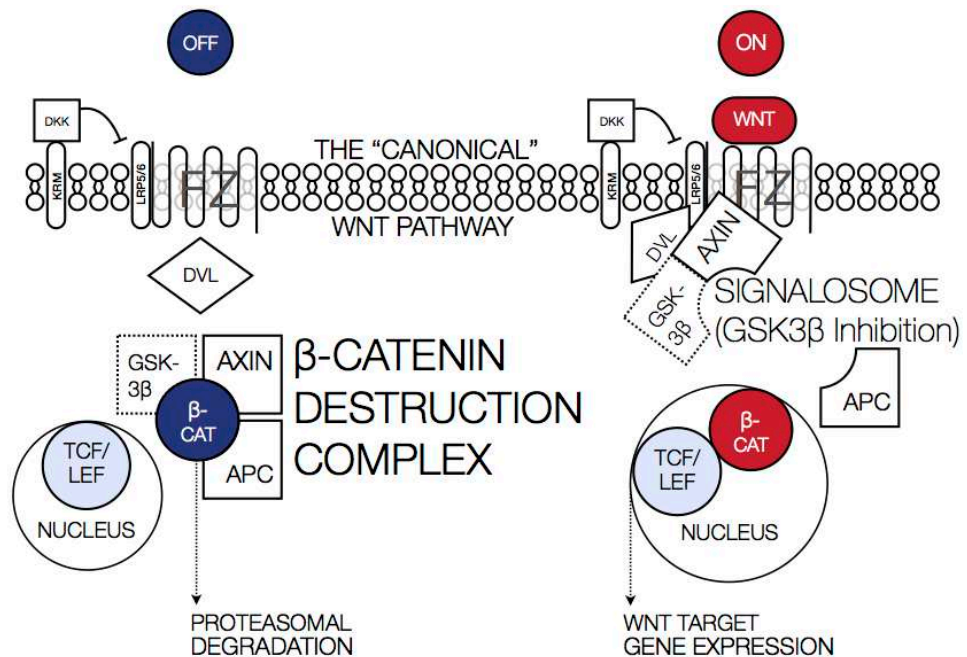


Fig. R2.a - Visual overview of canonical Wnt signalling structure and activation mechanisms.

In summary, the evidence discussed here provides key information on the importance of β -catenin, the destruction complex and the DKKs as key protein markers for investigation of Wnt dysfunction. Building upon this foundation, the work described in this chapter utilised this approach to determine whether protein level alterations of Wnt functions were present in DS mouse models and humans.

4.2.2 Results

This section details biochemical and quantitative real-time PCR (qPCR) experiments conducted on DS mouse model and human tissue. Particularly, the cerebral cortex and hippocampus of Tc1 and Dp1Tyb mice were examined. The hippocampus of two additional segmental trisomy models, the Ts(10)Yey and Ts(17)Yey, was also analysed, as well as postmortem hippocampal tissue derived from AD-DS humans. Building upon results in chapter 4.1 (4.1.2), the main aim of this study was to investigate any potential differences in key Wnt signalling components and assessing levels of canonical Wnt signalling activity *ex vivo*. The results were obtained combining tissue dissection, protein extraction, immunoblotting and qPCR. For all figures displaying box plots, box span represents first to third quartiles, bands represent the median of each sample group, and whiskers represent minimum/maximum values.

4.2.2.1 Tc1 mouse

Background details on the Tc1 model (27) are discussed in the general introduction (1.1.5) and in results chapter 4.1.

4.2.2.1.1 qPCR Validation of RNAseq data

In order to validate the Tc1 RNAseq data presented in results chapter 4.1 (4.1.2), hippocampal expression of *Dkk3* and *axin2* was investigated by qPCR. As introduced, these are two key components of canonical Wnt signalling, which were identified as DEX genes by RNAseq. *Dkk3* is a Wnt inhibitor, whilst *axin2* is a Wnt target gene which provides negative feedback regulation of β -catenin.

RNAseq detected *Dkk3* overexpression at approximately 1.3-fold relative to WT mice, while *Axin2* was found to be reduced to about 0.6-fold (see 4.1.2). A total of 8 (***n*=4, 3 months**) Tc1 mice were analysed by qPCR. Hippocampal RNA was isolated and reverse-transcribed into cDNA (see 3.4 for primer design and testing). The resultant genetic material was then amplified and quantified employing standard protocols. For both *Dkk3* and *axin2*, two housekeeping genes were used as loading controls, β -actin and glyceraldehyde-3-phosphate dehydrogenase (*GAPDH*). Final qPCR quantification results were expressed as **normalised to loading control and relative to the reference sample WT A**. Additionally, descriptive statistics are reported in brackets in the format (***Internally normalised quantity mean \pm SD, mean threshold cycle- $C_t \pm SD$***).

Dkk3 qPCR

β-actin control - Hippocampal Tc1 cDNA ($n=4$) was analysed for expression of *Dkk3*. Levels of *Dkk3* for WT A were assumed as reference and quantified to 1 (0.99 ± 0.008 , $C_t=28.76\pm 0.054$). The remaining WT samples displayed homogenous levels of *Dkk3* expression, with WT B relatively quantified to 1.004 (0.99 ± 0.03 , $C_t=29.43\pm 0.015$), WT C to 0.98 (0.97 ± 0.12 , $C_t=30.3\pm 0.008$), and WT D to 0.88 (0.87 ± 0.04 , $C_t=30.23\pm 0.18$). In the Tc1 samples, *Dkk3* levels were increased, with Tc1 A relatively quantified to 1.46 (1.45 ± 0.02 , $C_t=27.93\pm 0.03$), Tc1 B to 1.37 (1.36 ± 0.09 , $C_t=29.13\pm 0.13$), Tc1 C to 1.68 (1.66 ± 0.11 , $C_t=27.65\pm 0.01$), and Tc1 D to 1.89 (1.87 ± 0.03 , $C_t=21.22\pm 0.07$). Overall, and in accordance with RNAseq data, the Tc1 relative quantity mean indicates that hippocampal *Dkk3* expression is significantly increased 1.6-fold relative to the WT mean (1.65 ± 0.24 , $P=0.0017$, Fig. R2.1b).

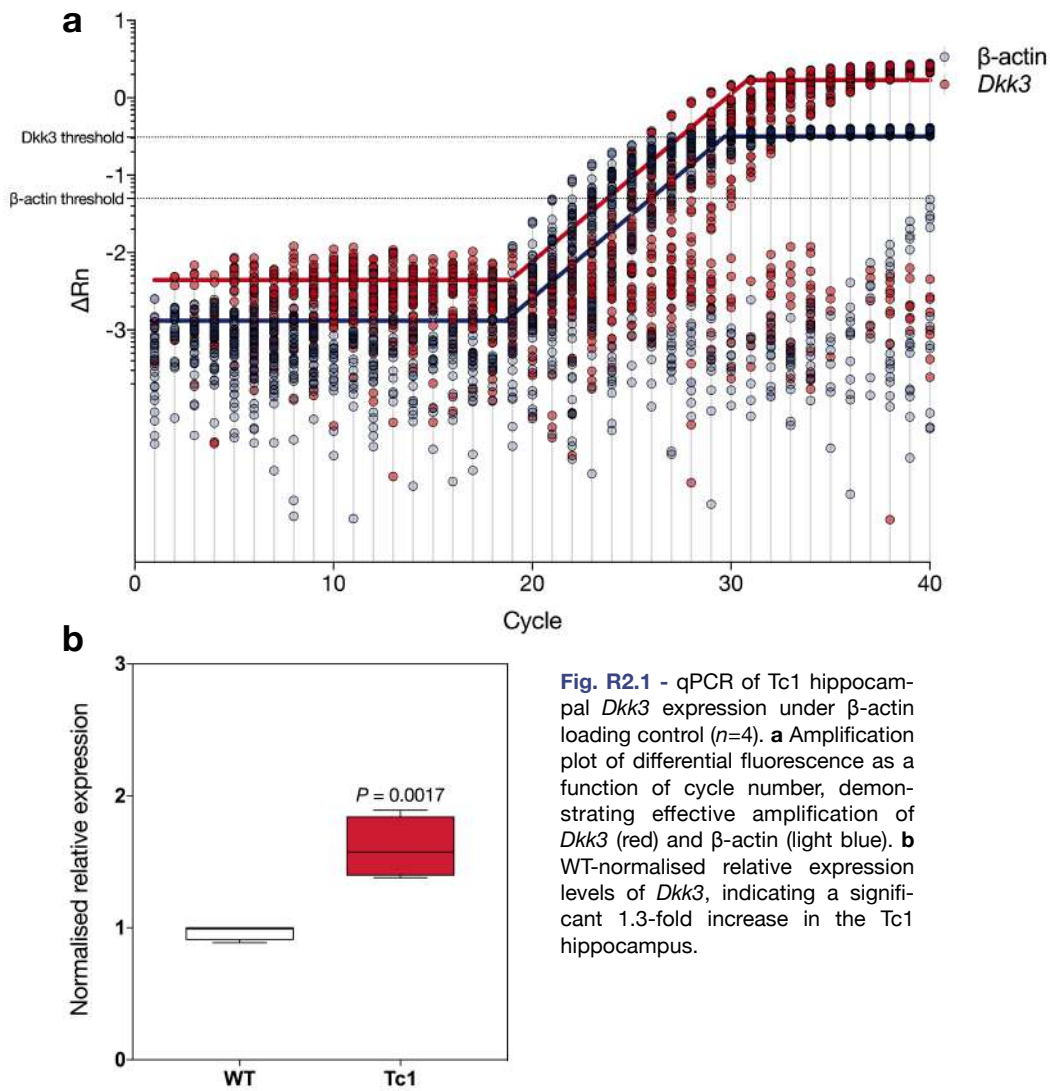


Fig. R2.1 - qPCR of Tc1 hippocampal *Dkk3* expression under β -actin loading control ($n=4$). **a** Amplification plot of differential fluorescence as a function of cycle number, demonstrating effective amplification of *Dkk3* (red) and β -actin (light blue). **b** WT-normalised relative expression levels of *Dkk3*, indicating a significant 1.3-fold increase in the Tc1 hippocampus.

GAPDH control - Hippocampal Tc1 cDNA ($n=4$) was analysed for expression of *Dkk3*, identically to the previous experiment. Levels of *Dkk3* for WT A were assumed as reference and quantified to 1 (01.05 ± 0.15 , $C_t=24.01\pm0.29$). The remaining WT samples displayed homogenous levels of *Dkk3* expression, with WT B relatively quantified to 1 (1.05 ± 0.18 , $C_t=23.27\pm0.24$), WT C to 0.86 (0.90 ± 0.09 , $C_t=24.81\pm0.19$), and WT D to 1.05 (1.12 ± 0.43 , $C_t=24.71\pm0.63$). In the Tc1 samples, *Dkk3* levels were increased, although higher variability was observed than with β -actin normalisation. Tc1 A relatively quantified to 1.53 (1.61 ± 0.06 , $C_t=22.74\pm0.09$), Tc1 B to 3.25 (3.42 ± 1.13 , $C_t=23.55\pm0.40$), Tc1 C to 2.28 (2.40 ± 0.33 , $C_t=22.65\pm0.36$), and Tc1 D to 2.37 (2.49 ± 0.74 , $C_t=20.89\pm0.27$). Consistently to β -actin normalisation and RNAseq, the Tc1 relative quantity mean for *GAPDH* indicates that *DKK3* expression is significantly increased 2.4-fold relative to WT (2.36 ± 0.71 , $P=0.008$, Fig. R2.2b).

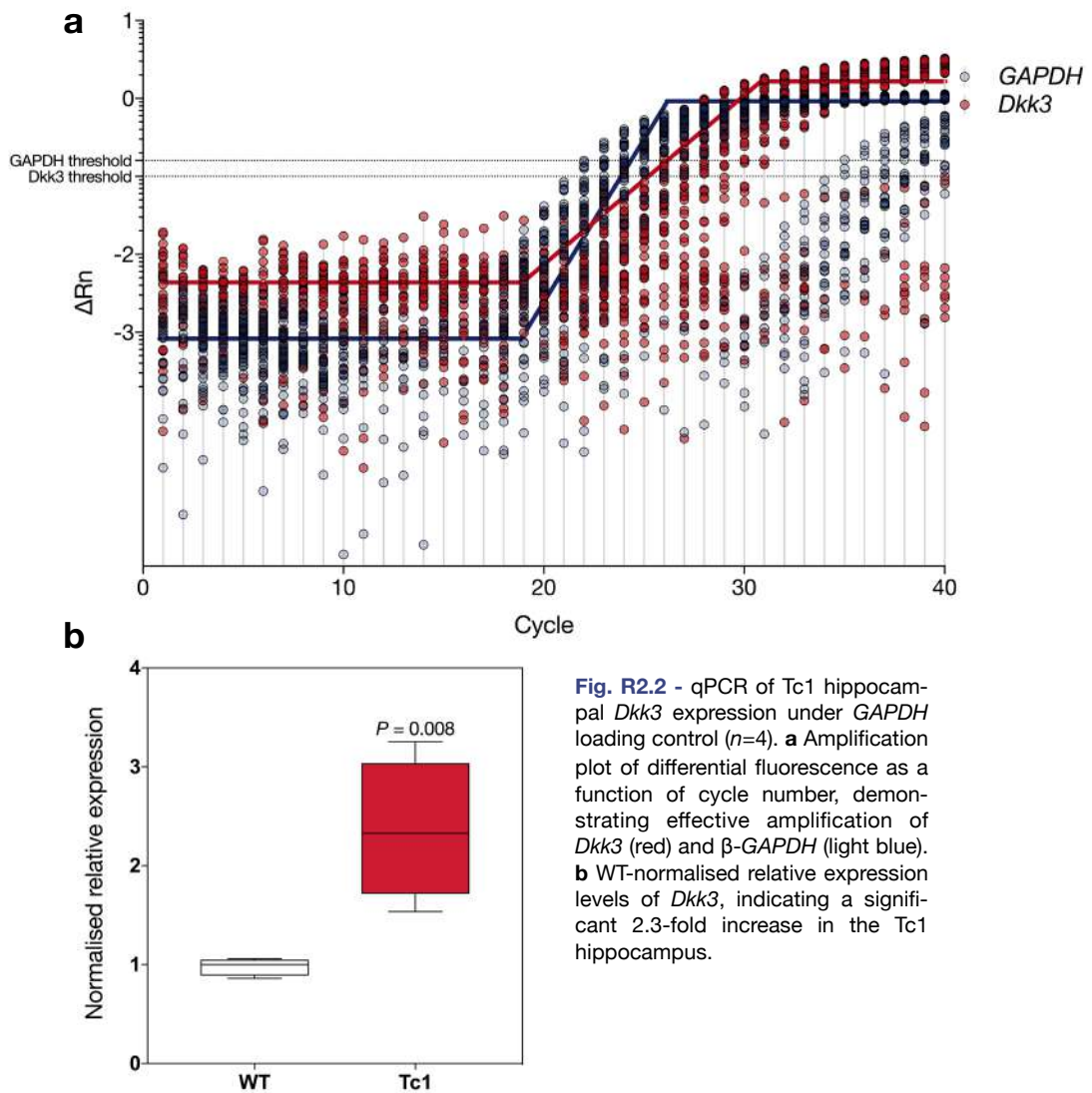


Fig. R2.2 - qPCR of Tc1 hippocampal *Dkk3* expression under *GAPDH* loading control ($n=4$). **a** Amplification plot of differential fluorescence as a function of cycle number, demonstrating effective amplification of *Dkk3* (red) and β -*GAPDH* (light blue). **b** WT-normalised relative expression levels of *Dkk3*, indicating a significant 2.3-fold increase in the Tc1 hippocampus.

Axin2 qPCR

β-actin control - Hippocampal Tc1 cDNA ($n=4$) was analysed for expression of *Axin2*. Levels of *Axin2* for WT A were assumed as reference and quantified to 1 (1.54 ± 0.15 , $C_t=30.92 \pm 0.08$). The remaining WT samples displayed slightly less homogenous levels of *Axin2* expression compared to *Dkk3*, with WT B relatively quantified to 0.83 (1.28 ± 0.26 , $C_t=31.77 \pm 0.010$), WT C to 0.91 (1.40 ± 0.02 , $C_t=30.62 \pm 0.09$), and WT D to 1.32 (2.04 ± 0.09 , $C_t=28.52 \pm 0.13$). In the Tc1 samples, *Axin2* levels displayed downregulation, with Tc1 A relatively quantified to 0.79 (1.22 ± 0.10 , $C_t=32.46 \pm 0.20$), Tc1 B to 0.62 (0.95 ± 0.21 , $C_t=32.36 \pm 0.19$), Tc1 C to 0.83 (1.28 ± 0.12 , $C_t=30.63 \pm 0.08$), and Tc1 D to 0.62 (0.96 ± 0.07 , $C_t=32.73 \pm 0.13$). Overall, and in accordance to RNAseq data, the Tc1 relative quantity mean indicates a significant 0.7-fold downregulation of *Axin2* relative to the WT mean (0.71 ± 0.11 , $P=0.048$, Fig. R2.3b).

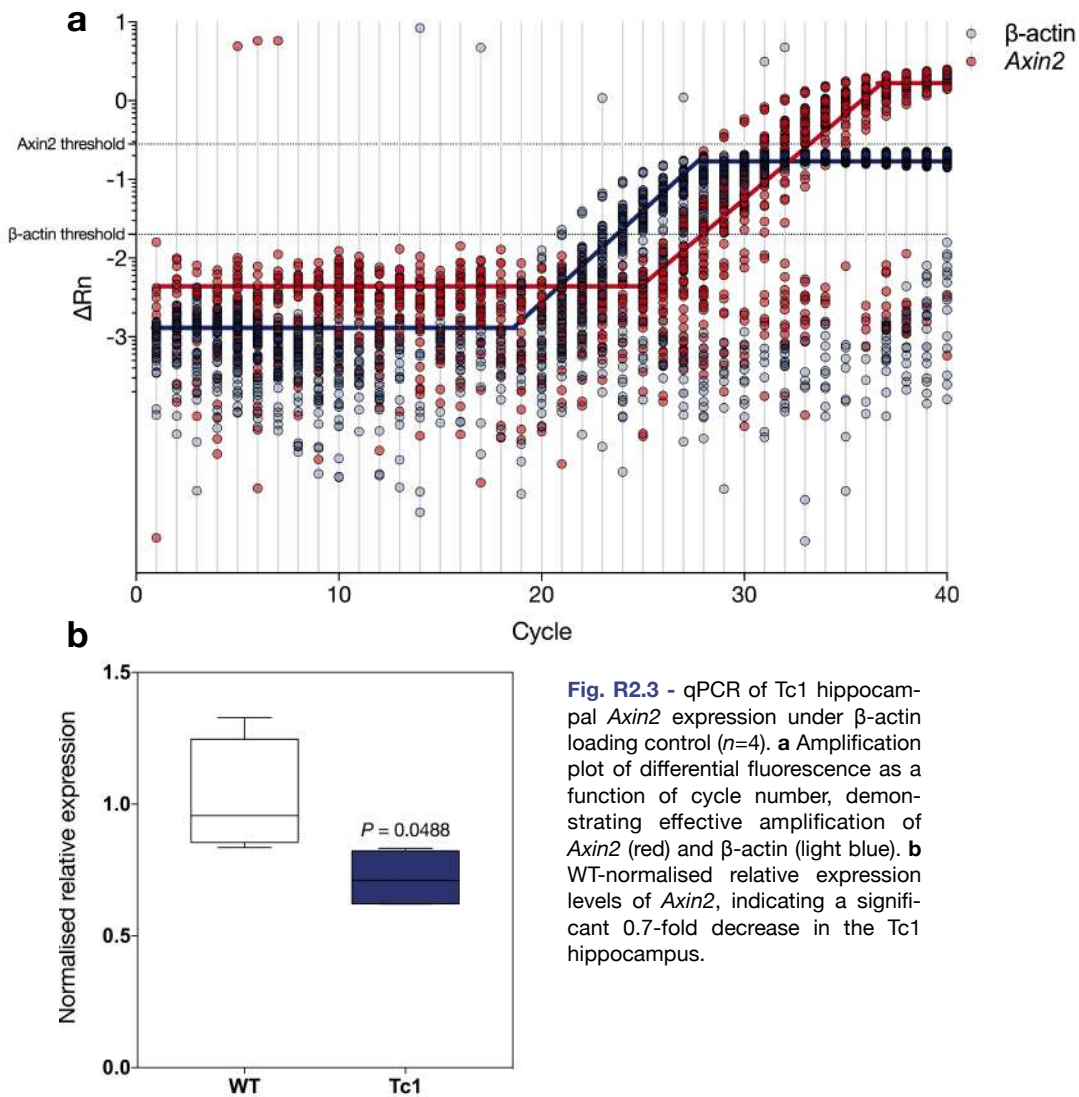


Fig. R2.3 - qPCR of Tc1 hippocampal *Axin2* expression under β -actin loading control ($n=4$). **a** Amplification plot of differential fluorescence as a function of cycle number, demonstrating effective amplification of *Axin2* (red) and β -actin (light blue). **b** WT-normalised relative expression levels of *Axin2*, indicating a significant 0.7-fold decrease in the Tc1 hippocampus.

GAPDH control - Hippocampal Tc1 cDNA ($n=4$) was analysed for expression of *Axin2*. In this experiment, higher variability between samples was observed, compared to previous results. Samples WT C and Tc1 B were excluded from the analysis due to ineffective amplification with undetectable signal. Levels of *Axin2* for WT A were assumed as reference and quantified to 1 (1.60 ± 0.20 , $C_t=25.9 \pm 0.20$). The remaining WT samples displayed variable levels of *Axin2* expression, with WT B relatively quantified to 0.59 (0.95 ± 0.13 , $C_t=25.79 \pm 0.33$) and WT D to 0.62 (1.00 ± 2.34 , $C_t=27.26 \pm 3.12$). In the Tc1 samples, *Axin2* displayed variable expression, with Tc1 A relatively quantified to 0.42 (0.66 ± 0.26 , $C_t=25.95 \pm 0.65$), Tc1 C to 0.95 (1.52 ± 0.37 , $C_t=26.11 \pm 0.59$), and Tc1 D to 0.75 (1.21 ± 0.17 , $C_t=24.57 \pm 0.26$). Overall, the Tc1 relative quantity mean indicates that *Axin2* expression was not significantly altered under GAPDH control conditions, but displayed a trend toward downregulation (0.78 ± 0.32 , $P=0.66$, Fig. R2.4b).

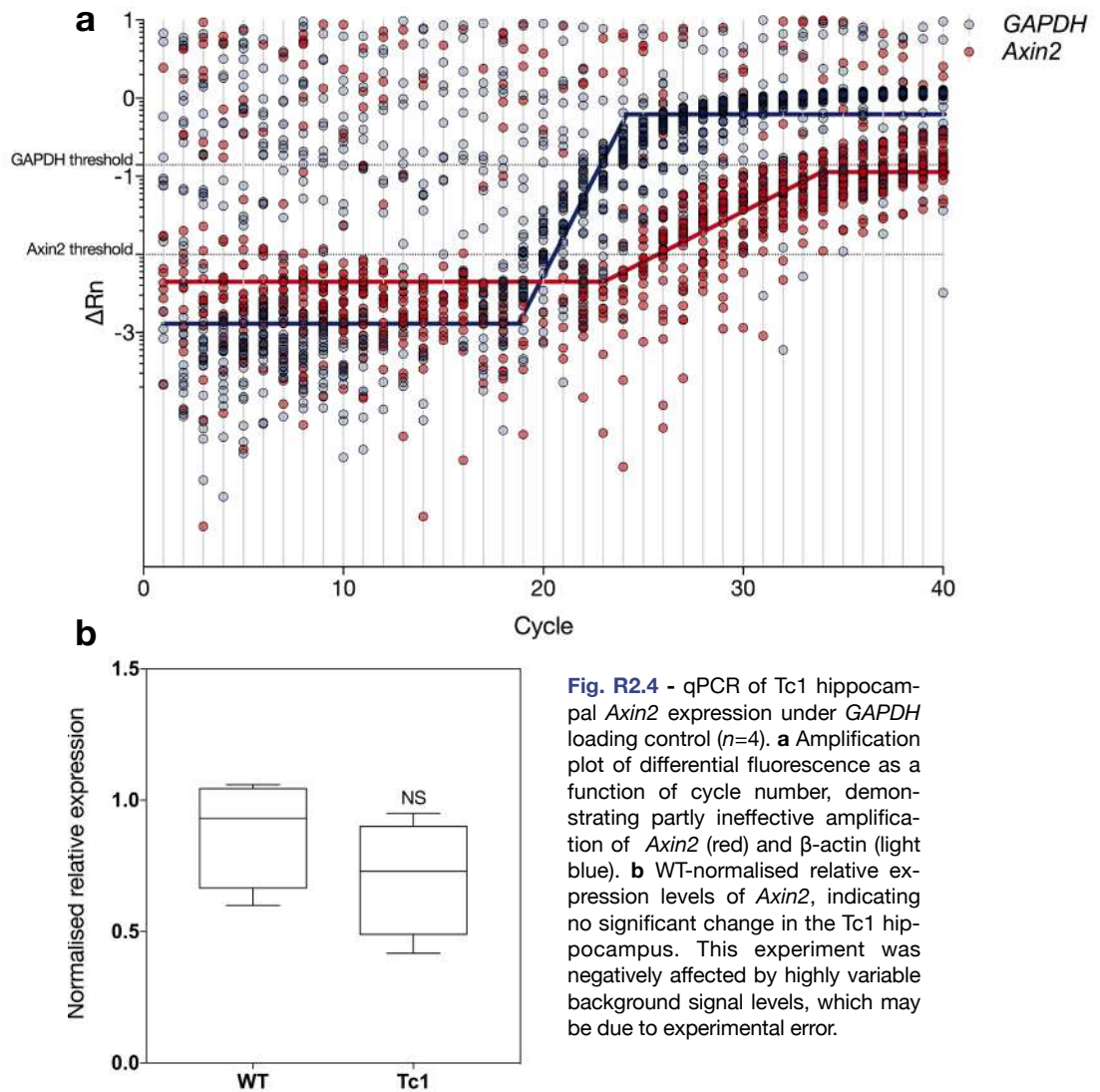


Fig. R2.4 - qPCR of Tc1 hippocampal *Axin2* expression under GAPDH loading control ($n=4$). **a** Amplification plot of differential fluorescence as a function of cycle number, demonstrating partly ineffective amplification of *Axin2* (red) and β -actin (light blue). **b** WT-normalised relative expression levels of *Axin2*, indicating no significant change in the Tc1 hippocampus. This experiment was negatively affected by highly variable background signal levels, which may be due to experimental error.

4.2.2.1.2 Canonical Wnt signalling in the Tc1 hippocampus

A total of 16 Tc1 mouse hippocampi ($n=8$, 6 months) were analysed for immunoblotting experiments. Quantified Western blot chemiluminescence values were normalised to loading control (β -actin) and thereby expressed as ratio to the wild-type (WT) sample mean. Descriptive statistics are reported in brackets in the format (*mean Tc1 relative normalised chemiluminescence \pm SD, p-value*).

Ex vivo Wnt signalling activity

To first confirm the aneuploid status of the tissue examined, hippocampal Tc1 samples were probed for total levels of DYRK1A. As expected, DYRK1A was found to be significantly increased at approximately 1.5-fold in Tc1 hippocampi (1.74 ± 0.15 , $P < 0.0001$, Fig. R2.5a). To determine levels of active Wnt signalling, hippocampal Tc1 samples were probed for total and active β -catenin. As introduced, the biochemical correlate of active β -catenin is represented by the de-phosphorylated form of the protein at the S33/37 and T41 residues. A specific, validated antibody was employed for immunoblotting (6). Active β -catenin levels were expressed as a ratio to total protein. No significant difference was observed in overall levels of β -catenin (0.96 ± 0.19 , $P = 0.94$, Fig. R2.5b). However, the active β -catenin fraction was significantly decreased 0.3-fold relative to WT samples (0.36 ± 0.17 , $P = 0.01$, Fig. R2.5c). Overall, immunoblotting revealed significant downregulation of canonical Wnt signalling activity in adult Tc1 hippocampi.

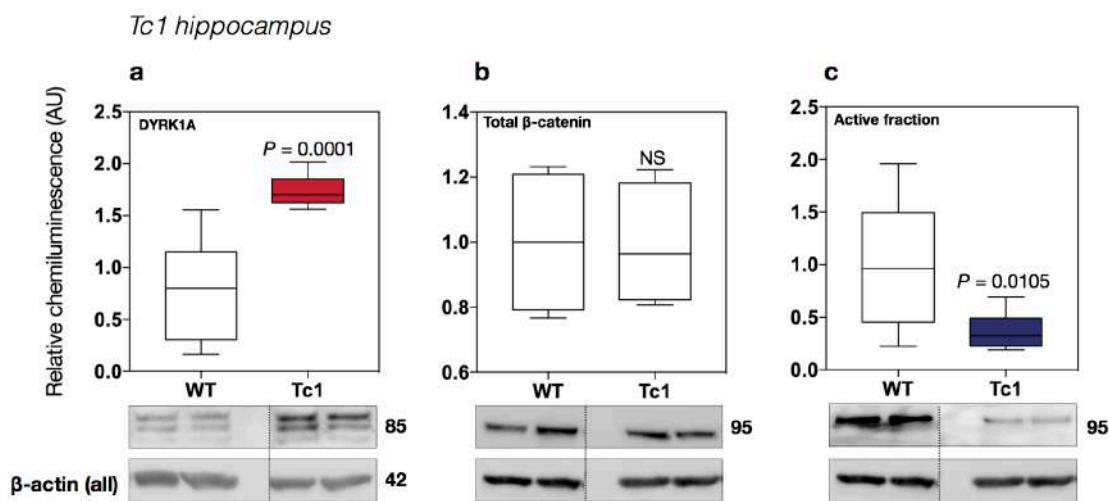


Fig. R2.5 - Immunoblotting quantification of Wnt signalling activity in the Tc1 hippocampus ($n=8$). **a** Significant ~1.5-fold elevation in DYRK1A protein levels. **b** No change in total β -catenin. **c** Significant 0.3-fold downregulation of the active β -catenin fraction.

Component profiling

Hippocampal samples were probed for three additional Wnt signalling proteins: the β -catenin inhibitor GSK3 β , its S9-phosphorylated form (p-S9) and the secreted inhibitor DKK3. As introduced, p-S9 GSK3 β is reportedly elevated in 20 months but not 3 months old Tc1 hippocampi (28). DKK3 was found to be increased by RNAseq and qPCR, and was thus tested for further validation. Levels of total GSK3 β were not significantly altered (0.76 ± 0.20 , $P=0.67$, Fig. R2.6a). Similarly to young Tc1 mice (28), no changes in amounts of p-GSK3 β -S9 were detected (1.24 ± 0.20 , $P=0.21$, Fig. R2.6b). DKK3, however, was found to be significantly increased (1.59 ± 0.52 , $P=0.015$, Fig. R2.6c). Overall, these data suggest that whilst GSK3 β levels are unaffected, the Tc1 mouse presents a consistent elevation of DKK3, detected across multiple techniques. Given its role as a Wnt inhibitor, DKK3 might contribute to the observed downregulation of active β -catenin in the Tc1 hippocampus.

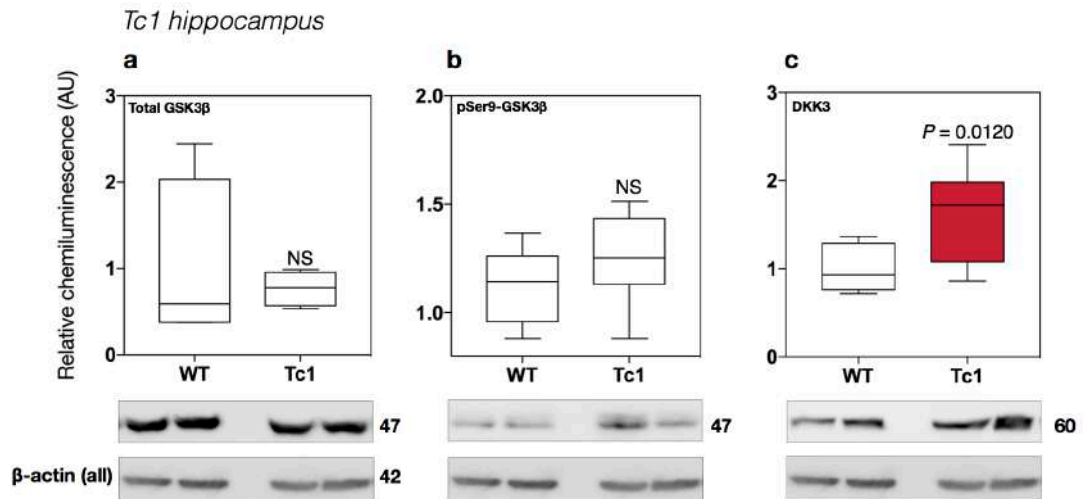


Fig. R2.6 - Immunoblotting quantification of Wnt signalling components in the Tc1 hippocampus ($n=8$). **a** No change in total GSK3 β levels. **b** No change in p-S9 GSK3 β levels. **c** Significant 1.6-fold increase in DKK3 protein levels, in accordance with RNAseq and qPCR results.

In summary, biochemical profiling of the Tc1 hippocampus revealed a state of suppressed Wnt signalling, with downregulation of active β -catenin, elevated DKK3 and unaltered GSK3 β .

4.2.2.1.3 Canonical Wnt signalling in the Tc1 cortex

A total of 16 Tc1 mouse cerebral cortices ($n=8$, 6 months) were analysed in immunoblotting experiments. Data were analysed and reported as in 4.2.2.1.2.

Ex vivo Wnt signalling activity

To first confirm the aneuploid status of the tissue examined, cerebral cortical Tc1 samples were probed for total levels of DYRK1A. As expected, DYRK1A was found to be significantly increased at approximately 1.5-fold in Tc1 hippocampi (1.58 ± 0.13 , $P=0.018$, Fig. R2.7a). No significant difference was observed in

total cortical levels of β -catenin (1.05 ± 0.25 , $P=0.52$, Fig. R2.7b). However, the active β -catenin fraction was significantly increased 2.3-fold relative to WT samples (2.28 ± 1.21 , $P=0.012$, Fig. R2.7c). In contrast to hippocampal results, these data suggest significant activation of the pathway in the Tc1 cortex, a trend which warrants careful interpretation and further validation.

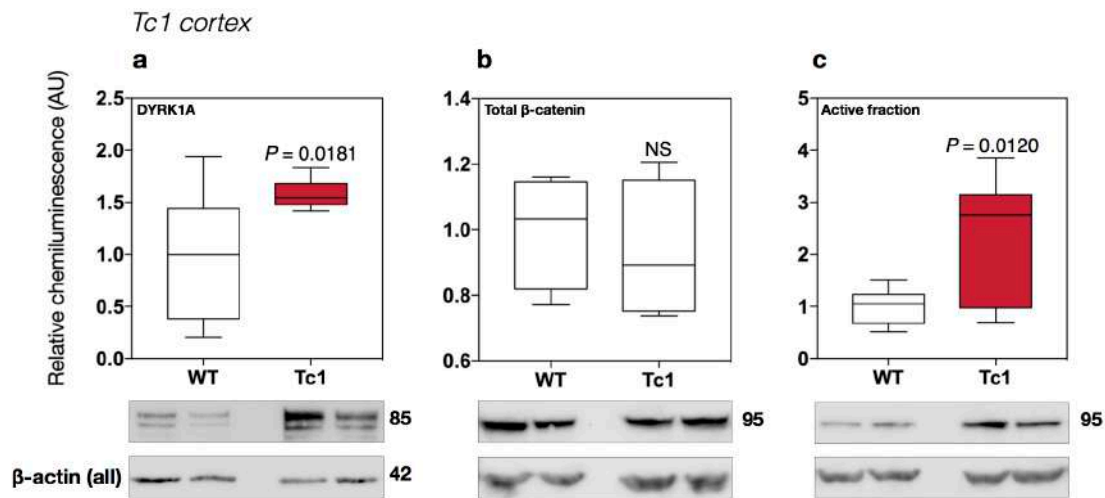


Fig. R2.7 - Immunoblotting quantification of Wnt signalling activity in the Tc1 cerebral cortex ($n=8$). **a** Significant ~1.5-fold elevation in DYRK1A protein levels. **b** No change in total β -catenin. **c** Significant 2.3-fold increase of the active β -catenin fraction.

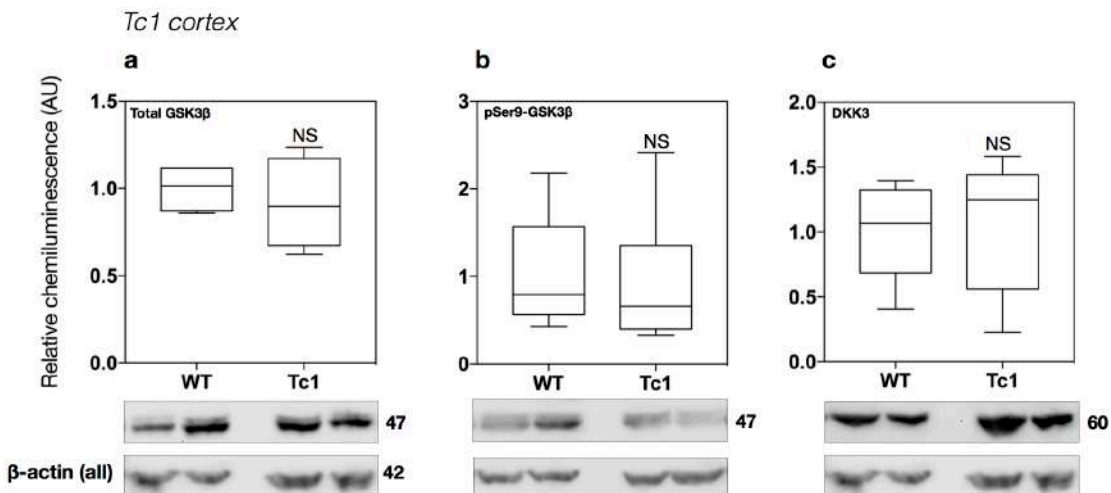


Fig. R2.8 - Immunoblotting quantification of Wnt signalling components in the Tc1 hippocampus ($n=8$). **a** No change in total GSK3 β levels. **b** No change in p-S9 GSK3 β levels. **c** No change in DKK3 levels.

Component profiling

Tc1 cortical samples were also probed for the Wnt components GSK3 β , p-S9-GSK3 β and DKK3. Levels of total GSK3 β were found not to be altered in the Tc1 cortex (0.91 ± 0.26 , $P=0.57$, Fig. R2.8a), and neither were levels of p-GSK3 β -S9 (0.93 ± 0.71 , $P=0.85$, Fig. R2.8b). Similarly, no difference the amount of DKK3 was identified (1.08 ± 0.51 , $P=0.71$, Fig. R2.8c). In summary, biochemical profiling of the Tc1 cortex revealed a state of overactive Wnt signalling. However, protein levels of the Wnt components examined were normal.

4.2.2.2 Dp1Tyb mouse

Details on the Dp1Tyb model (29) are discussed in the introduction (1.1.5) and results chapter 4.1 (4.1.1).

4.2.2.2.1 Canonical Wnt signalling in the Dp1Tyb hippocampus

A total of 20 Dp1Tyb mice hippocampi ($n=10$, 5 months) were analysed for immunoblotting experiments. Data were analysed and reported as in 4.2.2.1.2-3.

Ex vivo Wnt signalling activity

To first confirm the aneuploid status of the tissue examined, hippocampal Dp1Tyb samples were probed for total levels of DYRK1A. As expected, DYRK1A was found to be significantly increased at approximately 2-fold (2.22 ± 0.69 , $P=0.0001$, Fig. R2.9a). No significant difference was observed in total levels of β -catenin (0.77 ± 0.38 , $P=0.45$, Fig. R2.9b). However, and similarly to the Tc1 cortex, the active β -catenin fraction was substantially increased over 3-fold relative to WT samples (3.36 ± 1.54 , $P=0.0001$, Fig. R2.9c).

Component profiling

Dp1Tyb hippocampal samples were also probed for the Wnt components GSK3 β and DKK3. Levels of total GSK3 β did not appear to be altered (0.90 ± 0.32 , $P=0.62$, Fig. R2.10a). However, amounts of DKK3 were significantly elevated nearly 3-fold (2.78 ± 1.5 , $P=0.004$, Fig. R2.10b).

In summary, biochemical profiling of the Dp1Tyb hippocampus revealed a state of upregulated Wnt signalling, with unaltered GSK3 β levels. The prominent elevation in DKK3 is also of particular interest, as it apparently contrasts with its known Wnt inhibitory role.

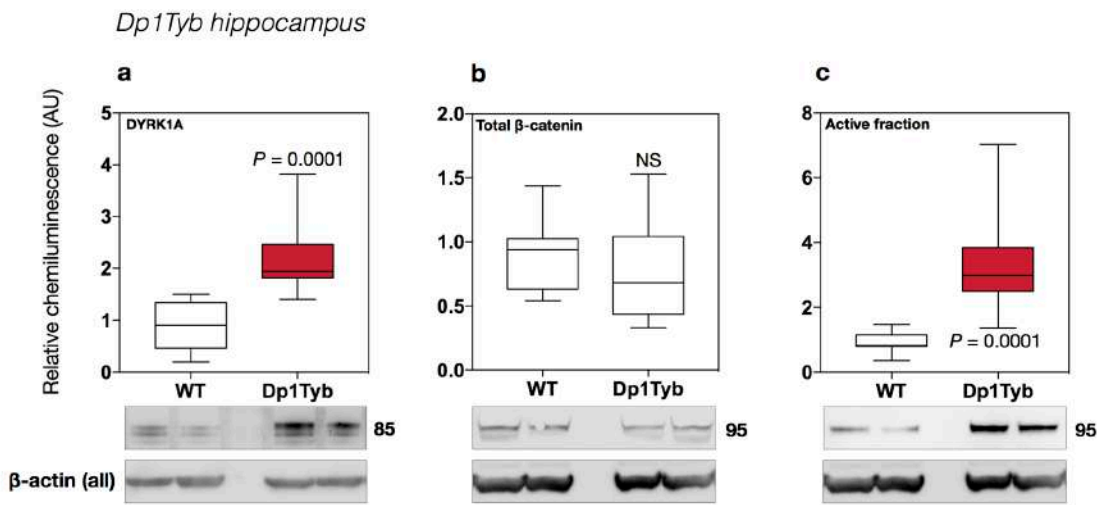


Fig. R2.9 - Immunoblotting quantification of Wnt signalling activity in the Dp1Tyb hippocampus ($n=10$). **a** Significant ~2-fold elevation in DYRK1A protein levels. **b** No change in total β -catenin. **c** Significant increase of the active β -catenin fraction to a substantial ~3.4-fold.

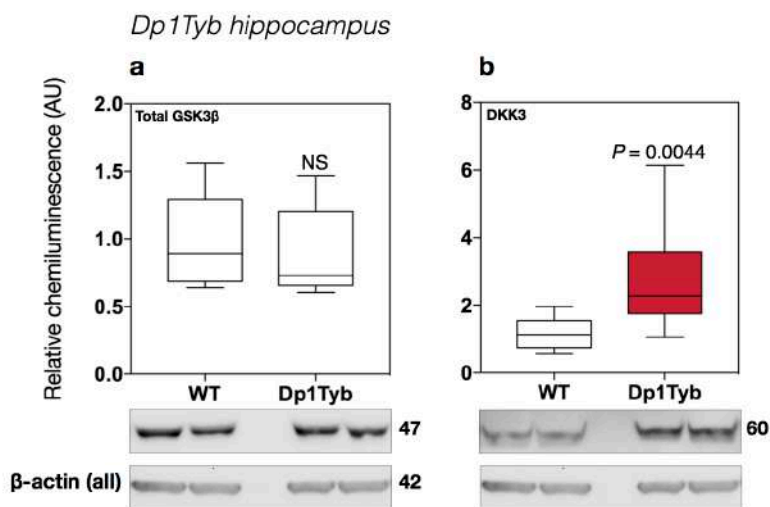


Fig. R2.10 - Immunoblotting quantification of Wnt signalling components in the Tc1 hippocampus ($n=8$). **a** No change in total GSK3 β levels. **b** Significant 2.8-fold increase in DKK3 protein levels.

4.2.2.2.2 Canonical Wnt signalling in the Dp1Tyb cortex

A total of 20 Dp1Tyb mouse cerebral cortices ($n=10$, 5 months) were analysed for immunoblotting experiments. Data were analysed and reported as in 4.2.2.1.2.

Ex vivo Wnt signalling activity

To first confirm the aneuploid status of the tissue examined, cerebral cortical Dp1Tyb samples were probed for total levels of DYRK1A. As expected, DYRK1A was found to be significantly increased at approximately 2-fold (2.18 ± 0.66 , $P=0.0005$, Fig. R2.11a). However, Wnt signalling activity was normal in the Dp1Tyb cerebral cortex, with unaltered levels of total (1.04 ± 0.88 , $P=0.78$, Fig. R2.11b) and active (1.44 ± 0.64 , $P=0.11$, Fig. R2.11c) β -catenin.

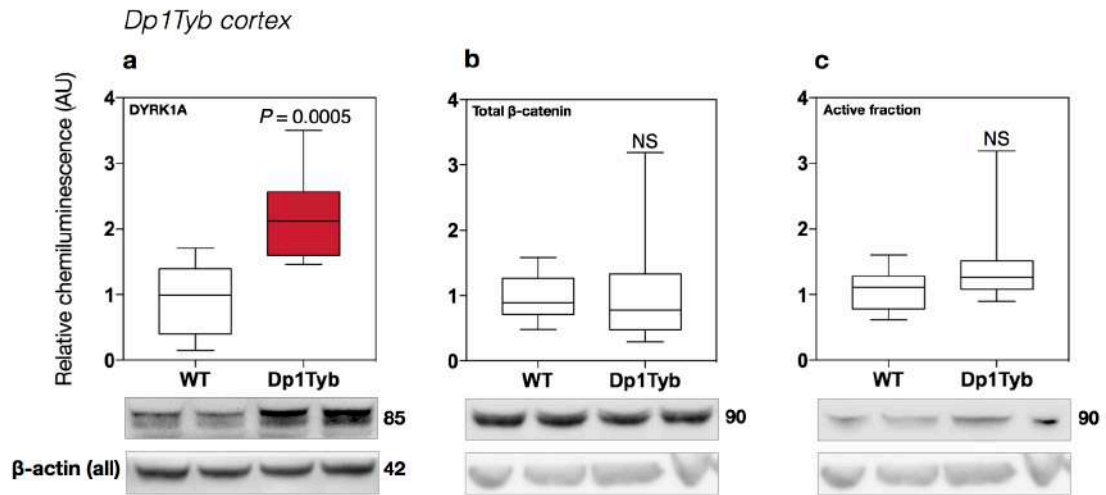


Fig. R2.11 - Immunoblotting quantification of Wnt signalling activity in the Dp1Tyb cerebral cortex ($n=10$). **a** Significant ~2-fold elevation in DYRK1A protein levels. **b** No change in total β -catenin. **c** No change in the active β -catenin fraction.

Overall, whilst the Dp1Tyb cortex displays enhanced DYRK1A levels, no differences in Wnt signalling activity are present at this time point. Therefore, no additional investigation of Wnt components was performed in this tissue type.

4.2.2.3 Additional segmental trisomy models

The presence of Wnt signalling activity alterations in the Tc1 and Dp1Tyb models provides support for the main hypothesis of this thesis, but also warrants the question of which Hsa21 genes are more likely to mediate the Wnt phenotype. Since Hsa21 genes are numerous, formulation of a candidate gene hypothesis for later study can be aided by further dissecting Hsa21 trisomy in smaller segments. For this purpose, canonical Wnt signalling activity was investigated in two additional segmental trisomy models, the Ts1(10)Yey and Ts1(17)Yey (30). As introduced, these mice possess duplications of Hsa21 syntenic regions on Mmu10 and 17, respectively, and do not include the DSCR.

4.2.2.3.1 Canonical Wnt signalling in the Ts1(10)Yey and Ts1(17)Yey hippocampus

A total of 10 Ts1(10-17)Yey mice hippocampi ($n=5$, 6 months) were analysed for immunoblotting experiments. Data were analysed and reported as in 4.2.2.1.2-3.

Ex vivo Wnt signalling activity

Overall, Wnt signalling activity was normal in the hippocampus of both models. Total β -catenin was unaffected (Ts1(10)Yey - 1.73 ± 1.31 , $P=0.30$; Ts1(17)Yey - 1.80 ± 1.23 , $P=0.75$, Fig. R2.12a/c). Similarly, no differences in active β -catenin were detected (Ts1(10)Yey - 0.85 ± 1.31 , $P=0.76$; Ts1(17)Yey - 1.55 ± 0.96 , $P=0.28$, Fig. R2.12b/d).

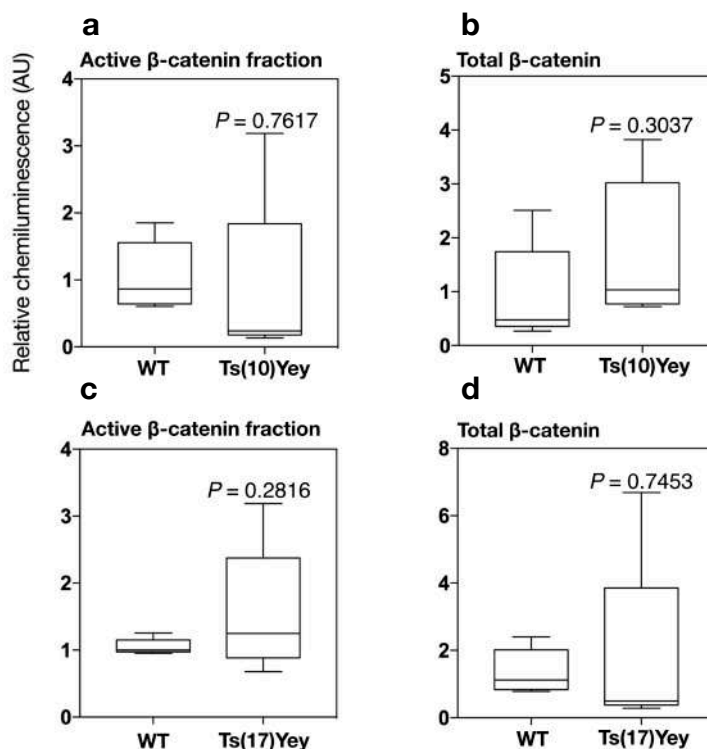
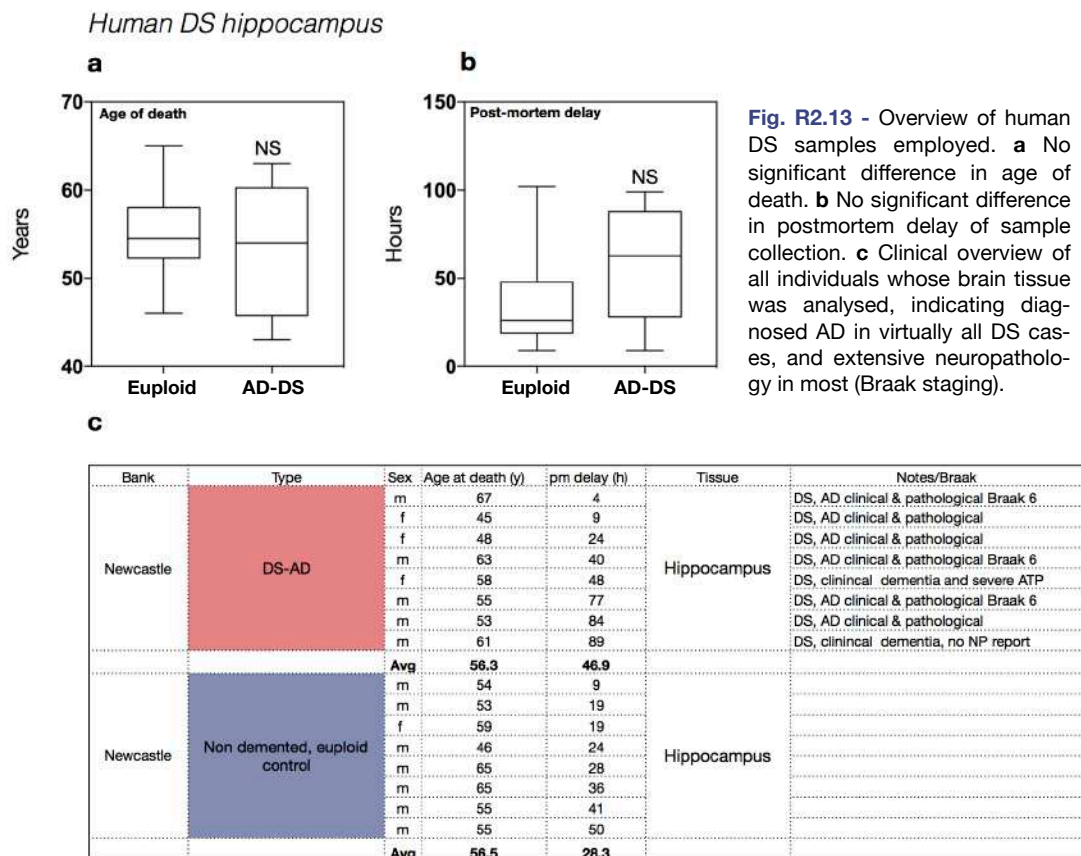


Fig. R2.12 - Immunoblotting quantification of Wnt signalling activity in the Ts1(10)Yey and Ts1(17)Yey hippocampus ($n=5$). **a/c** No change in total β -catenin. **b/d** No change in the active β -catenin fraction.

In summary, these results indicate unaffected Wnt signalling in the Ts1(10)Yey and Ts1(17)Yey models, suggesting that Hsa21 syntenic regions on Mmu10 and 17 are unlikely to mediate the phenotype observed in the Tc1 mouse. These data are particularly important, because they indicate that Hsa21 orthologs on Mmu16, overexpressed in the Dp1Tyb mouse, are more likely to underlie the observed Wnt alterations.

4.2.2.4 Human DS

Having established the presence of substantial Wnt alterations in the hippocampus of two key DS mouse models, the next logical step was to investigate whether this signalling pathway is affected in human DS individuals. The work conducted in mice provided validation of previous experiments, but it is by itself not sufficient to reliably conclude that abnormal Wnt signalling correlates with DS. Therefore, human DS brain tissue was employed to characterise potential Wnt signalling changes in Hsa21 trisomy. A total of $n=8$ postmortem human DS hippocampal samples were sourced from the Newcastle Brain Bank, along with 8 euploid controls. Both sample groups included a mix of males and females. Samples were age-matched, with no significant difference in age of death observed (**Euploid - 55 ± 5.5 yrs; DS - 53 ± 7 yrs, $P=0.62$, Fig. R2.13a**). Samples were also matched for postmortem delay of tissue collection, in order to minimise differences due to differential protein degradation. No significant difference in postmortem delay was observed (**Euploid - 36.5 ± 29.5 hrs; DS - 58.8 ± 33 hrs, $P=0.18$, Fig. R2.13b**). Clinical information for each group (Fig. R2.13c) indicated that all DS individuals suffered from AD at the time of death (AD-DS), with most displaying extensive brain pathology as classified by Braak staging. Conversely, all euploid controls were not affected by AD.



4.2.2.4.1 Canonical Wnt signalling in the adult human DS hippocampus

Ex vivo Wnt signalling activity

To first confirm the aneuploid status of the human tissue examined, hippocampal samples were probed for total levels of DYRK1A. As expected, DYRK1A was found to be significantly increased at approximately 1.5-fold (1.82 ± 0.69 , $P=0.0061$, Fig. R2.14a). Consistently with all mice examined, no significant difference was observed in total levels of β -catenin (1.34 ± 0.97 , $P=0.42$, Fig. R2.14b). However, similarly to the Tc1 hippocampus, the active β -catenin fraction was substantially downregulated nearly 3-fold (0.43 ± 0.22 , $P=0.0021$, Fig. R2.14c). These data indicate that, in human AD-DS hippocampi, canonical Wnt signalling is potently suppressed.

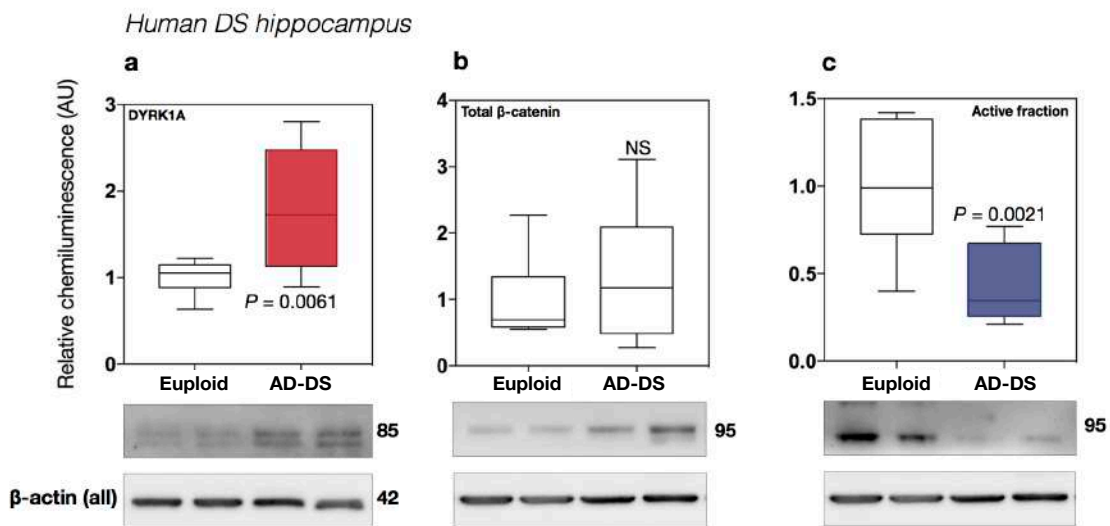


Fig. R2.14 - Immunoblotting quantification of Wnt signalling activity in the human DS hippocampus ($n=8$). **a** Significant ~1.5-fold elevation in DYRK1A protein levels. **b** No change in total β -catenin. **c** Significant 3-fold downregulation of the active β -catenin fraction to a similar extent to the Tc1 hippocampus.

Component profiling

Human DS hippocampal samples were also probed for the Wnt components GSK3 β and DKK3. Levels of total GSK3 β did not appear to be altered (0.90 ± 0.32 , $P=0.62$, Fig. R2.15a). However, amounts of DKK3 were significantly reduced 3-fold (0.33 ± 0.21 , $P=0.0147$, Fig. R2.15b). These data suggest that DKK3 alterations are associated with the DS hippocampus, since they were also present in both the Tc1 and Dp1-Tyb models, albeit in the opposite direction.

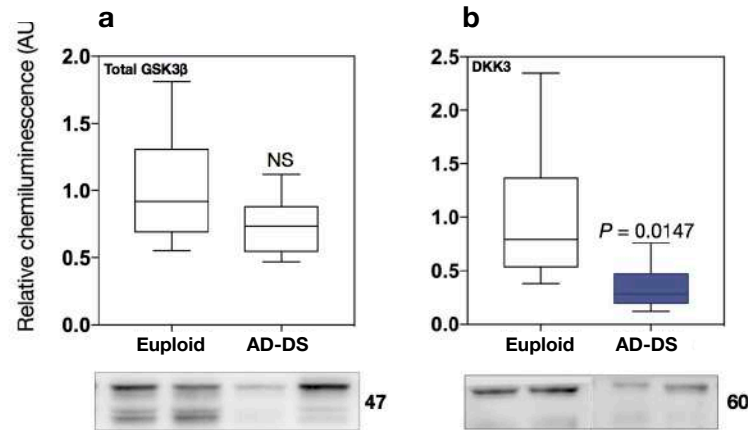


Fig. R2.15 - Immunoblotting quantification of Wnt signalling components in the Tc1 hippocampus ($n=8$). **a** No change in total GSK3 β levels. **b** Significant 3-fold increase in DKK3 protein levels.

In summary, the investigation conducted in humans DS individuals provided, for the first time, evidence of substantially suppressed canonical Wnt signalling activity, with an associated decrease in levels of DKK3.

4.2.3 Discussion

The work described in this chapter provided initial support to the main hypothesis of this thesis, by investigating potential protein level alterations of Wnt signalling activity and components in DS models and humans. The diverse array of proteomic alterations in DS was discussed in the main introduction (1.4), elucidating the associated high variability and relative contribution of a small number of Hsa21-encoded proteins. Overall, the data presented here clearly demonstrate that, at the protein level, Wnt signalling is dysfunctional in DS. Given that abnormalities were found in both models as well as human hippocampi, the combined interpretation of chapter 4.2 data lends support to the main hypothesis of this thesis. However, a non-trivial degree of variability was observed between tissue types and models examined. This further elucidates the idea put forth previously i.e. that, if present, Wnt alterations in DS are likely multi-directional, given the complexity and fine regulation of the pathway. Thus, possible interpretations and implications for later work are explored in this section.

4.2.3.1 Functional significance

Overall, qPCR and protein studies in this chapter provided one key finding in the understanding of DS: Wnt abnormalities are present at the protein level. It has to be noted, however, that given the available data, this notion is presently only applicable to the DS brain, and particularly the hippocampus. It remains to be determined whether such abnormalities are present in other cell types critical to DS pathology, such as heart tissue or the haematopoietic system. Given the statistical significance of differences in observed active β -catenin levels, however, it can be generally concluded that cerebral Wnt signalling is indeed affected by Hsa21 trisomy.

Out of all the data presented, studies conducted in the Tc1 and human DS hippocampi are perhaps the most compelling, for a number of reasons. In both conditions, a substantial downregulation of active β -catenin was observed. Given current knowledge on the importance of Wnt signalling in nervous system development and homeostatic function (11, 31, 32), it can be inferred that the observed degree of suppression, 3-fold on average, is likely to result in significant downstream effects. Particularly, inhibition of Wnt signalling in the DS hippocampus may primarily affect adult neurogenesis, a critical process in memory formation. Lie *et al.* reported on the essential regulatory role of canonical Wnt signalling on hippocampal neurogenesis (33), a mechanism through which the Wnt pathway is well known to affect memory formation processes such as LTP and neuronal network signal processing (34). Therefore, although no functional circuit data is available in this study, literature knowledge supports the inference that the observed extent of Wnt signalling dysregulation in DS may deleteriously affect hippocampal function. This is particularly relevant to AD. Given that all human samples examined originated from DS individuals affected by clinical AD, the data are consistent with previous reports of Wnt signalling downregulation in AD (26, 35).

Additionally, alterations in DKK3, an AD-related Wnt inhibitor regulating hippocampal development and neurogenesis (24, 25), are present in both mouse models and human DS. It remains unclear, however, why DKK3 alterations go in opposite directions in the Tc1 and human DS hippocampus. Given that DKK3 functions as a Wnt antagonist, an enhancement in protein levels would be expected in the human DS hippocampus, which was not the case for the data reported here. Similarly, enhanced active β -catenin levels in the Dp1Tyb hippocampus would be expected to correlate with decreases in DKK3 protein levels. A significant enhancement in DKK3 was observed instead. These data are difficult to reconcile, but may in part be due to possibly dual DKK3 functions in Wnt regulation. Reports exist suggesting that, in particular tissue types, DKK3 may function as a promoter of canonical Wnt signalling. For example, Nakamura *et al.* reported potent Wnt-stimulating effects of DKK3 in a retinal glial cell line, a tissue type relevant to nervous system function (36). It is possible, therefore, that DKK3 alterations might positively drive Wnt signalling in specific contexts, which however remain to be determined.

In parallel, *AXIN2* expression was decreased in the Tc1 hippocampus. This gene has a distinct pattern of expression, specific to both the developing and adult hippocampal dentate gyrus (37), and its protein levels are proportionally related to canonical Wnt signalling activity (38). The downregulation of *AXIN2* observed in the Tc1 hippocampus could further account for the concomitant decrease in Wnt signalling activity. The observed absence of alterations in GSK3 β levels in all tissues examined suggests, on the other hand, that the described Wnt phenotypes are possibly independent of GSK3 β activity. However, since abnormal S9 phosphorylation of GSK3 β is indeed observed in the brain of aged Tc1 mice (28), it is possible that GSK3 β changes are age-dependent, and only become detectable at later stages of life.

Another unclear finding is the observed enhancement of active Wnt signalling in the Tc1 cortex. Whilst all Wnt components were normal, significantly increased active β -catenin was observed. There are two possible interpretations for this finding. Overactive Wnt signalling in the cerebral cortex may represent an early feedback compensation, given the high degree of connectivity between hippocampal and cortical areas in the brain. Alternatively, this result might suggest that Hsa21-encoded proteins potentially responsible for Wnt alterations may be capable of bidirectional regulation of signalling activity, depending on basal activation levels and/or developmental stage. Some studies have reported that aberrant Wnt signalling activation in mature mouse neurons may result in transient neuronal progenitor proliferation, also followed by apoptosis (39). Interestingly, Cyclin D1 levels were found to be elevated in FAD post mortem brain samples (40, 41). Upregulation of this key mitotic regulation may induce forced cell cycle entry and subsequent apoptosis. Thus, it is possible that negative effects of Wnt signalling upregulation might also be present in DS. This implies that physiological, basal Wnt activity requirements might influence the direction of change induced by aberrant expression of Hsa21 genes. This idea warrants further mechanistic studies aimed at clarifying the underlying mechanisms.

In summary, if the Tc1 and human DS hippocampal data are considered independently of other results, a consistent pattern of Wnt suppression emerges, whereby Hsa21 trisomy may facilitate neurodegeneration with a some contribution from suppressed Wnt signalling. Overall, considering all data available, it can be concluded that, albeit somewhat inconsistent in direction of change, Wnt signalling is indeed functioning abnormally in DS (**Fig. R2.16**). This novel finding suggests that, provided mechanisms are clarified in future work, Wnt signalling function may be established as a critical contributor to DS brain pathology, with the consequential hypothesis that pharmacological targeting of this pathway might constitute a viable strategy for therapeutic development (see 5.2.2).

4.2.3.2 Implications

The presence of substantial Wnt dysregulation in the DS brain at the protein level (**Fig. R2.16**) warrants the subsequent need of determining which Hsa21 genes are more likely to underlie the observed phenotypes. This experimental question is critical to convincingly establish whether or not Hsa21 trisomy truly affects Wnt signalling in DS. While data discussed so far reliably demonstrate the presence of abnormalities of the pathway, they provide no insight into the underlying *causal relationship* between Hsa21 and Wnt signalling. It is indeed possible that, in DS, Wnt dysfunction might not result from aberrant activity of primarily overexpressed genes, especially given the genome-wide effects of Hsa21 trisomy on gene expression (4.1.3).

To answer this question, candidate Hsa21 genes must be functionally investigated in relation to Wnt signalling. In this respect, observations made in the Ts1(10/17)Yey hippocampus are particularly important. Specifically, given that no Wnt signalling alterations were detected in the hippocampus of either model, Hsa21 genes syntenic to Mmu10/17 regions are most likely not responsible for the phenotypes observed in other DS models and humans. Conversely, since β -catenin activity was abnormal in the Dp1Tyb model, the scope of investigation can be restricted to Hsa21 syntenic genes on Mmu16. There are indeed multiple interesting candidates in this region, most importantly *APP* and *DYRK1A*, both reportedly crucial for DS and AD pathology. Given that *APP* is not functionally overexpressed in the Tc1 mouse, however (4.1.2., (27, 42)), *DYRK1A* was selected for further investigation in this thesis. The DYRK1A protein is already known to functionally interact with two key Wnt components, namely GSK3 β (43-45) and p120/ δ -catenin (46). Moreover, its known role as a regulator of signalling pathways (47, 48) makes it an ideal candidate for Wnt modulation in DS (see 4.3.1 for a detailed overview of DYRK1A function).

It cannot be excluded however, that *APP* may also contribute to the Wnt phenotype in DS, given its key importance in AD pathogenesis and its overexpression in the DS brain. The studies investigating a potential DYRK1A-Wnt functional interaction are discussed in chapter 4.3.

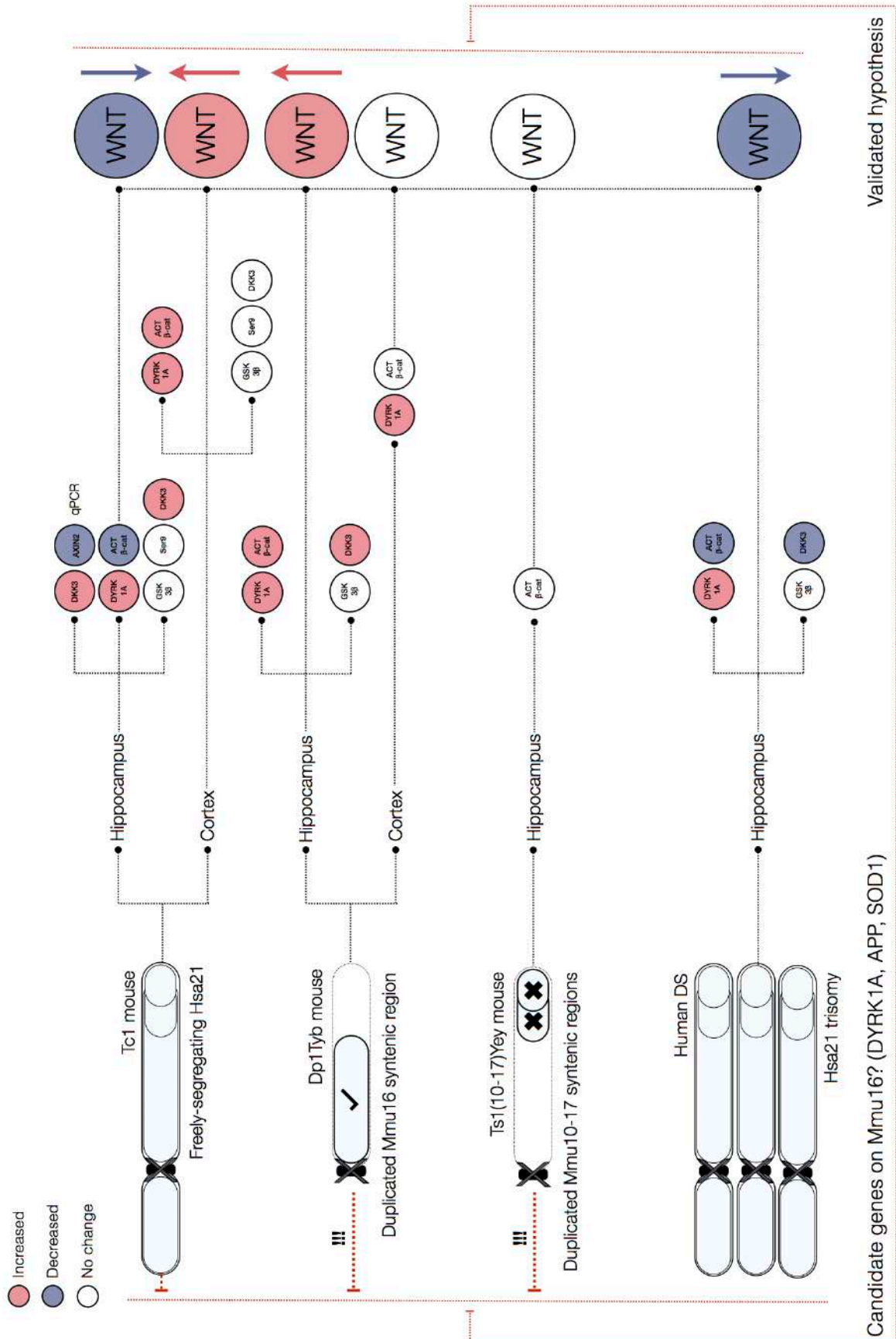


Fig. R2.16 - Visual summary of results discussed in chapter 4.2. Protein level Wnt signaling alterations in DS appear to be bidirectional and tissue dependent. Most importantly, however, hippocampal Tc1 and human DS Wnt signaling levels are consistently downregulated. Being the Tc1 the most faithful recapitulation of DS available here, these data strongly suggest Wnt suppression as characteristic of the adult DS hippocampus. Additionally, the absence of any alteration in mouse models with duplications of Mmu10/17 syntenic regions allows more refined hypothesis formulation i.e. Mmu16 orthologs to Hsa21 are more likely to mediate the observed phenotypes.

RESULTS

DYRK1A-mediated Wnt signalling modulation

4.3

4.3. Chapter 4.3 - DYRK1A-mediated Wnt signalling modulation

4.3.1 Introduction

The work described so far elucidated two key points: first, canonical Wnt signalling abnormalities in DS are *suggested* by transcriptional profiles in two mouse models. Second, Wnt alterations are also present at the protein level, with observed abnormalities in β -catenin activity and amounts of the inhibitor DKK3. This phenotype is observed in multiple tissue types of DS mouse models, as well as the postmortem hippocampus of DS individuals also diagnosed with AD. This phenotype is, however, directionally inconsistent, and may vary depending on tissue type. Particularly, the Tc1 mouse and human DS hippocampi both display substantially reduced Wnt signalling activity, whilst the Tc1 cerebral cortex and Dp1Tyb hippocampus possess enhanced activity of the pathway. Additionally, no alteration is observed in mice with duplications of Mmu10 and 17 regions syntenic to Hsa21, suggesting Mmu16 orthologs are more desirable candidates. Overall, these findings demonstrate that Wnt signalling alterations are present in DS, but do not provide any evidence as to which DS-relevant Hsa21 genes might be responsible. Several potential mechanisms may be envisioned: some Hsa21 genes may directly modulate Wnt signalling or influence certain cellular processes which then affect Wnt signalling. Alternatively, the Wnt alterations observed may be completely independent of the specific function of Hsa21 genes, and rather result from non-specific alterations in gene expression induced by aneuploidy.

To investigate which of these hypotheses best accounts for the observations made so far, a candidate gene approach was undertaken. As introduced, the most appealing candidate given the data currently available is DYRK1A, which is unequivocally overexpressed in the all DS tissues examined. This is in contrast to APP, another likely candidate for Wnt modulation, which is not functionally overexpressed in the Tc1 model, which nevertheless presents Wnt abnormalities. For these reasons, mechanistic studies into a potential Wnt modulatory role for DYRK1A were performed, and the results are described in this chapter.

Before discussing them, however, it is necessary to introduce scientific evidence on the known functions of DYRK1A and its role in DS and neurodegeneration. The available literature will serve as a conceptual basis to justify the experimental work presented thereafter. Given the CNS-oriented scope of this thesis, current knowledge on DYRK1A function is preferentially discussed in this context. Overall, four main themes deserve consideration: First, that DYRK1A is a multifaceted kinase with multiple roles in health and disease. Second, that abnormal DYRK1A function is a key feature of DS neurodegeneration. Third, that it is capable of finely regulating several signalling pathways. Fourth, that existing evidence preliminarily implicates DYRK1A in Wnt function, making it an ideal candidate for the studies carried out in this chapter.

4.3.1.1 DYRK1A: a multifaceted, dual-specificity kinase

DYRK1A is a member of the dual-specificity tyrosine-(Y)-phosphorylation-regulated kinase (DYRK) family of highly conserved protein kinases. From a phylogenetic perspective, the DYRK family is itself integral to the CMGC group of eukaryotic kinases. This group includes **C**yclin-dependent kinase (CDK), **M**itogen-activated protein kinase (MAPK), **G**lycogen synthase kinase (GSK - important in Wnt signalling) and **C**DK-like kinase (CLK) (1). Members of the DYRK family all possess a conserved kinase domain in close proximity to a DYRK homology domain, also known as DH-box [amino acid - (aa sequence: DDDNXDY)]. They however differ in the composition of amino/acid terminal regions (2). The DYRK family is additionally divided into three subclasses, one of which includes the vertebrate DYRK1A/B and DYRK2-4 genes.

DYRK1A itself is a highly conserved protein kinase with a multitude of phosphorylation functions. It was first identified in 1995 as the *Drosophila* gene *minibrain* (*Mbn*), encoding a protein essentially required for post-embryonic neurogenesis (3). The DYRK1A protein consists of 763 amino acids and multiple domains. Specifically, it possesses a kinase domain, two nuclear localisation signals (NLS), a PEST domain (rich in proline (**P**), glutamate (**E**), serine (**S**), and threonine (**T**), a highly conserved 13-histidine repeat (poly-H tail) and a C-terminal S/T rich region. The enzyme is able to self-activate or undergo priming by other kinases. The two NLSs, both functional, are located at the N-terminal and within the kinase domain (4). No known DYRK1A function is currently ascribed to the PEST domain or S/T rich region (5).

DYRK1A is a dual-specificity kinase, meaning it displays both tyrosine (**Y**) and serine/threonine kinase activities. However, the dual-specificity nature refers to its known autophosphorylation capabilities (5). DYRK1A in fact displays self-activation via phosphorylation of the Y321 residue. Particularly, the protein possesses a conserved Y-X-Y motif within the activation loop of the kinase domain, similarly to all other DYRK family members (2). Autophosphorylation of the second Y residue has been shown to be essential for DYRK1A kinase activation (6), hence the 'Y-regulated' nomenclature. This notion also reportedly applies to other DYRK members of the mammalian subclass (7). Whilst this activation modality is also present in MAPKs, it does not require a priming kinase and is instead an autophosphorylation event, as introduced (6). A key 2005 study by Lochhead *et al.* mechanistically characterised DYRK1A activation in *Drosophila* (8). This study demonstrated an important feature of DYRK1A function. The self-activating autophosphorylation was shown to occur during mid-translation, when the protein is not fully mature. A transient, intermediate form of DYRK1A catalyses this activating phosphorylation at the Y-X-**Y** motif, after which the Y-kinase activity is lost permanently. These findings also imply that once synthesised, the mature DYRK1A protein is constitutively active. Importantly, it follows that total protein levels of DYRK1A directly correlate with kinase activity. This notion is relevant to DS, as it suggests that in this condition, DYRK1A overexpression may result in a chronic 1.5-fold en-

hancement of kinase activity. Another study later demonstrated that, while common to all DYRK family members, this mechanism varies slightly between DYRKs (9). All known DYRK1A substrates undergo phosphorylation at S/T residues only. Overall, DYRK1A is thought to function as a proline-directed kinase, since its consensus phosphorylation sequence has been identified as RPX(S/T)**P** (10). More recent reviews however suggest that this might not be the only phosphorylation sequence, given that not all described DYRK1A substrates are compatible with the consensus motif (11, 12). Literature on DYRK1A and the DYRK family is extensive, and has been excellently reviewed in multiple instances, available for further consultation (5, 11-13).

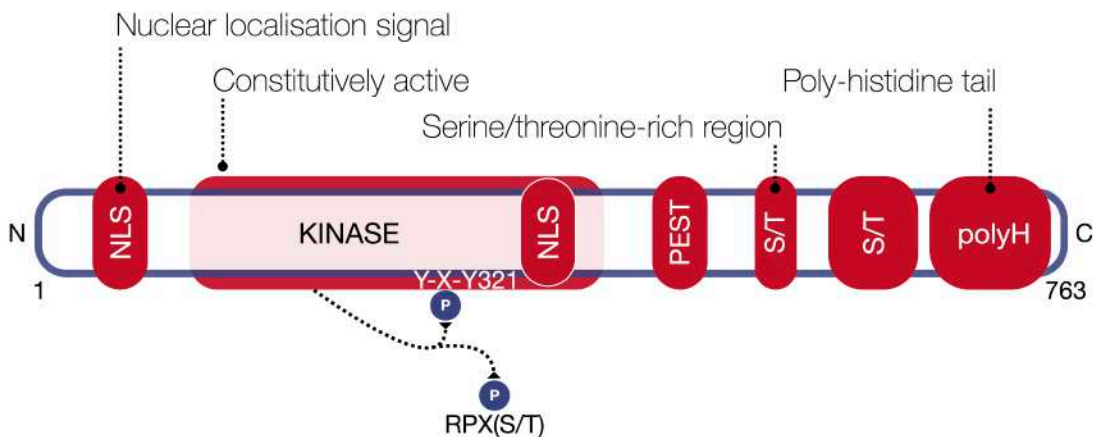


Fig. R3.a - Domains of the DYRK1A protein, 763 amino acids long. The kinase loop undergoes autophosphorylation at Y321 during DYRK1A synthesis, after which the enzyme remains constitutively active.

4.3.1.1.1 DYRK1A in health and disease

According to multiple reports, DYRK1A is virtually expressed ubiquitously under physiological conditions (13-15). These data underscore the critical importance of homeostatic DYRK1A function in health and disease. DYRK1A is known to functionally localise prominently to the nucleus, but also the cytosol, phosphorylating over 12 different substrates involved in several cellular functions (5, 12, 16). Well described DYRK1A substrates have been linked to mRNA splicing, protein translation and regulation of endocytic, catabolic and apoptotic mechanisms. For this reason, DYRK1A is understood to exert a pleiotropic role in multiple molecular aspects of development and adult life (5). Evidence has implicated DYRK1A function in multiple pathological processes, including tumour proliferation, regulation of bone stability and cardiac hypertrophy (17-20). DYRK1A has also been linked to neurodegenerative disease through identification of its substrates. Examples include α -synuclein and septin 4 (21, 22), two key proteins in Parkinson's disease (PD), and huntingtin interacting protein-1 (Hip-1) an important contributor to Huntington's disease (HD - (23)). Despite this knowledge, the precise role(s) of DYRK1A in CNS function remains elusive. Nonetheless, this question has been heavily investigated. As introduced, the seminal Tejedor et al. study (3), which first identified *Mbn* (DYRK1A) in *Drosophila*,

Chapter 4.3 - DYRK1A-mediated Wnt signalling modulation

emphasised its importance in CNS development. Loss-of-function *Mbn* mutations in fly larvae impaired neurogenesis, but also substantially reduced cerebral hemispheric volume. This *Mbn* phenotype was particularly shown to result from abnormal spatial arrangement of proliferating neuroblasts, implying direct *Mbn*-mediated modulation of developmental patterning in the *Drosophila* larval brain. Indeed, *Dyrk1a* knock-out (KO) studies in mice have long demonstrated the key importance of this kinase in CNS development and function. Fotaki *et al.* were among the first to investigate DYRK1A in this context (24). They showed that heterozygous *Dyrk1a* KO mice display overall smaller body size, with substantial reductions in brain and liver volume. Homozygous *Dyrk1a* KO, however, is embryonically lethal at mid-gestation, a phenotype accompanied by severe developmental delay. Additionally, the authors reported that homozygous *Dyrk1a* KO results in significantly decreased neuronal number in the developing superior colliculus. These data not only suggests that DYRK1A is a necessary requirement for embryonic survival and CNS development, but also that it directly affects neuronal organisation at the cellular level.

Another study later expanded on this notion, demonstrating alterations in cortical neuronal dendritic architecture in heterozygous *Dyrk1a* KO mouse embryos (25). At the whole brain level, *Dyrk1a* copy number significantly affects cerebral weight, volume, viability and growth in mice (26). Guedj *et al.* employed three DS models to characterise complex developmental effects of *Dyrk1a* dosage on cerebral morphology. These were highly dependent on brain region. For instance, DYRK1A gain-of-function increased ventricular and superior collicular volume, consistently with KO data by Fotaki *et al.*, which demonstrated a reduction (24). By contrast, cortical neuronal density was found to be reduced in mice overexpressing *Dyrk1a*, whilst, thalamic nuclear neuronal density positively correlated with *Dyrk1a* dosage (26). These highly complex phenotypes underscore the fundamental importance of fine DYRK1A regulation throughout CNS development. It follows that the impact of DYRK1A triplication in human DS neurodevelopment is likely heterogeneous. Similar observations have also been made in human cases of *DYRK1A* mutations. Two studies in fact demonstrated that *DYRK1A*-deleting or truncating mutations are sufficient to produce microcephaly (27, 28).

Importantly, DYRK1A is also a known regulator of the cell cycle. Najas *et al.* recently characterised interesting DYRK1A effects on the cell cycle in the context of cortical neuronal differentiation (29). This is particularly relevant to DS, since prenatal deficits in neuronal development are associated with intellectual disability in this condition. The authors reported that nuclear levels of Cyclin D1, a key mediator of cell cycle progression, are finely regulated by DYRK1A in Ts65Dn mouse embryonic neuronal progenitors. Enhanced DYRK1A levels in transgenic embryos reduced nuclear Cyclin D1, and prolonged G1 phase duration. This resulted in abnormal proliferation of progenitor cells, further leading to decreased neurogenic mitosis. An overall reduction in cortical neuronal number was observed, both embryonically and postnatally. Furthermore, reports indicate that DYRK1A may directly promote Cyclin

Chapter 4.3 - DYRK1A-mediated Wnt signalling modulation

D1 degradation (30). Single-cell analysis revealed that, in DS-derived human fibroblasts, *DYRK1A* overexpression prolongs G1 duration, similarly to mouse results by Najas *et al.* (29). This effect appears dependent on Cyclin D1 phosphorylation by DYRK1A, which leads to its degradation. Accordingly, pharmacological DYRK1A inhibition was sufficient to rescue this phenotype (30). These data overall suggest that downregulation of Cyclin D1 by aberrant DYRK1A activity may directly affect neuronal development in DS. Interestingly, Cyclin D1 is a well known canonical Wnt target gene (31). β -catenin activity indeed regulates its expression and mediates abnormal cell proliferation in several cancer types (32, 33). This established relationship implies that DYRK1A might modulate Cyclin D1 through Wnt signalling activity. Despite its inhibitory effect on Cyclin D1, DYRK1A may also promote neuronal differentiation. Hammerle *et al.* showed that DYRK1A is transiently expressed in the vertebrate CNS neuroepithelium prior to neuronal differentiation (34, 35). Interestingly, DYRK1A kinase activity positively correlated with arrested cell proliferation. In mouse and chick CNS tissue, DYRK1A appears to upregulate transcription of Cyclin-dependent kinase inhibitor p27 (KIP1), an important regulator of cell cycle exit. Another cell cycle regulator, Cyclin-dependent kinase-like 5 (CDKL5) is also a substrate of DYRK1A. The subcellular localisation of CDKL5 is reportedly controlled by DYRK1A via phosphorylation (36). With relevance to Wnt signalling, it has been shown that concomitant DYRK1A and GSK3 β inhibition positively regulates proliferation of human pancreatic β -cells (37). The authors interestingly argue that this effect might be mediated by enhancement of β -catenin signalling.

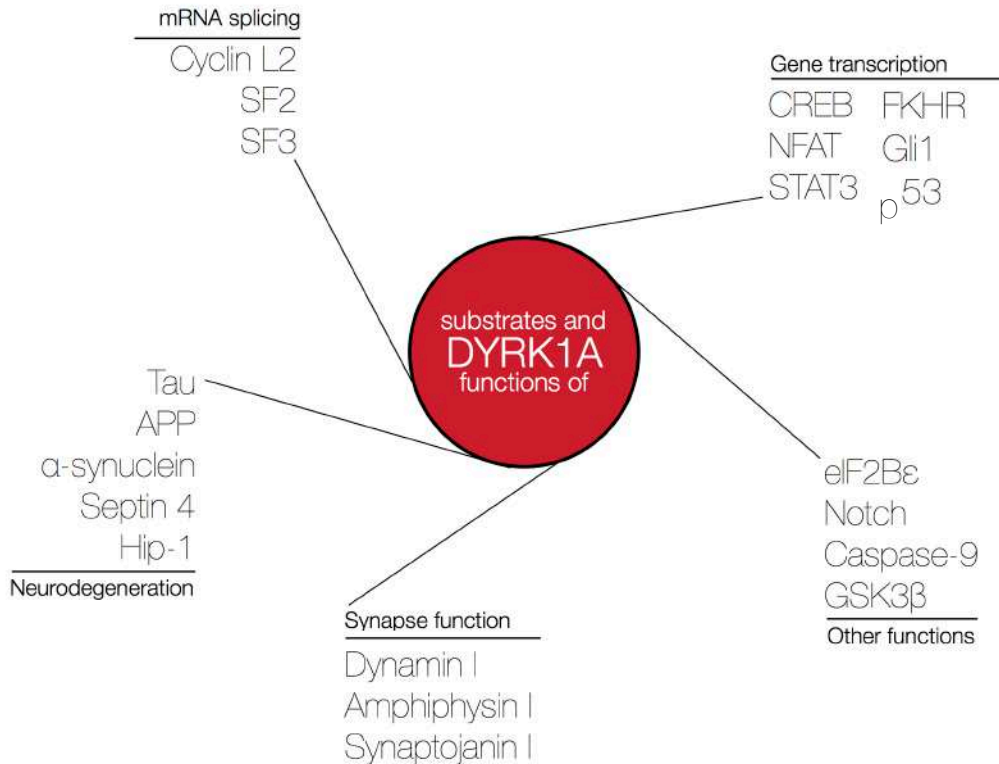


Fig. R3.b - Visual summary of DYRK1A substrates and function, demonstrating the importance of this kinase in a wide variety of biological processes.

In summary, extensive evidence implicates DYRK1A function in several cellular processes and particularly CNS development. The indispensable DYRK1A requirement for embryonic survival and homeostatic neurodevelopment support the role of this kinase as a key player in DS and as a candidate modulator for the Wnt phenotypes observed so far in this thesis.

4.3.1.1.2 The role of DYRK1A in DS and AD-DS

The DYRK1A gene is located on a portion of Hsa21 termed the Down syndrome critical region (DSCR - (38)). As introduced, the DSCR is currently thought to be a critical mediator of DS pathology (39), and particularly influences the development of intellectual disability in DS (40) (see 1.1.2 for an overview of the DSCR). Indeed, a DS-like phenotype is invariably associated with DYRK1A overexpression in mouse models (11, 14, 41, 42), and several studies have shown the contribution of this kinase to DS pathology. In the context of DS-related leukaemias, for instance, DYRK1A has been shown to be a potent megakaryoblastic oncogene due to its inhibitory effects on NFAT signalling, an important pathway in leukemogenesis (43). Abundant evidence now suggests that DYRK1A significantly contributes to several neuropathological features of DS (11, 38, 44). First, as introduced, *DYRK1A* overexpression correlates with enhanced DYRK1A transcript and protein levels in DS fetal and adult brains (41, 45). In mice, multiple *Dyrk1a* overexpression and deletion studies in the adult CNS (15, 46, 47) and embryonic brain (26, 29, 34, 35, 48) elucidated its key importance in homeostatic control of neuronal function and development.

With respect to AD-DS, DYRK1A is a favourable candidate to explain a potential mechanistic contribution of Hsa21 to the development of AD pathology. There are several lines of evidence supporting this view. As an initial consideration, both APP and tau, two proteins crucial to AD pathogenesis, have been identified as *in vitro* phosphorylation targets of DYRK1A in multiple independent studies (49-53), which are discussed in further detail below. From a biochemical viewpoint, the consistency of these data suggests a potential functional relationship between DYRK1A, APP and tau. In 2007, Kimura *et al.* (50) investigated potential Hsa21 markers in a Japanese population of AD patients. The analysis revealed a significant association between DYRK1A levels and the presence of AD. A more recent study corroborated this finding, by identifying levels of plasma DYRK1A as a previously unknown risk factor for sporadic AD (54). This further strengthens the functional DYRK1A-AD relationship by demonstrating that DYRK1A abnormalities extend, beyond the CNS, to the highly dynamic haematological system. Additionally, Kimura *et al.* (50) demonstrated that tau is a substrate of DYRK1A, phosphorylated at T212 (p-T212). Such interaction was observed both *in vivo* mouse brains and *in vitro*. In the same study, the authors additionally reported that acute administration of A β , in neuroblastoma cells and in mice, results in overexpression of DYRK1A. A concurrent, similar study also observed the same tau phosphorylation mechanism in the brain of transgenic DYRK1A mice (51). These findings suggest that DYRK1A may be a key player in both AD-DS and sporadic AD pathogenesis. According-

ly, elevated total DYRK1A and p-T212-tau levels have been observed in adult brains of both AD-DS and sporadic AD patients (52, 55). Liu *et al.* demonstrated that gain-of-function *Dyrk1a* mutations are sufficient to increase protein levels of APP, A β and p-p-T212-tau, resulting in tau inhibition and neurofibrillary aggregation (52). These findings were concurrently replicated in an independent study by Ryoo *et al.* (53). In DS, DYRK1A is also reportedly capable of indirectly regulating tau splicing, and its overexpression results in abnormal ratios of different tau isoforms (56). The authors showed that this mechanism relies on DYRK1A-mediated phosphorylation of alternative splicing factor (ASF), a regulator of tau-splicing. Furthermore, the protein presenilin 1 (PSEN1), an integral part of the γ -secretase complex regulating A β production, is reportedly phosphorylated by DYRK1A (57). In the phosphorylated state, PSEN1 appears to stabilise the enzymatic complex and enhance its amyloidogenic activity, with obvious implications for AD. Several studies also demonstrated deleterious functional effects of *Dyrk1a* overexpression in the hippocampus of DS mouse models. Overall, data indicate that aberrant DYRK1A activity produces deficits in hippocampal-dependent episodic and spatial memory (58-62).

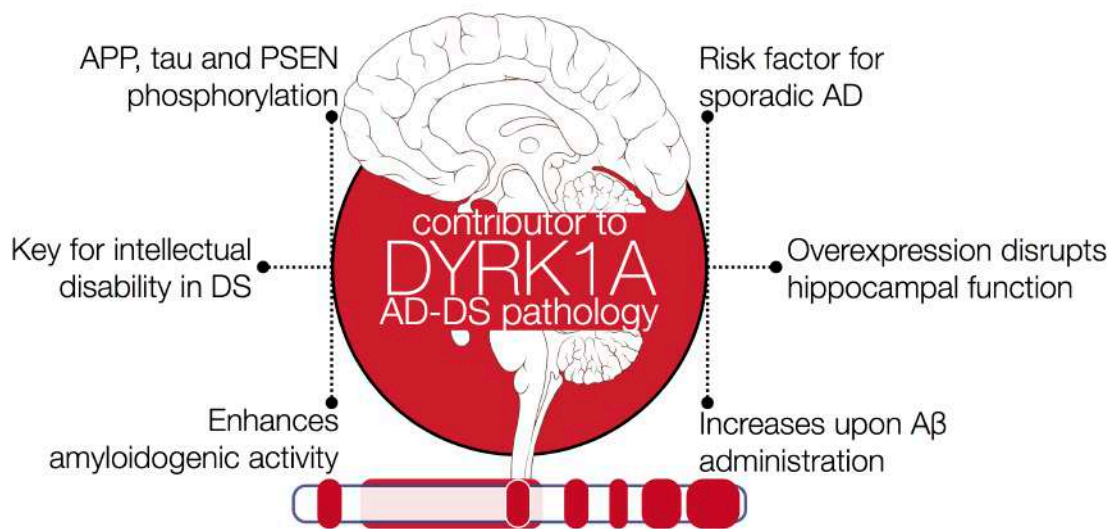


Fig. R3.c - Known contribution of DYRK1A to features of sporadic AD and AD-DS.

Taken together, these studies support the view that excessive amounts of DYRK1A might directly contribute to the AD-facilitatory effect of Hsa21 trisomy, and also provide a functional link between A β production and tau phosphorylation. Given the high spatiotemporal variability of *DYRK1A* overexpression in human DS discussed previously (4.1-2.1), however, the exact contribution of DYRK1A to AD-DS pathology might prove difficult to establish definitively. One overarching possibility may be found in the known regulatory role of DYRK1A over multiple signalling pathways important for brain development and function, which is discussed in the next section.

4.3.1.1.3 Signalling pathway regulation by DYRK1A

The evidence discussed so far elucidated the wide array of DYRK1A functions in several biological mechanisms, and essentially, its indispensable necessity for embryonic survival and CNS development. Indeed, intracellular signalling pathways are highly conserved key mechanism regulating development. It follows that the effects of abnormal *DYRK1A* expression in DS may be mediated by modulation of one or more signalling pathways. Combination of literature knowledge on DYRK1A with the Wnt phenotypes so far observed (see 4.1-2) led to the formulation of one of the main hypotheses of this thesis. That is, Wnt signalling dysfunction in the DS brain might occur through potential modulation by DYRK1A. Whilst not being the only feasible candidate gene, DYRK1A may contribute significantly to the Wnt-DS relationship (see next section). This hypothesis partly builds on the known regulatory functions of DYRK1A in several pathways with structural and functional similarity to Wnt signalling. Accumulating evidence, in fact, suggest that multiple DYRK1A substrates are involved in intracellular signalling pathways. These include NFAT, receptor tyrosine kinase (RTK), Notch and hedgehog (Hh) signalling, and are briefly considered here.

NFAT signalling is a conserved pathway regulating several aspects of immune, vascular and nervous system development (63). When dephosphorylated in the cytosol, NFAT transcription factors translocate to the nucleus and drive gene expression, similarly to β -catenin (64). Conversely, NFAT phosphorylation by multiple kinases, including GSK3 β , leads to inactivation of the pathway (65, 66). Interestingly, NFAT is reportedly phosphorylated by multiple DYRKs(1A) (44, 67). The data show this to be a priming phosphorylation event, a known property of DYRK1A, which stimulates further phosphorylation by GSK3 β and casein kinase 1 (CK1), ultimately leading to NFAT inactivation and cytoplasmic accumulation. The functional importance of GSK3 β and CK1 in Wnt signalling (68), as well its known overlap with NFAT, is strongly suggestive of a potential DYRK1A effect on Wnt activity. DYRK-mediated NFAT inhibition has observable functional consequences on NFAT-regulated processes such as differentiation of erythrocytes and osteoclasts (19, 69) as well as pathological cardiomyocyte hypertrophy (18).

DYRK1A also reportedly affects **RTK signalling**, a pathway important in cell metabolism, migration and differentiation. Particularly, RTK regulates synaptic plasticity, angiogenesis and tumour growth (70). This pathway possesses several well described positive and negative modulators, which fine tune RTK activity (71). Interestingly, DYRK1A was shown to upregulate RTK signalling activity through direct interaction with components of this pathway, in the neuronal cytosolic and membrane compartments (72, 73). A further study suggest that this effect is also dependent on DYRK1A kinase activity, which positively correlates with RTK output in rat and human cell lines (74).

The Notch signalling pathway is also highly conserved, and regulates developmental tissue patterning, cell fate specification, proliferation and apoptosis (75). The main mediators of this pathway are Notch receptors. These transmembrane receptors are enzymatically cleaved upon Notch activation, leading to nuclear translocation of their intracellular domain (NICD), which drive gene expression as transcriptional activators (75, 76). Evidence suggests that, in neurons, DYRK1A may physically interact with and phosphorylate NICD, thereby inhibiting Notch signalling activity (77). In the same study, this effect is accompanied by reduction of Notch-mediated suppression of neuronal differentiation.

Hh signalling is crucial for organ development and neural tube patterning (78), while also promoting mitosis in several neuronal precursor cell types throughout the CNS (79). The main mediators of Hh signalling belong to the Gli family (Gli1–3) of transcription factors (80), which translocate nuclearly upon Hh activation. Reports indicate that DYRK1A prolongs nuclear localisation of Gli1 in a kinase-dependent manner, thereby enhancing Hh activity (81, 82). Despite Gli1 being a DYRK1A substrate, however, Hh pathway activation does not in itself affect DYRK1A kinase activity (81).

In summary, these studies strongly suggest the presence of a functional relationship between DYRK1A and several signalling pathways structurally similar to Wnt signalling. Importantly, some of the pathways discussed here do indeed functionally overlap with Wnt, such as NFAT and hh (68). The evidence discussed thus provides a logical basis to the main hypothesis of this chapter.

4.3.1.1.4 DYRK1A: a potential Wnt signalling regulator?

In addition to the pathways discussed above, formulation of the Wnt-DYRK1A hypothesis in this thesis is also supported by a number of studies indicating a possible effect of DYRK1A on Wnt signalling activity. (see 1.2 for an overview of the pathway).

Importantly, DYRK1A has been shown to be a positive regulator of p120/ δ -catenin signalling (83). This pathway is a ramification of canonical Wnt signalling, with δ and β -catenin sharing high structural similarity. δ -catenin binds the Kaiso transcription factor, driving expression of several target genes, some of which are in common with canonical Wnt genes (e.g. *SIAMOSIS*, *WNT1*). In *X. laevis* embryos and mammalian cells, DYRK1A reportedly enhances δ -catenin levels and signalling activity (83). Co-expression of DYRK1A and δ -catenin in *X. laevis* resulted in dual head formation and severe developmental abnormalities. This suggests that a potential DYRK1A-mediated imbalance in developmental Wnt signalling activity might also be deleterious in human DS, given the enhanced gene dosage of this kinase.

Some studies have also revealed a relationship between DYRK1A and GSK3 β . DYRK1A appears to function as a GSK3 β priming kinase, tagging NFAT for further phosphorylation by GSK3 β , as discussed above, (44). This ultimately results in NFAT inactivation and degradation. Interestingly, this DYRK1A priming mechanism appears to also regulate other GSK3 β substrates. Degradation of the circadian protein CRY2, for instance, is reportedly promoted by an analogous priming phosphorylation by DYRK1A (84).

Chapter 4.3 - DYRK1A-mediated Wnt signalling modulation

With relevance to DS neuropathology, DYRK1A-GSK3 β priming also applies to tau metabolism. DYRK1A phosphorylates tau at T212, and this interaction has been shown to stimulate further phosphorylation by GSK3 β at S208 and eventual tau degradation (49, 85). Liu *et al* showed enhanced tau aggregation by DYRK1A overexpression, as discussed above (52). Interestingly, this phenotype was also dependent on secondary phosphorylation by GSK3 β . The occurrence of this phenomenon in three distinct and mostly unrelated processes suggest the presence of a general mechanism. Given the importance of GSK3 β in Wnt signalling activation, DYRK1A priming might also apply to GSK3 β -regulated Wnt substrates. Even if not the case, such a consistent functional link warrants the question of whether DYRK1A priming might secondarily affect multiple GSK3 β functions by modulating its substrate preference. As introduced previously, it has been shown that GSK3 β is abnormally phosphorylated at the S9 residue in aged but not young/adult Tc1 mouse brains ((86) - 4.2.2). Given that this phosphoresidue is inhibitory (87, 88), Shepard *et al.* argue that Hsa21 trisomy might lead to an age-dependent decrease in GSK3 β activity. It is thus possible to hypothesise that, because of the Wnt inhibitory role of GSK3 β , prolonged GSK3 β inhibition in DS might lead to an altered state of canonical Wnt signalling. As introduced above, Shen *et al.* (37) reported enhanced β -cell proliferation following concomitant kinase inhibition of DYRK1A and GSK3 β . The authors speculated that this effect might be mediated by modulation of β -catenin signalling.

A putative DYRK1A effect on Wnt signalling, however, need not solely be dependent on its relationship with GSK3 β . The complexity of both Wnt function and DYRK1A modulation of other pathways implies that other mechanisms may be at play, possibly synergistically. First, GSK3 β interacts with several cytosolic Wnt components. It may thus be argued that the primary DYRK1A effect on Wnt, if present, might occur through secondary DYRK1A interactions with other components of the pathway, for instance disheveled-1 (DVL1), CK1 or β -catenin itself. Second, it should be kept into consideration that DYRK1A is most prominently a nuclear kinase, as introduced. In parallel, Wnt signalling activation indeed ultimately relies on transcriptional activity of nuclear β -catenin. It is therefore possible that enhanced DYRK1A activity in the nucleus might also affect Wnt signalling within this compartment, independent of cytoplasmic effects. This overall implies the intriguing possibility that distinct Wnt-regulatory mechanisms by DYRK1A might exist in relation to its subcellular localisation. The functional importance of DYRK1A intracellular distribution is therefore introduced briefly here.

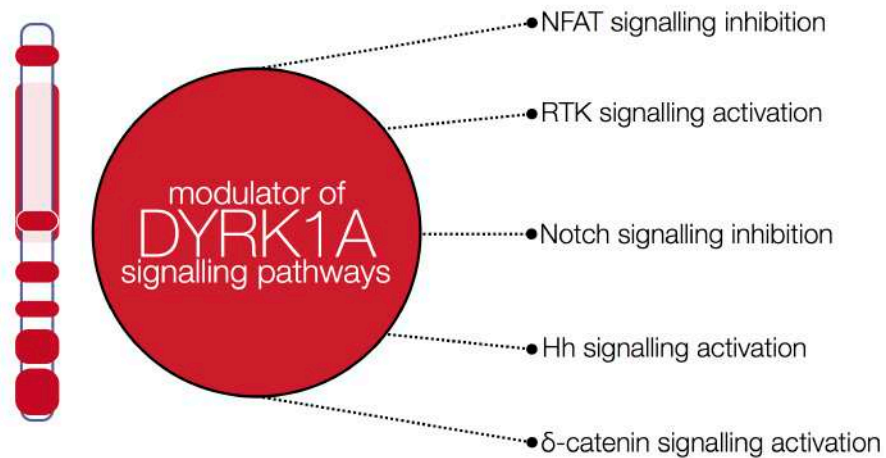


Fig. R3.d - Summary of DYRK1A-mediated modulation of signalling pathways, including the Wnt/ δ -catenin branch.

4.3.1.1.5 Subcellular localisation: the master key to DYRK1A function?

As introduced, DYRK1A functionally localises to both nuclear and cytosolic subcellular compartments. This has been clearly demonstrated endogenously, in a variety of neuronal cellular model systems including human, mouse and chick (15, 47, 89). This localisation pattern is variable, however. For example, DYRK1A expression is prominently cytosolic in glial cell lines (47). In the mouse brain, two studies identified an additional subdistribution of the DYRK1A cytosolic fraction (74, 90). DYRK1A reportedly segregates into three distinct functional pools: soluble, 'free' cytoplasmic DYRK1A, a pool associated with trafficking vesicles and a third in association with the neuronal plasma membrane. A number of studies have also shown that, under conditions of ectopic overexpression, DYRK1A preferentially localises to the nucleus of mouse hippocampal neurons, neural cells of the embryonic neocortex and several human cell lines (4, 13, 77, 81, 91-94). As introduced, DYRK1A sub-localises to the nucleus further by associating with nuclear speckles, when overexpressed and endogenously (4, 77).

Importantly, the nuclear-to-cytosolic ratio of DYRK1A is finely regulated. A 2002 study by Hammerle *et al.* (34) employed chicken cerebellar neuronal precursor cells to investigate DYRK1A localisation during neuronal differentiation. The authors detected a substantial rearrangement of subcellular DYRK1A distribution, in favour of the cytosolic compartment, at critical stages of Purkinje cell differentiation. This study also observed dynamic, persistent nuclear/cytosolic trafficking of DYRK1A. The presence of DYRK1A in both subcellular compartments, as well as fine regulation of its distribution, has been suggested to primarily serve as a means to segregate DYRK1A from its substrates (5). DYRK1A function may thus be modulated by influencing its availability to substrates. Interestingly, it appears that subcellular distribution of DYRK1A might be regulated through its differential phosphorylation. Kaczmarek *et al.* employed fractionation and 2DE to isolate three distinct DYRK1A pools in mouse and human brain lysates (95). DYRK1A was found in cytosolic, cytoskeletal and nuclear fractions with distinct isoelectric points, indicative of differential phosphorylation. This finding was further investigated via phosphate-affinity gel electrophoresis, which showed significant shifts in migration of DYRK1A bands depending on subcellular compartment. The authors then employed mass spectrometry to pinpoint this phosphorylation-dependent localisation to specific DYRK1A residues. The study however failed to identify any candidate kinases for this mechanism, which remain undetermined.

Overall, it is clear from the evidence discussed that DYRK1A localisation to subcellular compartments is highly dynamic, finely regulated and thus likely to significantly affect its function. It follows that its investigation, in the context of a potential DYRK1A-Wnt interaction, might provide important information on the nature of this putative relationship. If present, a functional overlap between DYRK1A and Wnt signalling is indeed likely to be reflected by specific localisation patterns of this kinase.

4.3.1.2 Luciferase-based quantification of Wnt signalling activity, an established approach

In this chapter, acute changes in Wnt signalling activity were measured in live cells. This was accomplished by measuring levels of active β -catenin via luciferase assay, a well established technique (see methods 3.5.5). This assay is widely employed in the investigation of a high number of biological processes, and is a validated tool for the study of Wnt signalling activity in live cells. Key evidence illustrating the advantages of this technique is briefly discussed below.

Luciferase (from the latin *Lucifer*, 'light carrier') collectively describes a family of oxidative enzymes capable of chemically producing light, a phenomenon termed bioluminescence. An array of different Luciferase enzymes exists in nature, and they are found in several organisms, most prominently in the firefly (*P. pyralis*), sea pansy (*R. reniformis*) and the *Photobacterium* prokaryotic genus. The former two are employed in the experiments described in this chapter. At a general level, luciferase produces light via ATP-dependent oxidation of a substrate termed luciferin to oxyluciferin. The energy produced by this reaction is released in the form of light. Upon oxidation, oxyluciferin electrons switch to a transient excited quantum state which is then followed by release of photons and return to the ground state. Thus, in contrast with fluorescent and photoproteins, bioluminescence is an active, energy-dependent and easily measurable process. This notion makes luciferase activity particularly useful for biological assays, which have now been employed for over half a century. The firefly luciferase system was characterised in the mid 20th century, by the pioneering work of William McElroy and colleagues. Luciferin was first purified in 1949 (96), and the same group later developed the first luciferase assay protocol. By the late 60s, studies employing this technique began to appear (97). Since then, the luciferase assay has been employed in several fields of molecular biology, the method has been perfected over time and is now standardised. Regardless of the specific application, this technique relies on quantifying luciferase bioluminescence under substrate-saturating conditions, whereby enzyme concentration is the only rate-limiting step. It follows that light output can be utilised as a direct, approximately linear correlate of whichever biological process is under study.

The luciferase assay is ideal for measuring activity of signalling pathways, and is widely employed in this sense. Luciferase genes have been cloned and their expression can thus be manipulated in several experimentally useful ways. With respect to intracellular signalling, the activity of transcription factors under study can be made to promote luciferase expression. Administration of luciferin consequently results in a measurable signal representative of pathway activity. This approach is employed in the study of several signalling pathways, indeed including canonical Wnt signalling. In the latter case, transcriptional activity of TCF/LEF factors stimulated by β -catenin is the preferred luciferase quantification method. The advent of molecular cloning allowed for the engineering of expression systems specifically driving luciferase output via TCF/LEF- β -catenin activation. Such systems can be employed as expression vectors in eukaryotic and prokaryotic cell lines, or genomically integrated into any mod-

Chapter 4.3 - DYRK1A-mediated Wnt signalling modulation

el organism. The first luciferase construct for Wnt quantification is a plasmid incorporating eight TCF/LEF sites upstream of a luciferase reporter gene. It was developed in 1997 by Van de Wetering *et al.*, in a study examining the role of TCF genes in *Drosophila* (98). The construct is usually referred to as (M50 Super 8x) TOPFlash. It was later improved and made publicly available by Veeman *et al.* (99), who employed the construct in a zebrafish study of developmental Wnt function. Since then, luciferase quantification has become an established and reliable approach in the field of Wnt signalling. TOPFlash vectors are now widely available, and continue to be used in recent high quality publications, for instance in the context of breast and colorectal cancer (100, 101).

Indeed, the Kirsten Harvey research group, which funded and directed the project of this thesis, has accumulated great expertise in luciferase-based Wnt signalling investigation. Several studies have been published by the group, in which the technique was employed and optimised. In 2012, Berwick & Harvey first demonstrated that leucine-rich repeat kinase 2 (LRRK2), an important contributor to familial Parkinson's disease (PD), plays a key structural role in Wnt signalling function (102). The protein was shown to act as a scaffold for multiple Wnt components through direct interaction. Luciferase assays in neuroblastoma cells importantly demonstrated that LRRK2 expression is sufficient to enhance active Wnt signalling levels. Additionally, PD-associated pathogenic LRRK2 mutations reduce this effect in the same system. The group also showed in a later study that a PD-protective LRRK2 mutant exerts the opposite effect, enhancing LRRK2-mediated elevation of active Wnt signalling (103). Luciferase assays were also recently employed by the same group to assess LRRK2 effects on basal Wnt signalling activity in modified embryonic fibroblasts (MEFs) of LRRK2 KO mice (104). Strikingly, KO cells displayed enhanced basal β -catenin and Axin2 transcriptional activity. Conversely LRRK2 expression significantly suppressed basal TOPFlash activity, a phenotype enhanced by pathogenic LRRK2 variants. Overall, combined evidence from the luciferase technique led to the discovery of a fine Wnt regulatory role of LRRK2, which is capable of both enhancement and repression of pathway activity dependent on previous activation state.

In summary, the luciferase assay is a validated and well-established technique in the Wnt signalling field. Building on its strength and reproducibility, and the expertise of the Kirsten Harvey Group, it was thus employed to address the primary experimental question of this chapter i.e. to determine whether DYRK1A is capable of modulating Wnt signalling activity.

4.3.2 Results

The link between DS and AD has long been documented (see 1.1.4), and several studies now suggest alterations in canonical Wnt signalling may play a significant role in the pathogenesis of AD (see 1.2.5). The existence of these relationships along with evidence implicating some Hsa21 genes in Wnt signalling (see 1.3), as well as the data gathered so far (4.1-2) led to a candidate gene hypothesis for the observed Wnt abnormalities in DS. Given the evidence discussed above, DYRK1A was selected as the initial Hsa21 candidate for effects on the Wnt pathway. However, this choice does not exclude the participation of other Hsa21 genes, such as *APP*. The aim of the studies presented here was threefold:

- I. **To characterise, explore and summarise Wnt-related protein-protein interaction networks for DYRK1A, combining public database knowledge (STRING), Yeast two hybrid screening (Y2H) and co-immunoprecipitation (co-IP) with Western blotting.**
- II. **To investigate whether acute manipulation of DYRK1A activity might exert modulatory effects on canonical Wnt signalling via luciferase assays and overexpression.**
- III. **To investigate the effects of Wnt signalling activation on the subcellular localisation of DYRK1A via quantitative immunocytochemistry.**

In the vast majority of experiments performed, human cell line systems were employed, to more closely represent human physiology.

4.3.2.1 DYRK1A-Wnt protein interaction networks

In order to preliminarily investigate DYRK1A as a candidate Wnt signalling modulator, the interactome of this kinase was interrogated for Wnt-relevant protein interactions, employing multiple techniques.

4.3.2.1.1 STRING-based DYRK family interaction with Wnt components

The Search Tool for the Retrieval of Interacting Genes/Proteins (STRING) is a large database combining known and predicted protein interaction networks (<http://string-db.org>; (105)). Its content is derived from “genomic context predictions, high-throughput lab experiments, conserved co-expression, automated text-mining and previous knowledge in databases”. STRING v10 was first employed to assess Wnt-related protein interactions for the entire vertebrate DYRK kinase family (DYRK1A/B, DYRK2-4). Each DYRK member was placed as the single starting node of a network comprising the first 50 or 100 best-scoring direct interactors. Overrepresentation/functional analysis was then performed on the resultant list of proteins by STRING, for enrichment with the Gene ontology (GO) or KEGG term “Wnt signalling pathway” (**Fig. R3.1**). In all conditions, and for all DYRK members, a significant association with Wnt signalling was detected whilst accounting for false-discovery rate ($FDR < 0.05$). Overall, DYRK family members were shown to possess from 3 up to 16 Wnt-related interaction partners. These data thus suggest that existing database and experimental knowledge already implicates the DYRK family in Wnt signalling.

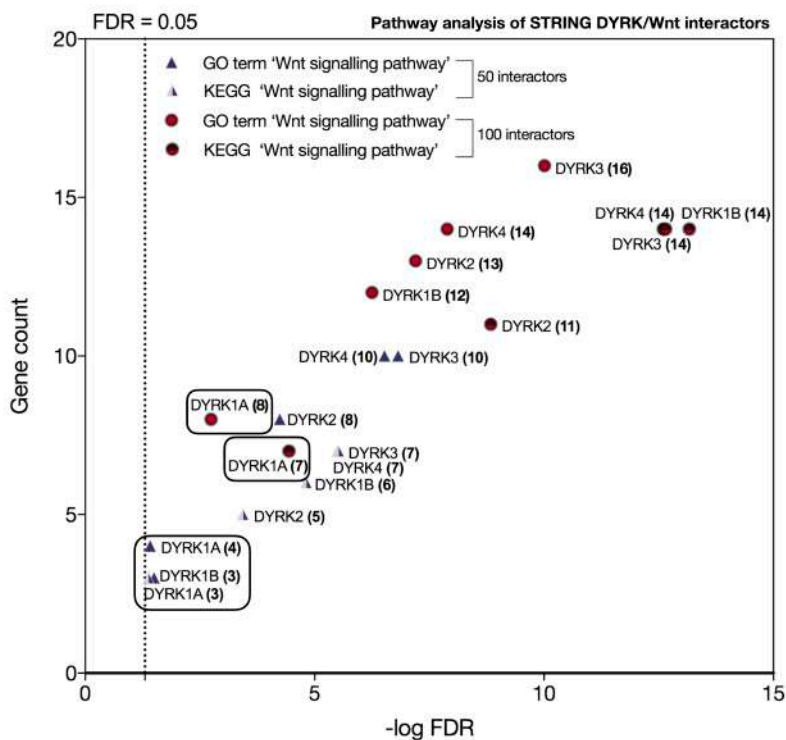


Fig. R3.1 - STRING-generated overview Wnt-relevant protein interactions for the entire DYRK family of kinases, plotting gene count as a function $-\log$ false discovery rate (FDR) of enrichment with the GO and KEGG terms ‘Wnt signalling pathway’.

4.3.2.1.2 Yeast two-hybrid screening reveals several DYRK1A-WNT interactions

Preliminary screening of the DYRK family indicated the presence of Wnt-related protein interactions. This finding was then further investigated by consulting a large protein interaction database part of the InterPP project, funded and conducted by Hybrigenics Ltd. on behalf of the Jerome LeJeune Foundation (Paris, Fr - fondationlejeune.org). This ongoing project represents an effort to identify and characterise protein-protein interactions in the DS brain. Interactions are detected via yeast two-hybrid screen (Y2HS) technology, employing all known Hsa21-encoded proteins as bait and/or prey against an adult brain cDNA library. For DYRK1A, a lex-A-based construct was employed. The database features a confidence scoring system termed PBS (PIM biological score) to assess the reliability of an observed interaction, ranging from A (extremely likely) to E (false positive/autoactivation ; see methods 3.7 for an overview of this database, techniques employed and scoring systems).

Setting the cut off at score C (moderate), the database was thus searched for DYRK1A partners with known functional relevance to Wnt signalling. The search identified an interesting array of potential DYRK1A interactions with Wnt-related proteins (**Fig. R3.2**). In yeast, DYRK1A reportedly interacts with DKK3, which was found to be altered in DS mice and humans, and LRP1B, a member of the LRP canonical Wnt signalling co-receptor family. Weaker protein protein interactions reported include Wnt inhibitory factor 1 (WIF1), LRP1 and 4. Additionally, the murine proteins Lrp1 and Lrp1b also interacted with mouse Dyrk1a in Y2H assays. The ligand Wnt3 and α -catenin were also reported to weakly interact with mouse and human DYRK1A, respectively. These data overall demonstrate multiple DYRK1A interactions with key Wnt components, and thus provide initial support to the main hypothesis of this chapter.

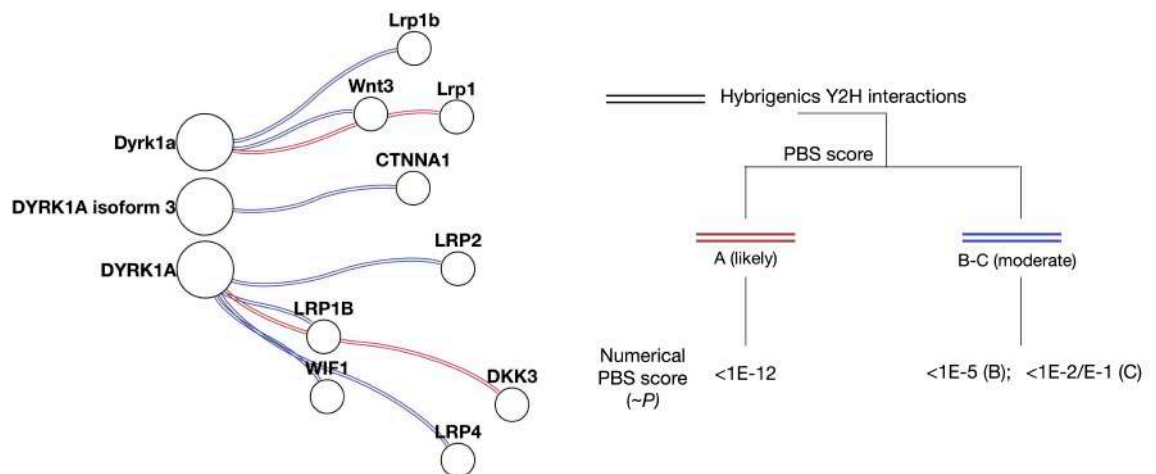


Fig. R3.2 - Visual summary of DYRK1A interactions with Wnt signalling components, as detected by Y2H screening. Lines are colour-coded to represent PIM Biological Score (PBS), a surrogate P value indicating the reliability of each interaction. Here, the highest scoring DYRK1A interactors were DKK3 and Lrp1b.

4.3.2.1.3 The poly-Histidine tail of DYRK1A interacts with DKK3

Given the presence of transcriptional and protein-level DKK3 alterations in DS (4.1-2), and the high PIM score of the hereby reported DYRK1A-DKK3 interaction, this relationship was further characterised by Hybrigenics via Y2H assay (see 3.7 for specifics of the Y2H protocol). Yeast cells were transformed with the *lexA-DYRK1A* expression construct employed as prey for screening in 4.3.2.1.2, and grown for 72 hours as liquid cultures. They were also co-transformed with either an empty *lexA* bait vector (*lexA-∅*), a construct comprising the dickkopf domain of DKK3 in isolation (**aa131-aa245**) or a portion of Family With Sequence Similarity 53 Member C (*Fam53C*; **aa339-452**). The latter is known interactor of DYRK1A at the kinase domain, here acting as positive control. To verify functionality of the assay, yeast cells were additionally co-transformed with positively (*Smad/Smurf*) and negatively (*lexA-∅/AD-∅*)-interacting control bait/prey constructs in separate, but parallel reactions.

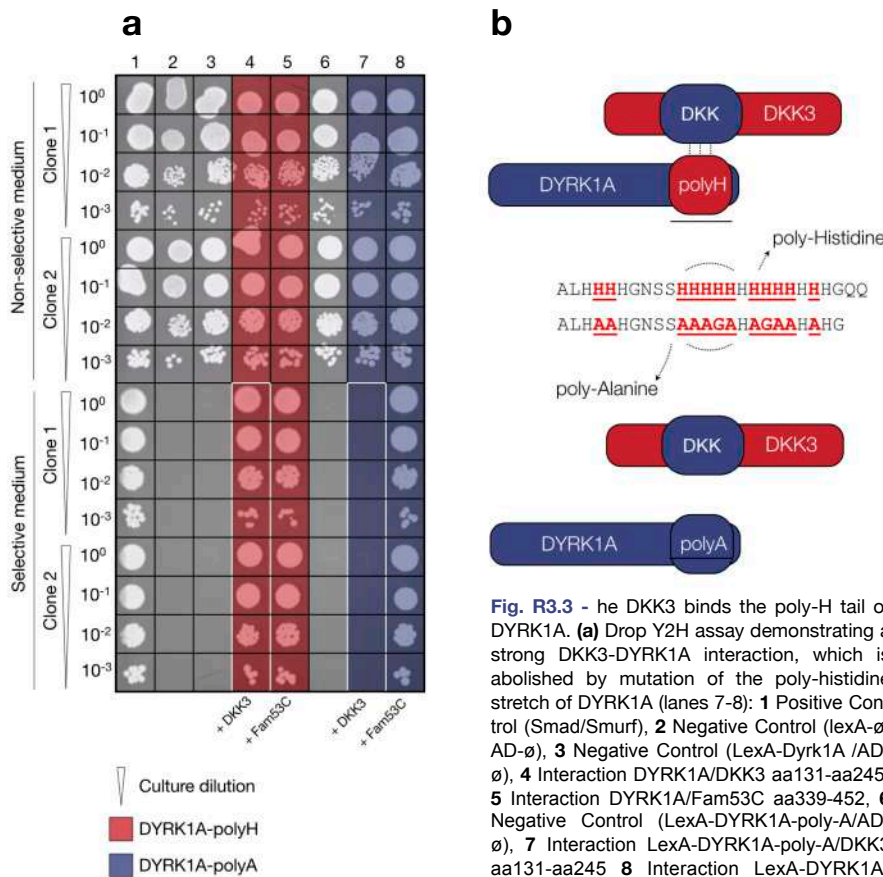


Fig. R3.3 - The DKK3 binds the poly-H tail of DYRK1A. **(a)** Drop Y2H assay demonstrating a strong DKK3-DYRK1A interaction, which is abolished by mutation of the poly-histidine stretch of DYRK1A (lanes 7-8): **1** Positive Control (*Smad/Smurf*), **2** Negative Control (*lexA-∅/AD-∅*), **3** Negative Control (*LexA-Dyrk1A /AD-∅*), **4** Interaction DYRK1A/DKK3 aa131-aa245, **5** Interaction DYRK1A/Fam53C aa339-452, **6** Negative Control (*LexA-DYRK1A-poly-A/AD-∅*), **7** Interaction *LexA-DYRK1A-poly-A/DKK3* aa131-aa245 **8** Interaction *LexA-DYRK1A-poly-H/Fam53C*. **(b)** Graphical summary depicting mutation sequence in **a** (lanes 7-8).

Thereafter, serial culture dilutions up to a factor of 10⁻³ were assessed via drop Y2H assay (**Fig. R3.3**). Cultures were grown on either non-selective and selective media (see 3.7). Under the former conditions all cultures grew successfully, throughout all dilution factors (**Fig. R3.3a, top square, lanes 1-5**). This result indicates successful yeast transformation and expression of the exogenous constructs.

Chapter 4.3 - DYRK1A-mediated Wnt signalling modulation

However when cultured in selective growth medium, which requires a positive interaction for yeast survival, only positive control- and DYRK1A+DKK3/Fam53C-positive cells grew successfully (**Fig. R3.3a, bottom square, lanes 1/4-5**). Overall, these data confirm the previously observed DYRK1A-DKK3 interaction against reliable controls.

Concomitantly, the sequence of the lex-A-DYRK1A construct was engineered in order to mutate its C-terminal poly-H tail (**aa 589-763**) into a poly-alanine (poly-A) sequence (**Fig. R3.3b, middle**). As discussed, the poly-H tail is important for DYRK1A interactions and nuclear speckle localisation (4, 11). Mutagenesis was thus performed to determine where the poly-H tail is necessary for the DKK3 interaction. The DYRK1A-poly-A construct was expressed in yeast cells under the same conditions as above. Whilst all cultures grew in non-selective medium (**Fig. R3.3a, top square, lanes 6-8**), no interaction was detected for DKK3 (**bottom square, lane 7**). The Fam53C interaction, being mediated by the kinase domain of DYRK1A, was unaffected by the poly-A mutation (**Fig. R3.3a, bottom square, lane 8**). Overall, these data demonstrate that the DYRK1A-DKK3 interaction is likely mediated by the poly-H tail of DYRK1A. Nevertheless, its mutation to poly-A does not appear to alter kinase domain binding of other DYRK1A substrates.

4.3.2.1.4 DYRK1A precipitates with DKK3 and DVL1, but not β -catenin

Following Y2H results, co-immunoprecipitation (co-IP) was employed to confirm the DKK3-DYRK1A interaction in human cells, and investigate other potential, Wnt-relevant DYRK1A protein partners. Three further Wnt signalling components were selected for this study, namely DVL1, GSK3 β and β -catenin. All are essential mediators of Wnt signalling activation and inhibition (68).

Co-IP was performed in HEK-293 cells (**$\sim 10^5$ cells/ml, $n=3$ cultures/condition**), via 24hr co-expression of 0.5 μ g/ml FLAG-tagged candidate interactors and HA-tagged DYRK1A, or relative empty control vector. Following FLAG bead-mediated precipitation and purification of tagged proteins, results were analysed via SDS-PAGE/IB alongside cell lysate control samples. For all interactors tested, immunoblotting with an endogenous antibody revealed expression of HA-DYRK1A in lysates, as a band migrating to ~ 90 kDa in accordance with its known molecular weight (11) (**Fig. R3.4-6, lanes 2/4, clear triangle**). DKK3 was also observed in control lysates, as a band migrating to approximately 60 kDa when probed for with an anti-FLAG antibody (**Fig. R3.4, lanes 3-4, clear arrow**). In contrast, the predicted molecular weight of DKK3 is theoretically ~ 30 kDa (106). It is however known that most of the DKK3 pool undergoes both *N*- and *O*-glycosylation in order to facilitate secretion (107, 108). This post-translational modification is likely to affect the observed molecular weight of DKK3. When expressed alone, DKK3 was precipitated by FLAG beads, also migrating to 60 kDa as a high-density band (**Fig. R3.4, lanes 7/8, dark arrow**).

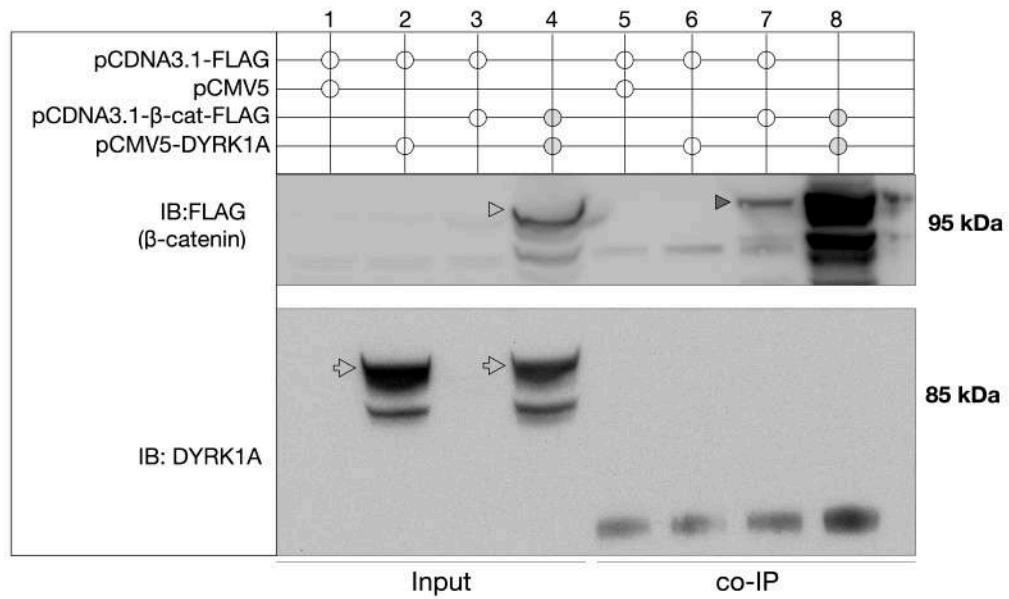


Fig. R3.6 - Expressed DYRK1A and β -catenin do not interact via FLAG pull-down in HEK293-cells. **Left:** input lanes demonstrating appropriate expression of both proteins (clear arrow/triangle). **Right:** co-IP lanes demonstrating precipitation of β -catenin when expressed alone and with DYRK1A (top dark triangle). No DYRK1A signal was detected in co-IP samples where both constructs were expressed. IB: immunoblotting antibody.

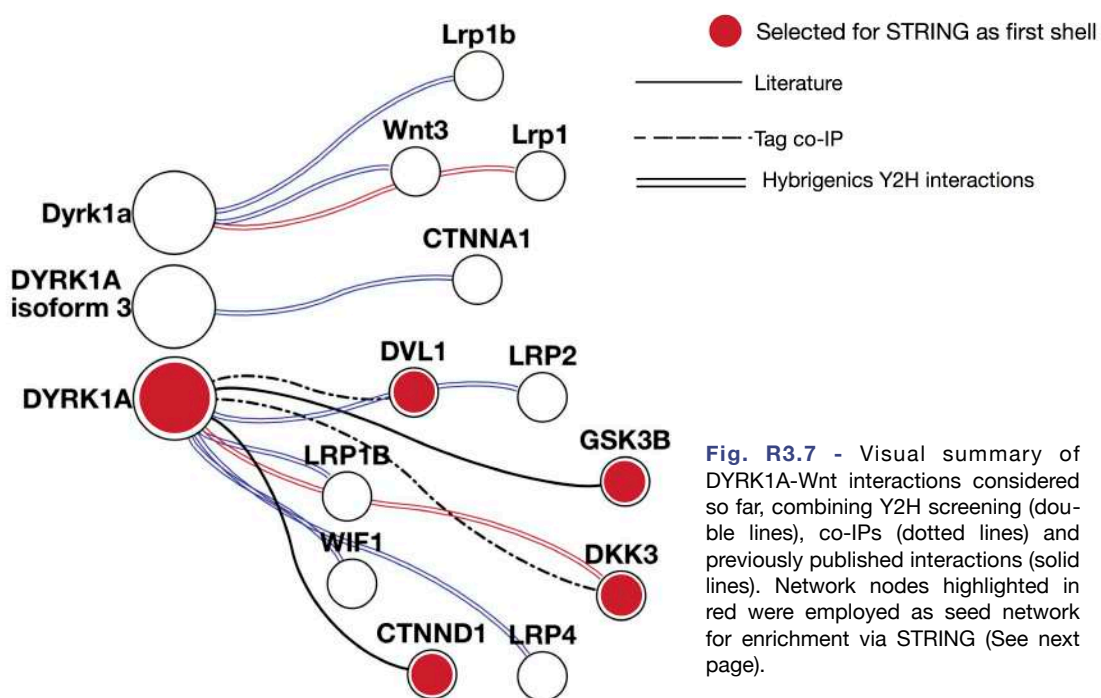
This finding helps guarantee the functionality and specificity of the FLAG bead co-IP reaction. Under these conditions, no DYRK1A signal was detected. Consistently with previous results, DYRK1A precipitated when co-expressed with DKK3-FLAG, and was detected in co-IP samples (**Fig. R3.4, lane 8, dark triangle**). DYRK1A was also co-expressed with FLAG-DVL1, a key second messenger for Wnt signalling (see 1.2). Expression of DVL1 was observed in cell lysates via FLAG staining (**Fig. R3.5, lanes 3-4, clear arrow**), and the protein was precipitated by FLAG beads when expressed alone (lane 7, dark arrow). Under these conditions, no DYRK1A signal was detected. Interestingly, however, DVL1 and DYRK1A co-precipitated when expressed together (**Fig. R3.5, lane 8, dark triangle**). Lastly, DYRK1A was also tested for interaction with β -catenin-FLAG. This protein was successfully detected in cell lysates as migrating to >100 kDa, in accordance with its known molecular weight (**Fig. R3.6, lanes 3-4, clear triangle**). β -catenin was also precipitated by FLAG beads, with or without DYRK1A co-expression (**Fig. R3.6, lanes 7-8, dark triangle**). In both conditions, however, DYRK1A did not precipitate, and was undetectable in co-IP samples despite substantial expression in cell lysates (**Fig. R3.6, lanes 2/4, clear arrow**).

Overall, these data provide further evidence on the participation of DYRK1A in Wnt protein networks. The previously detected DKK3 interaction was confirmed, and an additional interaction with DVL1, but not β -catenin, was also observed. This suggests that DYRK1A might be capable of modulating Wnt signalling activity on multiple levels, possibly affecting β -catenin indirectly.

4.3.2.1.5 STRING/Cytoscape interaction network analysis

The studies presented so far identified an array of DYRK1A protein interactions with components of Wnt signalling. Database knowledge and enrichment analysis preliminary suggested a functional Wnt relationship within the DYRK family interactome. Y2H screening confirmed the presence of multiple Wnt-relevant DYRK1A interactors, most notably DKK3 which binds the poly-H tail of DYRK1A. Additionally, co-IP evidence confirmed this interaction and identified a further association with DVL1. The presence of multiple interactions implies that DYRK1A might participate in a larger protein network influencing the Wnt pathway on several levels. To investigate this idea, the Cytoscape analysis software was employed along with STRING in order to build a network of potentially DS-relevant DYRK1A-Wnt interactions. This also served to summarise and contextualise all known and newly identified DYRK1A-Wnt interactions, aiding overall interpretation of the results available.

To achieve this goal, DYRK1A was first placed as the hub of a basic network (**Fig. R3.7**) comprising: **A)** The Hybrigenics-reported DKK3 interaction **B)** Previously published interactions between DYRK1A, p120 δ catenin (CTNND1- 83), and GSK3 β (109) **C)** The co-iP detected interactions with DVL1 and DKK3 (**Fig. R3.4-5**).



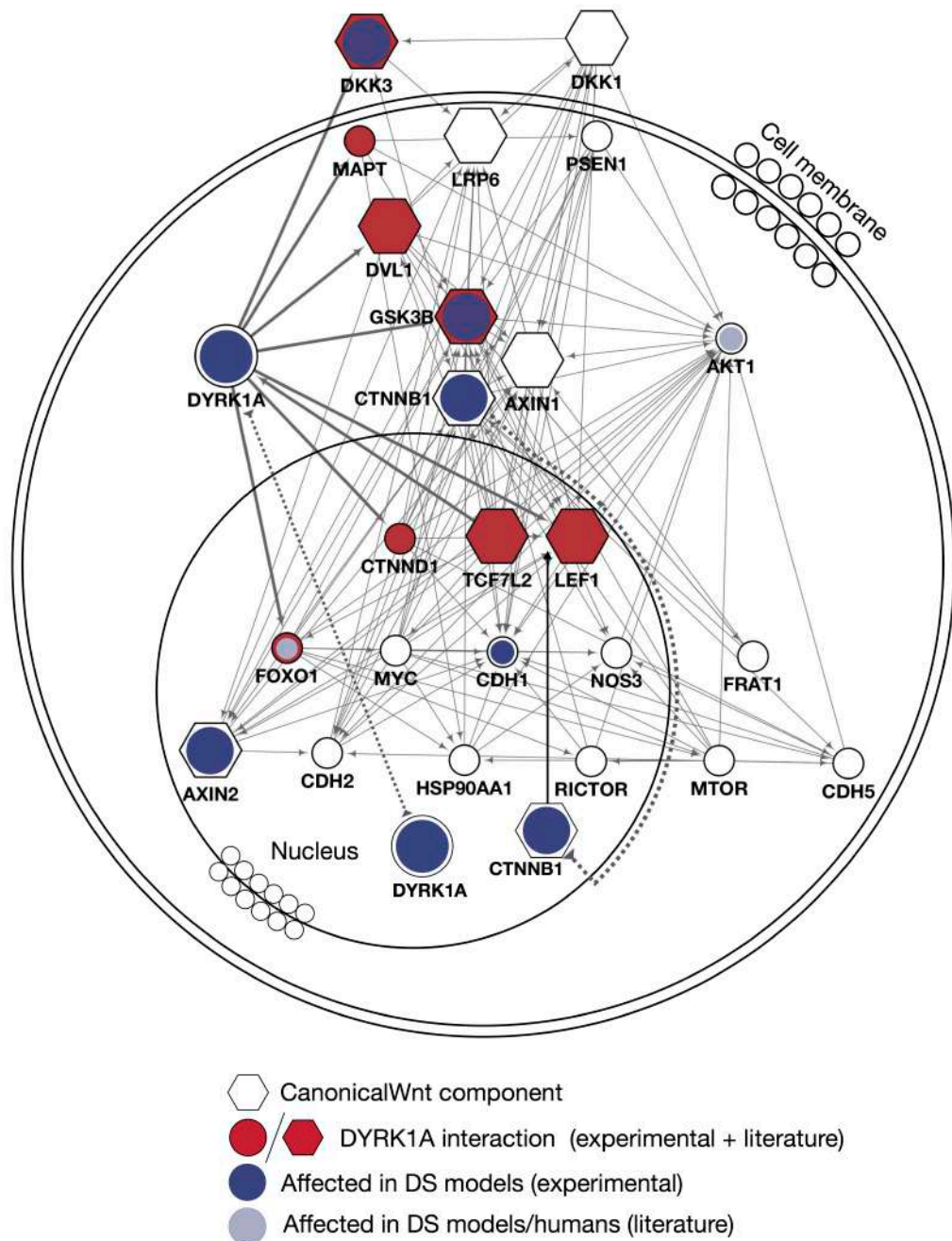


Fig. R3.8 - STRING-enriched DYRK1A-Wnt interaction network, displayed by Cytoscape. Following enrichment (See main text), the network was manually adjusted to reflect the known structure of canonical Wnt signalling, and contextualise the results for easier consultation.

The network was then enriched employing the STRING database. Components of the basic network in **R3.7** were used as starting nodes, selecting human as default organism (**Fig. R3.7, red circles**). This initial network, or first shell, was enriched with the 10 best-scoring interactors for any node, including DYRK1A. A further shell was then added, comprising the 10 best-scoring secondary interac-

Chapter 4.3 - DYRK1A-mediated Wnt signalling modulation

tors of any node in the enriched first shell. The network diameter, or distance between each node, was limited to 3, meaning that each node is no more than one degree of interaction away from DYRK1A, and from any other. This choice was made to better highlight interconnectedness. The resultant network (**Fig. R3.8**) has 140 edges and 25 nodes. The network was then displayed via the Cytoscape network analysis tool (see 3.8.2) in a spring-embedded layout, manually adjusted to reflect the known structure of canonical Wnt signalling (**Fig. R3.8**). Interestingly, some of the proteins automatically added to the network by STRING, such as, DKK3, Axin2, β -catenin and CDH1 were also found to be altered in DS models and humans (**Fig. R3.8, blue/grey circles** - see 4.1-2.2).

In summary, based on combined literature, database and experimental knowledge, these data suggest DYRK1A might be involved in a wide variety of Wnt signalling mechanisms, either directly or via modulation of other pathway components.

4.3.2.2 DYRK1A is a bimodal Wnt signalling regulator

The presence of a complex DYRK1A-Wnt interaction network suggests the possibility that DYRK1A may functionally affect signalling activity of this pathway, therefore potentially contributing to the Wnt phenotypes previously observed in DS models in humans (see 4.1-2). This possibility must therefore be studied further. In this section, potential effects of DYRK1A on Wnt signalling activity were investigated via luciferase assay and overexpression. Acute, transient manipulation of DYRK1A activity was achieved either via pharmacological kinase inhibition or DYRK1A overexpression. The latter approach relies on the notion that DYRK1A is constitutively active, and total protein levels thus linearly correlate with kinase activity.

4.3.2.2.1 DYRK1A inhibition and canonical Wnt signalling activity in SH-SY5Y cells

Descriptive statistics are reported in parentheses in the format (*mean, ±SD mean, P*). All luciferase values are reported as normalised to control in the text, but are expressed as log₂-transformed in figures to aid visualisation, due to large fold changes (see 3.9).

4.3.2.2.1.1 LiCl-mediated Wnt activation

SH-SY5Y cells (*n=3, ~2 · 10⁴ cells/ml, 3 replicates/condition*) stably expressing the TCF/LEF TOPFlash luciferase reporter (TF-stable, see 3.5.6), were administered a 5 hr 40 mM LiCl dose to activate canonical Wnt signalling. Concomitant DYRK1A inhibitor treatment was employed to investigate potential modulation of active β-catenin levels (**Fig. R3.9a-b**). All results are expressed as a ratio to the basal control condition mean (40mM NaCl treatment with ethanol or DMSO). LiCl+Ethanol treatment alone induced an approxi-

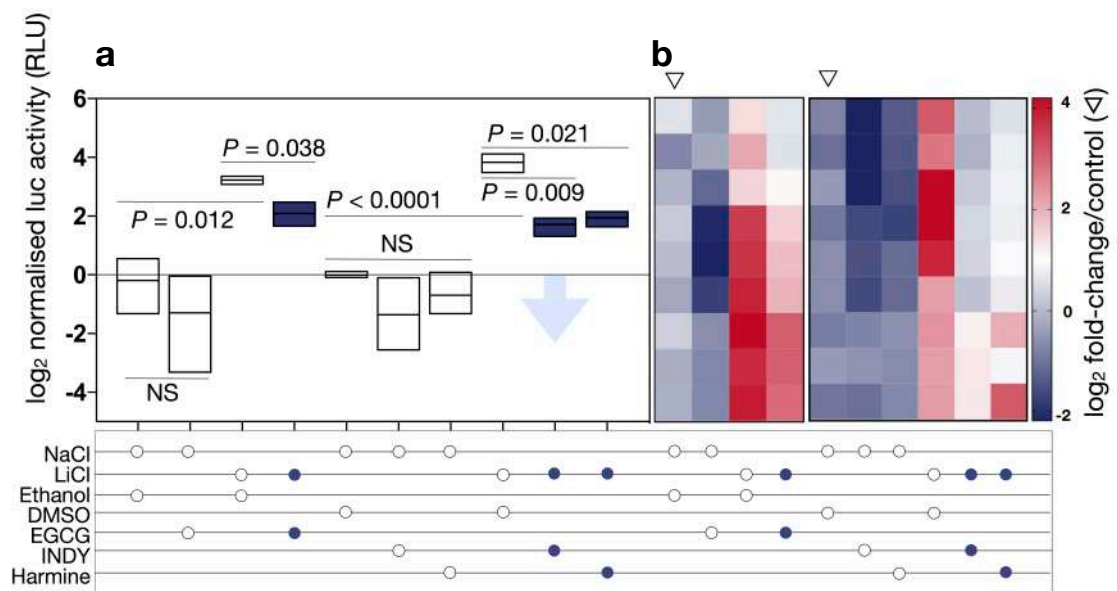


Fig. R3.9 - DYRK1A inhibition reduces levels of LiCl-induced canonical Wnt signalling activity quantified via TOPflash luciferase assay. **a** SH-SY5Y cells stably expressing the TCF-LEF luciferase reporter (*n=3*) were treated with 40 mM LiCl or NaCl control for 5 hours with or without 25 μM EGCG, 25 μM INDY or 10 μM Harmine. 0.1% ethanol and 0.01% DMSO were employed as negative control treatments for EGCG and INDY/Harmine, respectively. All inhibitors significantly reduced activation (blue bars). **b** Heat map representing log₂fold changes/NaCl alone for individual luciferase-expressing cultures. Data analysed by one-way ANOVA with post-hoc Sidak's multiple comparisons test.

mately 10-fold increase in luciferase signal relative to NaCl+Ethanol (9.7 ± 0.4 , $P=0.012$), and LiCl+DMSO treatment resulted in a 14-fold increase (14.5 ± 3.1 , $P<0.0001$) relative to NaCl+DMSO. The effect of LiCl is well reported in the literature and confirms successful Wnt signalling activation. Following, administration of LiCl+25 μ M EGCG led to a 4-fold increase in luciferase activity relative to NaCl+Ethanol (4.4 ± 1.2 , $P=0.013$). While the pathway was indeed stimulated, EGCG treatment resulted in a significantly reduced extent of activation, approximately 2-fold relative to LiCl+Ethanol (Fig. R3.9a, left blue - 2.2, $P=0.038$). A similar trend was observed for INDY and Harmine treatments. Administration of LiCl+25 μ M INDY induced a 4-fold increase in luciferase activity relative to NaCl+DMSO (3.9 ± 0.8 , $P=0.038$), corresponding to ~3-fold reduced extent of activation relative to LiCl+DMSO (Fig. R3.9a, right blue - 3.7, $P=0.009$). Similarly, LiCl+10 μ M Harmine treatment resulted in a 4-fold increase in signal relative to NaCl+DMSO (3.9 ± 0.7 , $P=0.017$). Compared to LiCl+DMSO activation, Harmine treatment also weakened the signal approximately 4-fold (Fig. R3.9a, far right blue - 3.7, $P=0.021$). In all conditions, none of the inhibitors exerted any detectable effect on basal luciferase activity. These data overall suggest that DYRK1A kinase inhibition may downregulate LiCl-activated, but not basal Wnt signalling.

4.3.2.2.1.2 Wnt3a-mediated Wnt activation

TF-stable cells ($n=3$, $\sim 2 \cdot 10^4$ cells/ml, 3 replicates/condition), were treated with 50 ng/ml Wnt3a for 5 hrs to activate canonical Wnt signalling in a physiological fashion (Fig. R3.10a-b). The same dose of DYRK1A inhibitor treatment from 4.3.2.2.1.1 was employed to investigate potential modulation of the pathway. Wnt3a+Ethanol treatment alone produced an approximately 7-fold increase in luciferase signal relative to PBS+Ethanol (6.9 ± 0.4 , $P=0.01$) while Wnt3a+DMSO treatment resulted in a 6-fold increase (6.3 ± 0.3 , $P=0.004$) relative to PBS+DMSO. Administration of Wnt3a+EGCG led to a 5-fold increase in luciferase ac-

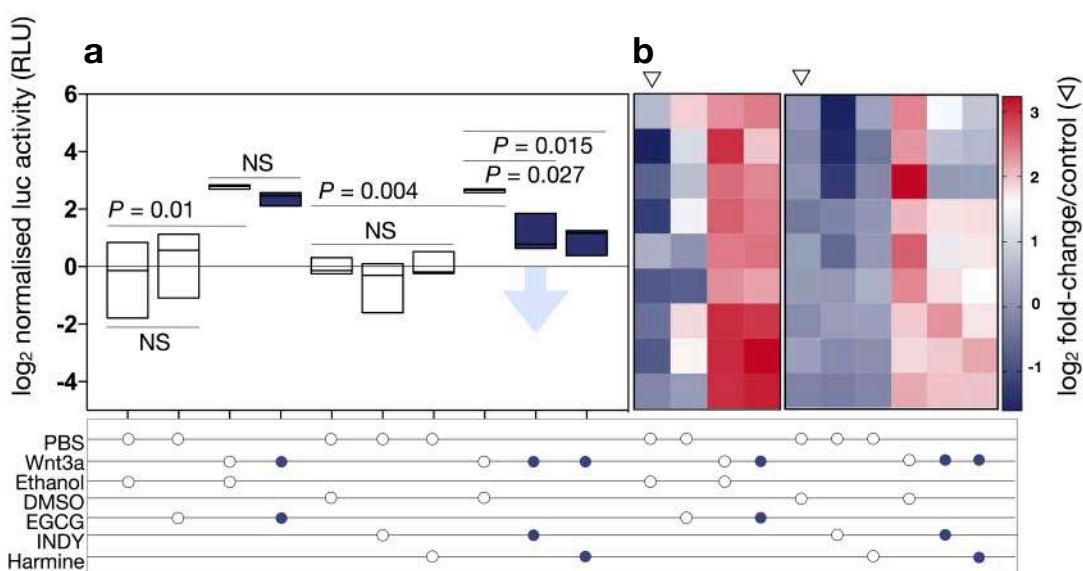


Fig. R3.10 - Same as Fig. R3.9 but employing 50ng/ml Wnt3a stimulation. All inhibitors but EGCG significantly reduced activation (blue bars). Data analysed by one-way ANOVA with post-hoc Sidak's multiple comparisons test.

Chapter 4.3 - DYRK1A-mediated Wnt signalling modulation

tivity relative to PBS+Ethanol (5.3 ± 0.9 , $P=0.021$). Under Wnt3a+EGCG stimulation, no significant difference in extent of activation was observed relative to Wnt3a+Ethanol (**Fig. R3.10a, left blue - 1.3, $P=0.97$**). Administration of Wnt3a+INDY induced a 2-fold increase in luciferase activity relative to PBS+DMSO (2.3 ± 1.1 , $P=0.043$), corresponding to a ~3-fold reduced extent of activation compared to Wnt3a+DMSO (**Fig. R3.9a, right blue - 2.7, $P=0.027$**). Similarly, Wnt3a+Harmine treatment resulted in a 2-fold increase in signal relative to PBS+DMSO (1.9 ± 0.6 , $P=0.032$). Harmine treatment also weakened the signal approximately 3-fold (**Fig. R3.9a, far right blue - 3.2, $P=0.015$**) compared to Wnt3a+DMSO activation. In all conditions, none of the inhibitors exerted any detectable effect on basal luciferase activity. These data suggest that under Wnt3a stimulation, the extent of pathway activation may be significantly reduced by DYRK1A inhibition with INDY and Harmine, but not with EGCG.

Taken together, the DYRK1A inhibition data suggest that interference with DYRK1A activity may reduce the ability of LiCl or Wnt3a to stimulate the canonical Wnt signalling pathway. According to the INDY results, DYRK1A might also act as a Wnt modulator in the absence of pathway stimulation. These preliminary findings suggest a potential interaction between DYRK1A and Wnt signalling activity.

4.3.2.1.3 Investigation of a dose-dependent relationship for INDY

Because of its reportedly superior specificity, INDY was selected for further investigation, in order to determine whether the observed downregulation of active Wnt signalling induced by INDY could fall under a dose-response function. A potential linear relationship between INDY treatment and Wnt signalling activity would suggest that DYRK1A modulates activity of the pathway in a dose-dependent fashion.

For this experiment, TF-stable cells ($n=3$, $\sim 2 \cdot 10^4$ cells/ml, 3 replicates/condition) were co-treated for 6 hrs with 40 mM LiCl or NaCl and a log-equidistant range of INDY doses (0, 1, 3, 10, 30, 100 μM - Fig. R3.11). Luciferase signal values were expressed as ratio to the basal control condition mean (NaCl treatment). LiCl treatment alone induced a 21-fold increase in luciferase signal (21.0 ± 2.9 , $P < 0.0001$). This was assumed as maximum response and tested against increasing INDY doses in the presence of LiCl. No significant effect was observed for LiCl+1 or 3 μM INDY, albeit the sample means displayed a trend towards decrease (1 μM - 19.3 ± 5.9 , $P=0.96$, 91%; 3 μM - 15.6 ± 1.0 , $P=0.072$, 75%). A dose-dependent significant decrease in pathway activation was observed throughout the remaining range of INDY treatments. A dose of 10 μM resulted in signal reduction to 62% (13.1 ± 2.7 , $P=0.004$), 30 μM to 54% (11.3 ± 4.7 , $P=0.0004$) and 100 μM to 16% (3.3 ± 0.9 , $P < 0.0001$). Regression analysis of the LiCl data showed linearity ($R^2=0.8$), fitting a function of significantly non-zero slope ($f(x)=-0.7x+84$, $P=0.009$; Fig. R3.11a, red). This finding suggests the presence of a dose-response relationship between INDY treatment and Wnt activation. Linearity was most evident between 3-30 μM INDY. Interestingly, the same dose range was identified by Ogawa *et al.*, the original developers (110), as linearly inhibiting tau phosphorylation and NFAT signalling activity. These are two common DYRK1A substrates, indicating the response observed here is possibly DYRK1A-specific. No significant effect of INDY treatment was observed with NaCl except at 100 μM , when basal response was decreased to 83% (0.8 ± 0.1 , $P=0.002$, not shown). Overall, these data suggest that DYRK1A inhibition may linearly modulate canonical Wnt signalling in the activated state.

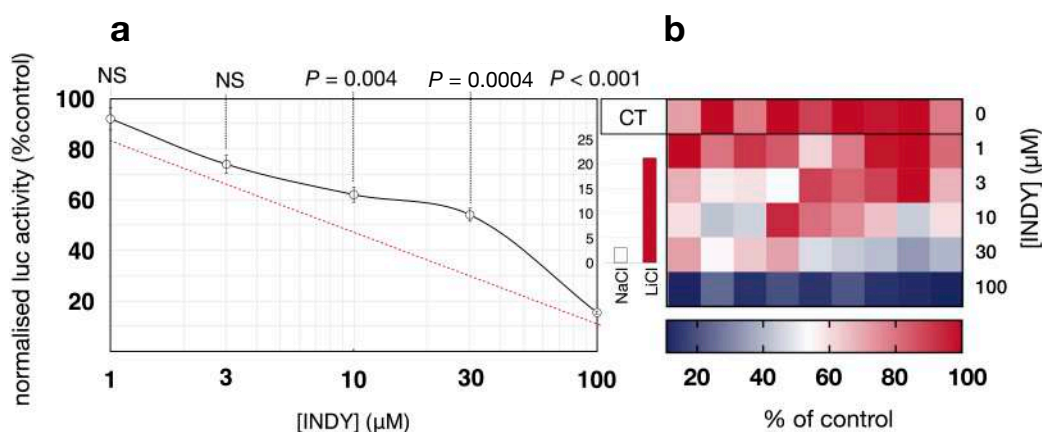


Fig. R3.11 - The inhibitory effect of INDY on LiCl-induced activation is dose-dependent. **a** Doses of 1-100 μM INDY ($n=3$) were administered for 5 hours and luciferase activity was plotted as percentage of control treatment. Linear regression analysis indicated a dose-response relationship ($P=0.009$, $R^2=0.8$, $f(x)=-0.7x+84$). **b** Heat map showing values normalised to LiCl + 0.01% DMSO for individual cultures. Data analysed by one-way ANOVA with post-hoc Sidak's multiple comparisons test. CT: control.

4.3.2.2.1.4 DYRK1A inhibition in live cells

The effects of INDY-mediated DYRK1A inhibition on canonical Wnt signalling activity were also tested in live, non-lysed cells from the TF-stable line (**Fig. R3.12**). Cells ($n=3$, $\sim 10^4$ cells/ml, 3 replicates/condition) were treated with either 40 mM LiCl or 50 ng/ml Wnt3a and relative controls for 5 hours, with or without administration of 25 μ M INDY. Following 20 min treatment with 150 μ g/mL D-luciferin, imaging through the IVIS system (see 3.5.5) detected significant Wnt stimulation with both LiCl (3.4 ± 1.5 , $P=0.026$) and Wnt3a (4.7 ± 1.0 , $P=0.0004$, **Fig. R3.12, left, rows 2/4**). In line with previous results, INDY treatment significantly reduced activation levels ~ 3 -fold with LiCl (1.3 ± 0.6 , $P=0.047$) and ~ 2 -fold with Wnt3a (2.5 ± 0.7 , $P=0.012$ - **Fig. R3.12, right, rows 2/4**). No effect was detected on basal activity levels (0.6 ± 0.2 , $P=0.94$; 0.7 ± 0.3 , $P=0.90$ - **right, rows 1/3**). These data further indicate that DYRK1A kinase inhibition reduces active, but not basal Wnt signalling activity.

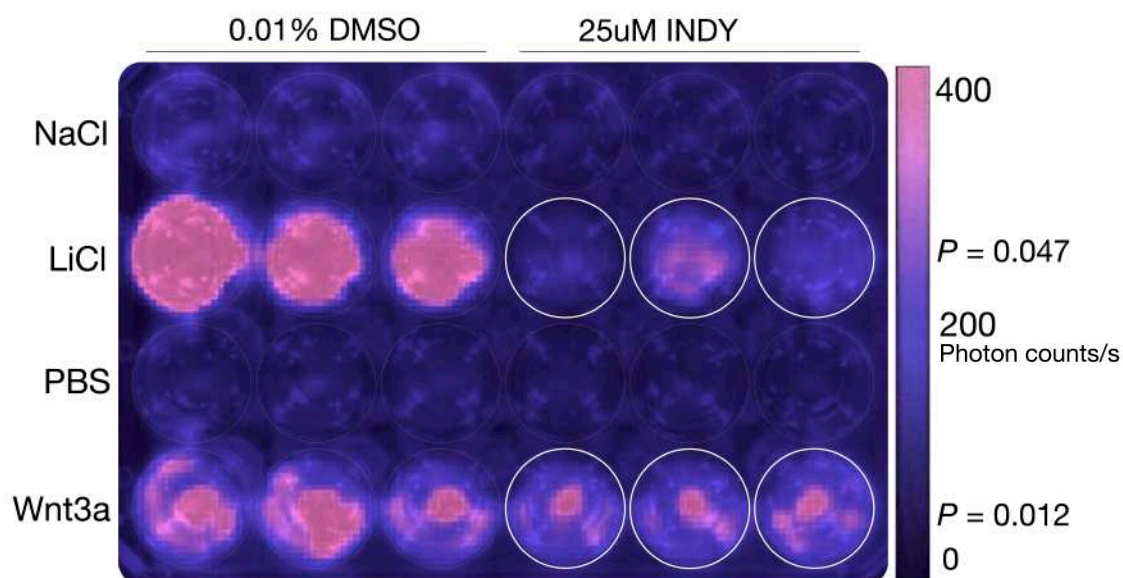


Fig. R3.12 - Effect of INDY in live, non-lysed stable SH-SY5Y cells ($n=3$). Samples were treated as in **R3.9-10**, with or without 25 μ M INDY and imaged live, employing the IVIS system. Signal intensity represents photon counts/s. In both stimulating conditions, DYRK1A inhibition significantly reduced active but not basal Wnt signalling activity (right side). Data analysed by student t-test.

4.3.2.2.2 DYRK1A overexpression and canonical Wnt signalling activity

4.3.2.2.2.1 DVL1-mediated Wnt activation

TOPFlash transfection

In this experiment, the effect of *DYRK1A* overexpression with or without Wnt signalling activation was investigated by co-transfection of the TOPFlash luciferase construct (**Fig. R3.13** - see 3.5.5) SH-SY5Y cells ($n=9$, $\sim 2 \cdot 10^4$ cells/ml, 3 replicates/condition) were co-transfected with 0.25 μ g/ml DYRK1A, DVL1, both or relative control vector. Similarly to experiments 1-3, luciferase signal values were expressed as a ratio to the basal control condition mean (pCMV5-empty+pRK5-myc-empty). Surprisingly, *DYRK1A* overexpression alone induced a significant 4-fold decrease in luciferase signal (**Fig. R3.13a, blue** - 0.2 ± 0.2 , $P=0.007$) relative to basal control. Activation of the pathway was confirmed by DVL1 overexpression, which resulted in a 8-fold increase in signal (8.5 ± 7.8 , $P<0.0001$). Concomitant overexpression of DVL1 and DYRK1A produced a remarkable 40-fold increase in signal relative to basal control (**Fig. R3.13a, red** - 35.5 ± 35.7 , $P<0.0001$), corresponding to a 4-fold enhancement of Wnt activation relative to DVL1 transfection alone (**4.2**, $P=0.002$). These data suggest that, in the active state, canonical Wnt signalling activity may be positively modulated by *DYRK1A* overexpression.

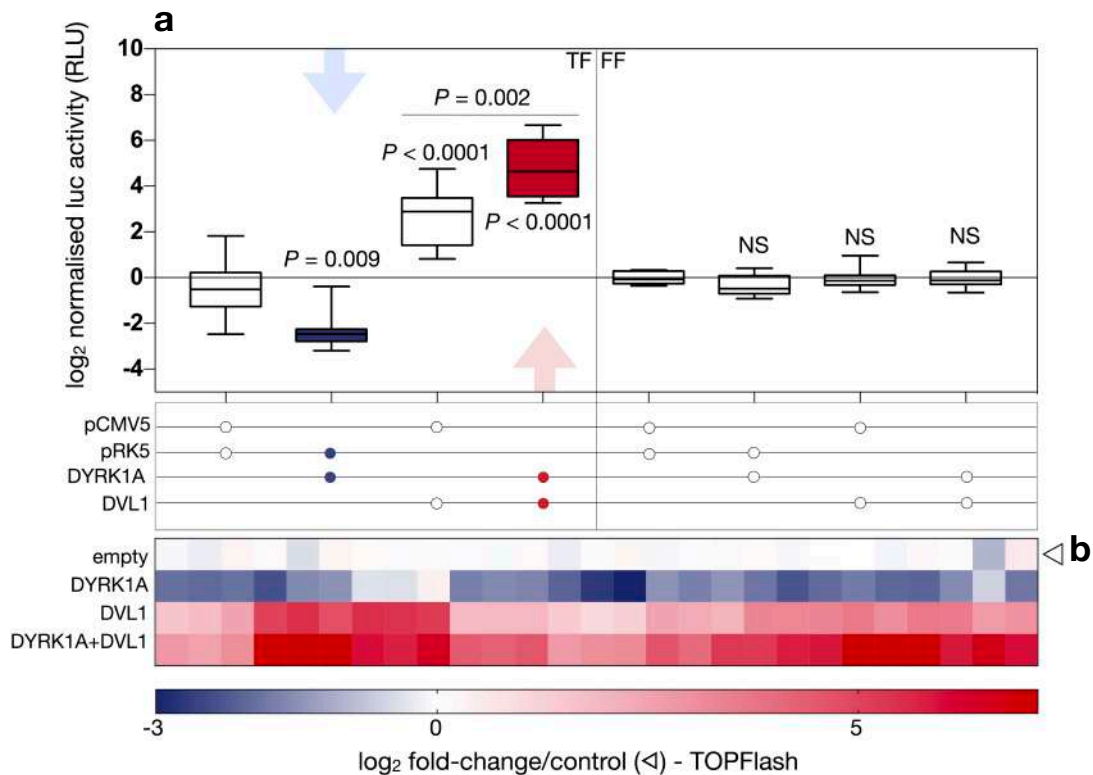


Fig. R3.13 - Bimodal Wnt effects of DYRK1A expression in the SH-SY5Y line. **a** Cells ($n=9$) were co-transfected with 0.25 μ g/ml HA-DYRK1A, FLAG-DVL1, both, or empty vector controls for 24 hrs. 0.25 μ g/ml TOPflash and 0.025 μ g/ml constitutively active renilla luciferase constructs were employed as reporters, with signal quantified as TOPflash/Renilla ratio. All values displayed as log₂fold transform relative to empty vector transfection. Adjacent graph demonstrates same experiment employing mutant reporter construct FOPflash-luciferase. **b** Heat map represent values for individual luciferase-expressing cultures. TF - TOPFlash, FF - FOPFlash. Data analysed by one-way ANOVA with post-hoc Sidak's multiple comparisons test.

FOPFlash transfection

In order to control for any non-specific signal effect of DNA transfection, the same experiment was carried out by transfection of the mutated FOPflash construct which does not relate canonical Wnt signalling activity to a luciferase signal (**Fig. R3.13a**, right panel). DYRK1A overexpression alone had no effect on luciferase signal (0.8 ± 0.2 , $P=0.91$) relative to basal control. DVL1 overexpression alone produced no significant change in signal intensity (0.9 ± 0.4 , $P=0.68$). Similarly, concomitant overexpression of DVL1 and DYRK1A did not exert a significant effect on luciferase signal (0.8 ± 0.2 , $P=0.58$).

4.3.2.2.2.2 Combined effects of DYRK1A and DKK3 expression on Wnt signalling activity

Given the consistently observed DYRK1A-DKK3 interaction, the individual and combined effects of these two proteins on canonical Wnt signalling activity were also investigated via luciferase assay (**Fig. R3.14**). For this experiment, 0.25 µg/ml HA-DYRK1A, DKK3-FLAG and FLAG-DVL1 were expressed for 24 hrs in SH-SY5Y cells ($n=3$, $\sim 2 \cdot 10^4$ cells/ml, 3 replicates/condition), either alone or in all possible combinations. Similarly to results discussed above, DYRK1A induced a significant decrease in Wnt signalling activity when expressed alone (**Fig. R3.14a, blue - 0.4 ± 0.1 , $P=0.01$**). DKK3, however, had no detectable effect when expressed alone (0.9 ± 0.2 , $P=0.99$). Also similarly, DVL1 expression induced a significant increase in Wnt activation (32.4 ± 25.4 , $P < 0.005$), further enhanced by the presence of DYRK1A (**Fig. R3.14a, red - 62.7 ± 18.4 , $P=0.02$**). When co-expressed with DVL1, DKK3 did not affect Wnt activation (33.5 ± 22.7 , $P=0.006$, comparative $P=0.97$). However, in the presence of all three proteins, DKK3 expression prevented the DYRK1A-enhancing effect, with luciferase levels comparable to DVL1 alone (**Fig. R3.14a, light red - 28.9 ± 16.5 , $P=0.008$, comparative $P=0.99$**). Overall, luciferase signals in this study were overall more variable than previous experiments, and it is more difficult to reliably interpret the data. DKK3 does not exert a detectable effect on basal or active Wnt signalling in this system. However, it might be able to reduce or prevent DYRK1A-mediated enhancement of DVL1 Wnt signalling.

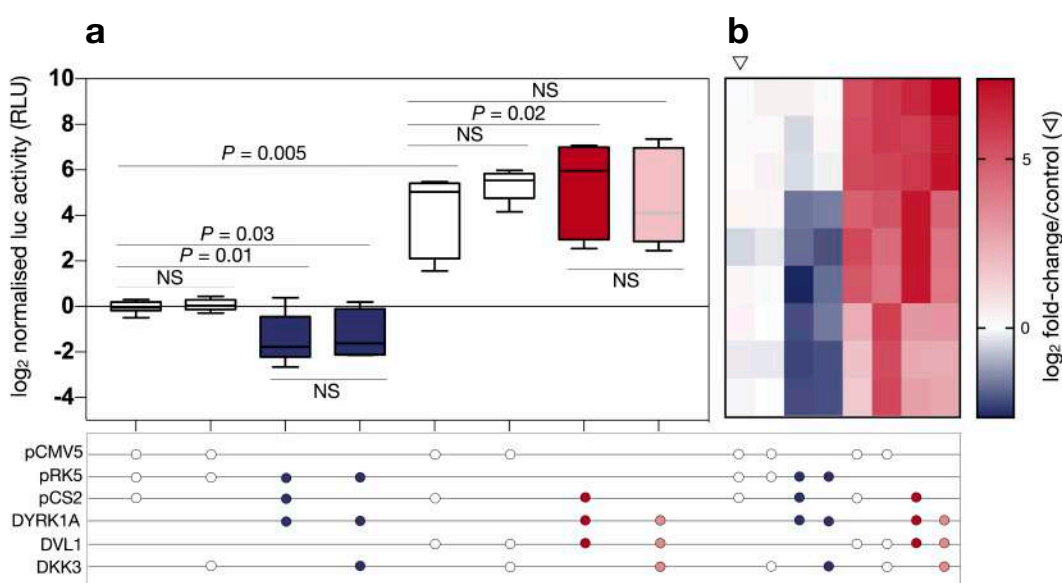


Fig. R3.14 - Combined Wnt effects of DYRK1A and DKK3 expression in the SH-SY5Y line. **a** Cells ($n=3$) were co-transfected with 0.5 µg HA-DYRK1A, DKK3, DVL1, or empty vector controls in all combinations for 24 hrs. Luciferase assay conducted as above. Same effects of DYRK1A±DVL1 (blue, red). No effect of DKK3±DVL1. When all three present, the DYRK1A enhancing effect on DVL1 was removed (light red). **b** Heat map represent values for individual luciferase-expressing cultures. Data analysed by one-way ANOVA with post-hoc Sidak's multiple comparisons test.

4.3.2.2.2.3 Effects of DYRK1A expression on GSK3 β

The luciferase data above demonstrated that DYRK1A is capable of bimodal Wnt regulation in neuroblastoma cells. Active Wnt signalling is enhanced by DYRK1A overexpression, whilst basal activity levels are potently downregulated. The latter effect was further examined, by investigating whether the observed Wnt inhibition correlates with changes in GSK3 β protein levels. GSK3 β is a long established Wnt component and chief intracellular inhibitor of β -catenin (68). Additionally, it possesses a functional relationship with DYRK1A (84, 85, 109) (see 4.3.1). It is therefore possible that the substantial Wnt downregulation observed in the presence of DYRK1A (**Fig. R3.13, blue**) might be accompanied by changes in GSK3 β levels.

In order to investigate this hypothesis, 0.5 μ g/ml HA-DYRK1A or relative empty control vector were expressed in HEK-293 cells ($n=6$, $\sim 10^5$ cells/ml, 4 replicates/condition) for 24 hrs and analysed via SDS-PAGE/IB (**Fig. R3.15**). DYRK1A protein levels were found to be significantly elevated over 2-fold (2.4 ± 1.4 , $P=0.0006$) compared to control samples, as expected (**Fig. R3.15a**). Interestingly, DYRK1A overexpression also induced a significant ~ 1.5 -fold increase in total GSK3 β (1.5 ± 0.2 , $P=0.03$ - **Fig. R3.15b**). This result supports the hypothesis formulated above, and preliminarily indicates that protein amounts of GSK3 β may be directly affected by DYRK1A activity. Additionally, the p-S9 fraction of GSK3 β was also examined under DYRK1A overexpression. Phosphorylation of this residue is reportedly elevated in the cerebral cortex and hippocampus of aged Tc1 mice (86), but is unaltered in 2 months and 6 months old animals ((86), 4.2.2). The p-S9 phosphoresidue is also known to inhibit GSK3 β activity, and is regulated by AKT (111). Surprisingly, DYRK1A overexpression resulted in a significant 3-fold decrease of the p-S9-GSK3 β fraction, quantified as a ratio to total GSK3 β (0.3 ± 0.2 , $P=0.02$ - **Fig. R3.15c**). Overall, these data suggest that enhanced DYRK1A activity may be sufficient to elevate GSK3 β levels, and reduce its inhibitory phosphorylation at S9. This is consistent with the previously observed basal Wnt inhibition by DYRK1A, and imply that such an effect may be accompanied by enhanced GSK3 β activity.

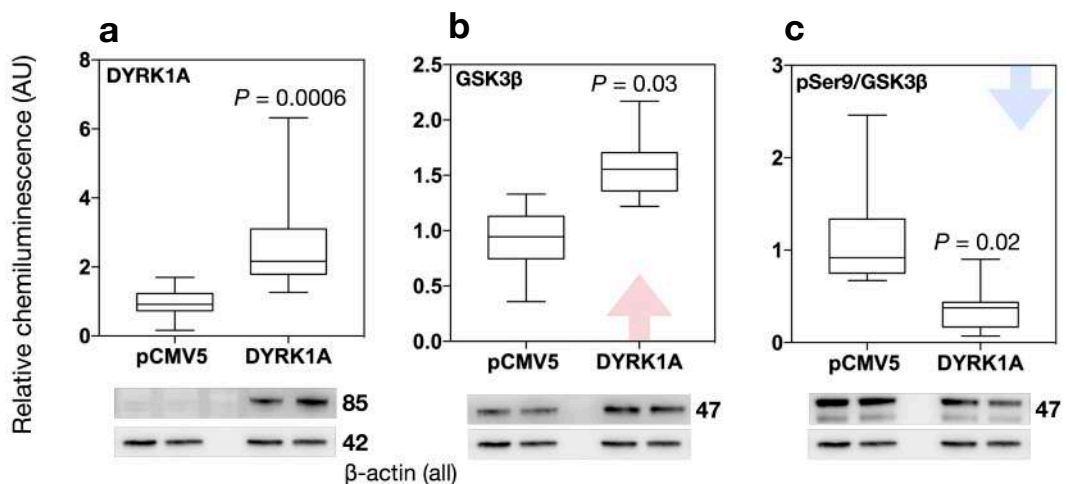


Fig. R3.15 - DYRK1A expression is sufficient to enhance total protein amounts of GSK3 β and alter its phosphorylation status at S9. SH-SY5Y cells ($n=4$) were transfected with 0.5 μ g/ml HA-DYRK1A for 24 hrs. **a** As expected, DYRK1A levels were elevated. **b** Total levels of GSK3 β were enhanced. **c** Phosphorylation at S9, as expressed by ratio to total protein, was significantly reduced.

4.3.2.3 Wnt signalling control over DYRK1A subcellular localisation

The experiments so far outlined in this chapter demonstrated that DYRK1A participates in complex Wnt protein interaction networks (4.3.2.1), and is also capable of bimodal Wnt regulation (4.3.2.2). These findings support the initial candidate gene hypothesis of DYRK1A-mediated Wnt signalling modulation, and must be investigated further. A wide variety of DYRK1A substrates and functions is currently known (11). If this kinase is indeed capable of regulating Wnt signalling intracellularly, such property should be reflected by detectable changes in DYRK1A homeostasis. Thus, the presence of this novel DYRK1A-Wnt relationship warrants the question of whether DYRK1A may itself be functionally regulated by Wnt activation states. As introduced, subcellular localisation is a key regulator of DYRK1A function (4.3.1.1.5). Whilst prominently a nuclear protein, DYRK1A does also localise to the cytoplasm, and the highly dynamic balance between these two subcellular compartments is finely regulated. Nuclear/cytoplasmic shuttling primarily serves the purpose of functionally directing DYRK1A to differential substrate pools. Indeed, the Wnt signalling pathway possesses both nuclear and cytoplasmic components important for activation. Given the hereby observed bimodal Wnt regulation by DYRK1A, which is activation dependent, it was thus hypothesised that such modulation might occur in distinct subcellular compartments.

In order to address this hypothesis, an imaging approach was undertaken. Employing quantitative immunocytochemistry and overexpression, the subcellular localisation of DYRK1A was investigated in relation to multiple Wnt activation states. Particularly, quantitation was used to objectively assess the subcellular distribution of DYRK1A. To ensure consistency, the same Wnt activation methods described above were employed (4.3.2.2), i.e. LiCl or Wnt3a stimulation, and DVL1 overexpression. All experiments were performed in the HeLa and HEK-293 human cell lines, combining high-resolution Airy-scan and confocal fluorescence microscopy (see 3.5.7-8 and 3.9 for info on sample preparation, primary and secondary (Alexa Fluor®) antibodies employed, fluorescence quantification protocols and statistical analysis).

4.3.2.3.1 Nuclear DYRK1A localises to the speckle compartment

Prior to addressing a potential Wnt-dependent effect on DYRK1A localisation, a qualitative pilot study was conducted with a dual purpose. First, to verify the consensus DYRK1A localisation as mostly nuclear in cell homeostatic conditions. Second, to replicate previous reports of DYRK1A sub-localisation to nuclear speckles (4). A GFP-tagged DYRK1A construct was expressed in HEK-293 cells ($\sim 2 \cdot 10^4$ cells/ml, $n=3$) for 24 hrs (**Fig. R3.16**). Cells were then collected, fixed and immunostained as described (see 3.5.7). DAPI staining was employed as nuclear marker, whilst a primary antibody to Serine/arginine-rich splicing factor 2 (SC35) was selected as nuclear speckle marker. Confocal microscopy demonstrated a detectable GFP-DYRK1A signal, which localised diffusely to the nucleus (**Fig. R3.16, green**) with discrete punctae of enhanced fluorescence (**green triangles**). DYRK1A also appeared to localise to the nuclear interchromatin

space, visible as a sharp reduction in DAPI signal (**Fig. R3.16, blue triangle**). SC-35 staining successfully identified nuclear speckles as distinct intranuclear punctae (**Fig. R3.17, red triangle**) also localising to the interchromatin space (**Fig. R3.17, blue triangle**). As previously reported, GFP-DYRK1A co-localised with SC-35 (**Fig. R3.17, yellow triangle**), thus confirming its association with nuclear speckles and the reliability of experimental setup employed thereafter.

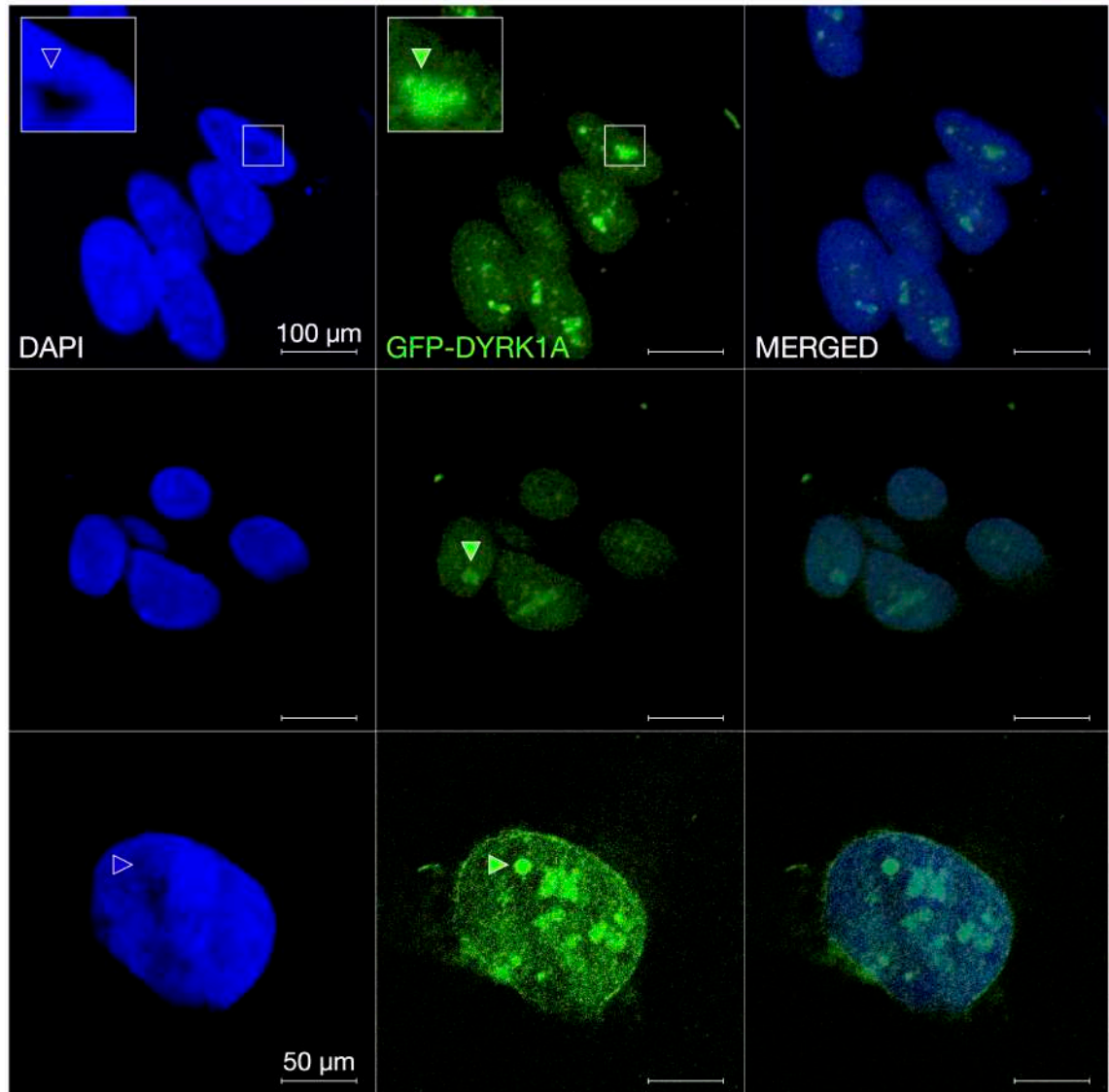


Fig. R3.16 - Pilot study of DYRK1A localisation. 24 hr expression of GFP-DYRK1A (green) resulted in nuclear localisation of the protein overlapping DAPI staining, and displaying fluorescent punctae (green arrow, centre) possibly within the interchromatin space (blue arrow, left).

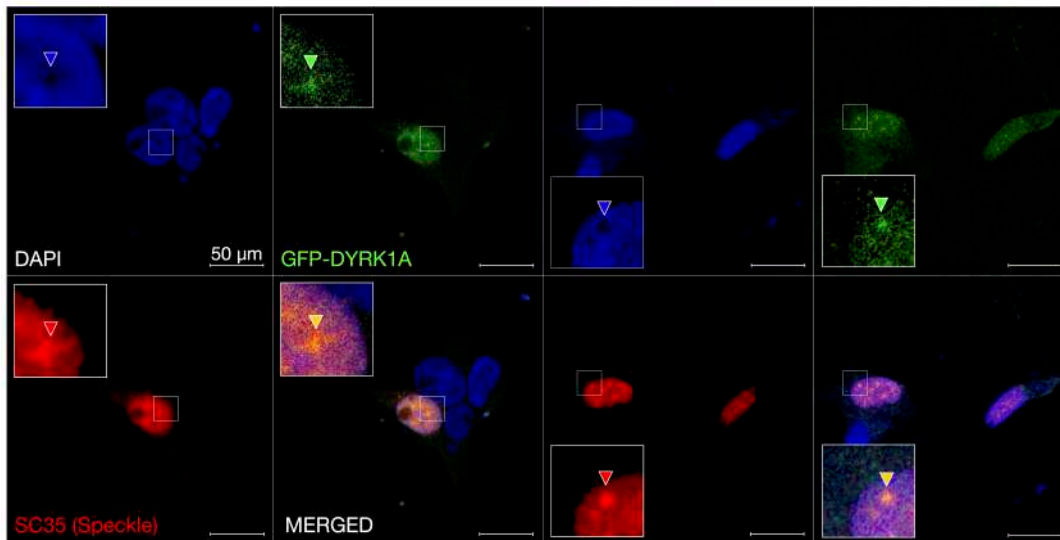


Fig. R3.17 - Pilot study of DYRK1A localisation with nuclear speckles. 24 hr expression of GFP-DYRK1A (green) resulted in nuclear localisation of the protein displaying intranuclear fluorescent punctae (green arrow). SC-35 staining demonstrated speckle morphology (red arrow) and co-localisation with DYRK1A punctae (yellow arrow).

4.3.2.3.2 LiCl-mediated Wnt activation

HeLa or HEK-293 cells were cultured ($\sim 2 \cdot 10^4$ cells/ml, $n=3$ cell clusters), expressing 0.5 µg/ml HA-DYRK1A for 24 hrs. (**Fig. R3.18-20**). Concomitantly, 40 mM LiCl or equimolar NaCl were administered for 5 hrs. Cells were then collected, fixed and immunostained. For all experiments hereafter, an anti-HA antibody was employed for DYRK1A detection. Hoechst and DAPI stains were employed to visualise the nucleus in HeLa and HEK-293 cells, respectively. F-actin staining was also performed in HeLa cells to visualise cell boundaries. The latter cell line served to produce representative, high-resolution images. HEK-293 cells were imaged at lower resolution, in order to generate ‘population’ samples for quantification and statistical testing.

Under basal Wnt signalling conditions, overexpressed DYRK1A mostly localised to the nucleus. Representative Airy-scan images demonstrated a prominent nuclear DYRK1A signal in HeLa cells, with little cytoplasmic fluorescence observable (**Fig. R3.18a, green**). This is consistent with previous reports on DYRK1A localisation (4, 11), confirming its role as a nuclear kinase. In the presence of LiCl stimulation, however, DYRK1A appeared to nearly completely redistribute out of the nucleus, with extremely low signal in this compartment. (**Fig. R3.18b, green**). This finding was accompanied by enhanced DYRK1A cytoplasmic fluorescence, which appeared diffuse. 3D z-stacking further illustrated this phenotype (**Fig. R3.19**). The same experiment was conducted in HEK-293 cells to quantify the ratio of nuclear to cytoplasmic (N/C) DYRK1A fluorescence (**Fig. R3.20a-b**). Under basal conditions, DYRK1A was predominantly nuclear ($n=3$ cell clusters, 2.0 ± 0.4). However, LiCl significantly decreased the DYRK1A N/C ratio in favour cytoplasmic localisation (0.4 ± 0.2 , $P=0.003$). Overall, this experiment demonstrates that LiCl treatment is sufficient to significantly redistribute DYRK1A out of the nucleus and into the cytoplasmic compartment.

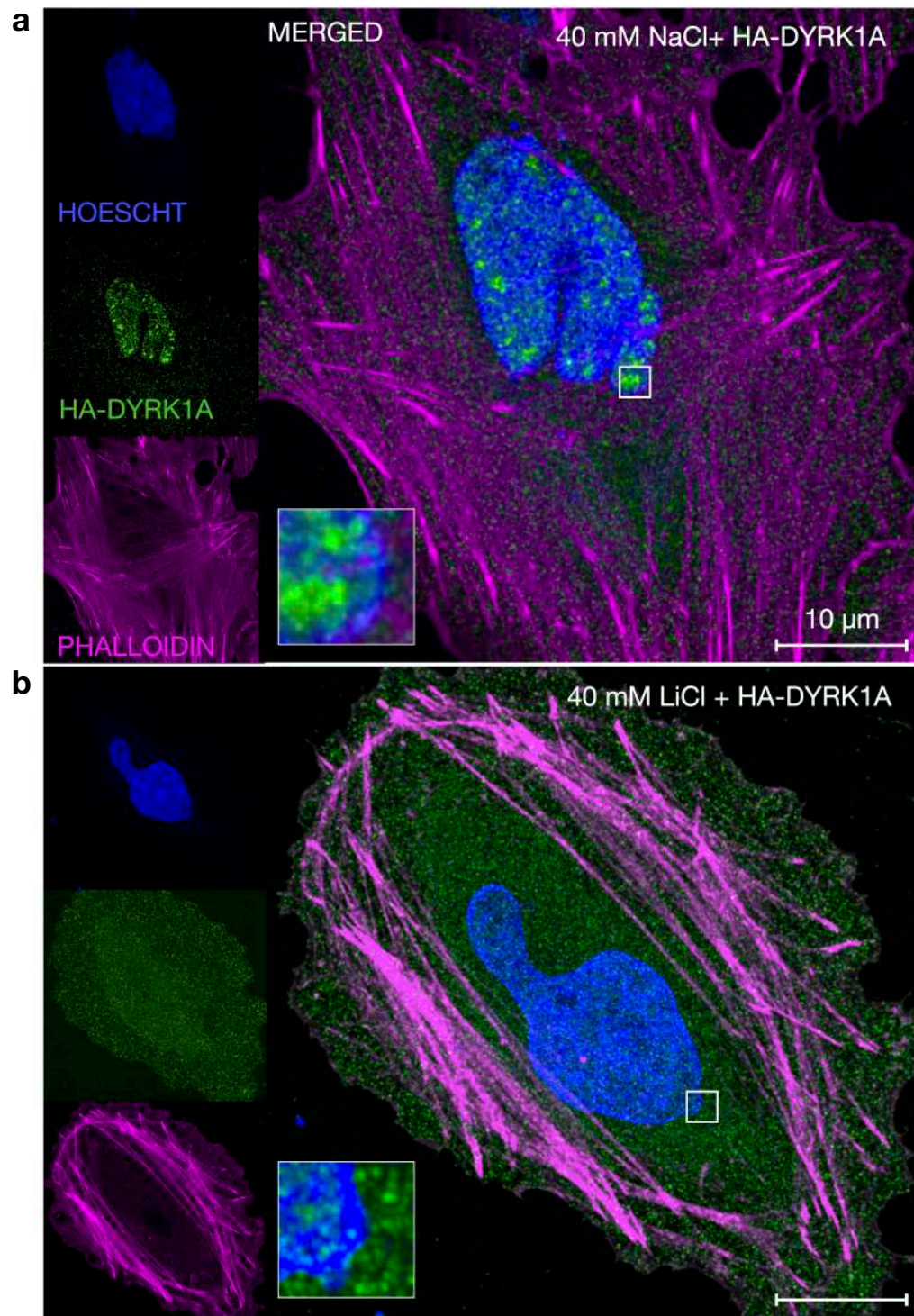


Fig. R3.18 - Wnt activation shuttles DYRK1A out of the nucleus. Airyscan microscopy of 5-hour 40mM NaCl (a) or LiCl (b) treatment in HeLa cells. DYRK1A (green) localised to the nucleus (blue) when expressed alone (a), but redistributed to the cytoplasm in the presence of Wnt activation (b).

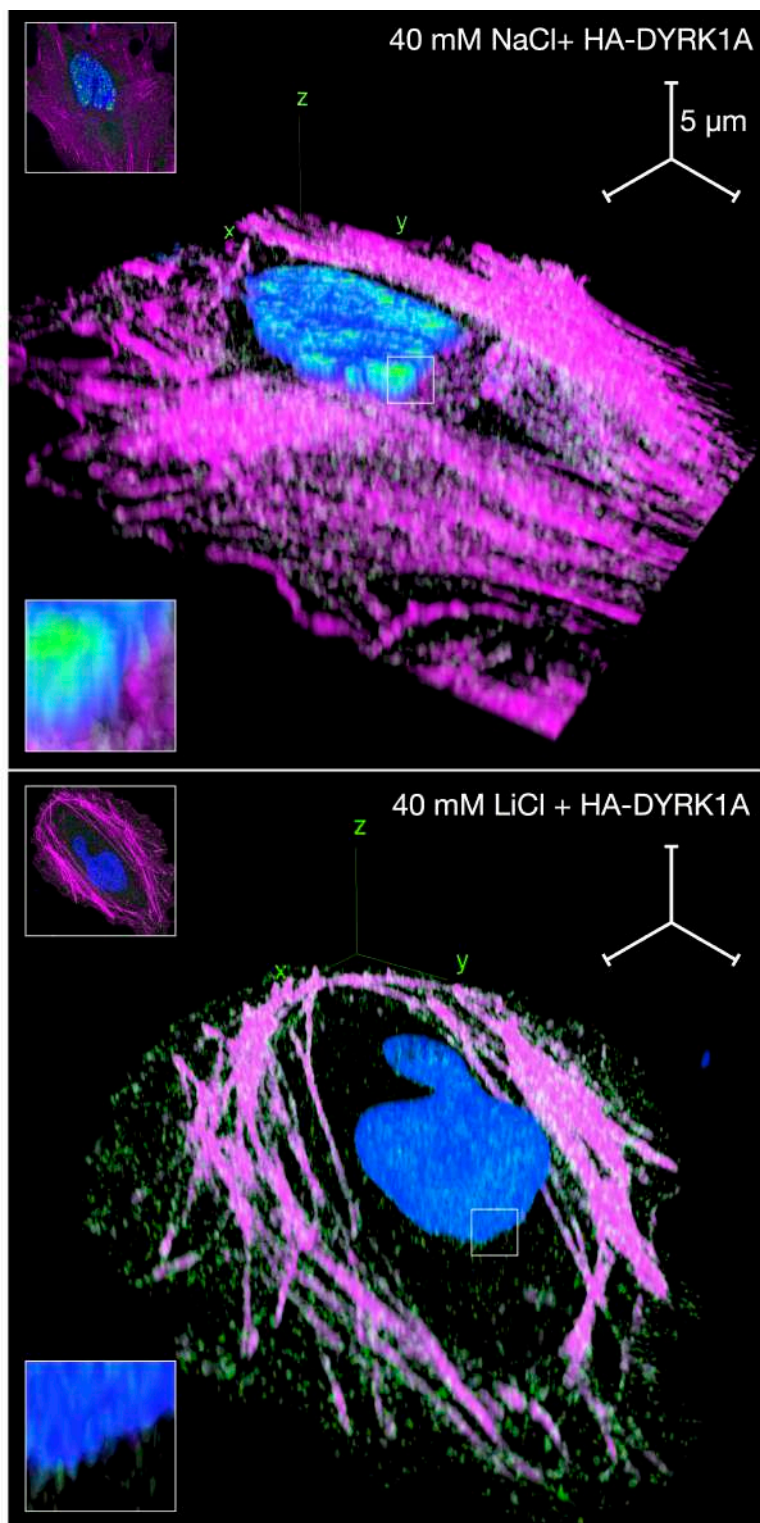


Fig. R3.19 - 3D reconstruction of z-stacks generated from images in R3.18, further demonstrating the observed phenotype.

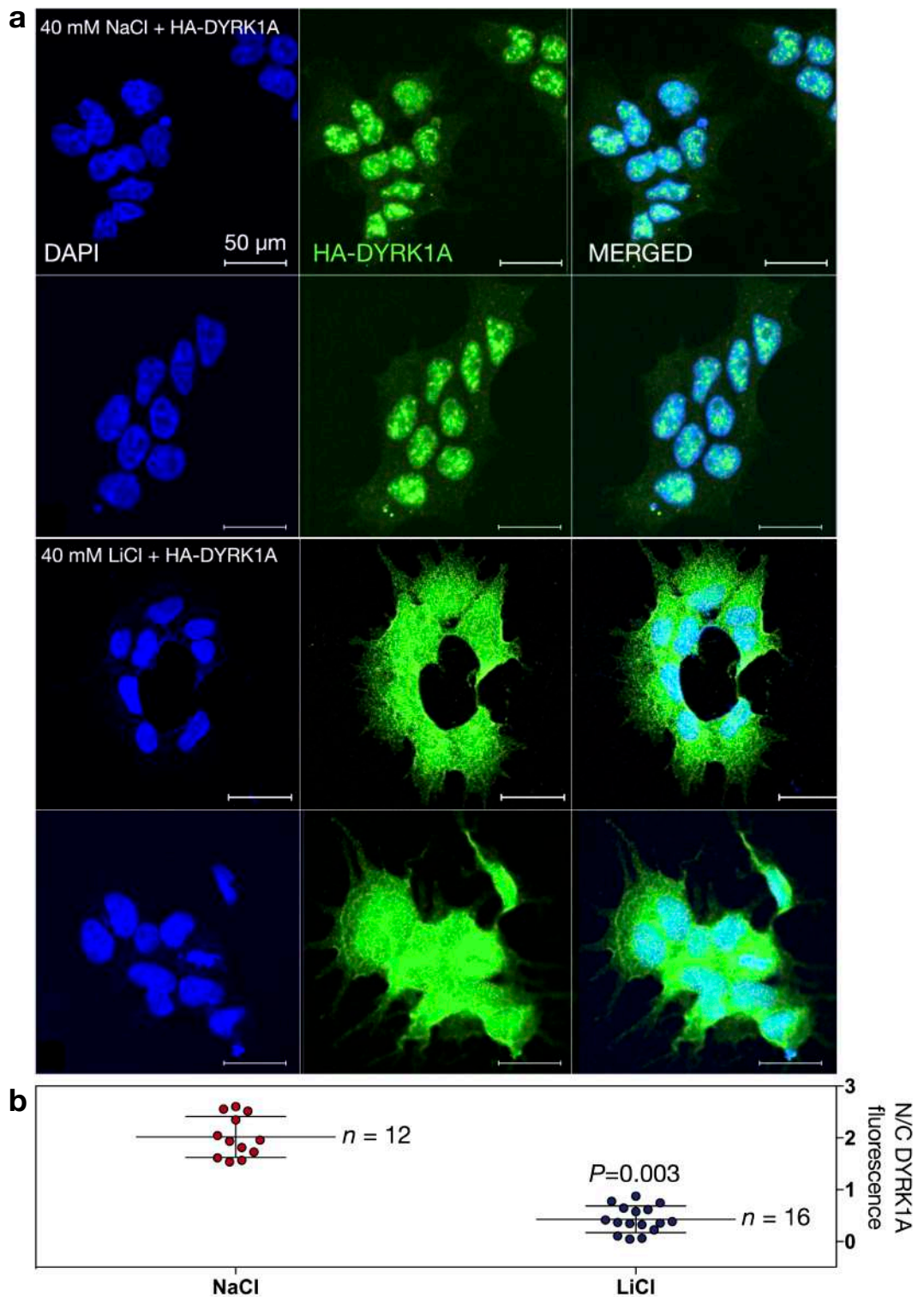


Fig. R3.20 - Nuclear/cytoplasmic DYRK1A ratio. **(a)** Same conditions as in **R3.18**, but in HEK-293 cells and imaged via confocal microscopy. **(b)** Significant reduction in DYRK1A nuclear localisation upon 5hr 40 mM LiCl treatment. For each condition, $n=3$ cell clusters were analysed, comprising $n=12$ and $n=16$ cells for NaCl and LiCl treatments, respectively.

4.3.2.3.3 Wnt3a-mediated Wnt activation

For this experiment HeLa or HEK-293 were cultured, transfected, stained and imaged as in 4.3.2.3.2. In this case, however, Wnt signalling activation was obtained via administration of 50 ng/ml Wnt3a or PBS, for 5 hours prior to sample collection (**Fig. R3.21-23**). Similarly to results above, overexpressed DYRK1A mostly localised to the nucleus under basal Wnt signalling conditions (**Fig. R3.21a, green**). Representative Airy-scan images demonstrated a prominent nuclear DYRK1A signal in HeLa cells, with little cytoplasmic fluorescence observable. In the presence of Wnt3a stimulation, however, DYRK1A redistributed out the nucleus similarly to LiCl treatment (**Fig. R3.21b, green**). Consistently, this finding was accompanied by diffuse DYRK1A cytoplasmic fluorescence. 3D z-stacking further illustrated this phenotype (**Fig. R3.22**).

The same experiment was conducted in HEK-293 cells to quantify the DYRK1A fluorescence N/C ratio (**Fig. R3.23a-b**). Under basal conditions, DYRK1A was predominantly nuclear ($n=3$ cell clusters, 2.2 ± 0.5). However, similarly to LiCl treatment, Wnt3a significantly decreased the DYRK1A N/C ratio in favour cytoplasmic localisation (0.8 ± 0.03 , $P=0.016$). Overall, this experiment demonstrates that, in addition to LiCl, the endogenous Wnt3a ligand may also significantly redistribute DYRK1A out of the nucleus and into the cytoplasmic compartment. Imaging data so far suggests that pharmacological Wnt activation may redirect DYRK1A activity to the cytoplasm, thus restricting its nuclear access.

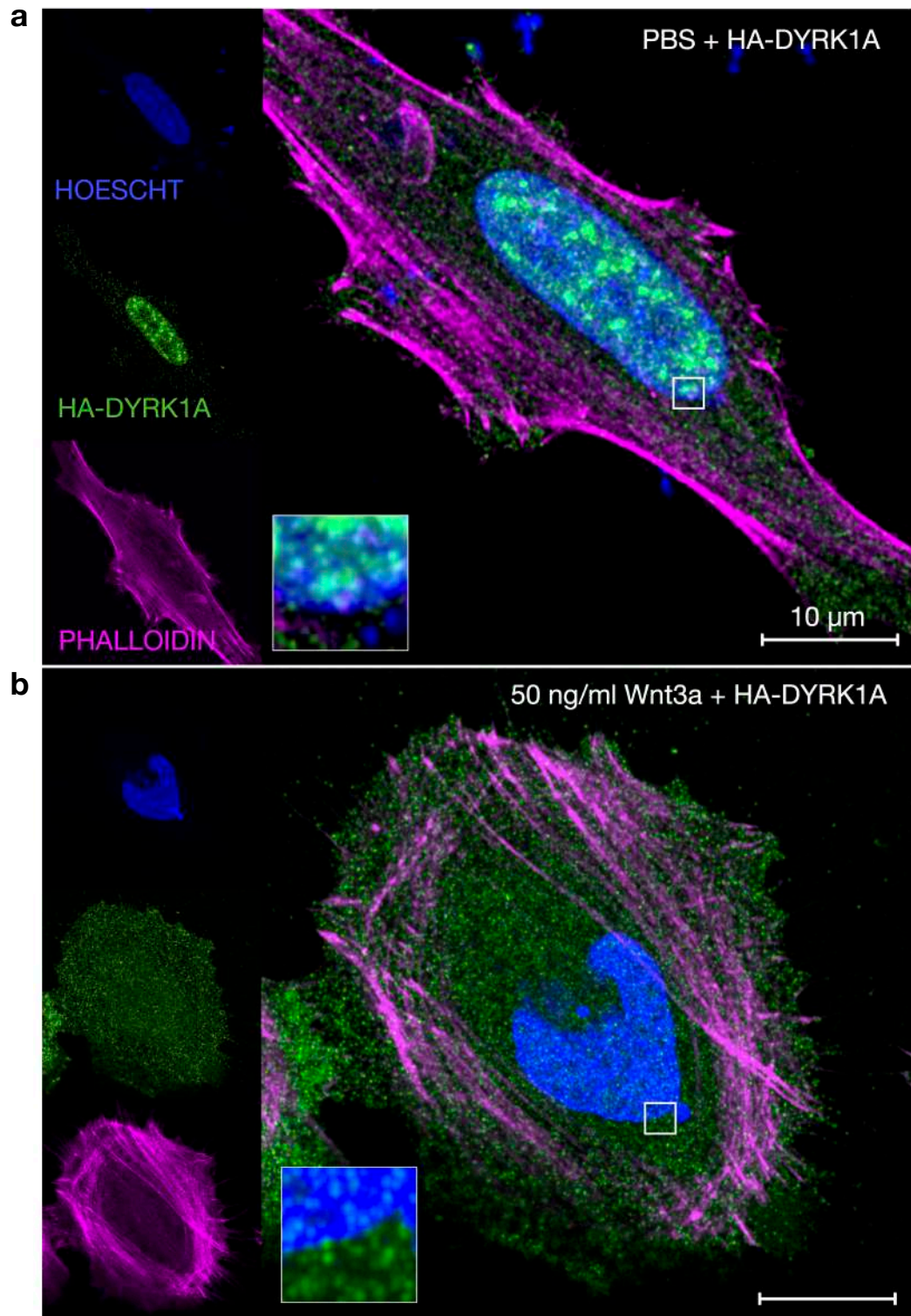


Fig. R3.21 - Same experiment as **R3.18**, but employing 5hr 50ng/ml Wnt3a stimulation. Under these conditions, nuclear DYRK1A (**a**, green) also redistributed into the cytoplasm (**b**).

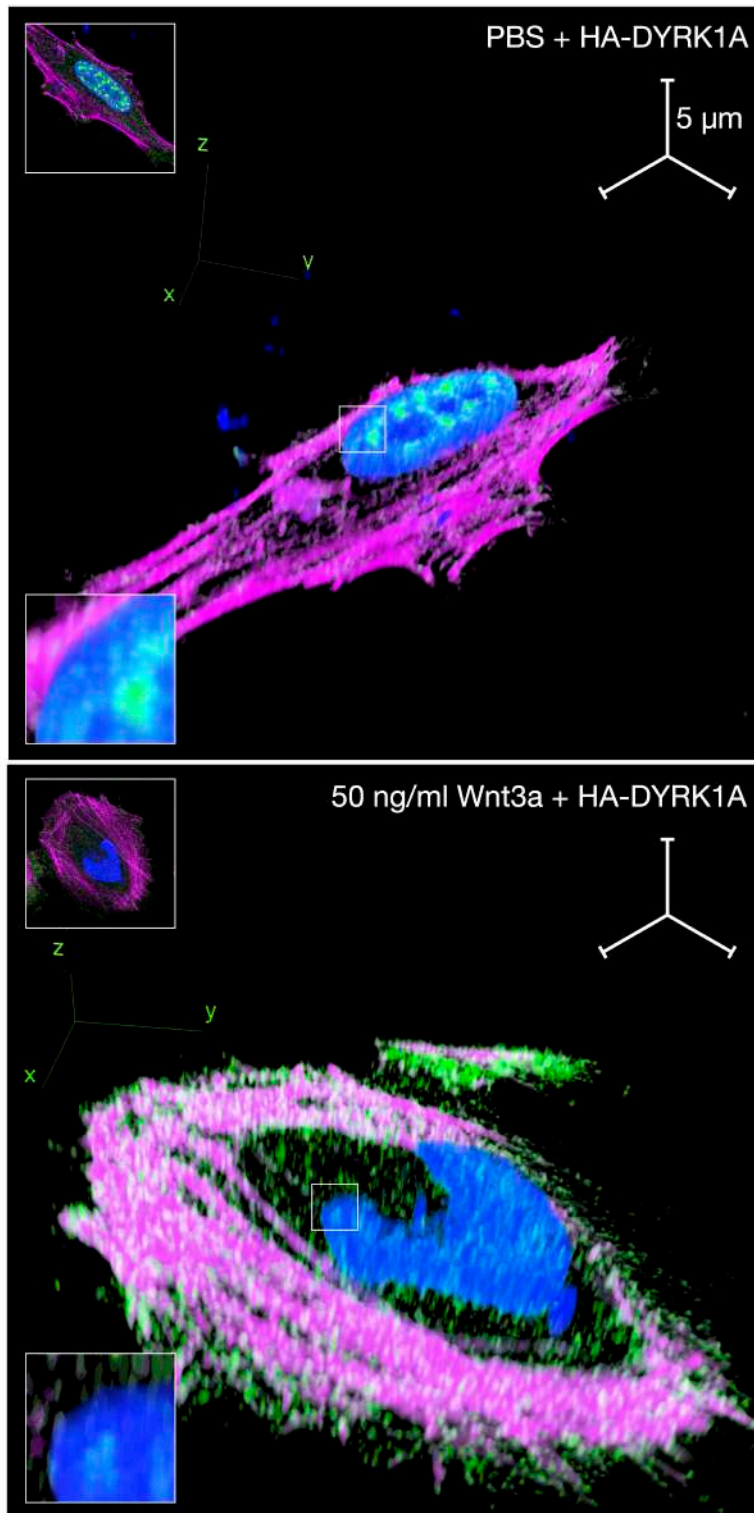


Fig. R3.22 - 3D reconstruction of z-stacks generated from images in R3.21, further demonstrating the observed phenotype.

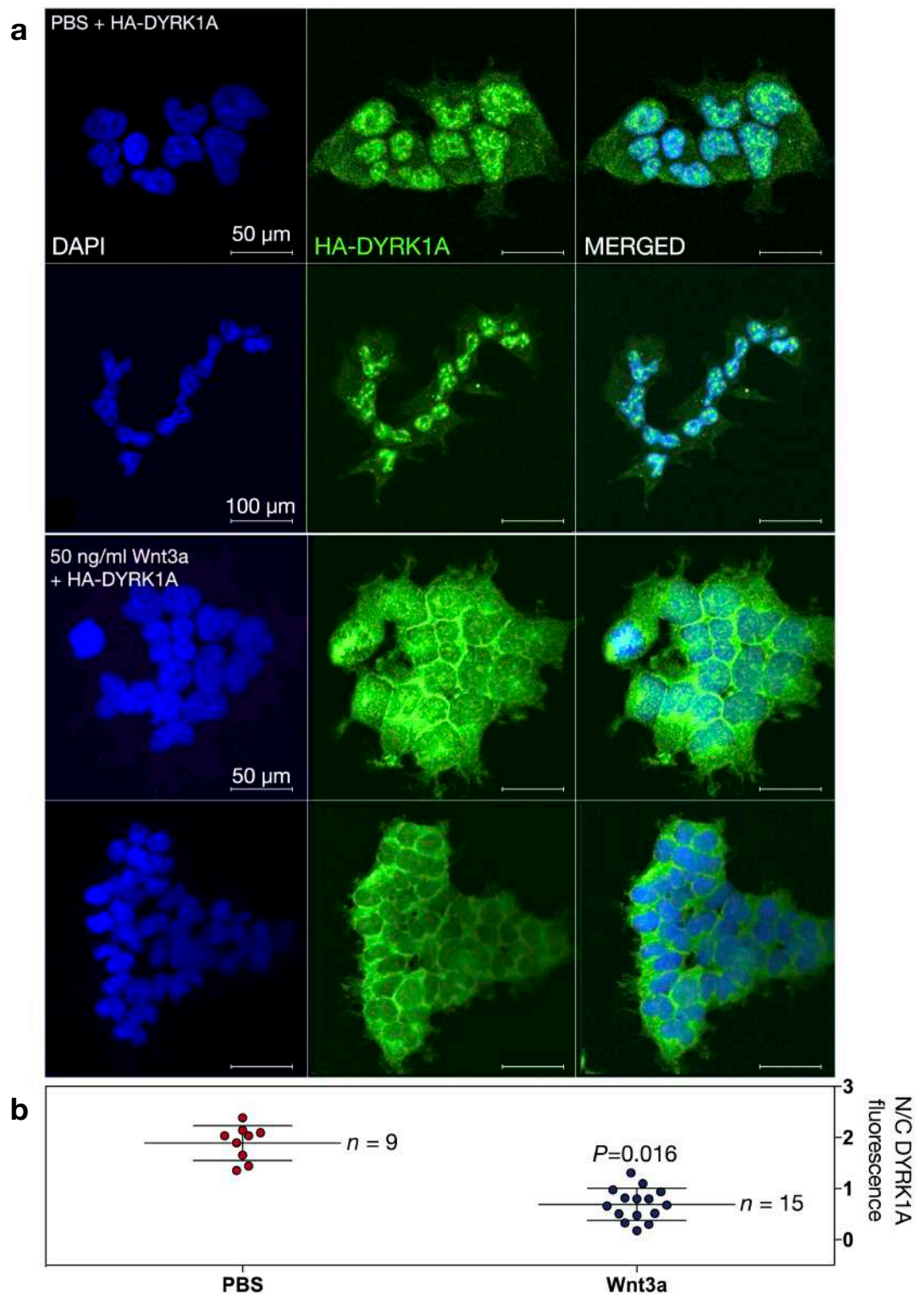


Fig. R3.23 - Nuclear/cytoplasmic DYRK1A ratio. **(a)** Same conditions as in **R3.21**, but in HEK-293 cells and imaged via confocal microscopy. **(b)** Significant reduction in DYRK1A nuclear localisation upon 5hr 50 ng/ml Wnt3a treatment. For each condition, $n=3$ cell clusters were analysed, comprising $n=9$ and $n=15$ cells for PBS and Wnt3a treatments, respectively.

4.3.2.3.4 DVL1 treatment: DYRK1A co-localises with DVL1 in cytoplasmic phase transitions

Given the observed DYRK1A interaction with DVL1 (**Fig. R3.5**), and their combined enhancement of active Wnt signalling (**Fig. R3.13**), the subcellular localisation of these two proteins was also investigated (**Fig. R3.24-26**). Its characterisation might provide important mechanistic information on the DYRK1A-DVL1 mediated enhancement of active Wnt signalling observed previously.

HeLa and HEK-293 cells were cultured, stained and imaged as in 4.3.2.3.2-3. HA-DYRK1A and FLAG-DVL1 along with relative control vectors were expressed at 0.5 µg/ml for 24 hrs. (**Fig. R3.24**). Cells were then collected, fixed and immunostained as described, with additional FLAG staining for DVL1 visualisation. As shown above, DYRK1A mostly localised to the nucleus when overexpressed alone (**Fig. R3.24a, green**). Representative Airy-scan images demonstrated a prominent nuclear DYRK1A signal in HeLa cells, with little cytoplasmic fluorescence observable. When DVL1 was overexpressed, imaging revealed its distinctive, vesicle-like cytoplasmic staining pattern (**Fig. R3.24b, red**). This is a known property of DVL1, which is prone to form 'aggregates' such as the ones observed here. This tendency is currently ascribed to membraneless compartmentalisation via liquid-liquid phase transitions (112) (see 4.3.3 for further discussion). When co-expressed with DVL1, DYRK1A appeared to redistribute out of the nucleus, as observed previously (**Fig. R3.24b, green**). Strikingly, however, DYRK1A prominently relocated to the DVL1 signal, assuming its vesicle-like staining pattern, with co-localisation of the the two proteins observed (**Fig. R3.24b, yellow**). 3D z-stacking further illustrated this phenotype (**Fig. R3.25**).

As before, the same experiment was conducted in HEK-293 cells to quantify the DYRK1A fluorescence N/C ratio (**Fig. R3.26a-b**). Under basal conditions, DYRK1A was predominantly nuclear ($n=3$ cell clusters, 1.6 ± 0.2). Consistently with pharmacological Wnt stimulation, DVL1 overexpression also resulted in a significant reduction of the DYRK1A N/C ratio, in favour cytoplasmic localisation (0.4 ± 0.2 , $P=0.002$). This finding represents a previously unreported intracellular configuration of DYRK1A, which appears to associate directly with DVL1 phase transitions. Additionally, the imaging data further validate the DYRK1A-DVL1 interaction, which was detected via co-IP under similar transfection conditions.

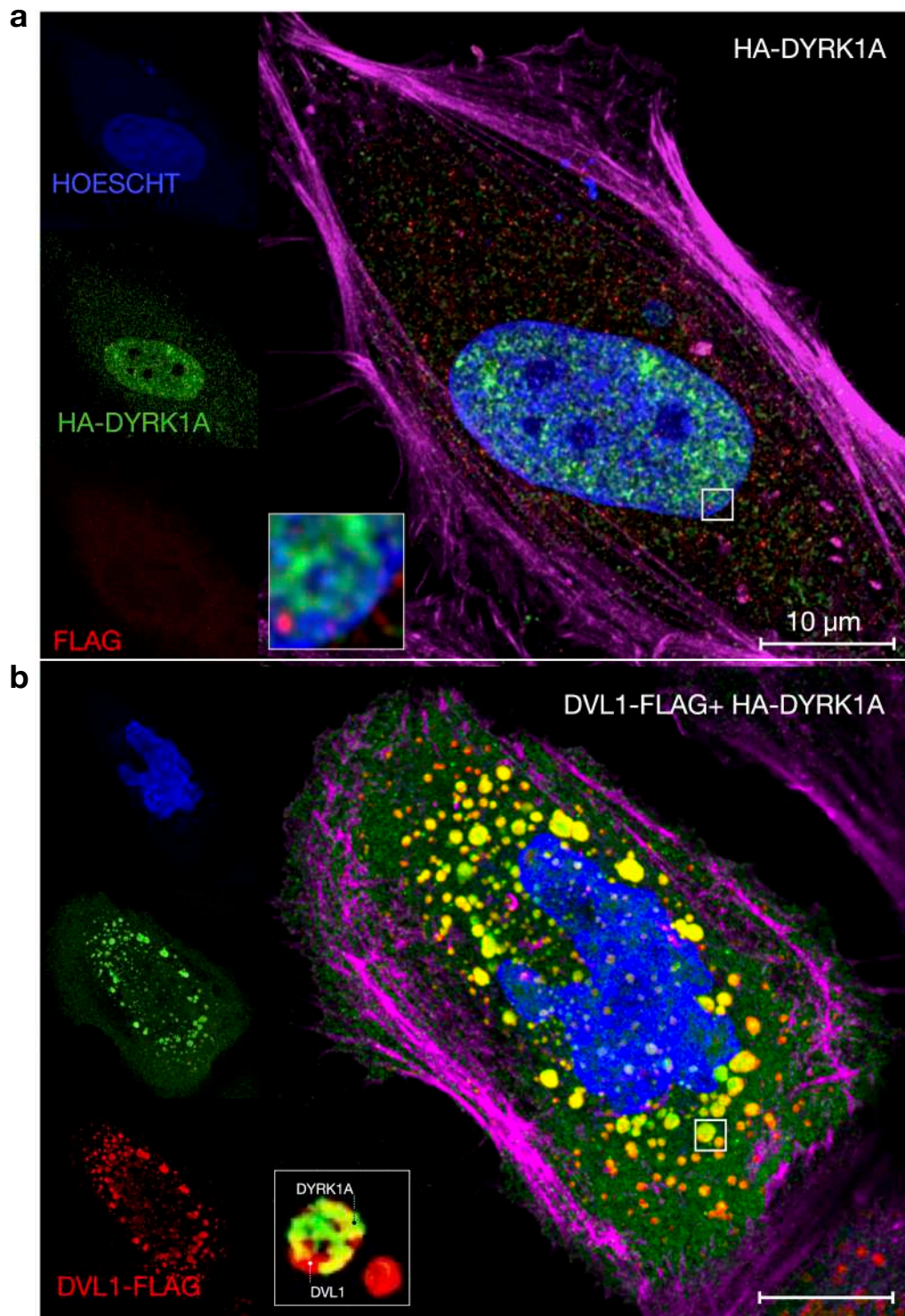


Fig. R3.24 - Same experiment as **R3.18/21**, but employing 0.5 µg/ml FLAG-DVL1 expression to stimulate Wnt activity. Under these conditions, nuclear DYRK1A (**a**, green) also redistributed into the cytoplasm (**b**), and prominently co-localised with DVL1 staining (**b**, yellow), in a pattern resembling liquid-liquid phase transitions.

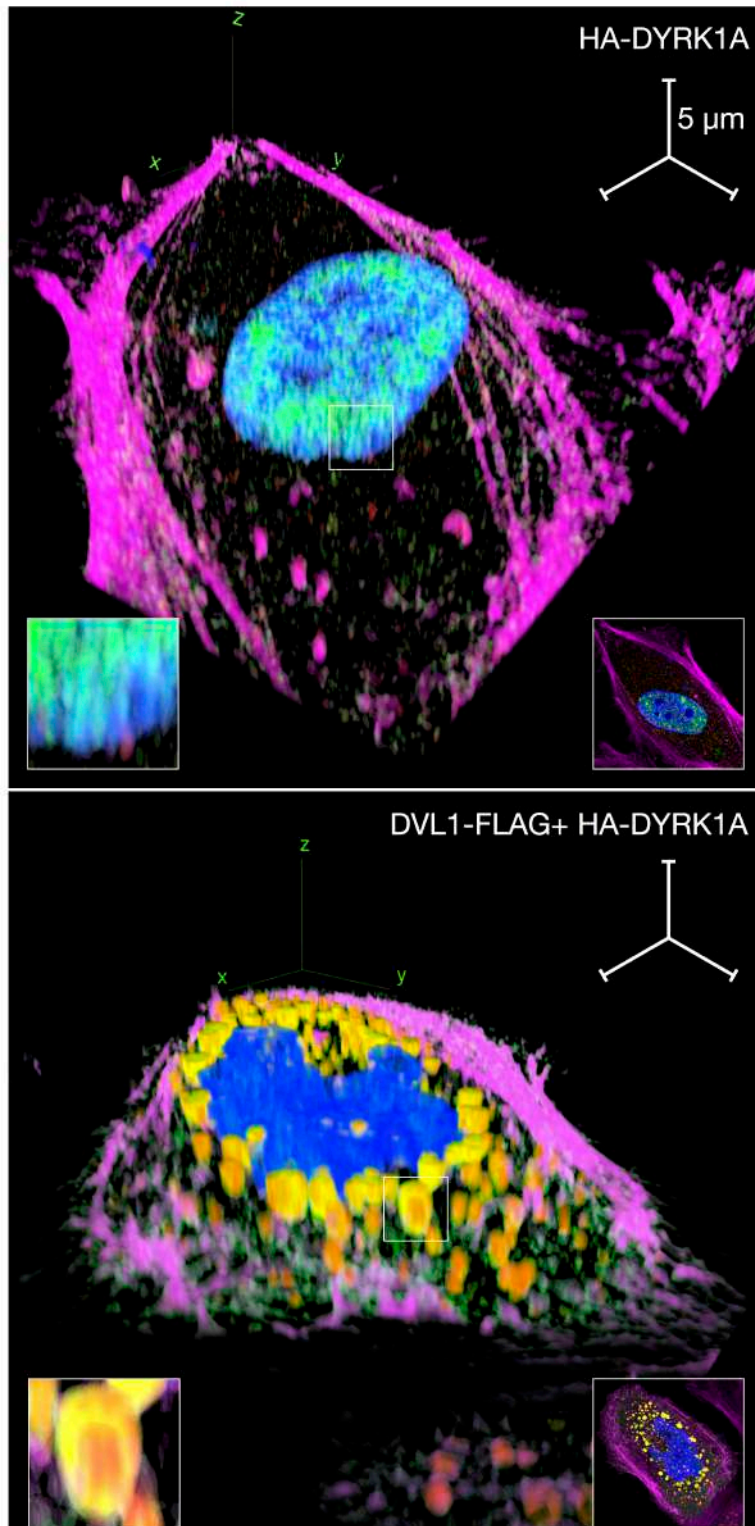


Fig. R3.25 - 3D reconstruction of z-stacks generated from images in **R3.24**, further demonstrating the observed phenotype and vesicle-like appearance of DYRK1A-DVL1 aggregates.

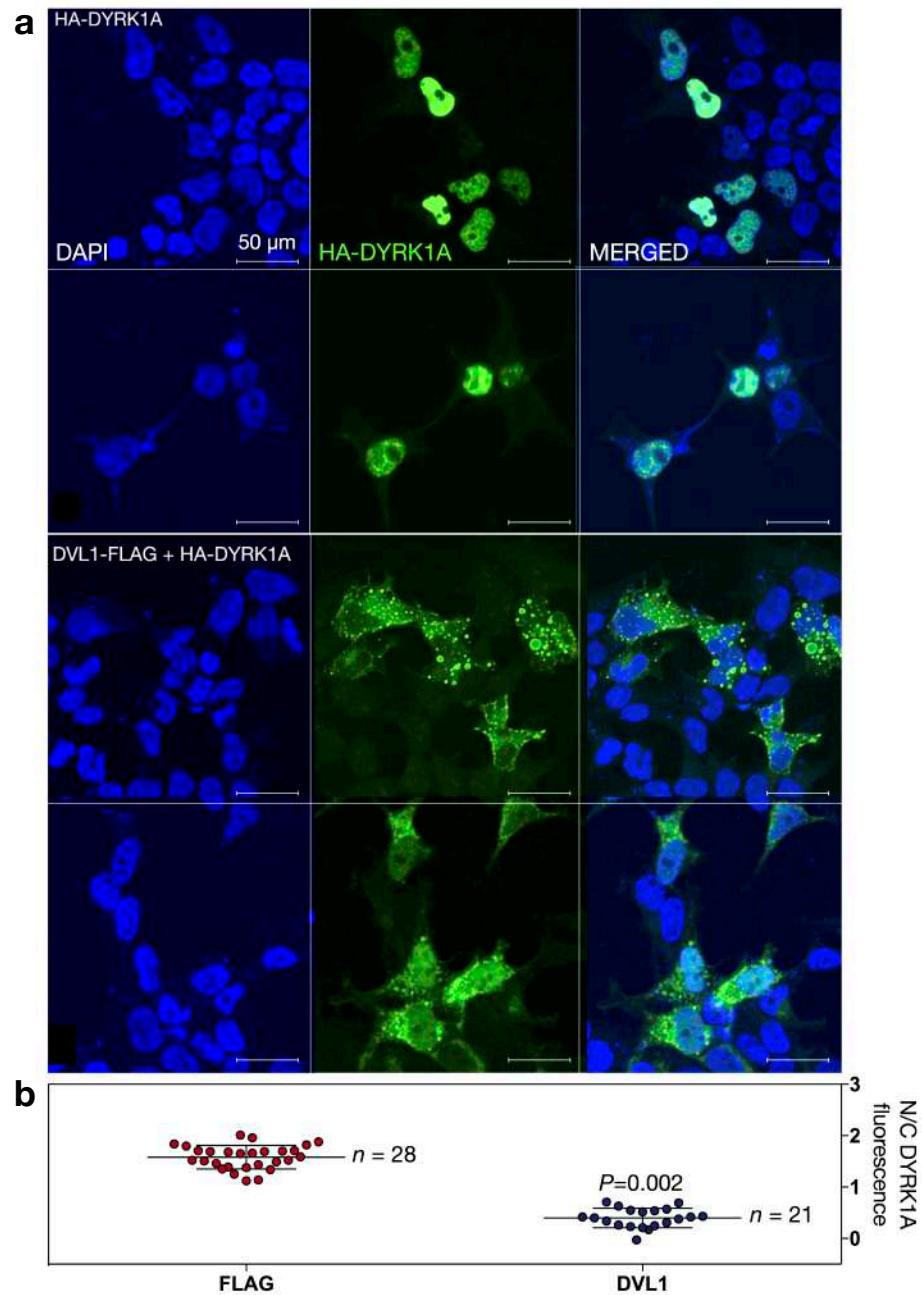


Fig. R3.26 - Nuclear/cytoplasmic DYRK1A fluorescence ratio. **(a)** Same conditions as in **R3.24**, but in HEK-293 cells and imaged via confocal microscopy. **(b)** Significant reduction in DYRK1A nuclear localisation with 24 hr DVL1 overexpression. For each condition, $n=3$ cell clusters were analysed, comprising $n=28$ and $n=28$ cells for FLAG-empty and FLAG-DVL1 vectors, respectively.

In summary, the imaging studies presented here elucidated a key aspect of the DYRK1A-Wnt relationship. Not only is DYRK1A capable of modulating Wnt signalling bidirectionally, but the pathway itself appears to regulate DYRK1A localisation. Wnt activation in fact may promote nuclear export of DYRK1A and its association with cytoplasmic DVL1 proteins.

4.3.3 Discussion

The key evidence concerning DYRK1A structure, function and localisation was discussed. The importance of DYRK1A in several biological mechanisms, most prominently CNS development and neuronal function, was also highlighted. DYRK1A is an essential contributor to DS neuropathology, and its aberrant activity is required for several features of the complex DS phenotype. Moreover, DYRK1A exerts significant control over multiple signalling pathways, and preliminary evidence also implicates the activity of this kinase in Wnt signalling regulation. Based on these lines of evidence, the experiments outlined in this chapter aimed to investigate DYRK1A as a candidate Wnt signalling modulator potentially contributing to the Wnt-DS phenotypes described previously (4.1-2).

The studies conducted here initially characterised a complex, multi-layered functional relationship between DYRK1A and canonical Wnt signalling. An unbiased STRING database screen first showed that the DYRK family interactome is significantly enriched with Wnt components, for all members. Following, Y2H screen and co-IP demonstrated that DYRK1A physically interacts with several Wnt components, most notably DKK3 and DVL1, but not β -catenin.

At this point, it is important to clarify that the significance of a DYRK1A-DKK3 interaction is contentious. Despite being detected by two distinct techniques, this interaction is unlikely to occur in intact cells. Multiple studies have in fact shown that, functionally, DKK3 is a secreted protein (106-108). Given that DYRK1A localisation is exclusively intracellular (11), the two proteins are extremely unlikely to functionally bind *in vivo*. It cannot thus be excluded that the DYRK1A-DKK3 interaction may instead result from the two proteins being artificially placed in proximity by cell lysis. This calls into question any functional relationship between DYRK1A and DKK3. For a counterpoint, however, it should be mentioned that DKK3 function and localisation are not as well established as for other Dickkopf family members, such as DKK1. As stated, DKK3 secretion has indeed been observed experimentally (106-108). Nevertheless, recent evidence suggests that an alternative, cytosolic function of DKK3 may exist. Leonard *et al.* (113) have in fact reported on a novel intracellular gene product encoded on the *Dkk3* locus in mice. The protein, termed Dkk3b, was shown to suppress β -catenin activity intracellularly, by preventing its nuclear translocation. This is purportedly achieved by Dkk3-mediated sequestration of β -catenin in cytosolic complexes with β -TrCP. Furthermore, the authors showed Dkk3b to be a key requirement for early mouse development. This study thus suggests that DKK3 might possess additional, non-secretory Wnt functions. It follows that the DYRK1A interaction reported here may apply to a potential cytosolic counterpart of DKK3, rather than to the secreted protein. Literature knowledge in this regard is limited, however, and the data generated here are not sufficient to exclude the potentially artefactual nature of the DYRK1A-DKK3 interaction. This remains a strong possibility, and no definitive conclusions can be drawn until further studies are performed.

Chapter 4.3 - DYRK1A-mediated Wnt signalling modulation

Despite this issue, current evidence suggests DYRK1A may indeed participate in Wnt-related protein networks. To explore this idea, all detected interactions were combined with the known DYRK1A-Wnt partners GSK3 β and p120/ δ -catenin (83, 109) into a larger, computationally enriched network. This approach exploited experimental and literature knowledge to highlight the tight functional proximity between DYRK1A and Wnt signalling components, either primarily or secondarily interacting. Following, potential effects of DYRK1A on β -catenin transcriptional activity were tested directly via luciferase assay. This revealed a novel, bimodal Wnt regulatory role of DYRK1A. Particularly, the data suggest that DYRK1A is capable of both suppressing and enhancing Wnt signalling activity. DYRK1A overexpression was shown to potently downregulate basal β -catenin activity. When the pathway was stimulated, however, DYRK1A exerted the opposite effect, further increasing activation several fold. This enhancement may also be prevented by co-expression of the DYRK1A interactor and Wnt antagonist DKK3. Accordingly, pharmacological inhibition of DYRK1A reduced active Wnt signalling in a dose-dependent manner. Basal Wnt activity levels were not detectably affected by kinase inhibition treatment, however. In support of DYRK1A-mediated downregulation of basal Wnt signalling, overexpression of this kinase also resulted in elevation of total GSK3 β levels. Such increase was accompanied by reduced GSK3 β phosphorylation at its inhibitory S9 residue, suggesting potential functional modulation by DYRK1A.

Bimodal Wnt signalling regulation by DYRK1A thus appears to be activation-dependent. Ultimately, the subcellular localisation of DYRK1A was investigated in relation to previously investigated Wnt activation states. Quantitative immunocytochemistry revealed that DYRK1A distribution may be affected by Wnt signalling stimulation. Whilst overexpressed DYRK1A was mostly nuclear under basal conditions, activation of Wnt signalling led to significant redistribution in favour of the cytoplasmic compartment.

In summary, the data overall indicate that DYRK1A interacts with Wnt components, regulates activity of the pathway and is itself controlled by Wnt signalling (**Fig. R3.27**). This set of findings generally establishes DYRK1A as a novel Wnt signalling modulator, with several ramifications for the understanding of DS pathology. However, the data presented here also convey a highly complex picture, with findings not always logically consistent, which requires careful interpretation before any conclusion can be drawn. The aim of this discussion is thus twofold:

- I. **To contextualise and predict the possible functional consequences of DYRK1A-mediated Wnt signalling modulation in cellular homeostasis and more generally, DS pathology.**
- II. **To outline the technical limitations of the present findings, and identify possible strategies to further explore the newly characterised DYRK1A-Wnt relationship.**

Generally speaking, the obvious implication of the data presented here is that DYRK1A might contribute to the abnormal Wnt phenotypes observed in DS mouse models and humans at the protein level (4.2). It follows that Wnt signalling, as regulated by DYRK1A, might in the future be established as a target pathway for therapeutic intervention in DS. This proposal, associated potential strategies, as well as current evidence on DS-DYRK1A therapies, are considered in detail in the general discussion of this thesis (5.2).

4.3.3.1 Bimodal DYRK1A regulation of Wnt signalling: potential mechanisms

It should first be stressed that the likelihood of functional Wnt regulation by DYRK1A is underscored by its participation in protein interaction networks relevant to this pathway. The power of the analysis conducted in this context relies on the combination of literature and experimental evidence. This demonstrated an important point: DYRK1A need not be placed more than two interactors away for the entire Wnt signalling pathway to be automatically included in a network. This suggests multiple potential access routes of DYRK1A to modulation of the Wnt pathway. However, an important consideration must be made at this point. The enriched network generated here should not necessarily be taken as factual in a definitive sense. It could be argued that seeding any network with a small number of Wnt components will yield a comprehensive Wnt signalling network, and this might indeed be the case. Rather, the purpose of generating a larger network was simply to place the observed and previously reported DYRK1A-Wnt interactions into the wider context of this pathway. For this reason, this network was not analysed for enrichment in functional terms, because doing so would incur significant bias, given that the network was originally constructed with several Wnt components. However, because the initial nodes were combined based on experimental evidence, it can be reliably concluded that the enriched network at least theoretically represents predicted but not definitively proven interactions. In support of this point, it is perhaps not surprising that some network nodes added by string (e.g. CDH1, FOS) were also identified as differentially expressed genes in DS models (4.1).

The notion that DYRK1A might participate in a highly-interconnected Wnt interaction network implies that its kinase activity might affect Wnt signalling. This was indeed the case when the pathway was investigated via luciferase assay. It should be conceded that the observed bimodal Wnt regulation by DYRK1A is somewhat counterintuitive. It may be generally argued that a kinase-regulated mechanism should exert consistent, homogeneous effects on its targets. For instance, DYRK1A effects on tau phosphorylation inevitably lead to its inhibition and accumulation (11), and no report currently suggests and opposite effect. Literature evidence however suggests that DYRK1A might indeed regulate target processes bidirectionally. For instance, it is well known that NFAT transcriptional activity is inhibited by DYRK1A (110). Another study however suggests that in specific contexts, DYRK1A might also enhance NFAT signalling (114). Additionally, as introduced, DYRK1A exerts bimodal effects on cell proliferation, both promoting and countering neuronal differentiation depending on tissue type (24, 26, 29). This suggests that DYRK1A may be expected to bimodally regulate Wnt signalling. And indeed,

Chapter 4.3 - DYRK1A-mediated Wnt signalling modulation

other known Wnt regulators are capable of such modulation. A prominent example mentioned here is LRRK2, which was shown to both promote and suppress Wnt signalling based on activation state, similarly to DYRK1A (102-104). It is interesting that the Wnt abnormalities here observed, in DS models and humans, were also bidirectional and varied based on tissue type and/or organism. It may be speculated that the bimodal Wnt effects of DYRK1A might be reflected in this phenotype, although this remains to be determined.

The imaging data presented here may shed light on why DYRK1A appears to drive Wnt signalling in both directions. When overexpressed under basal conditions, DYRK1A localised to the nucleus, and also suppressed Wnt signalling activity. It follows that, within the nucleus, DYRK1A might directly participate in transcriptional mechanisms suppressing β -catenin activation. Conversely, since DYRK1A was prominently cytoplasmic upon Wnt signalling activation, its enhancing effects might be mediated in this compartment, possibly via interaction with DVL1. An additional potential contributor to DYRK1A modulation of Wnt signalling is GSK3 β . Here, it was shown that *DYRK1A* overexpression is sufficient to increase protein levels of GSK3 β , with a small reduction in S9 phosphorylation. Importantly, a recent key finding by Song *et al* demonstrated that DYRK1A interacts with and phosphorylates GSK3 β at T356 (109). This interaction resulted in GSK3 β inactivation and amelioration of an obesity phenotype in TgGSK3 β mice. Reviewed evidence has clearly showed a prominent regulatory role of Wnt signalling in adipogenesis (115). Therefore, DYRK1A may contribute to Wnt signalling activation via GSK3 β inhibition. Whilst in the nucleus, DYRK1A has little access to cytosolic GSK3 β . Upon Wnt signalling activation, however, recruitment to DVL1 phase partitions may bring DYRK1A in close proximity to GSK3 β , resulting in inhibition of the latter and further enhancement of active Wnt signalling. GSK3 β might also be involved in nuclear effects of DYRK1A, given that it can itself localise to the nucleus and suppress Wnt signalling activity (116, 117). As introduced, DYRK1A employs priming phosphorylation to target substrates for further modification by GSK3 β and subsequent degradation (44, 49, 84, 85). A similar interaction might alternatively allow DYRK1A to direct GSK3 β phosphorylation to additional Wnt signalling components. These may include AXIN, APC, LRP5/6 and β -catenin itself, all substrates of GSK3 β . On the other hand, It is also possible that Wnt regulation by DYRK1A is achieved via multiple pathways including p120/ δ -catenin, NFAT, and non-Wnt GSK3 β substrates. At present, however, the nature of these mechanisms remains speculative, and they must be further investigated to clarify exactly how DYRK1A may control Wnt signalling activity. In summary, however, it can be concluded that the studies outlined here provide novel, preliminary insight into a complex, bimodal DYRK1A-Wnt relationship.

Assuming the reliability of these findings at least on a preliminary level, they can be further interpreted. The wider implication of this dualistic DYRK1A effect in DS is that a complex, multi-directional temporal and spatial alteration in Wnt target gene expression may occur throughout life. In addition to being

Chapter 4.3 - DYRK1A-mediated Wnt signalling modulation

dosage-sensitive, DYRK1A is also a constitutively active kinase. It follows that in DS, where the default level of DYRK1A expression is chronically elevated, Wnt signalling might be linearly affected as a consequence, in a direction determined by local activation states. This implies that tissue types with low basal Wnt signalling levels, such as adult neurons, may suffer from further downregulation. Conversely, developmental switches in Wnt signalling activity, or physiological activation in adult tissue may be abnormally enhanced by chronic DYRK1A overexpression. Both over- and under-activation of Wnt signalling in the hippocampus are expected to be deleterious during brain development (106), neurogenesis (118) and LTP (119), as fine regulation is crucial. Indeed, human DS hippocampi displayed decreased Wnt signalling activity (4.2.2), which is also known to contribute to idiopathic AD neuropathology [(120-123) see 5.1-2 for integrated discussion of all data generated in this thesis]. Overall, the original hypothesis formulated in this chapter was corroborated by experimental data and contextualised within the relevant literature. It appears that DYRK1A is capable of Wnt signalling regulation, with complex effects which may contribute to critical dysfunction of this pathway in DS. However, much remains to be determined on the mechanistic nature of the Wnt-DYRK1A relationship.

4.3.3.2 Limitations and future approaches

Despite the interesting nature of these novel findings, there are a number of technical limitations inherent to the methods employed which deserve consideration. They are briefly discussed here, along with potential countermeasures for subsequent work (see 5.2 and 6 for more general considerations on future directions). First, the majority of data presented were generated in overexpression systems. Whilst *DYRK1A* is indeed overexpressed in DS, the high protein abundance resulting from artificial expression might not faithfully recapitulate physiological conditions. It is possible that endogenous *DYRK1A* overexpression in DS might be much milder, and therefore unlikely to affect Wnt signalling to the extent observed in luciferase assays. This idea also applies to some of the interaction studies performed, which employed co-IP of FLAG-tagged proteins. Such approach greatly enhances throughput, but at the cost of specificity. It may be speculated that, under endogenous conditions, DYRK1A might be much less likely to interact with DVL1 or DKK3.

It is also important to mention that the employment of LiCl as a Wnt stimulation method (4.3.2.2) is not an entirely reliable approach if performed alone. Lithium is in fact well known to inhibit a wide range of kinases other than GSK3 β . Although Wnt activation was indeed detected with LiCl treatment, it cannot be excluded that other non-specific effects might be present, thus constituting a potential confounding factor. For this reason, Wnt3a treatment and *DVL1* overexpression were here employed alongside so as to improve the reliability of results. Future studies should therefore aim to replicate these results employing additional Wnt stimulation methods, such as alternative ligands and overexpression of other activating components (e.g. β -catenin, *FZD*).

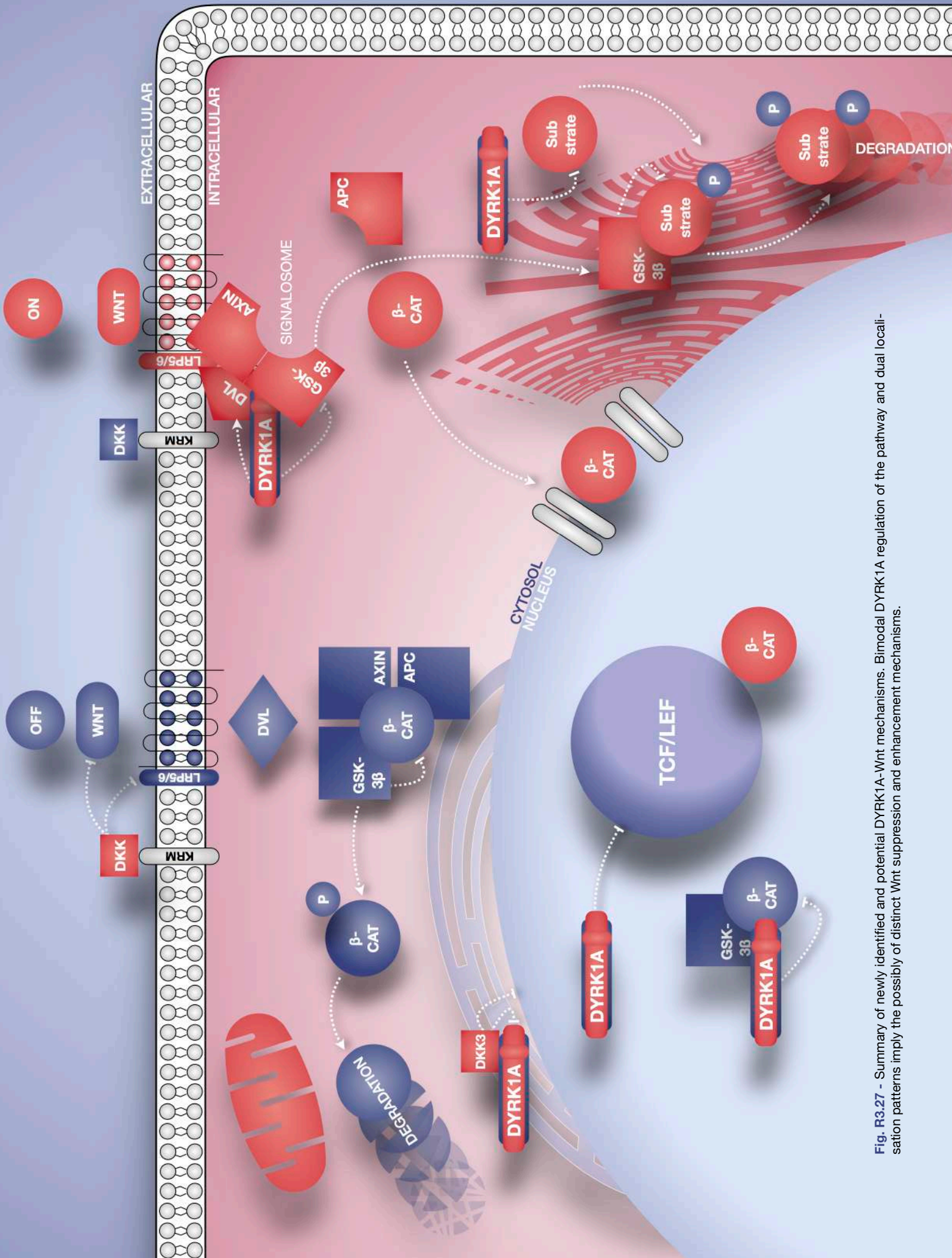


Fig. R3.27 - Summary of newly identified and potential DYRK1A-Wnt mechanisms. Bimodal DYRK1A regulation of the pathway and dual localization patterns imply the possibility of distinct Wnt suppression and enhancement mechanisms.

Chapter 4.3 - DYRK1A-mediated Wnt signalling modulation

With respect to the co-IP data, another key limitation is present. These experiments were performed employing beads pre-conjugated with a FLAG antibody. Whilst this approach enhances pull-down efficiency and reduces time required, it does not allow for the inclusion of important experimental controls. In traditional co-IP experiments, beads are generally conjugated to a specific antibody in-house, prior to pull-down. This ensures that the presence of non-specific binding products is controlled for, specifically by conjugating the beads to an unrelated antibody and by employing no antibody at all (mock IP). Since FLAG beads are not supplied with such controls, alternative non-conjugated beads should have been employed in the experiments here. This strategy introduces variability, since non-equivalent beads and additional conjugation steps would be performed specifically for the controls. They were thus not included here for these reasons. Instead, non-specific binding was controlled for by incubating the FLAG beads in empty vector-transfected cell lysates. This helped exclude spurious protein binding by the FLAG antibody. It is however essential to state that all co-IP interactions reported here must be validated by alternative approaches including the above mentioned controls. In summary, verification of these results must crucially be performed both via overexpression and endogenously before any definitive conclusion can be made.

Interpretation of imaging data might be limited by the fact that overexpression induces abnormally high intracellular accumulation of proteins under study, possibly resulting in non-physiological phenotypes. Without detracting from the validity of these results, future studies should aim to validate and characterise the Wnt-DYRK1A relationship from a more endogenous viewpoint. For instance, KO cell systems could be employed to determine the presence of any DYRK1A-mediated effects on basal and active Wnt signalling. Endogenous co-precipitation of proposed DYRK1A interactors should also be proven under physiological conditions, and in multiple tissue types. Likewise, imaging approaches should aim to reliably detect endogenous DYRK1A levels and investigate how they might, if at all, be altered by Wnt activation. Subsequent studies should also validate DYRK1A-mediated Wnt modulation in less artificial cell systems. The neuroblastoma cell lines employed here is highly proliferative, and might respond to Wnt signalling in non-physiological ways. Thus, the effects of DYRK1A could more appropriately be investigated in primary neuronal cultures derived from both mice and humans.

These proposed approaches might help further establish the novel findings presented here, and expand knowledge on the complex role of DYRK1A in DS and Wnt signalling.

General
DISCUSSION
5-6

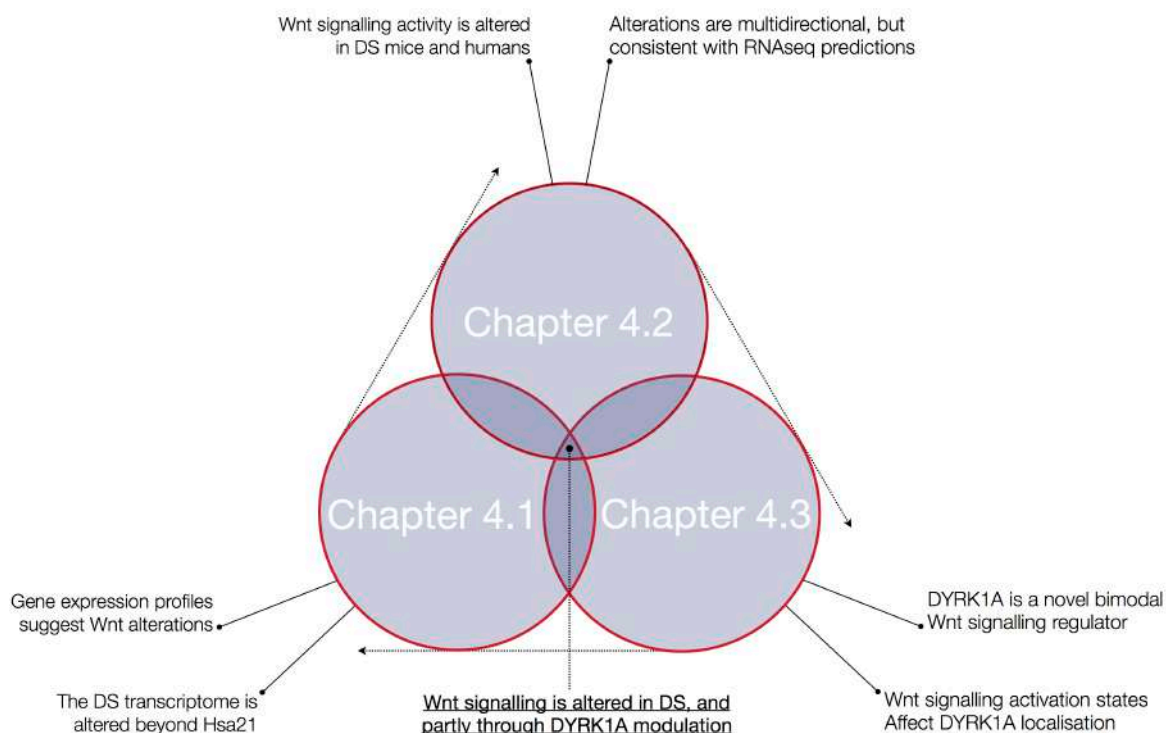


Fig. D.1 - Diagrammatic integrated summary of all results in this thesis.

Chapter 5 - General Discussion

The existence of a profound interplay between DS and early development of AD has long been documented (1). Moreover, alterations in canonical Wnt signalling are currently thought to contribute to AD pathogenesis (2-4). The well known importance of this signalling pathway in several neuronal developmental and homeostatic processes implies that Wnt dysfunction in AD or DS could reasonably lead to cell pathology. Despite preliminary evidence of multiple Hsa21 genes interacting with Wnt signalling, no direct Wnt-DS relationship has yet been described. For these reasons, this thesis sought to investigate a potential correlation between Hsa21 trisomy and Wnt signalling alterations (4.1-2) and to characterise the effects of a selected Hsa21 candidate, *DYRK1A*, on Wnt signalling function (4.3). The studies conducted thus generated multiple lines of evidence overall establishing, for the first time, Wnt signalling as a significant contributor to DS. These are briefly summarised here, and specifically discussed in each results chapter. The purpose of this concluding section is to consider all results in the general context of DS, and offer insight into how they might be expanded upon by future work, particularly in the context of therapeutic development.

5.1 Summary of all results

Results are first briefly summarised and discussed critically, in order to conceptually recap the conclusions of each set of studies and lay the basis for an integrative discussion (see 4.1-3.3 for chapter-specific discussion points).

5.1.1 Wnt signalling is potentially abnormal in DS

As discussed in the general introduction, genetic (1.4.1) and protein (1.4.2) work conducted in DS highlights complex alterations linked to several biological processes. Such abnormalities feature a degree of variability between tissue types and organisms examined. This phenomenon was similarly observed here, when DS-related and secondary transcriptional changes were examined (4.1) along with Wnt pathway components and activity (4.2). Nevertheless, this does not subtract from the preliminary conclusions that can be drawn from the data. First, modelled trisomy recapitulates phenotypes seen in human DS, as observed via hippocampal RNAseq (4.1). This confirms the reliability of Tc1 and Dp1Tyb mice. Second, Hsa21 trisomy is sufficient to affect Wnt signalling in the DS brain (4.2), at least for the parameters assessed here and most importantly the active β -catenin fraction. Given the presently limited understanding of molecular mechanisms in DS, this notion has important implications for the global understanding of this syndrome. The main findings in this regard can overall be summarised through the following key points:

I. The hippocampal transcriptome of DS mouse models recapitulates features of the human syndrome, and preliminarily suggests an association with altered Wnt signalling (4.1):

- A. DS-relevant Hsa21-Mmu16 genes are overexpressed, as seen in human DS.
- B. Genome-wide, secondary transcriptional alterations are observed, similarly to humans.
- C. In both mouse models, a number of secondarily affected genes are Wnt-related:
 1. The Tc1 hippocampal transcriptome displays reduced expression of the Wnt target gene *Axin2*, and enhanced expression of *Dkk3*, amongst others.
 2. The Dp1Tyb hippocampus displays reduced expression of the Wnt target gene *Axin2* and the Wnt receptor gene *Fzd2*, amongst others.

II. Wnt signalling activity dysfunction is observed at the protein level in the DS brain (4.2):

- A. β -catenin activity is significantly altered in the CNS tissue of DS mouse models and humans.
- B. The abnormalities detected correlate with enhancements in DYRK1A levels.
- C. Protein changes are **complex, tissue-specific and multidirectional**:
 1. The Tc1 and human DS hippocampus both display suppression of Wnt signalling activity.
 2. The Dp1Tyb hippocampus and Tc1 cerebral cortex, however, possess enhanced Wnt signalling activity, whilst the Dp1Tyb cortex is unaffected.
 3. The Wnt antagonist DKK3 is reduced in the human DS hippocampus, but enhanced in Tc1 and Dp1Tyb hippocampi, whilst GSK3 β remains unaffected throughout.

III. Candidate genes for the observed Wnt phenotype likely map to Mmu16 orthologs (4.2):

- A. Both Tc1 and Dp1Tyb mice overexpress Mmu16 orthologs, and displayed altered Wnt signalling.
- B. No alterations in hippocampal Wnt signalling activity were observed in Dp1(10-17)Yey mice.
- C. Therefore, Mmu10-17 orthologs are much less likely to mediate the Wnt phenotypes observed in DS mouse models and human hippocampi.

5.1.2 DYRK1A regulates canonical Wnt signalling activity

Conceptually, the second overarching finding of this thesis is the identification of the candidate Hsa21 gene *DYRK1A* as a novel Wnt signalling modulator. As discussed (4.3.1/3), *DYRK1A* is well placed to account for the Wnt phenotypes observed in mice and humans, given its location on Mmu16 and known importance for learning disability in DS. The evidence hereby generated linking *DYRK1A* to Wnt function can overall be summarised through the following key points:

IV. DYRK1A participates in complex Wnt signalling protein interaction networks:

- A. Unbiased STRING database screening identified significant Wnt-associated interaction partners for all members of the DYRK family of kinases.
- B. Yeast two-hybrid demonstrated multiple DYRK1A interactions with Wnt signalling components, most notably DKK3, which binds DYRK1A at a nuclear speckle-localising sequence.
- C. Co-immunoprecipitation showed DYRK1A interacts with DKK3 and DVL1, but not β -catenin.
- D. Integration of these results (B-C) with literature evidence for DYRK1A binding of p120/ δ -catenin and GSK3 β via STRING generated a highly interconnected network, demonstrating the functional proximity of DYRK1A to all major Wnt signalling components.

V. DYRK1A is a novel, bimodal canonical Wnt signalling regulator:

- A. DYRK1A kinase inhibition reduces *active* but not *basal* Wnt signalling activity.
- B. The Wnt inhibitory effects of INDY are dose-dependent.
- C. DYRK1A overexpression greatly reduces *basal* Wnt activity whilst enhancing *active* signalling.
- D. DYRK1A overexpression enhances total GSK3 β protein levels, whilst reducing p-S9.
- E. Whilst DKK3 exerts no effect on active or basal Wnt signalling, it may be able to prevent DYRK1A-mediated enhancement of DVL1/Wnt activation.

VI. Wnt signalling activation affects subcellular DYRK1A localisation:

- A. DYRK1A is prominently nuclear at basal Wnt activity levels.
- B. Wnt signalling activation induces significant cytoplasmic redistribution of DYRK1A.
- C. The effect applies to LiCl, Wnt3a and DVL1-induced activation.
- D. DYRK1A co-localises with cytoplasmic DVL1 phase transitions.

Overall, these results suggest a novel Wnt regulatory role for DYRK1A, which might influence Wnt signalling bimodally whilst being itself regulated by activity of the pathway. A further general principle may be preliminarily extrapolated from 5.1.1-2. Chronic dysregulation of Wnt and other transcriptional signalling pathways, due to triplication of modulators such as *DYRK1A*, may effectively extend gene dosage imbalance to a high number of secondary targets, possibly accounting for the known genome-wide transcriptional alterations typical of DS.

5.1.3 Critical evaluation of experimental results

Having summarised the main experimental conclusions of this thesis, it is important at this point to take a step back and critically evaluate results in light of some existing technical limitations. These might in fact hinder interpretative discussion of the data and, particularly in some cases, constitute non-trivial confounding factors. Alternative interpretations of key results, along with potential strategies to validate or confute them, must therefore be considered. They are discussed in this section, chapter by chapter and overall, so as to emphasise the preliminary nature of this thesis' findings and ensure neutrality is maintained.

5.1.3.1 Chapter 4.1 - Analysis of the DS transcriptome

In this chapter, hippocampal gene expression profiles of Tc1 and Dp1Tyb mice were investigated via RNAseq. The main purpose here was to preliminarily assess the aneuploid status of these two models. Results were quite clear in this respect, especially in light of the relevant literature discussed (1.4.1). It is not surprising that Tc1 and Dp1Tyb mice display the expected DS-like pattern of Hsa21/Mmu16 gene overexpression. In both cases, primary transcriptional alterations were consistent with previous reports (5-7). This reproducibility also applied to one of the main limitations inherent to the RNAseq data, i.e. the loss of functional trisomy for the *APP* gene in Tc1 mice. This finding implies the artificial silencing of any phenotypic contribution of *APP* to the Tc1 hippocampus, whereas this gene is of fundamental importance in human DS and AD-DS. It follows that transcriptional and biochemical abnormalities identified in this mouse, primary or secondary, cannot possibly be mediated by *APP* overexpression. Thus if present, they should occur independently of said gene, and must be considered as such. No conclusion regarding *APP* may then be made for the Tc1 mouse, and this is a significant limiting factor in the context of AD-DS. On the other hand, however, the absence of *APP* in this model might also be advantageous, in the sense that it allows for isolation of phenotypic contributions by other key DS genes, such as *DYRK1A*. Importantly, the functional loss of *APP* in the Tc1 mouse is not a novel finding, and has been previously reported (6). A sensible strategy to address this issue, as suggested by reviewers, is to crossbreed Tc1 mice with the established J20 line, an AD model which overexpresses two FAD-associated *APP* mutants (8). This would indeed provide a more faithful recapitulation of DS, by accounting for the full effects of *APP* trisomy. In the context of this thesis, it can be proposed that Tc1-J20 hybrids should be employed in further RNAseq and biochemical studies. Such an approach would aim to compare and contrast the phenotypes here observed and assess their validity. This consideration also applies to the primary hypothesis of this thesis, i.e. a potential contribution of Wnt signalling to DS.

In this regard, there is another key obstacle to the interpretation of results reported in 4.1. As already discussed (4.1.3.3), the RNAseq and IPA analyses, alone, are not sufficient to infer a significant contribution of abnormal Wnt signalling to the transcriptional profiles generated from either DS model. Granted, the objective *presence* of multiple DEX genes functionally associated to Wnt signalling was indeed observed. Prominent examples include the canonical Wnt target and negative regulator *Axin2*, reduced in both mice, the inhibitor *Dkk3*, increased in the Tc1, and the transmembrane receptor *Fzd2*, reduced in the Dp1Tyb. Addi-

tionally, canonical pathway analysis via IPA demonstrated a statistical association of canonical Wnt signalling with the Tc1 dataset, which was also the most significant enrichment for this mouse. By contrast, however, the Dp1Tyb data did not register a positive enrichment with the Wnt pathway, which only trended in association. Taken together, these findings only allow for the objective conclusion that, in the hippocampal transcriptome of two DS models, a number of secondary DEX genes are Wnt-related. This inference is supported by established literature knowledge of said genes (9, 10). Crucially, however, based on these data no further claim can be made without incurring considerable bias. There are simply too many confounding factors to deduce an overall involvement of Wnt in DS. As discussed (4.1.3.3), for instance, based on these findings it is impossible to dissect which individual hippocampal cell types contributed differential amounts of mRNA to the sequenced samples. This is indeed a critical issue. Determining the cellular origin of specific gene expression patterns is in fact paramount to even proposing the involvement of a coherent biological pathway. The transcriptional profiles detected here might distribute to distinct cell types, and not manifest concomitantly in any one population. Importantly, the hippocampus is notoriously composed of a wide spectrum of cell types beyond neurons, including microglia and oligodendrocytes. Even within these three types there are several known subclasses. For all these data show, the observed phenotypes might not even be neuronal at all. This calls into question the idea that such Wnt-related DEX genes may directly contribute to neurodegeneration. Moreover, there is little overlap in secondary expression patterns between the two mouse models, with *Axin2* being the sole primary Wnt component common to both. This may be at least partly accounted for by the significant genetic differences which set the two models apart, as discussed previously (4.1.3.2). However, this in itself may be seen as an additional confounding factor, preventing any further interpretation.

As a result it may only be stated that, for the scope of this thesis, some Wnt-related DEX genes are simply *present* in the hippocampus of two DS models. This constitutes a strictly *preliminary* indication, which might nevertheless deserve further inquiry. In order to clarify or equally refute this claim, additional studies are mandatory. For instance, it may be advisable to replicate the approach in 4.1.2 employing an extended range of DS models as well as human samples. Such a strategy should entail the use of genetic material obtained from dissected tissue, as in 4.1.2, as well as primary cultures derived from multiple, distinct cell types across all mouse models and/or humans. The latter effort should employ single-cell RNAseq in order to determine whether biologically-coherent signalling pathway defects are at all present and consistently replicable. In light of these reasons, therefore, great care must be exercised when considering results obtained in chapter 4.1. Overall, the only sensible conclusion to be drawn here is that these models recapitulate DS to a reasonable extent, and are thus reliable for employment in later studies.

5.1.3.2 Chapter 4.2 - Wnt signalling proteins in DS mouse models and humans

In this chapter, protein level analysis of DS model and human brain tissue was undertaken, in order to primarily investigate a hypothesis of Wnt signalling contribution to DS. It may overall be conceded that results, in this case, are more robust than those in 4.1. QPCR analysis of *Dkk3* and *Axin2* in the Tc1 mouse first demonstrated significantly enhanced and reduced expression, respectively, of the two genes. Importantly, this result was consistent with RNAseq data, providing support to the idea that the two Wnt components might indeed be abnormal in this model. Immunoblotting investigation of canonical Wnt activity and components then revealed what is perhaps the key finding of this thesis. That is, Wnt signalling alterations are present in the hippocampus of both mice as well as human DS individuals (4.2.2.1-4). The most significant observation here is that both Tc1 and human hippocampi display consistent suppression of canonical Wnt signalling activity, a notion which agrees with current evidence implicating suppression of this pathway in AD. However, some inconsistencies are present in these data which are difficult to reconcile. For instance, protein changes are, in some cases, directionally divergent across tissues. DKK3 levels are decreased in the human DS hippocampus, as opposed to Tc1 and Dp1Tyb mice. The latter two also display diametrically opposite Wnt signalling changes, with enhanced activity observed in the Dp1Tyb hippocampus. Even within the Tc1 brain there is variability, as cortical samples display an increase in Wnt activity, opposite to hippocampal tissue. Overall, the observed differences compared to control samples are however statistically significant and replicable. It is therefore difficult to absolutely question their presence, which might provisionally be assumed. However, the inconsistencies outlined above suggest considerable complexity of Wnt dysregulation in DS, with a potentially heterogeneous, variable picture. As such, based on these data, it is neither recommended nor possible to extrapolate a uniform conclusion as to the *direction* of Wnt abnormalities in the DS brain. It should also be stressed that the cell type origin issue raised in the previous section also applies here. It is not possible, at present, to clearly dissect the source of altered β -catenin activity levels.

The evidence gathered in 4.2 overall suggest novel, significant Wnt signalling abnormalities in the DS brain, which are more likely to manifest *in vivo* as suppression in the hippocampus. These findings are however somewhat contradictory, and further exploratory studies must be performed for full validation or eventual refutation. A sensible strategy in this regard may be to replicate all analyses in 4.2 employing an extended range of DS tissues. Additional mouse models must be incorporated, as well as a greater number of tissue types, within the brain and beyond. Furthermore, it is crucial to determine whether Wnt changes vary, or are present at all, over a comprehensive age range. Here, mice were assessed at a single time point of 4-6 months of age, whilst human tissue was examined post-mortem. It follows that the available evidence only allows to *preliminary* conclude the presence of Wnt abnormalities at a specific age. No further inferences can be made without speculation. In summary, chapter 4.2 results indicate a possible contribution of altered, and likely suppressed, canonical Wnt signalling to the DS brain. These findings must however be clarified and validated before being considered scientifically sound.

5.1.3.3 Chapter 4.3 - DYRK1A-mediated Wnt signalling modulation

This chapter investigated a candidate gene hypothesis for *DYRK1A*, a crucial contributor to DS, as a potential Wnt signalling modulator. This hypothesis was formulated to at least partly account for the Wnt phenotypes observed in 4.2. Such proposal is based on current knowledge on the key roles of *DYRK1A* in DS (11), as well as the observation that segmental trisomy models for Mmu10/17, which lack *DYRK1A* overexpression, do not display abnormal Wnt signalling biochemically (4.2.2.3). To address this hypothesis, yeast and human cell lines were employed to investigate *DYRK1A*-Wnt effects, combining studies on protein interactions, luciferase-mediated Wnt activity and, lastly, subcellular localisation. Data in this chapter overall suggest *DYRK1A* might participate in Wnt protein interaction networks and regulate Wnt signalling bimodally, whilst being itself influenced by the pathway via subcellular localisation. These key results, along with the associated limitations and proposed clarifying strategies, are assessed and detailed in sections 4.3.3.1-2 and 5.2.2.2. The most critical example in this regard, requiring validation, is the surprising finding of a *DYRK1A* interaction with *DKK3*, the reportedly secreted inhibitor also altered in DS models and humans.

In summary, it should be reiterated that whilst the data collected in 4.3 do suggest *DYRK1A* has the *ability* to modulate Wnt signalling across multiple model systems, the existence of these effects *in vivo* cannot be postulated, due to lack of evidence. Therefore, extensive further studies are an absolute requirement to clarify if, and how, *DYRK1A* overexpression might impact Wnt signalling in DS. The importance of this necessity is unquestionable. Nevertheless, it does not detract from the novel findings of chapter 4.3, which for the first time demonstrated Wnt modulation by *DYRK1A*, a fundamental kinase in DS and DS-AD.

5.1.3.4 Overall considerations

The evidence gathered here, due to its novel nature, is limited by several factors. These were discussed along with some alternative interpretations. It is obvious that, at present, the preliminary implication of Wnt signalling in DS is far from clear. This thesis only aims to provide an initial direction for further scientific inquiry. An in depth mechanistic account of how Wnt signalling may induce pathology in DS remains to be provided. The process by which bimodal Wnt regulation by *DYRK1A* alters finely tuned developmental and adult Wnt signalling remains elusive. Ultimately, the complex tapestry of Wnt dysregulation in a multifaceted condition such as DS has only been scratched at the surface. Its directionality, extent and exact contribution to DS phenotypes are yet to be fully determined.

5.2 Wider implications of a DS-Wnt relationship

Despite the limitations outlined in 5.1.3, a Wnt signalling contribution to DS is likely, at the very least partially. For the purpose of this extended discussion, this principle can thus be initially assumed as valid, and utilised as a framework to argue in favour of two wider implications. First, that several aspects of DS, beyond neurodegeneration, may be accounted for by underlying alterations in Wnt signalling function. Second, that a Wnt-DYRK1A pathway may, in the future, be targeted therapeutically in DS.

It should be stressed that this discussion does not presume the absolute validity of results discussed. Rather, it builds on the key *preliminary* findings of this thesis, in order to explore more far-reaching implications. These nevertheless essentially rely on further validation of the data generated here. This necessity, without doubt, takes experimental priority. It is in fact logically required before knowledge on a Wnt-DS relationship, if any, may at all be translated therapeutically.

5.2.1 Links between Wnt signalling and known DS phenotypes

The evidence generated in this thesis demonstrates the involvement of Wnt signalling in a least three distinct tissue types in DS: the hippocampus, cerebral cortex and fibroblasts. Despite no presently available data on other physiological systems or tissues, the known pervasiveness of Wnt signalling function in many biological mechanisms warrants the question of whether this pathway is globally affected in DS, beyond the CNS. The main logical premise of this idea is based on the fact that Hsa21 trisomy extends to all cell types in DS, regardless of individual variability or mosaicism. Consequently, the Wnt modulatory properties of Hsa21 genes such as *DYRK1A* most likely apply to any tissue in which such genes are overexpressed. Without speculating on exactly how Wnt modulation may occur, it is nevertheless possible to superimpose the general notion of dysfunctional Wnt signalling on several DS phenotypes other than CNS pathology. Interestingly, multiple characteristics of DS might be conceptually accounted for by underlining alterations in Wnt signalling activity, by integrating evidence generated here with literature knowledge on Wnt function. This approach may help establish a conceptual basis for future investigation.

Characteristic craniofacial morphology - Individuals affected by DS possess distinctive physical traits which are especially manifest in the face and head, and through altered growth patterns (12). A key study outlining such features was produced in 1993 by Allanson *et al.* (13). The authors recruited 199 DS individuals spanning a wide age range (0.5-61 years) and performed a measured set of 21 'anthropometric' craniofacial traits. Amongst these, three were identified as 98-99% likely to uniquely distinguish DS individuals from controls: reduced ear length and maxillary arc growth, as well as brachycephaly. Such findings reflect the core developmental component of DS. It follows that these physical characteristics must arise as a direct result of finely altered developmental body/head patterning. Indeed, Wnt signalling is known to regulate key aspects of facial development. Brugmann *et al.*, for instance, demonstrated the profound effects of Wnt signalling disruption in mouse and chicken facial morphogenesis (14). *Tcf/Lef* null mice reportedly presented substantially altered facial features and brachycephaly. *In utero* administration of DKK1 accordingly

produced similar defects. Analogous mechanisms were also observed in chick embryos. In mice, facial morphogenesis is also associated with expression of canonical Wnt ligand genes (15). These data suggest highly conserved regulation of facial development by Wnt signalling in vertebrate organisms. In humans, altered Wnt activity or responsiveness at critical stages of development might indeed contribute to the characteristic craniofacial morphology of DS. The largely homogeneous features of this DS trait amongst individuals point to a consistent mechanism, to which Wnt signalling is well placed to participate in accordance with current evidence.

Congenital heart disease - Another well described feature of DS is the wide occurrence of congenital heart disease (CHD), which poses considerable risk to neonatal and adult survival, and usually requires surgical intervention. As introduced (1.1.1), CHD in DS mostly affects ventricular and atrioventricular septal development (16, 17), significantly impairing physiological cardiac function. CHD encompasses a variety of conditions, but it generally arises as a result of abnormal cardiogenesis. At the cellular level, this implies disrupted developmental control over renewal, migration and differentiation of cardiovascular progenitor cells. Interestingly, all three mechanisms are well known to be finely regulated by the Wnt signalling pathway, which plays fundamental roles in all aspects of cardiogenesis. Wnt gradients of activity control fate specification of precursor cells, cardiac morphogenesis, valve and conduction system development (18). The Wnt pathway also controls tissue remodelling and growth responses of the mature heart, in physiological and pathological conditions (19). In the context of CHD, one critical component affected is the outflow tract (OFT). This is a transient structure connecting the developing ventricles with the aortic sac, and is remodelled throughout cardiogenesis. The OFT ultimately gives rise to the aortic and pulmonary trunks and associated valves, whilst also contributing endocardial cell layers to the developing septa. Defects in OFT morphogenesis are a major contributor to CHD. Qyang *et al.* demonstrated that canonical Wnt signalling is necessary for normal OFT development (20). Deletion of β -catenin in cardiovascular precursors prevents differentiation and results in their accumulation, ultimately leading to substantial OFT morphogenic defects. The authors conclude that the canonical Wnt pathway is a fundamental mediator of cardiac progenitor development, and a key player in CHD development. These data overall imply that the wide occurrence of CHD in DS may be underscored by dysfunctional Wnt signalling, given the critical importance of this pathway in cardiogenesis.

Differential susceptibility to cancer - DS produces complex alterations in cancer risk relative to the euploid population. A 2007 report on the Australian DS population (21) identified no overall difference in total cancer incidence. Risk ratios for individual cancer types were however significantly altered. Interestingly, DS people suffer from higher rates of leukaemia, whilst solid tumours occur less frequently. This compound differential risk is intriguing, as it suggests a potential multi-faceted mechanism. It is well established that enhanced Wnt activity is a primary event in the development of several cancer types (10, 22-28). In euploid individuals, Wnt-initiated tumorigenesis is generally thought to arise from activation of degradation-resistant β -catenin or APC mutations. In DS, chronic Wnt signalling modulation by Hsa21 genes such as *DYRK1A*

might produce similar, or opposite outcomes. Thus, Wnt dysfunction might potentially contribute to the differential cancer susceptibility in DS (21). High basal Wnt levels in proliferative haematopoietic cells may, for example, be exacerbated by DYRK1A overexpression, which does indeed play a role in DS-related leukemias (29). Conversely, the decreased incidence of certain types of solid tumour may arise from suppression of Wnt signalling. A prominent example is colonic carcinoma, which is less common in DS (30). Reports indicate that Wnt signalling inhibition may reduce tumour growth in mouse models of colon cancer (31). Therefore, it may be hypothesised that chronic Wnt dysfunction in DS might contribute to secondary alterations in cancer susceptibility.

Immune system dysfunction - A striking characteristic of DS pathology is the known global dysfunction of the immune system. Accumulating evidence in the past four decades suggests a substantial deficiency in overall immune function inherent to DS and manifest throughout life, worsening in an age-dependent manner (32, 33). An early report by Cossarizza *et al.* demonstrated complex alterations in numbers of circulating lymphocytes (34). The authors assessed all subtypes of peripheral blood cells in adult DS, and identified reductions in the number B lymphocytes and CD4+ (helper) T cells. Conversely, CD8+ (cytotoxic) T lymphocytes were significantly increased along with natural killer (NK) cells. Interestingly, these changes are somewhat analogous to those observed in euploid individuals of advanced age. However, immune system defects in DS are reportedly present in infancy as well. A flow cytometry study conducted in DS children aged 0-12 years identified overall reductions in lymphocyte, monocyte and granulocyte numbers, suggestive of immune suppression (35). One subclass of pro-inflammatory monocytes (CD16+), however, was significantly elevated, potentially underlying chronic inflammatory disease in DS. Together, these data suggest that a key component of the innate immune system might be overactive in DS infancy, whilst adaptive immunity may be suppressed or deficient altogether in both infancy and adulthood. The haematopoietic stem cell system plays a crucial role in determining the immunological makeup of circulating leukocytes, by regulating precursor fate and rate of differentiation. As introduced (1.2.2), the Wnt signalling pathway is an essential modulator of haematopoietic stem cell function (36). Several lines of evidence now heavily implicate this pathway in regulation of lymphocyte development (37). Reviewers suggest that homeostatic Wnt signalling activity is important for regulation of undifferentiated lymphocyte precursor pools and rate of terminal differentiation (38). Aside from the resulting impact on development of haematological malignancies, which are indeed more common in DS, these data imply that Wnt dysfunction may also result in abnormal immunological profiles akin to those observed in DS individuals. Thus, immune dysfunction in DS may partly result from chronic dysregulation of Wnt-mediated haematopoiesis.

Overall, these evidence-based considerations demonstrate that multidirectional alterations in Wnt signalling are likely to affect biological processes regulated by the pathway, inevitably leading to highly complex phenotypes. Given the tight regulation and differential tissue requirements of Wnt signalling function, a number of key manifestations of DS may thus be considered in this light. It should be stressed, however, that these associations remain inferential at present, and require experimental validation of each potential hypothesis.

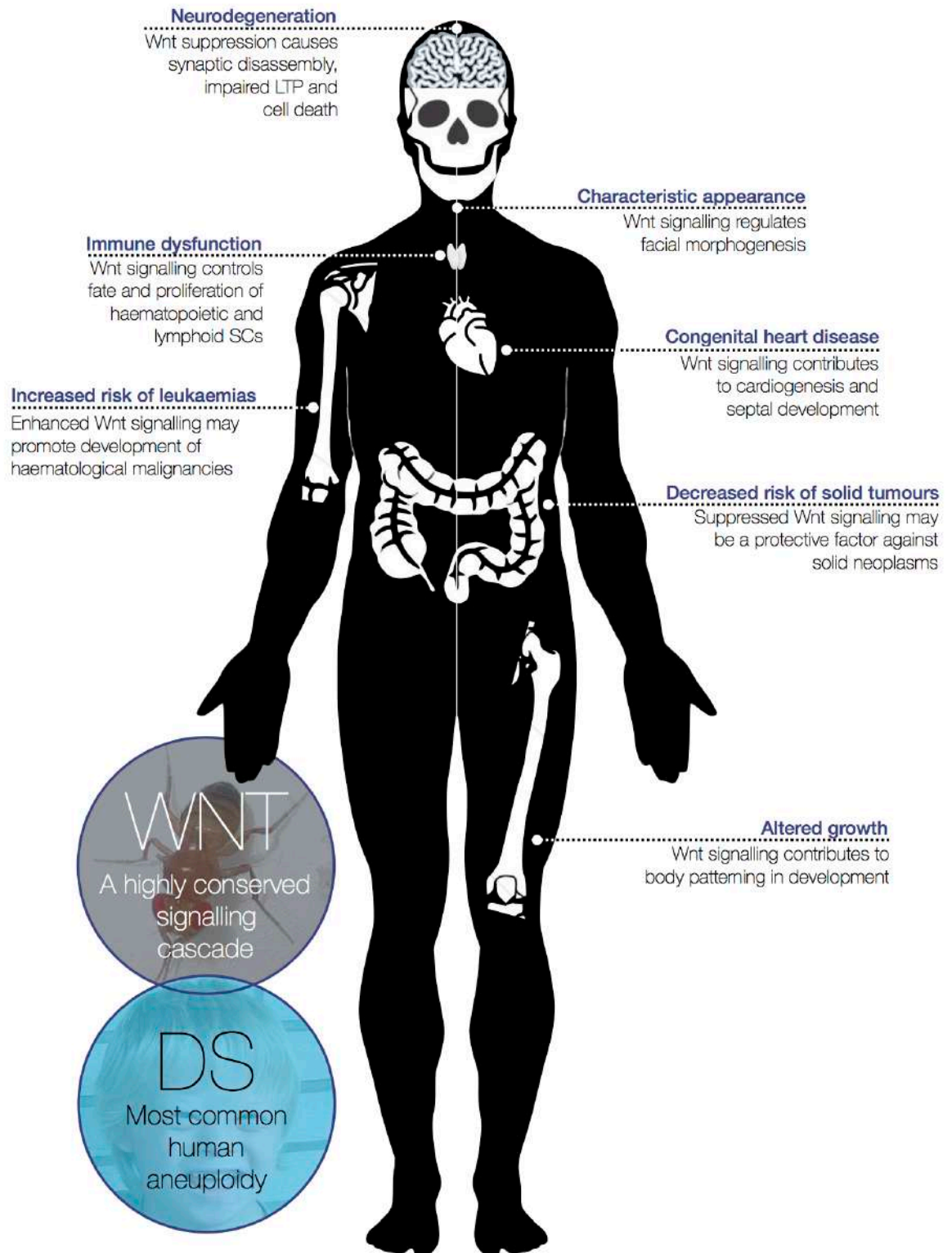


Fig. D.2 - Several features of DS are potentially accounted for, at least partly, by underlying Wnt signalling abnormalities. These considerations are derived from literature knowledge and experimental evidence generated here.

5.2.2 Potential therapeutic strategies: establishing Wnt signalling as a target pathway in DS

The key implication of the findings presented throughout this thesis is that Wnt signalling regulation by DYRK1A may be established as a novel target for therapeutic development in DS neuropathology and beyond. Such a strategy might entail a three-sided approach: **1)** Targeting aberrant DYRK1A activity in particularly Wnt-susceptible tissue types such as the adult hippocampus **2)** Directly targeting under/over-activation of Wnt signalling and target genes, depending on tissue-specific directional changes. **3)** Differentially tackling Wnt signalling dysfunction in both development and adulthood. These approaches are particularly attractive, chiefly because Wnt signalling and DYRK1A have been heavily investigated therapeutically. Therefore, future translation of the present findings into a viable therapeutic approach, aimed at normalising Wnt function in DS, would build upon solid foundations.

5.2.2.1 Wnt-based therapies in AD and neurodegeneration

As introduced (1.2.5), canonical Wnt signalling activity appears suppressed in the AD brain, leading to synaptic degeneration particularly in the hippocampus. Several lines of evidence clearly suggest that A β -induced Wnt signalling defects contribute heavily to AD pathogenesis and progression (2-4, 39, 40). Stimulation of neuronal Wnt signalling is thus currently viewed as a promising strategy in AD and other neurodegenerative diseases (41-43). Given the strong link between AD-DS, and the involvement of Wnt signalling newly identified here, therapeutic targeting of this pathway may prove beneficial in DS neuropathology as well. Due to its complexity, the Wnt pathway may be effectively targeted at multiple levels.

One prominent example is the employment of Wnt ligands as candidate agents. This family of small glycoproteins is well suited for therapeutic development, mainly because of small molecular size as well as the ability to activate Wnt signalling physiologically. It is now well established that Wnt signalling stimulation is neuroprotective in AD (39, 44). In hippocampal neurons, A β accumulation leads to suppression of excitatory post synaptic currents (EPSCs), a hallmark of early synaptic degeneration. Cerpa *et al.* demonstrated that, in cultured hippocampal slices, co-administration of Wnt5a and A β prevents EPSC suppression relative to A β alone (40), whilst Wnt7a stabilises the synaptic vesicle cycle (45). Wnt3a treatment, employed in this thesis to activate Wnt signalling, similarly prevents A β neurotoxicity and improves neuronal viability in rat hippocampal neurons (39). In the same study, A β administration reduced expression of the Wnt target gene engrailed-1 whilst enhancing GSK-3 β and tau phosphorylation. Both effects were prevented by Wnt3a. Consistently, Kawamoto *et al.* demonstrated that Wnt3a also rescues A β neurotoxicity in PC-12 cells, an effect accompanied by enhanced β -catenin protein levels (46).

In addition to Wnt ligand administration, GSK3 β activity may also be modulated pharmacologically to achieve significant Wnt stimulation. In this thesis, the GSK3 β inhibitor LiCl was employed successfully with this purpose. This compound is currently prescribed as a mood stabiliser for the treatment of

bipolar disorder. In hippocampal progenitor cells, LiCl promotes proliferation and neuronal differentiation via Wnt signalling activation (47, 48). GSK3 β inhibition is reportedly sufficient to achieve neuroprotection in primary hippocampal neurons and transgenic murine models of AD (3). Particularly, Fiorentini *et al.* showed that long-term LiCl administration in APP transgenic mice reduces neuropathology, promotes hippocampal neurogenesis and improves cognitive defects (48). Another candidate method targeting GSK3 β activity is administration of curcumin, a derivative of turmeric currently employed in a variety of industries as a cosmetic product or food colouring agent. In neuroblastoma cells expressing the APP^{swe} mutant, curcumin treatment was shown to activate Wnt signalling in a dose-dependent manner (49). The authors also observed that Wnt stimulation was accompanied by enhanced β -catenin expression and nuclear translocation, increased Cyclin D1 levels as well as reduced GSK3 β activity. GSK3 β is also inhibited by AF267B, a small molecule previously known as an M1 muscarinic Acetylcholine (ACh) receptor agonist. AF267B is thus capable of Wnt signalling activation via GSK3 β (50). In APP transgenic mice, this property was shown to result in reduced hippocampal A β /tau pathological burden and improved cognitive performance in spatial tasks (51). These findings also raise the possibility of cross-talk between Wnt function and cholinergic transmission. Consistently, nicotinic receptor activation also appears to stimulate canonical Wnt signalling activity, as shown by Inestrosa *et al.* (52). Nicotine administration in cultured hippocampal neurons prevented suppression of the pathway induced by A β and enhanced expression of the α 7 nicotinic ACh receptor gene, which the authors identified as a novel Wnt target. Another study also reported that enhancement of ACh activity, through acetylcholinesterase inhibition, results in Wnt signalling activation and reduced amyloidogenic activity in an APP transgenic mouse model (53).

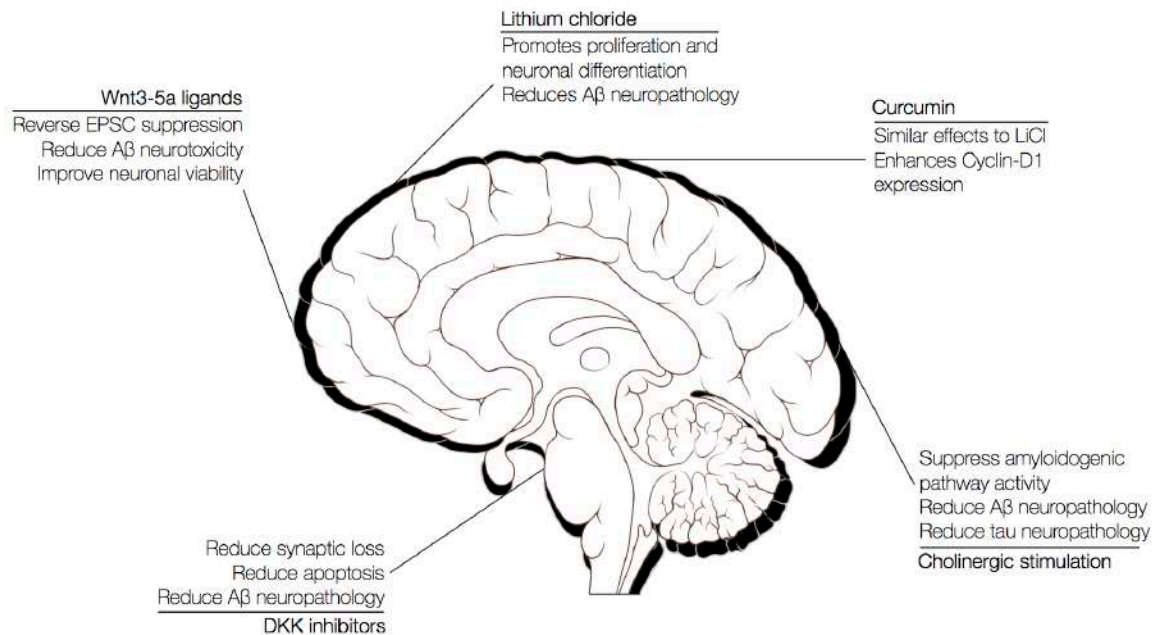


Fig. D.3 - Overview of Wnt-based therapeutic approaches in AD. Current evidence indicate Wnt stimulation as a promising strategy in the treatment of AD and other neurodegenerative diseases.

Another appealing target is the DKK family of Wnt inhibitors. As introduced, DKKs are secreted glycoproteins which bind to LRP5/6 and Kremen receptors, preventing Wnt ligand binding (54). Multiple DKK members have been linked to AD. DKK3 is important in hippocampal development and neurogenesis, and is elevated in plasma and CSF of AD patients (9, 55). Similarly, *DKK1* expression is enhanced by A β treatment in primary rat hippocampal neurons, and is increased in AD brains as reported by Caricasole *et al.* (56). The authors also showed that DKK1 knockdown in cultured neurons treated with A β enhances GSK3 β inhibition and reduces apoptosis, thus suggesting Wnt-mediated neuroprotective effects. DKKs may be targeted pharmacologically with antagonist to LRP5/6 binding. Given that DKKs and Wnt ligands interact with two distinct binding sequences on LRP5/6, such an approach would likely not affect Wnt ligand binding, which is desirable (57). To this end, Iozzi *et al.* developed NCI8642, a small molecule DKK1 inhibitor (58). The compound was shown to compete with DKK1 for LRP6 binding, thus reducing its Wnt antagonistic effects. Alternatively, neutralising antibodies targeted against DKK1 have also shown promise. Purro *et al.* employed anti-DKK1 in mouse brain slices treated with A β , demonstrating a substantial reduction in synaptic loss (59). These data overall illustrate that Wnt-based therapeutic development for AD is already well underway, and offers promising results, potentially translatable to DS.

5.2.2.2 Targeting DYRK1A in DS

According to the data generated here, the flip side of a Wnt-based therapeutic approach in DS is targeting of aberrant DYRK1A activity. And indeed, employment of DYRK1A inhibitors to target cognitive deficits in DS is a rapidly developing field with promising results (11, 60-64). As outlined in methods (3.5.2) and results (4.3.2), three DYRK1A inhibitors were employed in this thesis, EGCG, INDY and Harmine (60, 65, 66). All three are reasonably well described, and preliminary evidence on their potential therapeutic application has been generated.

The green tea polyphenol EGCG is an appealing candidate, primarily due to its ability to cross the placenta and blood-brain barrier (BBB), both very useful in the context of DS (67). A variety of approaches has explored the potential therapeutic effects of EGCG-mediated DYRK1A inhibition. In *Dyrk1a* transgenic (Tg) mouse models, several lines of evidence suggest long-term EGCG treatment might be beneficial. Young and adult TgDyrk1a mice fed green tea extracts or EGCG display improvements in hippocampal neurogenesis, prefrontal cortical LTP, neurotransmission and cognitive deficits (68-70). Additionally, developmental brain defects in TgDyrk1a mice may be corrected by chronic EGCG administration via a green tea polyphenol diet starting at gestation (65). Similar effects have been reported in the Ts65Dn mouse model of DS. Long-term EGCG treatment in this model reportedly rescues defects in hippocampal LTP and learning/memory behavioural tasks (71, 72). However, contradicting reports also showed no improvement in cognitive performance, including memory tasks, of Ts65Dn mice treated with purified EGCG up to a dose of 100mg/kg/day (73). On the other hand, Valenti *et al.* showed a beneficial effect of EGCG treatment on mitochondrial function in Ts65Dn hippocampal

neural progenitor cells (74). A recent study by Stagni *et al.* investigated acute and long-term effects of EGCG treatment (75). Postnatal Ts65Dn mice (day 3-15) were administered daily intravenous EGCG treatment at 25 mg/kg. Beneficial effects were observed at treatment cessation, with improved hippocampal/cortical cell number, connectivity, and neurogenesis. However, such improvements were lost in adulthood, with persistent cognitive impairment and cellular defects observed in EGCG-treated Ts65Dn mice at 42 days. Interestingly, the authors also reported enhanced total GSK3 β levels in the Ts65Dn hippocampus, an effect rescued by EGCG treatment. This result is consistent with the enhancement of total GSK3 β levels induced by *DYRK1A* overexpression observed in this thesis (4.3.2), and supports the finding of EGCG-mediated effects on canonical Wnt signalling activity.

A number of preliminary investigations has also considered EGCG-based therapies in human DS. Two consecutive studies by De la Torre *et al.* showed that long term (3-12 months) EGCG treatment in young DS adults improves cognitive performance and visual memory, whilst also enhancing the efficacy of cognitive training (72, 76). However, these effects were lost 3 months post treatment cessation, suggesting the potential requirement of life-long *DYRK1A* inhibition therapy in DS. EGCG treatment also rescued mitochondrial function and stimulated mitochondrial biogenesis in human DS-derived fibroblast and lymphoblast cell cultures (77). These trials, whilst promising, still suffer from design limitations due to the low number of participants and heterogeneous composition of the treatment administered, which included several green tea compounds other than EGCG.

In a similar fashion, the plant-derived *DYRK1A* inhibitor harmine has reportedly produced biologically relevant effects. In cellular models, harmine is able to reduce phosphorylation of multiple *DYRK1A* substrates including tau (78, 79) and rescue premature neuronal progenitor differentiation (80). INDY is relatively less characterised, despite its high *DYRK1A* specificity. However, Ogawa *et al.* showed that INDY treatment may correct abnormal morphogenesis in *DYRK1A* transgenic *Xenopus* embryos (66).

It should be stressed that a potential *DYRK1A* inhibition therapy in DS is not without significant risk of unwanted side effects. Excessive suppression of *DYRK1A* activity is known to result in severe developmental abnormalities, given that heterozygous loss-of-function mutations are deleterious in mice and humans (81-83). Future effort should thus be aimed at devising target-specific approaches focusing *DYRK1A* inhibition to relevant tissues and developmental stages. These data nevertheless demonstrate that *DYRK1A* inhibition is a promising approach for treatment of cognitive deficits and brain developmental abnormalities in DS, although this remains to be heavily investigated. Taken together, these lines of evidence suggest that modulation of *DYRK1A* activity in DS preliminarily appears beneficial, though continuing treatment might be necessary for sustained effects.

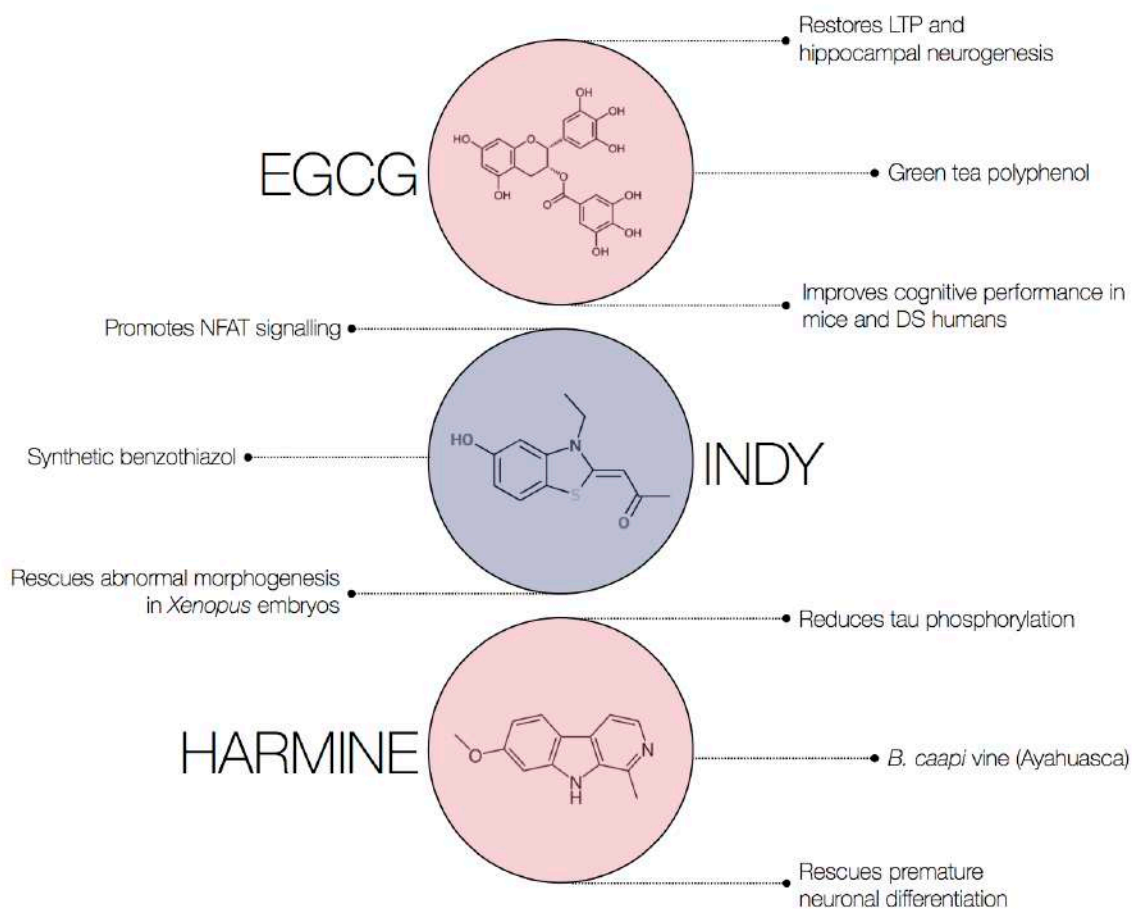


Fig. D.4 - Summary of therapeutically beneficial effects of DYRK1A inhibition reported so far in the literature. EGCG is the sole inhibitor to have been employed in pilot clinical trials by De la Torre *et al.*, with promising results.

5.2.2.3 A Wnt-DYRK1A therapy for DS neurodevelopment and AD-DS?

Mounting evidence convincingly suggests that multiple types of Wnt stimulation therapy might provide substantial benefit to AD patients. Concomitantly, standalone DYRK1A inhibition therapy also shows encouraging results in DS. It is important to appreciate that Wnt stimulation in AD should be directly translatable to DS, since AD neuropathology in this condition is essentially similar to sporadic disease, save for the much earlier age of onset and accelerated pathogenesis. This notion implies a further point for discussion, in light of the results of this thesis. That is, the more aggressive nature of AD-DS compared to sporadic AD might be, at least partly, underpinned by enhanced Wnt modulation due to Hsa21 trisomy. Surely *APP* triplication is in itself sufficient to enhance A β deposition (8), and this idea is not disputed here. However, if genes such as *APP* (84) and *DYRK1A* (4.3.2) are indeed capable of reducing basal Wnt signalling, Hsa21 trisomy in DS might significantly enhance AD development through Wnt modulation. Specifically, A β /tau pathology and overexpressed *DYRK1A* would synergistically suppress basal Wnt signalling in a vicious cycle, to a greater extent than in sporadic AD. The opposite of this phenomenon could however be exploited therapeutically in AD-DS, and may actually be

advantageous. As discussed, basal Wnt signalling activity is predicted to be downregulated further by DYRK1A overexpression. If, however, Wnt signalling were to be activated by means of any of the methods outlined above, the evidence presented in this thesis would suggest a potential further enhancement of their Wnt stimulatory effects in DS, due to *DYRK1A overexpression* (4.3.2-3). This poses the fundamental question of *how* DYRK1A should be targeted. Intuitively, it would seem obvious that DYRK1A *inhibition* is the necessary approach, given its excessive activity in DS. However, taking into account the bimodal Wnt regulatory effects of DYRK1A, one could argue that its overexpression in the adult DS hippocampus, in the presence of pharmacological Wnt stimulation, might be *beneficial*. Chronic administration of Wnt ligands or GSK3 β inhibitors might induce cytoplasmic redistribution of DYRK1A (4.3.2) and further enhance β -catenin activity. This nevertheless remains to be determined, as a precondition to further exploring the feasibility of a DYRK1A-Wnt therapy in DS.

Prospective study design - An initial approach to answer this question would be to design a study investigating the effects of \pm Wnt stimulation \pm DYRK1A inhibition on validated markers of AD and DS pathology, employing primary hippocampal cultures, human cell lines and animal models. The four treatment combinations should be tested with or without the presence of AD and/or DS pathology, induced either via pharmacological treatment or via an animal model. Markers should include A β /tau aggregation and species ratio, synaptic degeneration (Neurogranin, YKL-40), neurogenesis (BrdU), apoptosis (Annexin V, DNA fragmentation), neuronal number (NeuN), LTP (EPSCs), inflammation, behaviour (Learning and memory, spatial tasks) or any other identified in the literature as reliable. In parallel, Wnt signalling activity and expression of target genes should be monitored for each condition via a combination of genetic/bioinformatic, biochemical and imaging studies. This approach would provide basic evidence on **1**) Whether Wnt modulation at all has any beneficial effect in AD-DS and **2**) If DYRK1A inhibition provides any additional improvement on AD-DS pathology. Current evidence is strongly predictive of observing positive effects of Wnt signalling stimulation alone in the proposed model systems. Regarding **2**), the luciferase data generated here (4.3.2) suggests that DYRK1A inhibition would *reduce* the extent of activation produced by Wnt treatments, whilst overexpression should produce the opposite effects. According to the evidence available in AD, which associates Wnt activity with neuroprotection, such a result would be predictive of improved beneficial effects *without* DYRK1A inhibition. This seems counterintuitive, given that DYRK1A is overactive in DS. Its default overexpression may however be advantageous to improve the potency of Wnt stimulating treatments in AD-DS. This is an intriguing possibility, but it must be determined experimentally. It is equally feasible that DYRK1A inhibition might, at least initially, be more beneficial, or that either condition has no measurable effect on Wnt-mediated amelioration of AD markers. If proven beneficial, DYRK1A modulation therapy as an adjuvant to Wnt stimulation might also be advantageous in sporadic AD, given the involvement of DYRK1A in this condition (85, 86). It may be further speculated that whilst DYRK1A enhancement is unlikely to be beneficial in DS, given its default high activity, exploiting DYRK1A to further stimulate active Wnt signalling might prove useful in AD. This possibility also merits further inquiry.

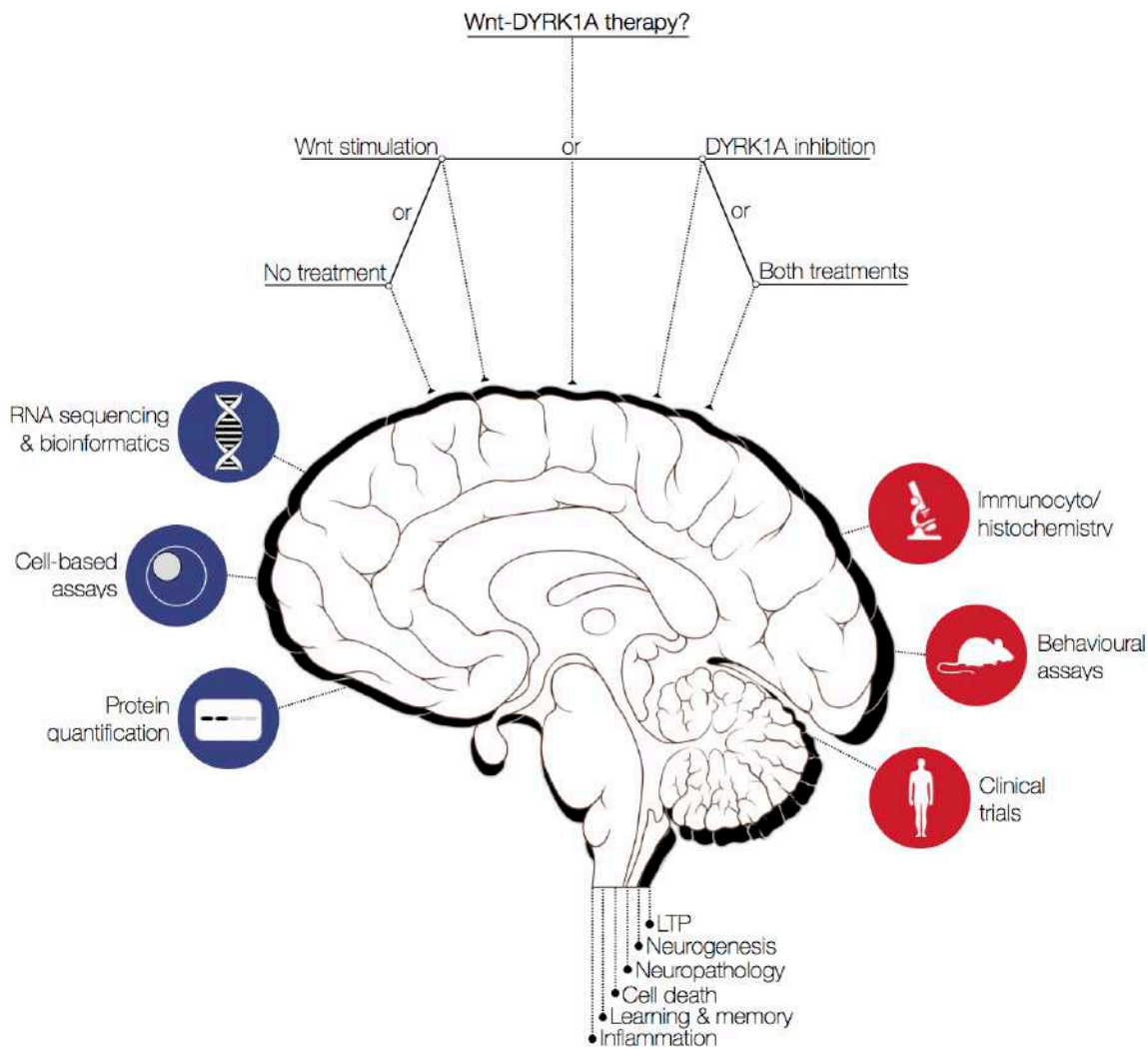


Fig. D.5 - Visual summary of a proposed study design for immediate follow up of the data generated here. Different combinations of Wnt stimulation and DYRK1A inhibition methods should be tested for efficacy against multiple AD and DS markers whilst monitoring Wnt signalling activity in parallel.

Ultimately, it should be kept into consideration that brain pathology in DS is complex and multifaceted, and likely to require combinatorial drug therapy. Multiple approaches aside from DYRK1A inhibition are being investigated at present, and have been excellently reviewed by Dierssen (87). Additional therapeutic strategies include normalisation of gene dosage, neurotransmitter replacement to stimulate both excitatory and inhibitory networks as well as targeting of cellular pathways controlling neurogenesis and plasticity. The latter approach may well include Wnt signalling modulation, given the involvement of this pathway in both mechanisms.

5.2.2.4 Beyond neurodegeneration and the DS brain

The other important CNS aspect of DS which could be tackled therapeutically is neurodevelopment. This is a crucial time point for the onset of learning disability and cognitive deficits, and restoration of homeostatic DYRK1A-Wnt function could prove beneficial. The observed enhancement of active Wnt signalling by DYRK1A implies that, during brain development, the high basal levels of Wnt activity might be deleteriously enhanced by *DYRK1A* overexpression. Aberrant over activation of Wnt signalling has indeed been shown to negatively impact neurogenesis and forebrain development in multiple instances (88-90). Thus, provided that the exact direction of Wnt dysfunction in DS neurodevelopment is established by future studies, a potential therapy might seek to *suppress* Wnt signalling activity, with or without concomitant normalisation of DYRK1A. To this end, the field of cancer therapy provides several attractive possibilities. As discussed, excessive β -catenin activity is now recognised as a key pathogenic event in several cancers (91, 92). For this reason, a high number of pharmaceutical agents which inhibit Wnt signalling on multiple levels already exists (93-95). These include synthetic small molecule β -catenin blockers, neutralising antibodies targeted against several Wnt components, and modulatory peptides mimicking the binding properties of Wnt ligands. Reviewers have argued, however, that Wnt inhibition therapy alone might not be sufficient to arrest cancer progression, but may nevertheless be beneficial in combination with other therapeutic approaches (93). These compounds might thus be prospectively employed in DS tissues displaying excessive Wnt signalling.

The complex landscape of Wnt function in AD, DS and AD-DS, and knowledge on potential therapeutic strategies imply that other features of DS might respond to a Wnt-DYRK1A normalising treatment. The most prominent examples are CHD and leukaemia, both highly prevalent in DS. As discussed, these secondary pathologies possess known links with Wnt signalling function, and might thus be ameliorated through Wnt modulation. Prenatal and perinatal Wnt stimulation in the developing DS heart may prevent development of CHD. Likewise, administration of Wnt antagonists in infancy may reduce the progression of haematological malignancies. These possibilities, however, cannot be investigated before the tissue specificity and directionality of Wnt changes in DS is established *in vivo*.

5.2.2.5 Overall considerations

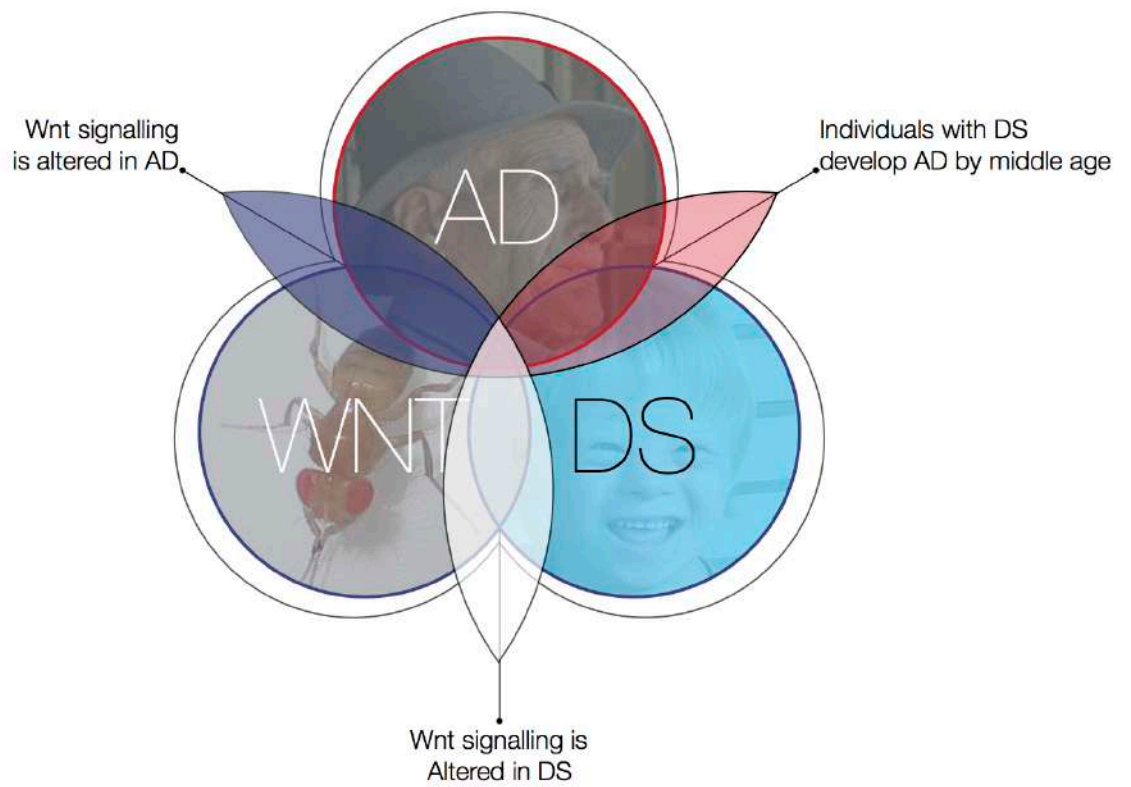
In summary, there is a long way ahead in the development of effective strategies for the treatment of DS and associated pathologies. Whilst available evidence is promising, a number of essential conditions must be satisfied for such strategies to prove successful. Perhaps the most important is devising a way to effectively target abnormal Wnt signalling in a tissue and direction-specific manner. Attempts at therapy design might otherwise prove ineffective or harmful. In the long term, therapeutic development will have to address more complex challenges inherent to drug design such as effective delivery to the brain, tissue selectivity, side effects and feasibility of prenatal treatment. These notions lie beyond the scope of this thesis, however, and are best addressed once more evidence has been generated.

6 Conclusions and future work: an avenue for the treatment of DS

DS remains the most common human aneuploidy and genetic cause of AD. For nearly 60 years since the discovery of trisomy of chromosome 21 as its primary cause, the cellular and molecular mechanisms underlying this condition have remained largely unclear. Despite improvements in life expectancy and quality of life for individuals affected, no pharmacological therapy is available to ameliorate the many features of DS. Additionally, the nearly universal occurrence of AD-DS poses an ever greater challenge to the ageing DS population. The studies discussed in this thesis have provided initial evidence of a functional Wnt-DS-AD relationship. There is preliminary indication that aberrant Wnt signalling may contribute to DS, primarily to abnormal neurodevelopment and AD-DS. Furthermore, such contribution is, at least partly, mediated by DYRK1A modulation of Wnt signalling. Both notions may be employed to develop therapies at a later date, though much evidence is yet to be gathered prior to achieving this. A set of pressing experimental questions should include:

- I. Does DYRK1A directly phosphorylate any Wnt signalling components? If so, how does this affect the Wnt substrate(s)?
- II. What is the molecular mechanism of DYRK1A-mediated Wnt modulation? How might it be interfered with pharmacologically? What are effects of DYRK1A overexpression on Wnt targets?
- III. Does DYRK1A phase transition with DVL1? If so, does this result in functional segregation of DYRK1A from cytoplasmic substrates? Does DYRK1A stimulate DVL1 activation, as observed, through this mechanism?
- IV. How do other Hsa21-encoded Wnt regulators mechanistically contribute to dysfunction of the pathway in DS? (E.g.: *APP*, *TIAM1*). Does A β suppress cerebral Wnt signalling similarly to AD?
- V. Is Wnt signalling affected in other brain areas? Do Wnt signalling alterations change with age?
- VI. Are there any Wnt abnormalities in other DS tissue types? E.g.: myocardium and heart conduction system, haematopoietic stem cells, pancreatic β -cells.
- VII. Which tissue types would benefit most from Wnt stimulation or suppression? E.g: hippocampus-stimulate, stem cells-suppress.
- VIII. What are the combined effects off Wnt \pm DYRK1A modulation on markers of AD in DS? E.g.: prospective study.

In the long term, the continuing study and potential clinical translation of this thesis' findings might open avenues for treatment strategies in DS, aimed at normalising Wnt signalling function throughout life. It is hoped that future research efforts will expand on this model, in order to control this condition therapeutically and improve the quality of life for those affected by it.



BIBLIOGRAPHY

7

7 Bibliography

Due to the high number of sources employed, citation numbers are reset between chapters, in order to avoid impractically long brackets for in-text referencing. Lists contains numbering according to each chapter. Some sources are employed in multiple chapters.

7.1 Chapter 1 - General Introduction

1. Lejeune, J.T.R.G.M., R. Turpin, and M. Gautier, Le mongolisme, premier exemple d'aberration autosomique humaine. *Ann Genet*, 1959. **1**: p. 1-49.
2. Patterson, D., Molecular genetic analysis of Down syndrome. *Human genetics*, 2009. **126**: p. 195-214.
3. Malamud, N., Neuropathology of organic brain: syndromes associated with aging. In *Aging and the Brain*, 1972. **Third edit**: p. 63-87.
4. Wisniewski, K.E., H.M. Wisniewski, and G.Y. Wen, Occurrence of neuropathological changes and dementia of Alzheimer's disease in Down's syndrome. *Ann Neurol*, 1985. **17**: p. 278-282.
5. Choong, X.Y., J.L. Tosh, L.J. Pulford, and E. Fisher, Dissecting Alzheimer disease in Down syndrome using mouse models. *Front Behav Neurosci*, 2015. **9**.
6. Hickey, F., E. Hickey, and K.L. Summar, Medical update for children with Down syndrome for the pediatrician and family practitioner. *Advances in pediatrics*, 2012. **59**: p. 137-157.
7. Antonarakis, S.E., R. Lyle, E.T. Dermitzakis, A. Raymond, and S. Deutsch, Chromosome 21 and down syndrome: from genomics to pathophysiology. *Nature Reviews Genetics*, 2004. **5**: p. 725-738.
8. Maslen, C.L., Molecular genetics of atrioventricular septal defects. *Current opinion in cardiology*, 2004. **19**: p. 205-210.
9. Malt, E.A., R.C. Dahl, T.M. Haugsand, I.H. Ulvestad, N.M. Emilsen, B. Hansen, and E.M. Davidsen, Health and disease in adults with Down syndrome. *Tidsskrift for den Norske laegeforening: tidsskrift for praktisk medicin, ny raekke*, 2013. **133**: p. 290-294.
10. Gamis, A.S. and F.O. Smith, Transient myeloproliferative disorder in children with Down syndrome: clarity to this enigmatic disorder. *British journal of haematology*, 2012. **159**: p. 277-287.
11. Penrose, L.S., The incidence of mongolism in the general population. *The British Journal of Psychiatry*, 1949. **95**: p. 685-688.
12. Rahmani, Z., J.L. Blouin, N. Creau-Goldberg, P.C. Watkins, J.F. Mattei, M. Poissonnier, and A. Aurias, Critical role of the D21S55 region on chromosome 21 in the pathogenesis of Down syndrome, in *Proceedings of the National Academy of Sciences*. 1989, 86(15). p. 5958-5962.
13. Korenberg, J.R., H. Kawashima, S.M. Pulst, T. Ikeuchi, N. Ogasawara, K. Yamamoto, and C.J. Epstein, Molecular definition of a region of chromosome 21 that causes features of the Down syndrome phenotype. *American journal of human genetics*, 1990. **47**: p. 236.
14. Hattori, M., A. Fujiyama, T.D. Taylor, H. Watanabe, T. Yada, H.S. Park, A. Toyoda, K. Ishii, Y. Totoki, D.K. Choi, Y. Groner, E. Soeda, M. Ohki, T. Takagi, Y. Sakaki, S. Taudien, K. Blechschmidt, A. Polley, U. Menzel, J. Delabar, K. Kumpf, R. Lehmann, D. Patterson, K. Reichwald, A. Rump, M.

Bibliography

- Schillhabel, A. Schudy, W. Zimmermann, A. Rosenthal, J. Kudoh, K. Schibuya, K. Kawasaki, S. Asakawa, A. Shintani, T. Sasaki, K. Nagamine, S. Mitsuyama, S.E. Antonarakis, S. Minoshima, N. Shimizu, G. Nordsiek, K. Hornischer, P. Brant, M. Scharfe, O. Schon, A. Desario, J. Reichelt, G. Kauer, H. Blocker, J. Ramser, A. Beck, S. Klages, S. Hennig, L. Riesselmann, E. Dagand, T. Haaf, S. Wehrmeyer, K. Borzym, K. Gardiner, D. Nizetic, F. Francis, H. Lehrach, R. Reinhardt, M.L. Yaspo, and C.M. Sequencing, The DNA sequence of human chromosome 21 (vol 405, pg 311, 2000). *Nature*, 2000. **407**(6800): p. 110-110.
- 15.**Chakrabarti, L., T.K. Best, N.P. Cramer, R.S. Carney, J.T. Isaac, Z. Galdzicki, and T.F. Haydar, Olig1 and Olig2 triplication causes developmental brain defects in Down syndrome. *Nature neuroscience*, 2010. **13**: p. 927-934.
- 16.**Olson, L.E., J.T. Richtsmeier, J. Leszl, and R.H. Reeves, A chromosome 21 critical region does not cause specific Down syndrome phenotypes. *Science*, 2004. **306**: p. 687-690.
- 17.**Kuhn, D.E., G.J. Nuovo, A.V. Terry, M.M. Martin, G.E. Malana, S.E. Sansom, and T.S. Elton, Chromosome 21-derived microRNAs provide an etiological basis for aberrant protein expression in human Down syndrome brains. *Journal of Biological Chemistry*, 2010. **285**: p. 1529-1543.
- 18.**Graeber, M.B., S. Kösel, R. Egensperger, R.B. Banati, U. Müller, K. Bise, P. Hoff, H.J. Möller, K. Fujisawa, and P. Mehraein, Rediscovery of the case described by Alois Alzheimer in 1911: historical, histological and molecular genetic analysis. *Neurogenetics*, 1997. **1**.
- 19.**Birks, J. and R.J. Harvey, Donepezil for dementia due to Alzheimer's disease. *Cochrane Database Syst Rev*, 2006(1): p. CD001190.
- 20.**Morris, J.C., Mild cognitive impairment is early-stage Alzheimer disease: time to revise diagnostic criteria. *Archives of Neurology*, 2006. **63**: p. 15-16.
- 21.**Sperling, R.A., P.S. Aisen, L.A. Beckett, D.A. Bennett, S. Craft, A.M. Fagan, and C.H. Phelps, Toward defining the preclinical stages of Alzheimer's disease: Recommendations from the National Institute on Aging-Alzheimer's Association workgroups on diagnostic guidelines for Alzheimer's disease. *Alzheimer's & Dementia*, 2011. **7**: p. 280-292.
- 22.**Abramov, E., I. Dolev, H. Fogel, G.D. Ciccotosto, E. Ruff, and I. Slutsky, Amyloid- β as a positive endogenous regulator of release probability at hippocampal synapses. *Nature neuroscience*, 2009. **12**: p. 1567-1576.
- 23.**Alonso, A.D.C., I. Grundke-Iqbal, and K. Iqbal, Alzheimer's disease hyperphosphorylated tau sequesters normal tau into tangles of filaments and disassembles microtubules. *Nature medicine*, 1996. **2**: p. 783-787.
- 24.**Taniguchi, K., L.R. Roberts, I.N. Aderca, X. Dong, C. Qian, L.M. Murphy, D.M. Nagorney, L.J. Burgart, P.C. Roche, D.I. Smith, J.A. Ross, and W. Liu, Mutational spectrum of β -catenin, AXIN1, and AXIN2 in hepatocellular carcinomas and hepatoblastomas. *Oncogene*, 2002. **21**: p. 4863-4871.
- 25.**Selkoe, D.J., Resolving controversies on the path to Alzheimer's therapeutics. *Nature medicine*, 2011. **17**: p. 1060-1065.
- 26.**Kamenetz, F., T. Tomita, H. Hsieh, G. Seabrook, D. Borchelt, T. Iwatsubo, and R. Malinow, APP processing and synaptic function. *Neuron*, 2003. **37**: p. 925-937.
- 27.**Palop, J.J., J. Chin, E.D. Roberson, J. Wang, M.T. Thwin, N. Bien-Ly, and L. Mucke, Aberrant excitatory neuronal activity and compensatory remodeling of inhibitory hippocampal circuits in mouse models of Alzheimer's disease. *Neuron*, 2007. **55**: p. 697-711.

- 28.** Shankar, G.M., B.L. Bloodgood, M. Townsend, D.M. Walsh, D.J. Selkoe, and B.L. Sabatini, Natural oligomers of the Alzheimer amyloid- β protein induce reversible synapse loss by modulating an NMDA-type glutamate receptor-dependent signaling pathway. *The Journal of neuroscience*, 2007. **27**: p. 2866-2875.
- 29.** Wang, Q., D.M. Walsh, M.J. Rowan, D.J. Selkoe, and R. Anwyl, Block of long-term potentiation by naturally secreted and synthetic amyloid β -peptide in hippocampal slices is mediated via activation of the kinases c-Jun N-terminal kinase, cyclin-dependent kinase 5, and p38 mitogen-activated protein kinase as well as m. *The Journal of neuroscience*, 2004. **24**: p. 3370-3378.
- 30.** Shankar, G.M., S. Li, T.H. Mehta, A. Garcia-Munoz, N.E. Shepardson, I. Smith, and D.J. Selkoe, Amyloid- β protein dimers isolated directly from Alzheimer's brains impair synaptic plasticity and memory. *Nature medicine*, 2008. **14**: p. 837-842.
- 31.** Walsh, D.M., M. Townsend, M.B. Podlisny, G.M. Shankar, J.V. Fadeeva, and E. Agnaf, O., & Selkoe, D. J. Certain inhibitors of synthetic amyloid β -peptide (A β) fibrillogenesis block oligomerization of natural A β and thereby rescue long-term potentiation. *The Journal of neuroscience*, 2005. **25**: p. 2455-2462.
- 32.** Kimura, T., D.J. Whitcomb, J. Jo, P. Regan, T. Piers, S. Heo, and K. Cho, Microtubule-associated protein tau is essential for long-term depression in the hippocampus. *Philosophical Transactions of the Royal Society B: Biological Sciences*, 2014. **369**: p. 20130144.
- 33.** Walsh, D.M. and D.J. Selkoe, A β oligomers: a decade of discovery. *Journal of neurochemistry*, 2007. **101**: p. 1172-1184.
- 34.** Ferreira, S.T. and W.L. Klein, The A β oligomer hypothesis for synapse failure and memory loss in Alzheimer's disease. *Neurobiology of learning and memory*, 2011. **96**: p. 529-543.
- 35.** Larson, M.E. and S.E. Lesné, Soluble A β oligomer production and toxicity. *Journal of neurochemistry*, 2012. **120**: p. 125-139.
- 36.** Fraser, J. and A. Mitchell, Kalmuc idiocy: Report of a case with autopsy. 1876.
- 37.** Struwe, F., Histopathologische Untersuchungen über entstehung und wesen der senilen Plaques. *Zeitschrift für die gesamte Neurologie und Psychiatrie*, 1929. **122**(1): p. 291-307.
- 38.** Jervis, G.A., Early senile dementia in mongoloid idiocy. *Am J Psychiatry*, 1948. **105**(2): p. 102-6.
- 39.** Schweber, M.S., Alzheimer's disease and Down syndrome. *Progress in clinical and biological research*, 1988. **317**: p. 247-267.
- 40.** Leverenz, J.B. and M.A. Raskind, Early amyloid deposition in the medial temporal lobe of young Down syndrome patients: a regional quantitative analysis. *Exp neurol*, 1998. **150**: p. 296-304.
- 41.** Lemere, C.A., J.K. Blusztajn, H. Yamaguchi, T. Wisniewski, T.C. Saido, and D.J. Selkoe, Sequence of deposition of heterogeneous amyloid β -peptides and APO E in Down syndrome: implications for initial events in amyloid plaque formation. *Neurobiology of disease*, 1996. **3**: p. 16-32.
- 42.** Teipel, S.J. and H. Hampel, Neuroanatomy of Down syndrome in vivo: a model of preclinical Alzheimer's disease. *Behavior Genetics*, 2006. **36**: p. 405-415.
- 43.** Lemere, C., Alzheimer's disease and Down syndrome. *Alzheimer's & Dementia: The Journal of the Alzheimer's Association*, 2013. **9**: p. 4.

Bibliography

- 44.**Rovelet-Lecrux, A., D. Hannequin, G. Raux, L. Meur, L. N., and C.D. A. Vital A., APP locus duplication causes autosomal dominant early-onset Alzheimer disease with cerebral amyloid angiopathy. *Nature genetics*, 2005. **38**: p. 24-26.
- 45.**Tejedor, F., X.R. Zhu, E. Kaltenbach, A. Ackermann, A. Baumann, I. Canal, M. Heisenberg, K.F. Fischbach, and O. Pongs, minibrain: a new protein kinase family involved in postembryonic neurogenesis in *Drosophila*. *Neuron*, 1995. **14**(2): p. 287-301.
- 46.**Park, J., W.J. Song, and K.C. Chung, Function and regulation of Dyrk1A: towards understanding Down syndrome. *Cell Mol Life Sci*, 2009. **66**: p. 3235-3240.
- 47.**Davisson, M.T., C. Schmidt, and E.C. Akeson, Segmental trisomy of murine chromosome 16: a new model system for studying Down syndrome. *Prog Clin Biol Res*, 1990. **360**: p. 263-80.
- 48.**Reinholdt, L.G., Y. Ding, G.T. Gilbert, A. Czechanski, J.P. Solzak, R.J. Roper, M.T. Johnson, L.R. Donahue, C. Lutz, and D. Mt., Molecular characterization of the translocation breakpoints in the Down syndrome mouse model Ts65Dn. *Mamm Genome*, 2011. **22**: p. 685-691.
- 49.**O'Doherty, A., S. Ruf, C. Mulligan, V. Hildreth, M.L. Errington, S. Cooke, and E.M. Fisher, An aneuploid mouse strain carrying human chromosome 21 with Down syndrome phenotypes. *Science*, 2005. **309**: p. 2033-2037.
- 50.**Devlin, L. and P.J. Morrison, Mosaic Down's syndrome prevalence in a complete population study. *Archives of disease in childhood*, 2004. **89**: p. 1177.
- 51.**Gribble, S.M., F.K. Wiseman, S. Clayton, E. Prigmore, E. Langley, F. Yang, S. Maguire, B. Fu, D. Rajan, O. Sheppard, C. Scott, H. Hauser, P.J. Stephens, L.A. Stebbings, B.L. Ng, T. Fitzgerald, M.A. Quail, R. Banerjee, K. Rothkamm, V.L. Tybulewicz, E.M. Fisher, and N.P. Carter, Massively parallel sequencing reveals the complex structure of an irradiated human chromosome on a mouse background in the Tc1 model of Down syndrome. *PLoS One*, 2013. **8**(4): p. e60482.
- 52.**Sheppard, O., F. Plattner, A. Rubin, A. Slender, J.M. Linehan, S. Brandner, V.L.J. Tybulewicz, E.M.C. Fisher, and F.K. Wiseman, Altered regulation of tau phosphorylation in a mouse model of down syndrome aging. *Neurobiol Aging*, 2012. **33**(4).
- 53.**Raz, N., I.J. Torres, S.D. Briggs, W.D. Spencer, A.E. Thornton, W.J. Loken, and J.D. Acker, Selective neuroanatomic abnormalities in Down's syndrome and their cognitive correlates Evidence from MRI morphometry. *Neurology*, 1995. **45**: p. 356-366.
- 54.**Aylward, E.H., R. Habbak, A.C. Warren, M.B. Pulsifer, P.E. Barta, M. Jerram, and G.D. Pearlson, Cerebellar volume in adults with Down syndrome. *Archives of neurology*, 1997. **54**: p. 209-212.
- 55.**Dunlevy, L., M. Bennett, A. Slender, E. Lana-Elola, V.L. Tybulewicz, E.M. Fisher, and T. Mohun, Down's syndrome-like cardiac developmental defects in embryos of the transchromosomal Tc1 mouse. *Cardiovascular research, cvq*, 2010. **193**.
- 56.**Alford, K.A., A. Slender, L. Vanes, Z. Li, E.M. Fisher, D. Nizetic, and V.L. Tybulewicz, Perturbed hematopoiesis in the Tc1 mouse model of Down syndrome. *Blood*, 2010. **115**: p. 2928-2937.
- 57.**Galante, M., H. Jani, L. Vanes, H. Daniel, E.M.C. Fisher, V.L.J. Tybulewicz, T.V.P. Bliss, and E. Morice, Impairments in motor coordination without major changes in cerebellar plasticity in the Tc1 mouse model of Down syndrome. *Human Molecular Genetics*, 2009. **18**(8): p. 1449-1463.

Bibliography

- 58.** Yu, T., Z. Li, Z. Jia, S.J. Clapcote, C. Liu, S. Li, and Y.E. Yu, A mouse model of Down syndrome trisomic for all human chromosome 21 syntenic regions. *Hum mol gen*, 2010. **179**.
- 59.** Lana-Elola, E., S. Watson-Scales, A. Slender, D. Gibbins, A. Martineau, C. Douglas, T. Mohun, E.M.C. Fisher, and V.L.J. Tybulewicz, Genetic dissection of Down syndrome-associated congenital heart defects using a new mouse mapping panel. *Elife*, 2016. **5**.
- 60.** Yu, T., C.H. Liu, P. Belichenko, S.J. Clapcote, S.M. Li, A.N. Pao, A. Kleschevnikov, A.R. Bechard, S. Asrar, R.Q. Chen, N. Fan, Z.Y. Zhou, Z.P. Jia, C. Chen, J.C. Roder, B. Liu, A. Baldini, W.C. Mobley, and Y.E. Yu, Effects of individual segmental trisomies of human chromosome 21 syntenic regions on hippocampal long-term potentiation and cognitive behaviors in mice. *Brain Research*, 2010. **1366**: p. 162-171.
- 61.** Nyberg, D.A., R.G. Resta, D.A. Luthy, D.E. Hickok, B.S. Mahony, and J.H. Hirsch, Prenatal sonographic findings of Down syndrome: review of 94 cases. *Obstetrics & Gynecology*, 1990. **76**: p. 370-377.
- 62.** Nusse, R. and H. Varmus, Three decades of Wnts: a personal perspective on how a scientific field developed. *The EMBO journal*, 2012. **31**: p. 2670-2684.
- 63.** Ashton-Rickardt, P.G., M.G. Dunlop, Y. Nakamura, R.G. Morris, C.A. Purdie, C.M. Steel, H.J. Evans, C.C. Bird, and A.H. Wylie, High frequency of APC loss in sporadic colorectal carcinoma due to breaks clustered in 5q21.22. *Oncogene*, 1989. **1169**.
- 64.** Groden, J., A. Thliveris, W. Samowitz, M. Carlson, L. Gelbert, H. Albertsen, and R. White, Identification and characterization of the familial adenomatous polyposis coli gene. *Cell*, 1991. **66**: p. 589-600.
- 65.** Zeng, L., F. Fagotto, T. Zhang, W. Hsu, T.J. Vasicek, P. Iij, W. L., and F. Costantini, The Mouse Fused Locus Encodes Axin, an Inhibitor of the Wnt Signaling Pathway That Regulates Embryonic Axis Formation. *Cell*, 1997. **90**: p. 181-192.
- 66.** Sakanaka, C., P. Leong, L. Xu, and L. Harrison S. D. Williams, Casein kinase 1 ϵ in the Wnt pathway: Regulation of β -catenin function. *Proceedings of the National Academy of Sciences of the United States of America*, 1999. **96**: p. 12548-12552.
- 67.** Amit, S., A. Hatzubai, Y. Birman, J.S. Andersen, E. Ben-Shushan, M. Mann, and I. Alkalay, Axin-mediated CKI phosphorylation of β -catenin at Ser 45: a molecular switch for the Wnt pathway. *Genes & development*, 2002. **16**: p. 1066-1076.
- 68.** Aberle, H., A. Bauer, J. Stappert, A. Kispert, and R. Kemler, β -catenin is a target for the ubiquitin-proteasome pathway. *EMBO Journal*, 1997. **16**: p. 3797-3804.
- 69.** Behrens, J., B.A. Jerchow, M. Würtele, J. Grimm, C. Asbrand, R. Wirtz, and W. Birchmeier, Functional interaction of an axin homolog, conductin, with β -catenin, APC, and GSK3 β . *Science*, 1998. **280**: p. 596-599.
- 70.** Hart M. J., d.I.S.R.A.I.N.R.B.P.P., Downregulation of β -catenin by human Axin and its association with the APC tumor suppressor, β -catenin and GSK3 β . *Current Biology*, 1998. **8**: p. 573-581.
- 71.** Beals, C.R., C.M. Sheridan, C.W. Turck, P. Gardner, and G.R. Crabtree, Nuclear export of NF-ATc enhanced by glycogen synthase kinase-3. *Science*, 1997. **275**(5308): p. 1930-4.
- 72.** Woods, Y.L., P. Cohen, W. Becker, R. Jakes, M. Goedert, X. Wang, and C.G. Proud, The kinase DYRK phosphorylates protein-synthesis initiation factor eIF2Bepsilon at Ser539 and the

Bibliography

microtubule-associated protein tau at Thr212: potential role for DYRK as a glycogen synthase kinase 3-priming kinase. *Biochem. J.*, 2001. **355**: p. 609-615.

73. Woods, Y.L., G. Rena, N. Morrice, A. Barthel, W. Becker, S. Guo, T.G. Unterman, and P. Cohen, The kinase DYRK1A phosphorylates the transcription factor FKHR at Ser329 in vitro, a novel in vivo phosphorylation site. *Biochem J.*, 2001. **355**: p. 597.

74. Reya, T. and H. Clevers, Wnt signalling in stem cells and cancer. *Nature*, 2005. **434**(7035): p. 843-50.

75. Krylova, O., J. Herreros, K.E. Cleverley, E. Ehler, J.P. Henriquez, S.M. Hughes, and P.C. Salinas, WNT-3, expressed by motoneurons, regulates terminal arborization of neurotrophin-3-responsive spinal sensory neurons. *Neuron*, 2002. **35**(6): p. 1043-56.

76. Ciani, L., K.A. Boyle, E. Dickins, M. Sahores, D. Anane, D.M. Lopes, and P.C. Salinas, Wnt7a signaling promotes dendritic spine growth and synaptic strength through Ca²⁺/Calmodulin-dependent protein kinase II, in *Proceedings of the National Academy of Sciences*. 2011, **108**(26). p. 10732-10737.

77. Wang, Z., W. Shu, M.M. Lu, and E.E. Morrisey, Wnt7b activates canonical signaling in epithelial and vascular smooth muscle cells through interactions with Fzd1, Fzd10, and LRP5. *Molecular and cellular biology*, 2005. **25**(12): p. 5022-5030.

78. Bilić, J., Y.L. Huang, G. Davidson, T. Zimmermann, C.M. Cruciat, M. Bienz, and C. Niehrs, Wnt induces LRP6 signalosomes and promotes dishevelled-dependent LRP6 phosphorylation. *Science*, 2007. **316**: p. 1619-1622.

79. Schwarz-Romond, T., C. Metcalfe, and M. Bienz, Dynamic recruitment of axin by Dishevelled protein assemblies. *Journal of cell science*, 2007. **120**: p. 2402-2412.

80. Niehrs, C., Function and biological roles of the Dickkopf family of Wnt modulators. *Oncogene*, 2006. **25**: p. 7469-7481.

81. Killick, R., E.M. Ribe, R. Al-Shawi, B. Malik, C. Hooper, C. Fernandes, and S. Lovestone, Clusterin regulates β -amyloid toxicity via Dickkopf-1-driven induction of the Wnt/PCP/JNK pathway. *Molecular psychiatry*, 2012. **19**: p. 88-98.

82. Berge, T., K. D., B. D., K. T., M. W., and N.R. A. Eroglu E., Embryonic stem cells require Wnt proteins to prevent differentiation to epiblast stem cells. *Nature cell biology*, 2011. **13**: p. 1070-1075.

83. Wray, J., T. Kalkan, S. Gomez-Lopez, D. Eckardt, A. Cook, R. Kemler, and A. Smith, Inhibition of glycogen synthase kinase-3 alleviates Tcf3 repression of the pluripotency network and increases embryonic stem cell resistance to differentiation. *Nature cell biology*, 2011. **13**: p. 838-845.

84. Davidson, K.C., A.M. Adams, J.M. Goodson, C.E. McDonald, J.C. Potter, J.D. Berndt, and R.T. Moon, Wnt/ β -catenin signaling promotes differentiation, not self-renewal, of human embryonic stem cells and is repressed by Oct4, in *Proceedings of the National Academy of Sciences*. 2012, **109**(12). p. 4485-4490.

85. Lyashenko, N., M. Winter, D. Migliorini, T. Biechele, R.T. Moon, and C. Hartmann, Differential requirement for the dual functions of [beta]-catenin in embryonic stem cell self-renewal and germ layer formation. *Nature cell biology*, 2011. **13**: p. 753-761.

86. Holland, J.D., A. Klaus, A.N. Garratt, and W. Birchmeier, Wnt signaling in stem and cancer stem cells. *Current opinion in cell biology*, 2013. **25**: p. 254-264.

- 87.**Perry, J.M., X.C. He, R. Sugimura, J.C. Grindley, J.S. Haug, S. Ding, and L. Li, Cooperation between both Wnt/ β -catenin and PTEN/PI3K/Akt signaling promotes primitive hematopoietic stem cell self-renewal and expansion. *Genes & development*, 2011. **25**: p. 1928-1942.
- 88.**van Es, J.H., T. Sato, M. van de Wetering, A. Lyubimova, A.N.Y. Nee, A. Gregorieff, and H. Clevers, Dll1+ secretory progenitor cells revert to stem cells upon crypt damage. *Nature cell biology*, 2012. **14**: p. 1099-1104.
- 89.**Mou, H., R. Zhao, R. Sherwood, T. Ahfeldt, A. Lapey, J. Wain, and J. Rajagopal, Generation of multipotent lung and airway progenitors from mouse ESCs and patient-specific cystic fibrosis iPSCs. *Cell stem cell*, 2012. **10**: p. 385-397.
- 90.**Lian, X., C. Hsiao, G. Wilson, K. Zhu, L.B. Hazeltine, S.M. Azarin, and S.P. Palecek, Robust cardiomyocyte differentiation from human pluripotent stem cells via temporal modulation of canonical Wnt signaling, in *Proceedings of the National Academy of Sciences*. 2012, 109(27): E1848-E1857.
- 91.**Wend, P., J.D. Holland, U. Ziebold, and W. Birchmeier, Wnt signaling in stem and cancer stem cells *Semin Cell Dev Biol*, 21 (2010). pp. **855**.
- 92.**Shackleton, M., F. Vaillant, K.J. Simpson, J. Stingl, G.K. Smyth, M.L. Asselin-Labat, and J.E. Visvader, Generation of a functional mammary gland from a single stem cell. *Nature*, 2006. **439**: p. 84-88.
- 93.**Malanchi, I., A. Santamaria-Martínez, E. Susanto, H. Peng, H.A. Lehr, J.F. Delaloye, and J. Huelsken, Interactions between cancer stem cells and their niche govern metastatic colonization. *Nature*, 2012. **481**: p. 85-89.
- 94.**Waalder, J., O. Machon, L. Tumova, H. Dinh, V. Korinek, S.R. Wilson, and S. Krauss, A novel tankyrase inhibitor decreases canonical Wnt signaling in colon carcinoma cells and reduces tumor growth in conditional APC mutant mice. *Cancer research*, 2012. **72**: p. 2822-2832.
- 95.**Thomas, K.R. and M.R. Capecchi, Targeted disruption of the murine int-1 proto-oncogene resulting in severe abnormalities in midbrain and cerebellar development. *Nature*, 1990. **346**: p. 30.
- 96.**Ikeya, M., S.M. Lee, J.E. Johnson, A.P. McMahon, and S. Takada, Wnt signalling required for expansion of neural crest and CNS progenitors. *Nature*, 1997. **389**(6654): p. 966-70.
- 97.**Haegel, H., L. Larue, M. Ohsugi, L. Fedorov, K. Herrenknecht, and R. Kemler, Lack of beta-catenin affects mouse development at gastrulation. *Development*, 1995. **121**: p. 3529-3537.
- 98.**Huelsken, J., R. Vogel, V. Brinkmann, B. Erdmann, C. Birchmeier, and W. Birchmeier, Requirement for β -catenin in anterior-posterior axis formation in mice. *The Journal of cell biology*, 2000. **148**: p. 567-578.
- 99.**Kittappa, R., W.W. Chang, R.B. Awatramani, and R.D. McKay, The *foxa2* gene controls the birth and spontaneous degeneration of dopamine neurons in old age. *PLoS biology*, 2007. **5**: p. 12.
- 100.**Joksimovic, M., B.A. Yun, R. Kittappa, A.M. Anderregg, W.W. Chang, M.M. Taketo, and R.B. Awatramani, Wnt antagonism of Shh facilitates midbrain floor plate neurogenesis. *Nature neuroscience*, 2009. **12**: p. 125-131.
- 101.**Tang, M., Y. Miyamoto, and E.J. Huang, Multiple roles of beta-catenin in controlling the neurogenic niche for midbrain dopamine neurons. *Development*, 2009. **136**: p. 2027.

Bibliography

- 102.**Tang, M., J.C. Villaescusa, S.X. Luo, C. Guitarte, S. Lei, Y. Miyamoto, and E.J. Huang, Interactions of Wnt/ β -catenin signaling and sonic hedgehog regulate the neurogenesis of ventral midbrain dopamine neurons. *The Journal of Neuroscience*, 2010. **30**: p. 9280-9291.
- 103.**Joksimovic, M., M. Patel, M.M. Taketo, R. Johnson, and R. Awatramani, Ectopic Wnt/Beta-Catenin Signaling Induces Neurogenesis in the Spinal Cord and Hindbrain Floor Plate. *PloS one*, 2012. **7**: p. 1.
- 104.**Ribeiro, D., K. Ellwanger, D. Glagow, S. Theofilopoulos, N.S. Corsini, A. Martin-Villalba, and E. Arenas, Dkk1 regulates ventral midbrain dopaminergic differentiation and morphogenesis. *PLoS one*, 2011. **6**: p. 2.
- 105.**Purro, S.A., S. Galli, and P.C. Salinas, Dysfunction of Wnt signaling and synaptic disassembly in neurodegenerative diseases. *Journal of molecular cell biology*, mjt0, 2014. **49**.
- 106.**Hall, A.C., F.R. Lucas, and P.C. Salinas, Axonal remodeling and synaptic differentiation in the cerebellum is regulated by WNT-7a signaling. *Cell*, 2000. **100**: p. 525-535.
- 107.**Ahmad-Annuar, A., L. Ciani, I. Simeonidis, J. Herreros, N.B. Fredj, S.B. Rosso, and P.C. Salinas, Signaling across the synapse: a role for Wnt and Dishevelled in presynaptic assembly and neurotransmitter release. *The Journal of cell biology*, 2006. **174**: p. 127-139.
- 108.**Varela-Nallar, L., C.P. Grabowski, I.E. Alfaro, A.R. Alvarez, and N.C. Inestrosa, Role of the Wnt receptor Frizzled-1 in presynaptic differentiation and function. *Neural Dev*, 2009. **4**: p. 41.
- 109.**Sahores, M., A. Gibb, and P.C. Salinas, Frizzled-5, a receptor for the synaptic organizer Wnt7a, regulates activity-mediated synaptogenesis. *Development*, 2010. **137**: p. 2215-2225.
- 110.**Cerpa, W., J.A. Godoy, I. Alfaro, G.G. Farías, M.J. Metcalfe, R. Fuentealba, and N.C. Inestrosa, Wnt-7a modulates the synaptic vesicle cycle and synaptic transmission in hippocampal neurons. *Journal of Biological Chemistry*, 2008. **283**: p. 5918-5927.
- 111.**Cuitino, L., J.A. Godoy, G.G. Farías, A. Couve, C. Bonansco, M. Fuenzalida, and N.C. Inestrosa, Wnt-5a modulates recycling of functional GABAA receptors on hippocampal neurons. *The Journal of Neuroscience*, 2010. **30**: p. 8411-8420.
- 112.**Gogolla, N., I. Galimberti, Y. Deguchi, and P. Caroni, Wnt signaling mediates experience-related regulation of synapse numbers and mossy fiber connectivities in the adult hippocampus. *Neuron*, 2009. **62**: p. 510-525.
- 113.**Seib, D.R., N.S. Corsini, K. Ellwanger, C. Plaas, A. Mateos, C. Pitzer, and A. Martin-Villalba, Loss of Dickkopf-1 restores neurogenesis in old age and counteracts cognitive decline. *Cell Stem Cell*, 2013. **12**: p. 204-214.
- 114.**Purro, S.A., E.M. Dickins, and P.C. Salinas, The secreted Wnt antagonist Dickkopf-1 is required for amyloid β -mediated synaptic loss. *J Neurosci*, 2012. **32**: p. 3492-3498.
- 115.**De Ferrari, G.V., A. Papassotiropoulos, T. Biechele, F.W. De-Vrieze, M.E. Avila, M.B. Major, A. Myers, K. Sáez, J.P. Henríquez, and A. Zhao, Common genetic variation within the low-density lipoprotein receptor-related protein 6 and late-onset Alzheimer's disease. *Proceedings of the National Academy of Sciences*, 2007. **104**(22): p. 9434-9439.
- 116.**Caricasole, A., A. Copani, F. Caraci, E. Aronica, A.J. Rozemuller, A. Caruso, and F. Nicoletti, Induction of Dickkopf-1, a negative modulator of the Wnt pathway, is associated with neuronal degeneration in Alzheimer's brain. *J Neurosci*, 2004. **24**: p. 6021-6027.

Bibliography

- 117.**Zenzmaier, C., J. Marksteiner, A. Kiefer, P. Berger, and C. Humpel, Dkk3 is elevated in CSF and plasma of Alzheimer's disease patients. *J Neurochem*, 2009. **110**: p. 653-661.
- 118.**Zhang, Z., H. Hartmann, V.M. Do, D. Abramowski, C. Sturchler-Pierrat, M. Staufenbiel, and B.A. Yankner, Destabilization of β -catenin by mutations in presenilin-1 potentiates neuronal apoptosis. *Nature*, 1998. **395**: p. 698-702.
- 119.**Kang, D.E., S. Soriano, M.P. Frosch, T. Collins, S. Naruse, S.S. Sisodia, and E.H. Koo, Presenilin 1 facilitates the constitutive turnover of β -catenin: differential activity of Alzheimer's disease-linked PS1 mutants in the β -catenin signaling pathway. *The Journal of neuroscience*, 1999. **19**: p. 4229-4237.
- 120.**Takashima, A., M. Murayama, O. Murayama, T. Kohno, T. Honda, K. Yasutake, and B. Wolozin, Presenilin 1 associates with glycogen synthase kinase-3 β and its substrate tau, in *Proceedings of the National Academy of Sciences*. 1998, 95(16). p. 9637-9641.
- 121.**Lucas, J.J., F. Hernández, P. Gómez Ramos, M.A. Morán, R. Hen, and J. Avila, Decreased nuclear β -catenin, tau hyperphosphorylation and neurodegeneration in GSK3 β conditional transgenic mice. *The EMBO Journal*, 2001. **20**: p. 27-39.
- 122.**Noble, W., V. Olm, K. Takata, E. Casey, O. Mary, J. Meyerson, and K. Duff, Cdk5 is a key factor in tau aggregation and tangle formation in vivo. *Neuron*, 2003. **38**: p. 555-565.
- 123.**Rosso, S.B., D. Sussman, A. Wynshaw-Boris, and P.C. Salinas, Wnt signaling through Dishevelled, Rac and JNK regulates dendritic development. *Nature neuroscience*, 2005. **8**(1): p. 34-42.
- 124.**Alvarez, A.R., J.A. Godoy, K. Mullendorff, G.H. Olivares, M. Bronfman, and N.C. Inestrosa, Wnt-3a overcomes β -amyloid toxicity in rat hippocampal neurons. *Experimental cell research*, 2004. **297**: p. 186-196.
- 125.**Toledo, E.M. and N.C. Inestrosa, Wnt signaling activation reduces neuropathological markers in a mouse model of Alzheimer's disease. *Mol Psychiatry*, 2010. **15**: p. 228.
- 126.**Magdesian, M.H., M.M. Carvalho, F.A. Mendes, L.M. Saraiva, M.A. Juliano, L. Juliano, and S.T. Ferreira, Amyloid- β binds to the extracellular cysteine-rich domain of Frizzled and inhibits Wnt/ β -catenin signaling. *Journal of Biological Chemistry*, 2008. **283**: p. 9359-9368.
- 127.**Zhou, F., K. Gong, B. Song, T. Ma, T. van Laar, Y. Gong, and L. Zhang, The APP intracellular domain (AICD) inhibits Wnt signalling and promotes neurite outgrowth. *Biochim Biophys Acta*, 2012. **1823**: p. 1233-1241.
- 128.**Schepeler, T., F. Mansilla, L.L. Christensen, T.F. Orntoft, and C.L. Andersen, Clusterin expression can be modulated by changes in TCF1-mediated Wnt signaling. *J Mol Signal*, 2007. **2**: p. 6.
- 129.**Cisternas, P. and N.C. Inestrosa, Brain glucose metabolism: Role of Wnt signaling in the metabolic impairment in Alzheimer's disease. *Neurosci Biobehav Rev*, 2017. **80**: p. 316-328.
- 130.**Machhi, J., A. Sinha, P. Patel, A.M. Kanhed, P. Upadhyay, A. Tripathi, Z.S. Parikh, R. Chruvattil, P.P. Pillai, S. Gupta, K. Patel, R. Giridhar, and M.R. Yadav, Neuroprotective Potential of Novel Multi-Targeted Isoalloxazine Derivatives in Rodent Models of Alzheimer's Disease Through Activation of Canonical Wnt/beta-Catenin Signalling Pathway. *Neurotox Res*, 2016. **29**(4): p. 495-513.

Bibliography

- 131.**Jin, N., H. Zhu, X. Liang, W. Huang, Q. Xie, P. Xiao, J. Ni, and Q. Liu, Sodium selenate activated Wnt/beta-catenin signaling and repressed amyloid-beta formation in a triple transgenic mouse model of Alzheimer's disease. *Exp Neurol*, 2017. **297**: p. 36-49.
- 132.**Malliri, A., T.P. Rygiel, R.A. van der Kammen, J.Y. Song, R. Engers, A.F. Hurlstone, and J.G. Collard, The rac activator Tiam1 is a Wnt-responsive gene that modifies intestinal tumor development. *J Biol Chem*, 2006. **281**: p. 543-548.
- 133.**Hong, J.Y., J.I. Park, M. Lee, W.A. Muñoz, R.K. Miller, H. Ji, and P.D. McCrea, Down's-syndrome-related kinase Dyrk1A modulates the p120-catenin/Kaiso trajectory of the Wnt signaling pathway. *J cell sci*, 2012. **125**: p. 561-569.
- 134.**Ozsolak, F. and P.M. Milos, RNA sequencing: advances, challenges and opportunities. *Nat Rev Genet*, 2011. **12**(2): p. 87-98.
- 135.**Antonarakis, S.E., Down syndrome and the complexity of genome dosage imbalance. *Nat Rev Genet*, 2017. **18**(3): p. 147-163.
- 136.**Chrast, R., H.S. Scott, M.P. Pappasavvas, C. Rossier, E.S. Antonarakis, C. Barras, M.T. Davisson, C. Schmidt, X. Estivill, M. Dierssen, M. Pritchard, and S.E. Antonarakis, The mouse brain transcriptome by SAGE: differences in gene expression between P30 brains of the partial trisomy 16 mouse model of Down syndrome (Ts65Dn) and normals. *Genome Res*, 2000. **10**(12): p. 2006-21.
- 137.**Saran, N.G., M.T. Pletcher, J.E. Natale, Y. Cheng, and R.H. Reeves, Global disruption of the cerebellar transcriptome in a Down syndrome mouse model. *Hum Mol Genet*, 2003. **12**(16): p. 2013-9.
- 138.**Lyle, R., C. Gehrig, C. Neergaard-Henrichsen, S. Deutsch, and S.E. Antonarakis, Gene expression from the aneuploid chromosome in a trisomy mouse model of down syndrome. *Genome research*, 2004. **14**: p. 1268-1274.
- 139.**Kahlem, P., M. Sultan, R. Herwig, M. Steinfath, D. Balzereit, B. Eppens, N.G. Saran, M.T. Pletcher, S.T. South, G. Stetten, H. Lehrach, R.H. Reeves, and M.L. Yaspo, Transcript level alterations reflect gene dosage effects across multiple tissues in a mouse model of down syndrome. *Genome Res*, 2004. **14**(7): p. 1258-67.
- 140.**Ling, K.H., C.A. Hewitt, K.L. Tan, P.S. Cheah, S. Vidyadaran, M.I. Lai, H.C. Lee, K. Simpson, L. Hyde, M.A. Pritchard, G.K. Smyth, T. Thomas, and H.S. Scott, Functional transcriptome analysis of the postnatal brain of the Ts1Cje mouse model for Down syndrome reveals global disruption of interferon-related molecular networks. *BMC Genomics*, 2014. **15**: p. 624.
- 141.**Guedj, F., J.L. Pennings, H.C. Wick, and D.W. Bianchi, Analysis of adult cerebral cortex and hippocampus transcriptomes reveals unique molecular changes in the Ts1Cje mouse model of down syndrome. *Brain Pathol*, 2015. **25**(1): p. 11-23.
- 142.**Guedj, F., J.L. Pennings, M.A. Ferres, L.C. Graham, H.C. Wick, K.A. Miczek, D.K. Slonim, and D.W. Bianchi, The fetal brain transcriptome and neonatal behavioral phenotype in the Ts1Cje mouse model of Down syndrome. *Am J Med Genet A*, 2015. **167A**(9): p. 1993-2008.
- 143.**Walus, M., E. Kida, A. Rabe, G. Albertini, and A.A. Golabek, Widespread cerebellar transcriptome changes in Ts65Dn Down syndrome mouse model after lifelong running. *Behav Brain Res*, 2016. **296**: p. 35-46.
- 144.**Letourneau, A., F.A. Santoni, X. Bonilla, M.R. Sailani, D. Gonzalez, J. Kind, C. Chevalier, R. Thurman, R.S. Sandstrom, Y. Hibaoui, M. Garieri, K. Popadin, E. Falconnet, M. Gagnebin, C.

Bibliography

- Gehrig, A. Vannier, M. Guipponi, L. Farinelli, D. Robyr, E. Migliavacca, C. Borel, S. Deutsch, A. Feki, J.A. Stamatoyannopoulos, Y. Herault, B. van Steensel, R. Guigo, and S.E. Antonarakis, Domains of genome-wide gene expression dysregulation in Down's syndrome. *Nature*, 2014. **508**(7496): p. 345-+.
- 145.** FitzPatrick, D.R., J. Ramsay, N.I. McGill, M. Shade, A.D. Carothers, and N.D. Hastie, Transcriptome analysis of human autosomal trisomy. *Hum Mol Genet*, 2002. **11**(26): p. 3249-56.
- 146.** Mao, R., X. Wang, E.L. Spitznagel, Jr., L.P. Frelin, J.C. Ting, H. Ding, J.W. Kim, I. Ruczinski, T.J. Downey, and J. Pevsner, Primary and secondary transcriptional effects in the developing human Down syndrome brain and heart. *Genome Biol*, 2005. **6**(13): p. R107.
- 147.** Ait Yahya-Graison, E., J. Aubert, L. Dauphinot, I. Rivals, M. Prieur, G. Golfier, J. Rossier, L. Personnaz, N. Creau, H. Blehaut, S. Robin, J.M. Delabar, and M.C. Potier, Classification of human chromosome 21 gene-expression variations in Down syndrome: impact on disease phenotypes. *Am J Hum Genet*, 2007. **81**(3): p. 475-91.
- 148.** Esposito, G., J. Imitola, J. Lu, D. De Filippis, C. Scuderi, V.S. Ganesh, R. Folkerth, J. Hecht, S. Shin, T. Iuvone, J. Chesnut, L. Steardo, and V. Sheen, Genomic and functional profiling of human Down syndrome neural progenitors implicates S100B and aquaporin 4 in cell injury. *Hum Mol Genet*, 2008. **17**(3): p. 440-57.
- 149.** Prandini, P., S. Deutsch, R. Lyle, M. Gagnebin, C. Delucinge Vivier, M. Delorenzi, C. Gehrig, P. Descombes, S. Sherman, F. Dagna Bricarelli, C. Baldo, A. Novelli, B. Dallapiccola, and S.E. Antonarakis, Natural gene-expression variation in Down syndrome modulates the outcome of gene-dosage imbalance. *Am J Hum Genet*, 2007. **81**(2): p. 252-63.
- 150.** Lyle, R., F. Bena, S. Gagos, C. Gehrig, G. Lopez, A. Schinzel, J. Lespinasse, A. Bottani, S. Dahoun, L. Taine, M. Doco-Fenzy, P. Cornillet-Lefebvre, A. Pelet, S. Lyonnet, A. Toutain, L. Colleaux, J. Horst, I. Kennerknecht, N. Wakamatsu, M. Descartes, J.C. Franklin, L. Florentin-Arar, S. Kitsiou, E. Ait Yahya-Graison, M. Costantine, P.M. Sinet, J.M. Delabar, and S.E. Antonarakis, Genotype-phenotype correlations in Down syndrome identified by array CGH in 30 cases of partial trisomy and partial monosomy chromosome 21. *Eur J Hum Genet*, 2009. **17**(4): p. 454-66.
- 151.** Costa, V., C. Angelini, L. D'Apice, M. Mutarelli, A. Casamassimi, L. Sommese, M.A. Gallo, M. Aprile, R. Esposito, L. Leone, A. Donizetti, S. Crispi, M. Rienzo, B. Sarubbi, R. Calabro, M. Picardi, P. Salvatore, T. Infante, P. De Berardinis, C. Napoli, and A. Ciccocicola, Massive-scale RNA-Seq analysis of non ribosomal transcriptome in human trisomy 21. *PLoS One*, 2011. **6**(4): p. e18493.
- 152.** Sullivan, K.D., H.C. Lewis, A.A. Hill, A. Pandey, L.P. Jackson, J.M. Cabral, K.P. Smith, L.A. Liggett, E.B. Gomez, M.D. Galbraith, J. DeGregori, and J.M. Espinosa, Trisomy 21 consistently activates the interferon response. *Elife*, 2016. **5**.
- 153.** Noda, T., H. Nagano, I. Takemasa, S. Yoshioka, M. Murakami, H. Wada, S. Kobayashi, S. Marubashi, Y. Takeda, K. Dono, K. Umeshita, N. Matsuura, K. Matsubara, Y. Doki, M. Mori, and M. Monden, Activation of Wnt/beta-catenin signalling pathway induces chemoresistance to interferon-alpha/5-fluorouracil combination therapy for hepatocellular carcinoma. *Br J Cancer*, 2009. **100**(10): p. 1647-58.
- 154.** Nava, P., S. Koch, M.G. Laukoetter, W.Y. Lee, K. Kolegraff, C.T. Capaldo, N. Beeman, C. Addis, K. Gerner-Smidt, and I. Neumaier, Interferon- γ regulates intestinal epithelial homeostasis through converging β -catenin signaling pathways. *Immunity*, 2010. **32**(3): p. 392-402.
- 155.** Olmos-Serrano, J.L., H.J. Kang, W.A. Tyler, J.C. Silbereis, F. Cheng, Y. Zhu, M. Pletikos, L. Jankovic-Rapan, N.P. Cramer, Z. Galdzicki, J. Goodliffe, A. Peters, C. Sethares, I. Delalle, J.A.

Bibliography

Golden, T.F. Haydar, and N. Sestan, Down Syndrome Developmental Brain Transcriptome Reveals Defective Oligodendrocyte Differentiation and Myelination. *Neuron*, 2016. **89**(6): p. 1208-22.

156.Epstein, C.J., K.B. Avraham, M. Lovett, S. Smith, O. Elroy-Stein, G. Rotman, C. Bry, and Y. Groner, Transgenic mice with increased Cu/Zn-superoxide dismutase activity: animal model of dosage effects in Down syndrome. *Proc Natl Acad Sci U S A*, 1987. **84**(22): p. 8044-8.

157.Kadota, M., R. Nishigaki, C.C. Wang, T. Toda, Y. Shirayoshi, T. Inoue, T. Gojobori, K. Ikeo, M.S. Rogers, and M. Oshimura, Proteomic signatures and aberrations of mouse embryonic stem cells containing a single human chromosome 21 in neuronal differentiation: an in vitro model of Down syndrome. *Neuroscience*, 2004. **129**(2): p. 325-35.

158.Shukkur, E.A., A. Shimohata, T. Akagi, W. Yu, M. Yamaguchi, M. Murayama, D. Chui, T. Takeuchi, K. Amano, K.H. Subramhanya, T. Hashikawa, H. Sago, C.J. Epstein, A. Takashima, and K. Yamakawa, Mitochondrial dysfunction and tau hyperphosphorylation in Ts1Cje, a mouse model for Down syndrome. *Hum Mol Genet*, 2006. **15**(18): p. 2752-62.

159.Liu, F., Z. Liang, J. Wegiel, Y.W. Hwang, K. Iqbal, I. Grundke-Iqbal, N. Ramakrishna, and C.X. Gong, Overexpression of Dyrk1A contributes to neurofibrillary degeneration in Down syndrome. *FASEB J*, 2008. **22**(9): p. 3224-33.

160.Pollonini, G., V. Gao, A. Rabe, S. Palmiello, G. Albertini, and C.M. Alberini, Abnormal expression of synaptic proteins and neurotrophin-3 in the Down syndrome mouse model Ts65Dn. *Neuroscience*, 2008. **156**(1): p. 99-106.

161.Wang, Y., C. Mulligan, G. Denyer, F. Delom, F. Dagna-Bricarelli, V.L. Tybulewicz, E.M. Fisher, W.J. Griffiths, D. Nizetic, and J. Groet, Quantitative proteomics characterization of a mouse embryonic stem cell model of Down syndrome. *Mol Cell Proteomics*, 2009. **8**(4): p. 585-95.

162.Spoelgen, R., A. Hammes, U. Anzenberger, D. Zechner, O.M. Andersen, B. Jerchow, and T.E. Willnow, LRP2/megalin is required for patterning of the ventral telencephalon. *Development*, 2005. **132**(2): p. 405-14.

163.Ishihara, K., S. Kanai, H. Sago, K. Yamakawa, and S. Akiba, Comparative proteomic profiling reveals aberrant cell proliferation in the brain of embryonic Ts1Cje, a mouse model of Down syndrome. *Neuroscience*, 2014. **281**: p. 1-15.

164.Wu, D. and W. Pan, GSK3: a multifaceted kinase in Wnt signaling. *Trends Biochem Sci*, 2010. **35**(3): p. 161-8.

165.Griffin, W.S., L.C. Stanley, C. Ling, L. White, V. MacLeod, L.J. Perrot, C.L. White, 3rd, and C. Araoz, Brain interleukin 1 and S-100 immunoreactivity are elevated in Down syndrome and Alzheimer disease. *Proc Natl Acad Sci U S A*, 1989. **86**(19): p. 7611-5.

166.Oppermann, M., N. Cols, T. Nyman, J. Helin, J. Saarinen, I. Byman, N. Toran, A.A. Alaiya, T. Bergman, N. Kalkkinen, R. Gonzalez-Duarte, and H. Jornvall, Identification of foetal brain proteins by two-dimensional gel electrophoresis and mass spectrometry comparison of samples from individuals with or without chromosome 21 trisomy. *Eur J Biochem*, 2000. **267**(15): p. 4713-9.

167.Bajo, M., J. Fruehauf, S.H. Kim, M. Fountoulakis, and G. Lubec, Proteomic evaluation of intermediary metabolism enzyme proteins in fetal Down's syndrome cerebral cortex. *Proteomics*, 2002. **2**(11): p. 1539-46.

168.Shin, J.H., K. Krapfenbauer, and G. Lubec, Mass-spectrometrical analysis of proteins encoded on chromosome 21 in human fetal brain. *Amino Acids*, 2006. **31**(4): p. 435-47.

Bibliography

- 169.** Son, Y.O., L. Wang, P. Poyil, A. Budhraj, J.A. Hitron, Z. Zhang, J.C. Lee, and X. Shi, Cadmium induces carcinogenesis in BEAS-2B cells through ROS-dependent activation of PI3K/AKT/GSK-3 β /beta-catenin signaling. *Toxicol Appl Pharmacol*, 2012. **264**(2): p. 153-60.
- 170.** Sun, Y., M. Dierssen, N. Toran, D.D. Pollak, W.Q. Chen, and G. Lubec, A gel-based proteomic method reveals several protein pathway abnormalities in fetal Down syndrome brain. *J Proteomics*, 2011. **74**(4): p. 547-57.
- 171.** Yun, S., Y. Rim, and E.H. Jho, Induced expression of the transcription of tropomodulin 1 by Wnt5a and characterization of the tropomodulin 1 promoter. *Biochem Biophys Res Commun*, 2007. **363**(3): p. 727-32.
- 172.** Lee, H., S. Bae, and Y. Yoon, The anti-adipogenic effects of (-)epigallocatechin gallate are dependent on the WNT/beta-catenin pathway. *J Nutr Biochem*, 2013. **24**(7): p. 1232-40.
- 173.** Di Domenico, F., R. Coccia, A. Cocciolo, M.P. Murphy, G. Cenini, E. Head, D.A. Butterfield, A. Giorgi, M.E. Schinina, C. Mancuso, C. Cini, and M. Perluigi, Impairment of proteostasis network in Down syndrome prior to the development of Alzheimer's disease neuropathology: redox proteomics analysis of human brain. *Biochim Biophys Acta*, 2013. **1832**(8): p. 1249-59.
- 174.** Perluigi, M., F. Di Domenico, and D.A. Butterfield, Unraveling the complexity of neurodegeneration in brains of subjects with Down syndrome: insights from proteomics. *Proteomics Clin Appl*, 2014. **8**(1-2): p. 73-85.
- 175.** Swatton, J.E., L.A. Sellers, R.L. Faull, A. Holland, S. Iritani, and S. Bahn, Increased MAP kinase activity in Alzheimer's and Down syndrome but not in schizophrenia human brain. *Eur J Neurosci*, 2004. **19**(10): p. 2711-9.
- 176.** Dowjat, W.K., T. Adayev, I. Kuchna, K. Nowicki, S. Palmieriello, Y.W. Hwang, and J. Wegiel, Trisomy-driven overexpression of DYRK1A kinase in the brain of subjects with Down syndrome. *Neurosci Lett*, 2007. **413**(1): p. 77-81.
- 177.** Shin, J.H., R. Weitzdoerfer, M. Fountoulakis, and G. Lubec, Expression of cystathionine beta-synthase, pyridoxal kinase, and ES1 protein homolog (mitochondrial precursor) in fetal Down syndrome brain. *Neurochem Int*, 2004. **45**(1): p. 73-9.

7.2 Chapter 3 - Materials and Methods

1.Sancho, R.M., B.M. Law, and K. Harvey, Mutations in the LRRK2 Roc-COR tandem domain link Parkinson's disease to Wnt signalling pathways. *Hum Mol Genet*, 2009. **18**(20): p. 3955-68.

2.Veeman, M.T., D.C. Slusarski, A. Kaykas, S.H. Louie, and R.T. Moon, Zebrafish prickles, a modulator of noncanonical Wnt/Fz signaling, regulates gastrulation movements. *Curr Biol*, 2003. **13**(8): p. 680-5.

3.O'Doherty, A., S. Ruf, C. Mulligan, V. Hildreth, M.L. Errington, S. Cooke, and E.M. Fisher, An aneuploid mouse strain carrying human chromosome 21 with Down syndrome phenotypes. *Science*, 2005. **309**: p. 2033-2037.

4.Yu, T., Z. Li, Z. Jia, S.J. Clapcote, C. Liu, S. Li, and Y.E. Yu, A mouse model of Down syndrome trisomic for all human chromosome 21 syntenic regions. *Hum mol gen*, 2010. **179**.

5.Lana-Elola, E., S. Watson-Scales, A. Slender, D. Gibbins, A. Martineau, C. Douglas, T. Mohun, E.M.C. Fisher, and V.L.J. Tybulewicz, Genetic dissection of Down syndrome-associated congenital heart defects using a new mouse mapping panel. *Elife*, 2016. **5**.

6.Lucas, J.J., F. Hernández, P. Gómezâ Ramos, M.A. Morán, R. Hen, and J. Avila, Decreased nuclear β -catenin, tau hyperphosphorylation and neurodegeneration in GSK3 β conditional transgenic mice. *The EMBO Journal*, 2001. **20**: p. 27-39.

7.Nusse, R. and H. Varmus, Three decades of Wnts: a personal perspective on how a scientific field developed. *The EMBO journal*, 2012. **31**: p. 2670-2684.

7.3 Chapter 4.1 - Analysis of the DS transcriptome

1. O'Doherty, A., S. Ruf, C. Mulligan, V. Hildreth, M.L. Errington, S. Cooke, and E.M. Fisher, An aneuploid mouse strain carrying human chromosome 21 with Down syndrome phenotypes. *Science*, 2005. **309**: p. 2033-2037.
2. Lana-Elola, E., S. Watson-Scales, A. Slender, D. Gibbins, A. Martineau, C. Douglas, T. Mohun, E.M.C. Fisher, and V.L.J. Tybulewicz, Genetic dissection of Down syndrome-associated congenital heart defects using a new mouse mapping panel. *Elife*, 2016. **5**.
3. Esposito, G., J. Imitola, J. Lu, D. De Filippis, C. Scuderi, V.S. Ganesh, R. Folkerth, J. Hecht, S. Shin, T. Iuvone, J. Chesnut, L. Steardo, and V. Sheen, Genomic and functional profiling of human Down syndrome neural progenitors implicates S100B and aquaporin 4 in cell injury. *Hum Mol Genet*, 2008. **17**(3): p. 440-57.
4. Sullivan, K.D., H.C. Lewis, A.A. Hill, A. Pandey, L.P. Jackson, J.M. Cabral, K.P. Smith, L.A. Liggett, E.B. Gomez, M.D. Galbraith, J. DeGregori, and J.M. Espinosa, Trisomy 21 consistently activates the interferon response. *Elife*, 2016. **5**.
5. Kramer, A., J. Green, J. Pollard, Jr., and S. Tugendreich, Causal analysis approaches in Ingenuity Pathway Analysis. *Bioinformatics*, 2014. **30**(4): p. 523-30.
6. Ojalvo, L.S., C.A. Whittaker, J.S. Condeelis, and J.W. Pollard, Gene expression analysis of macrophages that facilitate tumor invasion supports a role for Wnt-signaling in mediating their activity in primary mammary tumors. *J Immunol*, 2010. **184**(2): p. 702-12.
7. Pena, E., G. Arderiu, and L. Badimon, Tissue factor induces human coronary artery smooth muscle cell motility through Wnt-signalling. *J Thromb Haemost*, 2013. **11**(10): p. 1880-91.
8. Gribble, S.M., F.K. Wiseman, S. Clayton, E. Prigmore, E. Langley, F. Yang, S. Maguire, B. Fu, D. Rajan, O. Sheppard, C. Scott, H. Hauser, P.J. Stephens, L.A. Stebbings, B.L. Ng, T. Fitzgerald, M.A. Quail, R. Banerjee, K. Rothkamm, V.L. Tybulewicz, E.M. Fisher, and N.P. Carter, Massively parallel sequencing reveals the complex structure of an irradiated human chromosome on a mouse background in the Tc1 model of Down syndrome. *PLoS One*, 2013. **8**(4): p. e60482.
9. Yue, W., Q. Sun, S. Dacic, R.J. Landreneau, J.M. Siegfried, J. Yu, and L. Zhang, Downregulation of Dkk3 activates beta-catenin/TCF-4 signaling in lung cancer. *Carcinogenesis*, 2008. **29**: p. 84-92.
10. Lee, E.-J., M. Jo, S.B. Rho, K. Park, Y.-N. Yoo, J. Park, M. Chae, W. Zhang, and J.-H. Lee, Dkk3, downregulated in cervical cancer, functions as a negative regulator of β -catenin. *Int J Cancer*, 2009. **124**: p. 287-297.
11. Diep, D.B., N. Hoen, M. Backman, O. Machon, and S. Krauss, Characterisation of the Wnt antagonists and their response to conditionally activated Wnt signalling in the developing mouse forebrain. *Dev Brain Res*, 2004. **153**(2): p. 261-270.
12. Katoh, M. and M. Katoh, WNT signaling pathway and stem cell signaling network. *Clin Cancer Res*, 2007. **13**(14): p. 4042-5.
13. Eger, A., A. Stockinger, B. Schaffhauser, H. Beug, and R. Foisner, Epithelial mesenchymal transition by c-Fos estrogen receptor activation involves nuclear translocation of beta-catenin and upregulation of beta-catenin/lymphoid enhancer binding factor-1 transcriptional activity. *J Cell Biol*, 2000. **148**(1): p. 173-88.

Bibliography

- 14.**Staal, F.J., F. Weerkamp, M.R. Baert, C.M. van den Burg, M. van Noort, E.F. de Haas, and J.J. van Dongen, Wnt target genes identified by DNA microarrays in immature CD34+ thymocytes regulate proliferation and cell adhesion. *J Immunol*, 2004. **172**(2): p. 1099-108.
- 15.**Park, J.I., S.W. Kim, J.P. Lyons, H. Ji, T.T. Nguyen, K. Cho, M.C. Barton, T. Deroo, K. Vleminckx, R.T. Moon, and P.D. McCrea, Kaiso/p120-catenin and TCF/beta-catenin complexes coordinately regulate canonical Wnt gene targets. *Dev Cell*, 2005. **8**(6): p. 843-54.
- 16.**Janssens, S., T. Denayer, T. Deroo, F. Van Roy, and K. Vleminckx, Direct control of Hoxd1 and Irx3 expression by Wnt/beta-catenin signaling during anteroposterior patterning of the neural axis in *Xenopus*. *Int J Dev Biol*, 2010. **54**(10): p. 1435-42.
- 17.**Ikeya, M., S.M. Lee, J.E. Johnson, A.P. McMahon, and S. Takada, Wnt signalling required for expansion of neural crest and CNS progenitors. *Nature*, 1997. **389**(6654): p. 966-70.
- 18.**Bebek, G., V. Patel, and M.R. Chance, PETALS: Proteomic Evaluation and Topological Analysis of a mutated Locus' Signaling. *BMC Bioinformatics*, 2010. **11**: p. 596.
- 19.**Mebarki, S., R. Desert, L. Sulpice, M. Sicard, M. Desille, F. Canal, H. Dubois-Pot Schneider, D. Bergeat, B. Turlin, P. Bellaud, E. Lavergne, R. Le Guevel, A. Corlu, C. Perret, C. Coulouarn, B. Clement, and O. Musso, De novo HAPLN1 expression hallmarks Wnt-induced stem cell and fibrogenic networks leading to aggressive human hepatocellular carcinomas. *Oncotarget*, 2016. **7**(26): p. 39026-39043.
- 20.**Witton, J., R. Padmashri, L.E. Zinyuk, V.I. Popov, I. Kraev, S.J. Line, T.P. Jensen, A. Tedoldi, D.M. Cummings, V.L.J. Tybulewicz, E.M.C. Fisher, D.M. Bannerman, A.D. Randall, J.T. Brown, F.A. Edwards, D.A. Rusakov, M.G. Stewart, and M.W. Jones, Hippocampal circuit dysfunction in the Tc1 mouse model of Down syndrome. *Nature Neuroscience*, 2015. **18**(9): p. 1291-+.
- 21.**Galante, M., H. Jani, L. Vanes, H. Daniel, E.M.C. Fisher, V.L.J. Tybulewicz, T.V.P. Bliss, and E. Morice, Impairments in motor coordination without major changes in cerebellar plasticity in the Tc1 mouse model of Down syndrome. *Human Molecular Genetics*, 2009. **18**(8): p. 1449-1463.
- 22.**Reya, T. and H. Clevers, Wnt signalling in stem cells and cancer. *Nature*, 2005. **434**(7035): p. 843-50.
- 23.**Oh, S., E. You, P. Ko, J. Jeong, S. Keum, and S. Rhee, Genetic disruption of tubulin acetyltransferase, α TAT1, inhibits proliferation and invasion of colon cancer cells through decreases in Wnt1/ β -catenin signaling. *Biochemical and Biophysical Research Communications*, 2017. **482**(1): p. 8-14.
- 24.**Pei, Z., X. Du, Y. Song, L. Fan, F. Li, Y. Gao, R. Wu, Y. Chen, W. Li, H. Zhou, Y. Yang, and J. Zeng, Down-regulation of lncRNA CASC2 promotes cell proliferation and metastasis of bladder cancer by activation of the Wnt/beta-catenin signaling pathway. *Oncotarget*, 2017.
- 25.**Inestrosa, N.C. and L. Varela-Nallar, Wnt signaling in the nervous system and in Alzheimer's disease. *J Mol Cell Biol*, 2014. **6**(1): p. 64-74.
- 26.**Arrazola, M.S., E. Ramos-Fernandez, P. Cisternas, D. Ordenes, and N.C. Inestrosa, Wnt Signaling Prevents the Abeta Oligomer-Induced Mitochondrial Permeability Transition Pore Opening Preserving Mitochondrial Structure in Hippocampal Neurons. *PLoS One*, 2017. **12**(1): p. e0168840.
- 27.**Hattori, M., A. Fujiyama, T.D. Taylor, H. Watanabe, T. Yada, H.S. Park, A. Toyoda, K. Ishii, Y. Totoki, D.K. Choi, Y. Groner, E. Soeda, M. Ohki, T. Takagi, Y. Sakaki, S. Taudien, K. Blechschmidt, A. Polley, U. Menzel, J. Delabar, K. Kumpf, R. Lehmann, D. Patterson, K. Reichwald, A. Rump, M.

Bibliography

Schillhabel, A. Schudy, W. Zimmermann, A. Rosenthal, J. Kudoh, K. Schibuya, K. Kawasaki, S. Asakawa, A. Shintani, T. Sasaki, K. Nagamine, S. Mitsuyama, S.E. Antonarakis, S. Minoshima, N. Shimizu, G. Nordsiek, K. Hornischer, P. Brant, M. Scharfe, O. Schon, A. Desario, J. Reichelt, G. Kauer, H. Blocker, J. Ramser, A. Beck, S. Klages, S. Hennig, L. Riesselmann, E. Dagand, T. Haaf, S. Wehrmeyer, K. Borzym, K. Gardiner, D. Nizetic, F. Francis, H. Lehrach, R. Reinhardt, M.L. Yaspo, and C.M. Sequencing, The DNA sequence of human chromosome 21 (vol 405, pg 311, 2000). *Nature*, 2000. **407**(6800): p. 110-110.

28.Dierssen, M., Y. Herault, and X. Estivill, Aneuploidy: From a Physiological Mechanism of Variance to Down Syndrome. *Physiological Reviews*, 2009. **89**(3): p. 887-920.

29.Li, Z., T. Yu, M. Morishima, A. Pao, J. LaDuca, J. Conroy, N. Nowak, S. Matsui, I. Shiraishi, and Y.E. Yu, Duplication of the entire 22.9 Mb human chromosome 21 syntenic region on mouse chromosome 16 causes cardiovascular and gastrointestinal abnormalities. *Hum Mol Genet*, 2007. **16**(11): p. 1359-66.

30.Yu, T., Z. Li, Z. Jia, S.J. Clapcote, C. Liu, S. Li, and Y.E. Yu, A mouse model of Down syndrome trisomic for all human chromosome 21 syntenic regions. *Human molecular genetics*, 2010. **179**.

31.Lee, A.Y., B. He, L. You, S. Dadfarmay, Z. Xu, J. Mazieres, I. Mikami, F. McCormick, and D.M. Jablons, Expression of the secreted frizzled-related protein gene family is downregulated in human mesothelioma. *Oncogene*, 2004. **23**(39): p. 6672-6676.

32.Bengochea, A., M.M. de Souza, L. Lefrancois, E. Le Roux, O. Galy, I. Chemin, M. Kim, J.R. Wands, C. Trepo, P. Hainaut, J.Y. Scoazec, L. Vitvitski, and P. Merle, Common dysregulation of Wnt/Frizzled receptor elements in human hepatocellular carcinoma. *Br J Cancer*, 2008. **99**(1): p. 143-50.

33.Choo, A.B., H.L. Tan, S.N. Ang, W.J. Fong, A. Chin, J. Lo, L. Zheng, H. Hentze, R.J. Philp, S.K. Oh, and M. Yap, Selection against undifferentiated human embryonic stem cells by a cytotoxic antibody recognizing podocalyxin-like protein-1. *Stem Cells*, 2008. **26**(6): p. 1454-63.

34.Ding, V.M., L. Ling, S. Natarajan, M.G. Yap, S.M. Cool, and A.B. Choo, FGF-2 modulates Wnt signaling in undifferentiated hESC and iPS cells through activated PI3-K/GSK3 β signaling. *Journal of cellular physiology*, 2010. **225**(2): p. 417-428.

35.Chassot, A.A., F. Ranc, E.P. Gregoire, H.L. Roepers-Gajadien, M.M. Taketo, G. Camerino, D.G. de Rooij, A. Schedl, and M.C. Chaboissier, Activation of beta-catenin signaling by Rspo1 controls differentiation of the mammalian ovary. *Hum Mol Genet*, 2008. **17**(9): p. 1264-77.

36.Gore, A.V., M.R. Swift, Y.R. Cha, B. Lo, M.C. McKinney, W. Li, D. Castranova, A. Davis, Y.S. Mukoyama, and B.M. Weinstein, Rspo1/Wnt signaling promotes angiogenesis via Vegfc/Vegfr3. *Development*, 2011. **138**(22): p. 4875-86.

37.Binnerts, M.E., K.A. Kim, J.M. Bright, S.M. Patel, K. Tran, M. Zhou, J.M. Leung, Y. Liu, W.E. Lomas, 3rd, M. Dixon, S.A. Hazell, M. Wagle, W.S. Nie, N. Tomasevic, J. Williams, X. Zhan, M.D. Levy, W.D. Funk, and A. Abo, R-Spondin1 regulates Wnt signaling by inhibiting internalization of LRP6. *Proc Natl Acad Sci U S A*, 2007. **104**(37): p. 14700-5.

38.Glinka, A., C. Dolde, N. Kirsch, Y.L. Huang, O. Kazanskaya, D. Ingelfinger, M. Boutros, C.M. Cruciat, and C. Niehrs, LGR4 and LGR5 are R-spondin receptors mediating Wnt/beta-catenin and Wnt/PCP signalling. *EMBO Rep*, 2011. **12**(10): p. 1055-61.

39.Yu, T., C.H. Liu, P. Belichenko, S.J. Clapcote, S.M. Li, A.N. Pao, A. Kleschevnikov, A.R. Bechard, S. Asrar, R.Q. Chen, N. Fan, Z.Y. Zhou, Z.P. Jia, C. Chen, J.C. Roder, B. Liu, A. Baldini, W.C. Mobley, and Y.E. Yu, Effects of individual segmental trisomies of human chromosome 21

Bibliography

syntenic regions on hippocampal long-term potentiation and cognitive behaviors in mice. *Brain Research*, 2010. **1366**: p. 162-171.

40.Das, I. and R.H. Reeves, The use of mouse models to understand and improve cognitive deficits in Down syndrome. *Disease Models & Mechanisms*, 2011. **4**(5): p. 596-606.

41.Rosso, S.B., D. Sussman, A. Wynshaw-Boris, and P.C. Salinas, Wnt signaling through Dishevelled, Rac and JNK regulates dendritic development. *Nature neuroscience*, 2005. **8**(1): p. 34-42.

42.Endo, Y. and J.S. Rubin, Wnt signaling and neurite outgrowth: insights and questions. *Cancer Sci*, 2007. **98**(9): p. 1311-7.

43.Chen, J.Y., C.S. Park, and S.J. Tang, Activity-dependent synaptic Wnt release regulates hippocampal long term potentiation. *Journal of Biological Chemistry*, 2006. **281**(17): p. 11910-11916.

44.Oliva, C.A., J.Y. Vargas, and N.C. Inestrosa, Wnt signaling: role in LTP, neural networks and memory. *Ageing Res Rev*, 2013. **12**(3): p. 786-800.

45.Yu, T., Z. Li, Z. Jia, S.J. Clapcote, C. Liu, S. Li, and Y.E. Yu, A mouse model of Down syndrome trisomic for all human chromosome 21 syntenic regions. *Hum mol gen*, 2010. **17**9.

46.Gitton, Y., N. Dahmane, S. Baik, A. Ruiz i Altaba, L. Neidhardt, M. Scholze, B.G. Herrmann, P. Kahlem, A. Benkahla, S. Schrinner, R. Yildirimman, R. Herwig, H. Lehrach, M.L. Yaspo, and H.S.A.e.m. initiative, A gene expression map of human chromosome 21 orthologues in the mouse. *Nature*, 2002. **420**(6915): p. 586-90.

47.Rachidi, M. and C. Lopes, Mental retardation and associated neurological dysfunctions in Down syndrome: a consequence of dysregulation in critical chromosome 21 genes and associated molecular pathways. *Eur J Paediatr Neurol*, 2008. **12**(3): p. 168-82.

7.4 Chapter 4.2 - Wnt signalling proteins in DS mouse models and humans

1. Nagafuchi, A. and M. Takeichi, Cell binding function of E-cadherin is regulated by the cytoplasmic domain. *EMBO J*, 1988. **7**(12): p. 3679-84.
2. McCrea, P.D., C.W. Turck, and B. Gumbiner, A homolog of the armadillo protein in *Drosophila* (plakoglobin) associated with E-cadherin. *Science*, 1991. **254**(5036): p. 1359-61.
3. McCrea, P.D., W.M. Brieher, and B.M. Gumbiner, Induction of a secondary body axis in *Xenopus* by antibodies to beta-catenin. *J Cell Biol*, 1993. **123**(2): p. 477-84.
4. Funayama, N., F. Fagotto, P. McCrea, and B.M. Gumbiner, Embryonic axis induction by the armadillo repeat domain of beta-catenin: evidence for intracellular signaling. *J Cell Biol*, 1995. **128**(5): p. 959-68.
5. Yost, C., M. Torres, J.R. Miller, E. Huang, D. Kimelman, and R.T. Moon, The axis-inducing activity, stability, and subcellular distribution of beta-catenin is regulated in *Xenopus* embryos by glycogen synthase kinase 3. *Genes Dev*, 1996. **10**(12): p. 1443-54.
6. Morin, P.J., A.B. Sparks, V. Korinek, N. Barker, H. Clevers, B. Vogelstein, and K.W. Kinzler, Activation of beta-catenin-Tcf signaling in colon cancer by mutations in beta-catenin or APC. *Science*, 1997. **275**(5307): p. 1787-90.
7. Reya, T. and H. Clevers, Wnt signalling in stem cells and cancer. *Nature*, 2005. **434**(7035): p. 843-50.
8. Clevers, H., Wnt/beta-catenin signaling in development and disease. *Cell*, 2006. **127**(3): p. 469-80.
9. Nusse, R. and H. Varmus, Three decades of Wnts: a personal perspective on how a scientific field developed. *The EMBO journal*, 2012. **31**: p. 2670-2684.
10. Holland, J.D., A. Klaus, A.N. Garratt, and W. Birchmeier, Wnt signaling in stem and cancer stem cells. *Current opinion in cell biology*, 2013. **25**: p. 254-264.
11. Inestrosa, N.C. and L. Varela-Nallar, Wnt signalling in neuronal differentiation and development. *Cell Tissue Res*, 2015. **359**(1): p. 215-23.
12. Behrens, J., B.A. Jerchow, M. Würtele, J. Grimm, C. Asbrand, R. Wirtz, and W. Birchmeier, Functional interaction of an axin homolog, conductin, with β -catenin, APC, and GSK3 β . *Science*, 1998. **280**: p. 596-599.
13. Farr, G.H., 3rd, D.M. Ferkey, C. Yost, S.B. Pierce, C. Weaver, and D. Kimelman, Interaction among GSK-3, GBP, axin, and APC in *Xenopus* axis specification. *J Cell Biol*, 2000. **148**(4): p. 691-702.
14. Kimelman, D. and W. Xu, beta-catenin destruction complex: insights and questions from a structural perspective. *Oncogene*, 2006. **25**(57): p. 7482-91.
15. Yang, K., X. Wang, H.M. Zhang, Z.L. Wang, G.X. Nan, Y.S. Li, F.G. Zhang, M.K. Mohammed, R.C. Haydon, H.H. Luu, Y. Bi, and T.C. He, The evolving roles of canonical WNT signaling in stem cells and tumorigenesis: implications in targeted cancer therapies. *Lab Invest*, 2016. **96**(2): p. 116-136.
16. Sancho, R.M., B.M. Law, and K. Harvey, Mutations in the LRRK2 Roc-COR tandem domain link Parkinson's disease to Wnt signalling pathways. *Hum Mol Genet*, 2009. **18**(20): p. 3955-68.

Bibliography

17. Berwick, D.C. and K. Harvey, LRRK2 functions as a Wnt signaling scaffold, bridging cytosolic proteins and membrane-localized LRP6. *Hum Mol Genet*, 2012. **21**(22): p. 4966-79.
18. Nie, X., Dkk1, -2, and -3 expression in mouse craniofacial development. *Journal of Molecular Histology*, 2005. **36**: p. 367-372.
19. Chamorro, M.N., D.R. Schwartz, A. Vonica, A.H. Brivanlou, K.R. Cho, and H.E. Varmus, FGF-20 and DKK1 are transcriptional targets of β -catenin and FGF-20 is implicated in cancer and development. *The EMBO Journal*, 2005. **24**: p. 73-84.
20. Ribeiro, D., K. Ellwanger, D. Glasgow, S. Theofilopoulos, N.S. Corsini, A. Martin-Villalba, and E. Arenas, Dkk1 regulates ventral midbrain dopaminergic differentiation and morphogenesis. *PLoS one*, 2011. **6**: p. 2.
21. Lee, E.-J., M. Jo, S.B. Rho, K. Park, Y.-N. Yoo, J. Park, M. Chae, W. Zhang, and J.-H. Lee, Dkk3, downregulated in cervical cancer, functions as a negative regulator of β -catenin. *Int J Cancer*, 2009. **124**: p. 287-297.
22. Abarzua, F., Adenovirus-Mediated Overexpression of REIC/Dkk-3 Selectively Induces Apoptosis in Human Prostate Cancer Cells through Activation of c-Jun-NH2-Kinase. *Cancer Research*, 2005. **65**: p. 9617-9622.
23. Medinger, M., A. Tzankov, J. Kern, A. Pircher, M. Hermann, H.-W. Ott, G. Gastl, G. Untergasser, and E. Gunsilius, Increased Dkk3 protein expression in platelets and megakaryocytes of patients with myeloproliferative neoplasms. *Thrombosis and Haemostasis*, 2010. **105**: p. 72-80.
24. Diep, D.B., N. Hoen, M. Backman, O. Machon, and S. Krauss, Characterisation of the Wnt antagonists and their response to conditionally activated Wnt signalling in the developing mouse forebrain. *Dev Brain Res*, 2004. **153**(2): p. 261-270.
25. Zenzmaier, C., J. Marksteiner, A. Kiefer, P. Berger, and C. Humpel, Dkk3 is elevated in CSF and plasma of Alzheimer's disease patients. *J Neurochem*, 2009. **110**: p. 653-661.
26. Purro, S.A., E.M. Dickins, and P.C. Salinas, The secreted Wnt antagonist Dickkopf-1 is required for amyloid β -mediated synaptic loss. *J Neurosci*, 2012. **32**: p. 3492-3498.
27. O'Doherty, A., S. Ruf, C. Mulligan, V. Hildreth, M.L. Errington, S. Cooke, and E.M. Fisher, An aneuploid mouse strain carrying human chromosome 21 with Down syndrome phenotypes. *Science*, 2005. **309**: p. 2033-2037.
28. Sheppard, O., F. Plattner, A. Rubin, A. Slender, J.M. Linehan, S. Brandner, V.L.J. Tybulewicz, E.M.C. Fisher, and F.K. Wiseman, Altered regulation of tau phosphorylation in a mouse model of down syndrome aging. *Neurobiol Aging*, 2012. **33**(4).
29. Lana-Elola, E., S. Watson-Scales, A. Slender, D. Gibbins, A. Martineau, C. Douglas, T. Mohun, E.M.C. Fisher, and V.L.J. Tybulewicz, Genetic dissection of Down syndrome-associated congenital heart defects using a new mouse mapping panel. *Elife*, 2016. **5**.
30. Yu, T., Z. Li, Z. Jia, S.J. Clapcote, C. Liu, S. Li, and Y.E. Yu, A mouse model of Down syndrome trisomic for all human chromosome 21 syntenic regions. *Hum mol gen*, 2010. **179**.
31. Inestrosa, N.C. and E. Arenas, Emerging roles of Wnts in the adult nervous system. *Nature Rev Neurosci*, 2010. **11**(2): p. 77-86.

Bibliography

- 32.**Inestrosa, N.C. and L. Varela-Nallar, Wnt signaling in the nervous system and in Alzheimer's disease. *J Mol Cell Biol*, 2014. **6**(1): p. 64-74.
- 33.**Lie, D.C., S.A. Colamarino, H.J. Song, L. Desire, H. Mira, A. Consiglio, E.S. Lein, S. Jessberger, H. Lansford, A.R. Dearie, and F.H. Gage, Wnt signalling regulates adult hippocampal neurogenesis. *Nature*, 2005. **437**(7063): p. 1370-1375.
- 34.**Oliva, C.A., J.Y. Vargas, and N.C. Inestrosa, Wnt signaling: role in LTP, neural networks and memory. *Ageing Res Rev*, 2013. **12**(3): p. 786-800.
- 35.**Purro, S.A., S. Galli, and P.C. Salinas, Dysfunction of Wnt signaling and synaptic disassembly in neurodegenerative diseases. *Journal of molecular cell biology*, mjt0, 2014. **49**.
- 36.**Nakamura, R., D. Hunter, W. Brunken, and A. Hackam, Dickkopf-3 (Dkk3) is an Anti-Apoptotic Protein That Regulates Wnt Signaling in Retinal Muller Glia. *Investigative Ophthalmology & Visual Science*, 2007. **48**(13): p. 621-621.
- 37.**Bowman, A.N., R. van Amerongen, T.D. Palmer, and R. Nusse, Lineage tracing with Axin2 reveals distinct developmental and adult populations of Wnt/beta-catenin-responsive neural stem cells. *Proc Natl Acad Sci U S A*, 2013. **110**(18): p. 7324-9.
- 38.**Leung, J.Y., F.T. Kolligs, R. Wu, Y. Zhai, R. Kuick, S. Hanash, K.R. Cho, and E.R. Fearon, Activation of AXIN2 expression by beta-catenin-T cell factor. A feedback repressor pathway regulating Wnt signaling. *J Biol Chem*, 2002. **277**(24): p. 21657-65.
- 39.**Chevallier, N.L., S. Soriano, D.E. Kang, E. Masliah, G. Hu, and E.H. Koo, Perturbed neurogenesis in the adult hippocampus associated with presenilin-1 A246E mutation. *Am J Pathol*, 2005. **167**(1): p. 151-9.
- 40.**Malik, B., A. Currais, A. Andres, C. Towilson, D. Pitsi, A. Nunes, M. Niblock, J. Cooper, T. Hortobagyi, and S. Soriano, Loss of neuronal cell cycle control as a mechanism of neurodegeneration in the presenilin-1 Alzheimer's disease brain. *Cell Cycle*, 2008. **7**(5): p. 637-46.
- 41.**Malik, B., A. Currais, and S. Soriano, Cell cycle-driven neuronal apoptosis specifically linked to amyloid peptide A β 1-42 exposure is not exacerbated in a mouse model of presenilin-1 familial Alzheimer's disease. *J Neurochem*, 2008. **106**(2): p. 912-6.
- 42.**Gribble, S.M., F.K. Wiseman, S. Clayton, E. Prigmore, E. Langley, F. Yang, S. Maguire, B. Fu, D. Rajan, O. Sheppard, C. Scott, H. Hauser, P.J. Stephens, L.A. Stebbings, B.L. Ng, T. Fitzgerald, M.A. Quail, R. Banerjee, K. Rothkamm, V.L. Tybulewicz, E.M. Fisher, and N.P. Carter, Massively parallel sequencing reveals the complex structure of an irradiated human chromosome on a mouse background in the Tc1 model of Down syndrome. *PLoS One*, 2013. **8**(4): p. e60482.
- 43.**Kurabayashi, N., T. Hirota, M. Sakai, K. Sanada, and Y. Fukada, DYRK1A and glycogen synthase kinase 3 β , a dual-kinase mechanism directing proteasomal degradation of CRY2 for circadian timekeeping. *Mol Cell Biol*, 2010. **30**(7): p. 1757-1768.
- 44.**Shen, W., B. Taylor, Q. Jin, V. Nguyen-Tran, S. Meeusen, Y.Q. Zhang, A. Kamireddy, A. Swafford, A.F. Powers, J. Walker, J. Lamb, B. Bursalaya, M. DiDonato, G. Harb, M. Qiu, C.M. Filippi, L. Deaton, C.N. Turk, W.L. Suarez-Pinzon, Y. Liu, X. Hao, T. Mo, S. Yan, J. Li, A.E. Herman, B.J. Hering, T. Wu, H. Martin Seidel, P. McNamara, R. Glynne, and B. Laffitte, Inhibition of DYRK1A and GSK3B induces human beta-cell proliferation. *Nat Commun*, 2015. **6**: p. 8372.
- 45.**Song, W.-J., E.-A.C. Song, M.-S. Jung, S.-H. Choi, H.-H. Baik, B.K. Jin, J.H. Kim, and S.-H. Chung, Phosphorylation and inactivation of glycogen synthase kinase 3 β (GSK3 β) by dual-

Bibliography

specificity tyrosine phosphorylation-regulated kinase 1A (Dyrk1A). *J Biol Chem*, 2015. **290**(4): p. 2321-2333.

46. Hong, J.Y., J.I. Park, M. Lee, W.A. Muñoz, R.K. Miller, H. Ji, and P.D. McCrea, Down's-syndrome-related kinase Dyrk1A modulates the p120-catenin/Kaiso trajectory of the Wnt signaling pathway. *J cell sci*, 2012. **125**: p. 561-569.

47. Arron, J.R., M.M. Winslow, A. Polleri, C.-P. Chang, H. Wu, X. Gao, J.R. Neilson, L. Chen, J.J. Heit, and S.K. Kim, NFAT dysregulation by increased dosage of DSCR1 and DYRK1A on chromosome 21. *Nature*, 2006. **441**(7093): p. 595-600.

48. Park, J., W.J. Song, and K.C. Chung, Function and regulation of Dyrk1A: towards understanding Down syndrome. *Cell Mol Life Sci*, 2009. **66**: p. 3235-3240.

7.5 Chapter 4.3 - DYRK1A-mediated Wnt signalling modulation

1. Manning, G., D.B. Whyte, R. Martinez, T. Hunter, and S. Sudarsanam, The protein kinase complement of the human genome. *Science*, 2002. **298**(5600): p. 1912-34.
2. Becker, W. and H.G. Joost, Structural and functional characteristics of Dyrk, a novel subfamily of protein kinases with dual specificity. *Prog Nucleic Acid Res Mol Biol*, 1999. **62**: p. 1-17.
3. Tejedor, F., X.R. Zhu, E. Kaltenbach, A. Ackermann, A. Baumann, I. Canal, M. Heisenberg, K.F. Fischbach, and O. Pongs, minibrain: a new protein kinase family involved in postembryonic neurogenesis in *Drosophila*. *Neuron*, 1995. **14**(2): p. 287-301.
4. Álvarez, M., X. Estivill, and S. de la Luna, DYRK1A accumulates in splicing speckles through a novel targeting signal and induces speckle disassembly. *J cell sci*, 2003. **116**(15): p. 3099-3107.
5. Becker, W., Recent insights into the function of DYRK1A. *FEBS J*, 2011. **278**(2): p. 222-222.
6. Himpel, S., P. Panzer, K. Eirnbter, H. Czajkowska, M. Sayed, L.C. Packman, T. Blundell, H. Kentrup, J. Grotzinger, H.G. Joost, and W. Becker, Identification of the autophosphorylation sites and characterization of their effects in the protein kinase DYRK1A. *Biochem J*, 2001. **359**(Pt 3): p. 497-505.
7. Papadopoulos, C., K. Arato, E. Lilienthal, J. Zerweck, M. Schutkowski, N. Chatain, G. Muller-Newen, W. Becker, and S. de la Luna, Splice variants of the dual specificity tyrosine phosphorylation-regulated kinase 4 (DYRK4) differ in their subcellular localization and catalytic activity. *J Biol Chem*, 2011. **286**(7): p. 5494-505.
8. Lochhead, P.A., G. Sibbet, N. Morrice, and V. Cleghon, Activation-loop autophosphorylation is mediated by a novel transitional intermediate form of DYRKs. *Cell*, 2005. **121**(6): p. 925-36.
9. Kinstrie, R., N. Luebbering, D. Miranda-Saavedra, G. Sibbet, J. Han, P.A. Lochhead, and V. Cleghon, Characterization of a domain that transiently converts class 2 DYRKs into intramolecular tyrosine kinases. *Sci Signal*, 2010. **3**(111): p. ra16.
10. Himpel, S., W. Tegge, R. Frank, S. Leder, H.G. Joost, and W. Becker, Specificity determinants of substrate recognition by the protein kinase DYRK1A. *J Biol Chem*, 2000. **275**(4): p. 2431-8.
11. Park, J., W.J. Song, and K.C. Chung, Function and regulation of Dyrk1A: towards understanding Down syndrome. *Cell Mol Life Sci*, 2009. **66**: p. 3235-3240.
12. Aranda, S., A. Laguna, and S. de la Luna, DYRK family of protein kinases: evolutionary relationships, biochemical properties, and functional roles. *FASEB J*, 2011. **25**(2): p. 449-62.
13. Becker, W., Y. Weber, K. Wetzel, K. Eirnbter, F.J. Tejedor, and H.G. Joost, Sequence characteristics, subcellular localization, and substrate specificity of DYRK-related kinases, a novel family of dual specificity protein kinases. *J Biol Chem*, 1998. **273**(40): p. 25893-902.
14. Guimerá, J., C. Casas, C. Pucharcós, A. Solans, A. Domènech, A.M. Planas, and M.A. Pritchard, A human homologue of *Drosophila* minibrain (MNB) is expressed in the neuronal regions affected in Down syndrome and maps to the critical region. *Human molecular genetics*, 1996. **5**: p. 1305-1310.
15. Wegiel, J., I. Kuchna, K. Nowicki, J. Frackowiak, K. Dowjat, W.P. Silverman, B. Reisberg, M. DeLeon, T. Wisniewski, T. Adayev, M.C. Chen-Hwang, and Y.W. Hwang, Cell type- and brain structure-specific patterns of distribution of minibrain kinase in human brain. *Brain Res*, 2004. **1010**(1-2): p. 69-80.

- 16.**Becker, W. and H.G. Joost, Structural and functional characteristics of Dyrk, a novel subfamily of protein kinases with dual specificity. *Progress in nucleic acid research and molecular biology*, 1998. **62**: p. 1-17.
- 17.**Baek, K.H., A. Zaslavsky, R.C. Lynch, C. Britt, Y. Okada, R.J. Siarey, M.W. Lensch, I.H. Park, S.S. Yoon, T. Minami, J.R. Korenberg, J. Folkman, G.Q. Daley, W.C. Aird, Z. Galdzicki, and S. Ryeom, Down's syndrome suppression of tumour growth and the role of the calcineurin inhibitor DSCR1. *Nature*, 2009. **459**(7250): p. 1126-30.
- 18.**Kuhn, C., D. Frank, R. Will, C. Jaschinski, R. Frauen, H.A. Katus, and N. Frey, DYRK1A is a novel negative regulator of cardiomyocyte hypertrophy. *J Biol Chem*, 2009. **284**(25): p. 17320-7.
- 19.**Lee, Y., J. Ha, H.J. Kim, Y.S. Kim, E.J. Chang, W.J. Song, and H.H. Kim, Negative feedback inhibition of NFATc1 by DYRK1A regulates bone homeostasis. *J Biol Chem*, 2009. **284**(48): p. 33343-51.
- 20.**Raaf, L., C. Noll, M. Cherifi, Y. Benazzoug, J.M. Delabar, and N. Janel, Hyperhomocysteinemia-induced Dyrk1a downregulation results in cardiomyocyte hypertrophy in rats. *Int J Cardiol*, 2010. **145**(2): p. 306-7.
- 21.**Kim, E.J., J.Y. Sung, H.J. Lee, H. Rhim, M. Hasegawa, T. Iwatsubo, S. Min do, J. Kim, S.R. Paik, and K.C. Chung, Dyrk1A phosphorylates alpha-synuclein and enhances intracellular inclusion formation. *J Biol Chem*, 2006. **281**(44): p. 33250-7.
- 22.**Sitz, J.H., K. Baumgartel, B. Hammerle, C. Papadopoulos, P. Hekerman, F.J. Tejedor, W. Becker, and B. Lutz, The Down syndrome candidate dual-specificity tyrosine phosphorylation-regulated kinase 1A phosphorylates the neurodegeneration-related septin 4. *Neuroscience*, 2008. **157**(3): p. 596-605.
- 23.**Kang, J.E., S.A. Choi, J.B. Park, and K.C. Chung, Regulation of the proapoptotic activity of huntingtin interacting protein 1 by Dyrk1 and caspase-3 in hippocampal neuroprogenitor cells. *J Neurosci Res*, 2005. **81**(1): p. 62-72.
- 24.**Fotaki, V., M. Dierssen, S. Alcántara, S. Martínez, E. Martí, C. Casas, J. Visa, E. Soriano, X. Estivill, and M.L. Arbones, Dyrk1A haploinsufficiency affects viability and causes developmental delay and abnormal brain morphology in mice. *Mol Cell Biol*, 2002. **22**(18): p. 6636-47.
- 25.**Benavides-Piccione, R., M. Dierssen, I. Ballesteros-Yanez, M. Martínez de Lagran, M.L. Arbones, V. Fotaki, J. DeFelipe, and G.N. Elston, Alterations in the phenotype of neocortical pyramidal cells in the Dyrk1A^{+/-} mouse. *Neurobiol Dis*, 2005. **20**(1): p. 115-22.
- 26.**Guedj, F., P.L. Pereira, S. Najas, M.J. Barallobre, C. Chabert, B. Souchet, C. Sebrie, C. Verney, Y. Herault, M. Arbones, and J.M. Delabar, DYRK1A: a master regulatory protein controlling brain growth. *Neurobiol Dis*, 2012. **46**(1): p. 190-203.
- 27.**Moller, R.S., S. Kubart, M. Hoeltzenbein, B. Heye, I. Vogel, C.P. Hansen, C. Menzel, R. Ullmann, N. Tommerup, H.H. Ropers, Z. Tumer, and V.M. Kalscheuer, Truncation of the Down syndrome candidate gene DYRK1A in two unrelated patients with microcephaly. *Am J Hum Genet*, 2008. **82**(5): p. 1165-70.
- 28.**Fujita, H., C. Torii, R. Kosaki, S. Yamaguchi, J. Kudoh, K. Hayashi, T. Takahashi, and K. Kosaki, Microdeletion of the Down syndrome critical region at 21q22. *Am J Med Genet A*, 2010. **152A**(4): p. 950-3.

Bibliography

- 29.**Najas, S., J. Arranz, P.A. Lochhead, A.L. Ashford, D. Oxley, J.M. Delabar, S.J. Cook, M.J. Barallobre, and M.L. Arbones, DYRK1A-mediated Cyclin D1 Degradation in Neural Stem Cells Contributes to the Neurogenic Cortical Defects in Down Syndrome. *EBioMedicine*, 2015. **2**(2): p. 120-34.
- 30.**Chen, J.Y., J.R. Lin, F.C. Tsai, and T. Meyer, Dosage of Dyrk1a shifts cells within a p21-cyclin D1 signaling map to control the decision to enter the cell cycle. *Mol Cell*, 2013. **52**(1): p. 87-100.
- 31.**Tetsu, O. and F. McCormick, Beta-catenin regulates expression of cyclin D1 in colon carcinoma cells. *Nature*, 1999. **398**(6726): p. 422-6.
- 32.**Reya, T. and H. Clevers, Wnt signalling in stem cells and cancer. *Nature*, 2005. **434**(7035): p. 843-50.
- 33.**Stewart, D.J., Wnt signaling pathway in non-small cell lung cancer. *J Natl Cancer Inst*, 2014. **106**(1): p. djt356.
- 34.**Hammerle, B., E. Vera-Samper, S. Speicher, R. Arencibia, S. Martinez, and F.J. Tejedor, Mnb/Dyrk1A is transiently expressed and asymmetrically segregated in neural progenitor cells at the transition to neurogenic divisions. *Dev Biol*, 2002. **246**(2): p. 259-73.
- 35.**Hammerle, B., E. Ulin, J. Guimera, W. Becker, F. Guillemot, and F.J. Tejedor, Transient expression of Mnb/Dyrk1a couples cell cycle exit and differentiation of neuronal precursors by inducing p27(KIP1) expression and suppressing NOTCH signaling. *Development*, 2011. **138**(12): p. 2543-2554.
- 36.**Oi, A., S. Katayama, N. Hatano, Y. Sugiyama, I. Kameshita, and N. Sueyoshi, Subcellular distribution of cyclin-dependent kinase-like 5 (CDKL5) is regulated through phosphorylation by dual specificity tyrosine-phosphorylation-regulated kinase 1A (DYRK1A). *Biochem Biophys Res Commun*, 2017. **482**(2): p. 239-245.
- 37.**Shen, W., B. Taylor, Q. Jin, V. Nguyen-Tran, S. Meeusen, Y.Q. Zhang, A. Kamireddy, A. Swafford, A.F. Powers, J. Walker, J. Lamb, B. Bursalaya, M. DiDonato, G. Harb, M. Qiu, C.M. Filippi, L. Deaton, C.N. Turk, W.L. Suarez-Pinzon, Y. Liu, X. Hao, T. Mo, S. Yan, J. Li, A.E. Herman, B.J. Hering, T. Wu, H. Martin Seidel, P. McNamara, R. Glynne, and B. Laffitte, Inhibition of DYRK1A and GSK3B induces human beta-cell proliferation. *Nat Commun*, 2015. **6**: p. 8372.
- 38.**Epstein, C.J., Down's syndrome: critical genes in a critical region. *Nature*, 2006. **441**(7093): p. 582-3.
- 39.**Lyle, R., F. Bena, S. Gagos, C. Gehrig, G. Lopez, A. Schinzel, J. Lespinasse, A. Bottani, S. Dahoun, L. Taine, M. Doco-Fenzy, P. Cornillet-Lefebvre, A. Pelet, S. Lyonnet, A. Toutain, L. Colleaux, J. Horst, I. Kennerknecht, N. Wakamatsu, M. Descartes, J.C. Franklin, L. Florentin-Arar, S. Kitsiou, E. Ait Yahya-Graison, M. Costantine, P.M. Sinet, J.M. Delabar, and S.E. Antonarakis, Genotype-phenotype correlations in Down syndrome identified by array CGH in 30 cases of partial trisomy and partial monosomy chromosome 21. *Eur J Hum Genet*, 2009. **17**(4): p. 454-66.
- 40.**Dahmane, N., G. Charron, C. Lopes, M.L. Yaspo, C. Maunoury, L. Decorte, P.M. Sinet, B. Bloch, and J.M. Delabar, Down syndrome-critical region contains a gene homologous to *Drosophila sim* expressed during rat and human central nervous system development. *Proc Natl Acad Sci U S A*, 1995. **92**(20): p. 9191-5.
- 41.**Guimera, J., C. Casas, X. Estivill, and M. Pritchard, Human minibrain homologue (MNBH/DYRK1): characterization, alternative splicing, differential tissue expression, and overexpression in Down syndrome. *Genomics*, 1999. **57**(3): p. 407-18.

Bibliography

- 42.** Park, J., E.J. Yang, J.H. Yoon, and K.C. Chung, Dyrk1A overexpression in immortalized hippocampal cells produces the neuropathological features of Down syndrome. *Mol Cell Neurosci*, 2007. **36**(2): p. 270-9.
- 43.** Malinge, S., M. Bliss-Moreau, G. Kirsammer, L. Diebold, T. Chlon, S. Gurbuxani, and J.D. Crispino, Increased dosage of the chromosome 21 ortholog Dyrk1a promotes megakaryoblastic leukemia in a murine model of Down syndrome. *The Journal of clinical investigation*, 2012. **122**: p. 948-962.
- 44.** Arron, J.R., M.M. Winslow, A. Polleri, C.-P. Chang, H. Wu, X. Gao, J.R. Neilson, L. Chen, J.J. Heit, and S.K. Kim, NFAT dysregulation by increased dosage of DSCR1 and DYRK1A on chromosome 21. *Nature*, 2006. **441**(7093): p. 595-600.
- 45.** Dowjat, W.K., T. Adayev, I. Kuchna, K. Nowicki, S. Palminiello, Y.W. Hwang, and J. Wegiel, Trisomy-driven overexpression of DYRK1A kinase in the brain of subjects with Down syndrome. *Neurosci Lett*, 2007. **413**(1): p. 77-81.
- 46.** Okui, M., T. Ide, K. Morita, E. Funakoshi, F. Ito, K. Ogita, Y. Yoneda, J. Kudoh, and N. Shimizu, High-level expression of the Mnb/Dyrk1A gene in brain and heart during rat early development. *Genomics*, 1999. **62**(2): p. 165-71.
- 47.** Marti, E., X. Altafaj, M. Dierssen, S. de la Luna, V. Fotaki, M. Alvarez, M. Perez-Riba, I. Ferrer, and X. Estivill, Dyrk1A expression pattern supports specific roles of this kinase in the adult central nervous system. *Brain Res*, 2003. **964**(2): p. 250-63.
- 48.** Hammerle, B., C. Elizalde, and F.J. Tejedor, The spatio-temporal and subcellular expression of the candidate Down syndrome gene Mnb/Dyrk1A in the developing mouse brain suggests distinct sequential roles in neuronal development. *Eur J Neurosci*, 2008. **27**(5): p. 1061-74.
- 49.** Woods, Y.L., G. Rena, N. Morrice, A. Barthel, W. Becker, S. Guo, T.G. Unterman, and P. Cohen, The kinase DYRK1A phosphorylates the transcription factor FKHR at Ser329 in vitro, a novel in vivo phosphorylation site. *Biochem J*, 2001. **355**: p. 597.
- 50.** Kimura, R., K. Kamino, M. Yamamoto, A. Nuripa, T. Kida, H. Kazui, and M. Takeda, The DYRK1A gene, encoded in chromosome 21 Down syndrome critical region, bridges between β -amyloid production and tau phosphorylation in Alzheimer disease. *Hum mol gen*, 2007. **16**: p. 15-23.
- 51.** Ryoo, S.R., H.K. Jeong, C. Radnaabazar, J.J. Yoo, H.J. Cho, H.W. Lee, I.S. Kim, Y.H. Cheon, Y.S. Ahn, S.H. Chung, and W.J. Song, DYRK1A-mediated hyperphosphorylation of Tau. A functional link between Down syndrome and Alzheimer disease. *J Biol Chem*, 2007. **282**(48): p. 34850-7.
- 52.** Liu, F., Z. Liang, J. Wegiel, Y.W. Hwang, K. Iqbal, I. Grundke-Iqbal, N. Ramakrishna, and C.X. Gong, Overexpression of Dyrk1A contributes to neurofibrillary degeneration in Down syndrome. *FASEB J*, 2008. **22**(9): p. 3224-33.
- 53.** Ryoo, S.R., H.J. Cho, H.W. Lee, H.K. Jeong, C. Radnaabazar, Y.S. Kim, M.J. Kim, M.Y. Son, H. Seo, S.H. Chung, and W.J. Song, Dual-specificity tyrosine(Y)-phosphorylation regulated kinase 1A-mediated phosphorylation of amyloid precursor protein: evidence for a functional link between Down syndrome and Alzheimer's disease. *J Neurochem*, 2008. **104**(5): p. 1333-44.
- 54.** Janel, N., M. Sarazin, F. Corlier, H. Corne, L.C. de Souza, L. Hamelin, A. Aka, J. Lagarde, H. Blehaut, V. Hindie, J.C. Rain, M.L. Arbones, B. Dubois, M.C. Potier, M. Bottlaender, and J.M. Delabar, Plasma DYRK1A as a novel risk factor for Alzheimer's disease. *Transl Psychiatry*, 2014. **4**.

Bibliography

55. Wegiel, J., K. Dowjat, W. Kaczmarek, I. Kuchna, K. Nowicki, J. Frackowiak, B. Mazur Kolecka, J. Wegiel, W.P. Silverman, B. Reisberg, M. DeLeon, T. Wisniewski, C.X. Gong, F. Liu, T. Adayev, M.C. Chen-Hwang, and Y.W. Hwang, The role of overexpressed DYRK1A protein in the early onset of neurofibrillary degeneration in Down syndrome. *Acta Neuropathol*, 2008. **116**(4): p. 391-407.
56. Shi, J., T. Zhang, C. Zhou, M.O. Chohan, X. Gu, J. Wegiel, J. Zhou, Y.W. Hwang, K. Iqbal, I. Grundke-Iqbal, C.X. Gong, and F. Liu, Increased dosage of Dyrk1A alters alternative splicing factor (ASF)-regulated alternative splicing of tau in Down syndrome. *J Biol Chem*, 2008. **283**(42): p. 28660-9.
57. Ryu, Y.S., S.Y. Park, M.S. Jung, S.H. Yoon, M.Y. Kwon, S.Y. Lee, and S.H. Chung, Dyrk1A-mediated phosphorylation of Presenilin 1: a functional link between Down syndrome and Alzheimer's disease. *J Neurochem*, 2010. **115**: p. 574-584.
58. Smith, D.J., M.E. Stevens, S.P. Sudanagunta, R.T. Bronson, M. Makhinson, A.M. Watabe, T.J. O'Dell, J. Fung, H.U. Weier, J.F. Cheng, and E.M. Rubin, Functional screening of 2 Mb of human chromosome 21q22.2 in transgenic mice implicates minibrain in learning defects associated with Down syndrome. *Nat Genet*, 1997. **16**(1): p. 28-36.
59. Altafaj, X., M. Dierssen, C. Baamonde, E. Martí, J. Visa, J. Guimera, M. Oset, J.R. Gonzalez, J. Florez, C. Fillat, and X. Estivill, Neurodevelopmental delay, motor abnormalities and cognitive deficits in transgenic mice overexpressing Dyrk1A (minibrain), a murine model of Down's syndrome. *Hum Mol Genet*, 2001. **10**(18): p. 1915-23.
60. Branchi, I., Z. Bichler, L. Minghetti, J.M. Delabar, F. Malchiodi-Albedi, M.C. Gonzalez, Z. Chettouh, A. Nicolini, C. Chabert, D.J. Smith, E.M. Rubin, D. Migliore-Samour, and E. Alleva, Transgenic mouse in vivo library of human Down syndrome critical region 1: association between DYRK1A overexpression, brain development abnormalities, and cell cycle protein alteration. *J Neuropathol Exp Neurol*, 2004. **63**(5): p. 429-40.
61. de Lagrán, M.M., X. Altafaj, X. Gallego, E. Martí, X. Estivill, I. Sahun, C. Fillat, and M. Dierssen, Motor phenotypic alterations in TgDyrk1a transgenic mice implicate DYRK1A in Down syndrome motor dysfunction. *Neurobiol Dis*, 2004. **15**(1): p. 132-142.
62. Ahn, K.J., H.K. Jeong, H.S. Choi, S.R. Ryoo, Y.J. Kim, J.S. Goo, S.Y. Choi, J.S. Han, I. Ha, and W.J. Song, DYRK1A BAC transgenic mice show altered synaptic plasticity with learning and memory defects. *Neurobiol Dis*, 2006. **22**(3): p. 463-72.
63. Mancini, M. and A. Toker, NFAT proteins: emerging roles in cancer progression. *Nat Rev Cancer*, 2009. **9**(11): p. 810-20.
64. Hogan, P.G., L. Chen, J. Nardone, and A. Rao, Transcriptional regulation by calcium, calcineurin, and NFAT. *Genes Dev*, 2003. **17**(18): p. 2205-32.
65. Beals, C.R., C.M. Sheridan, C.W. Turck, P. Gardner, and G.R. Crabtree, Nuclear export of NF-ATc enhanced by glycogen synthase kinase-3. *Science*, 1997. **275**(5308): p. 1930-4.
66. Zhu, J., F. Shibasaki, R. Price, J.C. Guillemot, T. Yano, V. Dotsch, G. Wagner, P. Ferrara, and F. McKeon, Intramolecular masking of nuclear import signal on NF-AT4 by casein kinase I and MEK1. *Cell*, 1998. **93**(5): p. 851-61.
67. Gwack, Y., S. Sharma, J. Nardone, B. Tanasa, A. Iuga, S. Srikanth, H. Okamura, D. Bolton, S. Feske, P.G. Hogan, and A. Rao, A genome-wide Drosophila RNAi screen identifies DYRK-family kinases as regulators of NFAT. *Nature*, 2006. **441**(7093): p. 646-50.

Bibliography

- 68.**Nusse, R. and H. Varmus, Three decades of Wnts: a personal perspective on how a scientific field developed. *The EMBO journal*, 2012. **31**: p. 2670-2684.
- 69.**Bogacheva, O., O. Bogachev, M. Menon, A. Dev, E. Houde, E.I. Valoret, H.M. Prosser, C.L. Creasy, S.J. Pickering, E. Grau, K. Rance, G.P. Livi, V. Karur, C.L. Erickson-Miller, and D.M. Wojchowski, DYRK3 dual-specificity kinase attenuates erythropoiesis during anemia. *J Biol Chem*, 2008. **283**(52): p. 36665-75.
- 70.**Lemmon, M.A. and J. Schlessinger, Cell signaling by receptor tyrosine kinases. *Cell*, 2010. **141**(7): p. 1117-34.
- 71.**Ebisuya, M., K. Kondoh, and E. Nishida, The duration, magnitude and compartmentalization of ERK MAP kinase activity: mechanisms for providing signaling specificity. *J Cell Sci*, 2005. **118**(Pt 14): p. 2997-3002.
- 72.**Kelly, P.A. and Z. Rahmani, DYRK1A enhances the mitogen-activated protein kinase cascade in PC12 cells by forming a complex with Ras, B-Raf, and MEK1. *Mol Biol Cell*, 2005. **16**(8): p. 3562-73.
- 73.**Ferron, S.R., N. Pozo, A. Laguna, S. Aranda, E. Porlan, M. Moreno, C. Fillat, S. de la Luna, P. Sanchez, M.L. Arbones, and I. Farinas, Regulated segregation of kinase Dyrk1A during asymmetric neural stem cell division is critical for EGFR-mediated biased signaling. *Cell Stem Cell*, 2010. **7**(3): p. 367-79.
- 74.**Aranda, S., M. Alvarez, S. Turro, A. Laguna, and S. de la Luna, Sprouty2-mediated inhibition of fibroblast growth factor signaling is modulated by the protein kinase DYRK1A. *Mol Cell Biol*, 2008. **28**(19): p. 5899-911.
- 75.**Yuan, J.S., P.C. Kousis, S. Suliman, I. Visan, and C.J. Guidos, Functions of notch signaling in the immune system: consensus and controversies. *Annu Rev Immunol*, 2010. **28**: p. 343-65.
- 76.**D'Souza, B., A. Miyamoto, and G. Weinmaster, The many facets of Notch ligands. *Oncogene*, 2008. **27**(38): p. 5148-67.
- 77.**Fernandez-Martinez, J., E.M. Vela, M. Tora-Ponsioen, O.H. Ocana, M.A. Nieto, and J. Galceran, Attenuation of Notch signalling by the Down-syndrome-associated kinase DYRK1A. *J Cell Sci*, 2009. **122**(Pt 10): p. 1574-83.
- 78.**Wong, S.Y. and J.F. Reiter, The primary cilium at the crossroads of mammalian hedgehog signaling. *Curr Top Dev Biol*, 2008. **85**: p. 225-60.
- 79.**Briscoe, J., Making a grade: Sonic Hedgehog signalling and the control of neural cell fate. *EMBO J*, 2009. **28**(5): p. 457-65.
- 80.**Ayers, K.L. and P.P. Therond, Evaluating Smoothed as a G-protein-coupled receptor for Hedgehog signalling. *Trends Cell Biol*, 2010. **20**(5): p. 287-98.
- 81.**Mao, J., P. Maye, P. Kogerman, F.J. Tejedor, R. Toftgard, W. Xie, G. Wu, and D. Wu, Regulation of Gli1 transcriptional activity in the nucleus by Dyrk1. *J Biol Chem*, 2002. **277**(38): p. 35156-61.
- 82.**Shimokawa, T., U. Tostar, M. Lauth, R. Palaniswamy, M. Kasper, R. Toftgard, and P.G. Zaphiropoulos, Novel human glioma-associated oncogene 1 (GLI1) splice variants reveal distinct mechanisms in the terminal transduction of the hedgehog signal. *J Biol Chem*, 2008. **283**(21): p. 14345-54.

Bibliography

- 83.**Hong, J.Y., J.I. Park, M. Lee, W.A. Muñoz, R.K. Miller, H. Ji, and P.D. McCrea, Down's-syndrome-related kinase Dyrk1A modulates the p120-catenin/Kaiso trajectory of the Wnt signaling pathway. *J cell sci*, 2012. **125**: p. 561-569.
- 84.**Kurabayashi, N., T. Hirota, M. Sakai, K. Sanada, and Y. Fukada, DYRK1A and glycogen synthase kinase 3 β , a dual-kinase mechanism directing proteasomal degradation of CRY2 for circadian timekeeping. *Mol Cell Biol*, 2010. **30**(7): p. 1757-1768.
- 85.**Woods, Y.L., P. Cohen, W. Becker, R. Jakes, M. Goedert, X. Wang, and C.G. Proud, The kinase DYRK phosphorylates protein-synthesis initiation factor eIF2Bepsilon at Ser539 and the microtubule-associated protein tau at Thr212: potential role for DYRK as a glycogen synthase kinase 3-priming kinase. *Biochem. J*, 2001. **355**: p. 609-615.
- 86.**Sheppard, O., F. Plattner, A. Rubin, A. Slender, J.M. Linehan, S. Brandner, V.L.J. Tybulewicz, E.M.C. Fisher, and F.K. Wiseman, Altered regulation of tau phosphorylation in a mouse model of down syndrome aging. *Neurobiol Aging*, 2012. **33**(4).
- 87.**Sutherland, C., I.A. Leighton, and P. Cohen, Inactivation of glycogen synthase kinase-3 beta by phosphorylation: new kinase connections in insulin and growth-factor signalling. *Biochem. J*, 1993. **296**: p. 15-19.
- 88.**Cohen, P. and S. Frame, The renaissance of GSK3. *Nature reviews Molecular cell biology*, 2001. **2**: p. 769-776.
- 89.**Hammerle, B., A. Carnicero, C. Elizalde, J. Ceron, S. Martinez, and F.J. Tejedor, Expression patterns and subcellular localization of the Down syndrome candidate protein MNB/DYRK1A suggest a role in late neuronal differentiation. *Eur J Neurosci*, 2003. **17**(11): p. 2277-86.
- 90.**Murakami, N., D. Bolton, and Y.W. Hwang, Dyrk1A binds to multiple endocytic proteins required for formation of clathrin-coated vesicles. *Biochemistry*, 2009. **48**(39): p. 9297-305.
- 91.**Sitz, J.H., M. Tigges, K. Baumgartel, L.G. Khaspekov, and B. Lutz, Dyrk1A potentiates steroid hormone-induced transcription via the chromatin remodeling factor Arip4. *Mol Cell Biol*, 2004. **24**(13): p. 5821-34.
- 92.**Seifert, A., L.A. Allan, and P.R. Clarke, DYRK1A phosphorylates caspase 9 at an inhibitory site and is potently inhibited in human cells by harmine. *FEBS J*, 2008. **275**(24): p. 6268-80.
- 93.**Guo, X., J.G. Williams, T.T. Schug, and X. Li, DYRK1A and DYRK3 promote cell survival through phosphorylation and activation of SIRT1. *J Biol Chem*, 2010. **285**(17): p. 13223-32.
- 94.**Yabut, O., J. Domogauer, and G. D'Arcangelo, Dyrk1A overexpression inhibits proliferation and induces premature neuronal differentiation of neural progenitor cells. *J Neurosci*, 2010. **30**(11): p. 4004-14.
- 95.**Kaczmarek, W., M. Barua, B. Mazur-Kolecka, J. Frackowiak, W. Dowjat, P. Mehta, D. Bolton, Y.W. Hwang, A. Rabe, G. Albertini, and J. Wegiel, Intracellular distribution of differentially phosphorylated dual-specificity tyrosine phosphorylation-regulated kinase 1A (DYRK1A). *J Neurosci Res*, 2014. **92**(2): p. 162-73.
- 96.**Strehler, B.L. and E.W. Mc, Purification of firefly luciferin. *J Cell Comp Physiol*, 1949. **34**(3): p. 457-66.
- 97.**Cole, H.A., J.W. Wimpenny, and D.E. Hughes, The ATP pool in *Escherichia coli*. I. Measurement of the pool using modified luciferase assay. *Biochim Biophys Acta*, 1967. **143**(3): p. 445-53.

Bibliography

- 98.**van de Wetering, M., R. Cavallo, D. Dooijes, M. van Beest, J. van Es, J. Loureiro, A. Ypma, D. Hursh, T. Jones, A. Bejsovec, M. Peifer, M. Mortin, and H. Clevers, Armadillo coactivates transcription driven by the product of the *Drosophila* segment polarity gene dTCF. *Cell*, 1997. **88**(6): p. 789-99.
- 99.**Veeman, M.T., D.C. Slusarski, A. Kaykas, S.H. Louie, and R.T. Moon, Zebrafish prickles, a modulator of noncanonical Wnt/Fz signaling, regulates gastrulation movements. *Curr Biol*, 2003. **13**(8): p. 680-5.
- 100.**El Helou, R., G. Pinna, O. Cabaud, J. Wicinski, R. Bhajun, L. Guyon, C. Rioualen, P. Finetti, A. Gros, B. Mari, P. Barbry, F. Bertucci, G. Bidaut, A. Harel-Bellan, D. Birnbaum, E. Charafe-Jauffret, and C. Ginestier, miR-600 Acts as a Bimodal Switch that Regulates Breast Cancer Stem Cell Fate through WNT Signaling. *Cell Rep*, 2017. **18**(9): p. 2256-2268.
- 101.**Jiao, S., C. Li, Q. Hao, H. Miao, L. Zhang, L. Li, and Z. Zhou, VGLL4 targets a TCF4-TEAD4 complex to coregulate Wnt and Hippo signalling in colorectal cancer. *Nat Commun*, 2017. **8**: p. 14058.
- 102.**Berwick, D.C. and K. Harvey, LRRK2 functions as a Wnt signaling scaffold, bridging cytosolic proteins and membrane-localized LRP6. *Hum Mol Genet*, 2012. **21**(22): p. 4966-79.
- 103.**Nixon-Abell, J., D.C. Berwick, S. Grannó, V.A. Spain, C. Blackstone, and K. Harvey, Protective LRRK2 R1398H variant enhances GTPase and Wnt signaling activity. *Front Mol Neurosci*, 2016. **9**.
- 104.**Berwick, D.C., B. Javaheri, A. Wetzel, M. Hopkinson, J. Nixon-Abell, S. Granno, A.A. Pitsillides, and K. Harvey, Pathogenic LRRK2 variants are gain-of-function mutations that enhance LRRK2-mediated repression of beta-catenin signaling. *Mol Neurodegener*, 2017. **12**(1): p. 9.
- 105.**Szklarczyk, D., A. Franceschini, S. Wyder, K. Forslund, D. Heller, J. Huerta-Cepas, M. Simonovic, A. Roth, A. Santos, K.P. Tsafou, M. Kuhn, P. Bork, L.J. Jensen, and C. von Mering, STRING v10: protein-protein interaction networks, integrated over the tree of life. *Nucleic Acids Res*, 2015. **43**(Database issue): p. D447-52.
- 106.**Diep, D.B., N. Hoen, M. Backman, O. Machon, and S. Krauss, Characterisation of the Wnt antagonists and their response to conditionally activated Wnt signalling in the developing mouse forebrain. *Dev Brain Res*, 2004. **153**(2): p. 261-270.
- 107.**Yue, W., Q. Sun, S. Dacic, R.J. Landreneau, J.M. Siegfried, J. Yu, and L. Zhang, Downregulation of Dkk3 activates beta-catenin/TCF-4 signaling in lung cancer. *Carcinogenesis*, 2008. **29**: p. 84-92.
- 108.**Lee, E.-J., M. Jo, S.B. Rho, K. Park, Y.-N. Yoo, J. Park, M. Chae, W. Zhang, and J.-H. Lee, Dkk3, downregulated in cervical cancer, functions as a negative regulator of β -catenin. *Int J Cancer*, 2009. **124**: p. 287-297.
- 109.**Song, W.-J., E.-A.C. Song, M.-S. Jung, S.-H. Choi, H.-H. Baik, B.K. Jin, J.H. Kim, and S.-H. Chung, Phosphorylation and inactivation of glycogen synthase kinase 3 β (GSK3 β) by dual-specificity tyrosine phosphorylation-regulated kinase 1A (Dyrk1A). *J Biol Chem*, 2015. **290**(4): p. 2321-2333.
- 110.**Ogawa, Y., Y. Nonaka, T. Goto, E. Ohnishi, T. Hiramatsu, I. Kii, M. Yoshida, T. Ikura, H. Onogi, H. Shibuya, T. Hosoya, N. Ito, and M. Hagiwara, Development of a novel selective inhibitor of the Down syndrome-related kinase Dyrk1A. *Nat Commun*, 2010. **1**: p. 86.

Bibliography

- 111.** Bijur, G.N. and R.S. Jope, Proapoptotic stimuli induce nuclear accumulation of glycogen synthase kinase-3 beta. *J Biol Chem*, 2001. **276**(40): p. 37436-42.
- 112.** Sear, R.P., Dishevelled: a protein that functions in living cells by phase separating. *Soft Matter*, 2007. **3**(6): p. 680-684.
- 113.** Leonard, J.L., D.M. Leonard, S.A. Wolfe, J. Liu, J. Rivera, M. Yang, R.T. Leonard, J.P.S. Johnson, P. Kumar, K.L. Liebmann, A.A. Tutto, Z. Mou, and K.J. Simin, The Dkk3 gene encodes a vital intracellular regulator of cell proliferation. *PLoS One*, 2017. **12**(7): p. e0181724.
- 114.** da Costa Martins, P.A., K. Salic, M.M. Gladka, A.S. Armand, S. Leptidis, H. el Azzouzi, A. Hansen, C.J. Coenen-de Roo, M.F. Bierhuizen, R. van der Nagel, J. van Kuik, R. de Weger, A. de Bruin, G. Condorelli, M.L. Arbones, T. Eschenhagen, and L.J. De Windt, MicroRNA-199b targets the nuclear kinase Dyrk1a in an auto-amplification loop promoting calcineurin/NFAT signalling. *Nat Cell Biol*, 2010. **12**(12): p. 1220-7.
- 115.** Christodoulides, C., C. Lagathu, J.K. Sethi, and A. Vidal-Puig, Adipogenesis and WNT signalling. *Trends Endocrinol Metab*, 2009. **20**(1): p. 16-24.
- 116.** Zmijewski, J.W. and R.S. Jope, Nuclear accumulation of glycogen synthase kinase-3 during replicative senescence of human fibroblasts. *Aging Cell*, 2004. **3**(5): p. 309-17.
- 117.** Schmitz, Y., K. Rateitschak, and O. Wolkenhauer, Analysing the impact of nucleo-cytoplasmic shuttling of beta-catenin and its antagonists APC, Axin and GSK3 on Wnt/beta-catenin signalling. *Cell Signal*, 2013. **25**(11): p. 2210-21.
- 118.** Lie, D.C., S.A. Colamarino, H.J. Song, L. Desire, H. Mira, A. Consiglio, E.S. Lein, S. Jessberger, H. Lansford, A.R. Dearie, and F.H. Gage, Wnt signalling regulates adult hippocampal neurogenesis. *Nature*, 2005. **437**(7063): p. 1370-1375.
- 119.** Chen, J.Y., C.S. Park, and S.J. Tang, Activity-dependent synaptic Wnt release regulates hippocampal long term potentiation. *Journal of Biological Chemistry*, 2006. **281**(17): p. 11910-11916.
- 120.** Toledo, E.M. and N.C. Inestrosa, Wnt signaling activation reduces neuropathological markers in a mouse model of Alzheimer's disease. *Mol Psychiatry*, 2010. **15**: p. 228.
- 121.** Purro, S.A., E.M. Dickins, and P.C. Salinas, The secreted Wnt antagonist Dickkopf-1 is required for amyloid β -mediated synaptic loss. *J Neurosci*, 2012. **32**: p. 3492-3498.
- 122.** Inestrosa, N.C. and L. Varela-Nallar, Wnt signaling in the nervous system and in Alzheimer's disease. *J Mol Cell Biol*, 2014. **6**(1): p. 64-74.
- 123.** Purro, S.A., S. Galli, and P.C. Salinas, Dysfunction of Wnt signaling and synaptic disassembly in neurodegenerative diseases. *Journal of molecular cell biology, mjt0*, 2014. **49**.

7.6 Chapter 5 - General Discussion

1. Wisniewski, K.E., H.M. Wisniewski, and G.Y. Wen, Occurrence of neuropathological changes and dementia of Alzheimer's disease in Down's syndrome. *Ann Neurol*, 1985. **17**: p. 278-282.
2. Boonen, R.A., P. van Tijn, and D. Zivkovic, Wnt signaling in Alzheimer's disease: up or down, that is the question. *Ageing Res Rev*, 2009. **8**(2): p. 71-82.
3. Oliva, C.A., J.Y. Vargas, and N.C. Inestrosa, Wnt signaling: role in LTP, neural networks and memory. *Ageing Res Rev*, 2013. **12**(3): p. 786-800.
4. Inestrosa, N.C. and L. Varela-Nallar, Wnt signaling in the nervous system and in Alzheimer's disease. *J Mol Cell Biol*, 2014. **6**(1): p. 64-74.
5. O'Doherty, A., S. Ruf, C. Mulligan, V. Hildreth, M.L. Errington, S. Cooke, and E.M. Fisher, An aneuploid mouse strain carrying human chromosome 21 with Down syndrome phenotypes. *Science*, 2005. **309**: p. 2033-2037.
6. Gribble, S.M., F.K. Wiseman, S. Clayton, E. Prigmore, E. Langley, F. Yang, S. Maguire, B. Fu, D. Rajan, O. Sheppard, C. Scott, H. Hauser, P.J. Stephens, L.A. Stebbings, B.L. Ng, T. Fitzgerald, M.A. Quail, R. Banerjee, K. Rothkamm, V.L. Tybulewicz, E.M. Fisher, and N.P. Carter, Massively parallel sequencing reveals the complex structure of an irradiated human chromosome on a mouse background in the Tc1 model of Down syndrome. *PLoS One*, 2013. **8**(4): p. e60482.
7. Lana-Elola, E., S. Watson-Scales, A. Slender, D. Gibbins, A. Martineau, C. Douglas, T. Mohun, E.M.C. Fisher, and V.L.J. Tybulewicz, Genetic dissection of Down syndrome-associated congenital heart defects using a new mouse mapping panel. *Elife*, 2016. **5**.
8. Choong, X.Y., J.L. Tosh, L.J. Pulford, and E. Fisher, Dissecting Alzheimer disease in Down syndrome using mouse models. *Front Behav Neurosci*, 2015. **9**.
9. Diep, D.B., N. Hoen, M. Backman, O. Machon, and S. Krauss, Characterisation of the Wnt antagonists and their response to conditionally activated Wnt signalling in the developing mouse forebrain. *Dev Brain Res*, 2004. **153**(2): p. 261-270.
10. Nusse, R. and H. Varmus, Three decades of Wnts: a personal perspective on how a scientific field developed. *The EMBO journal*, 2012. **31**: p. 2670-2684.
11. Park, J., W.J. Song, and K.C. Chung, Function and regulation of Dyrk1A: towards understanding Down syndrome. *Cell Mol Life Sci*, 2009. **66**: p. 3235-3240.
12. Hickey, F., E. Hickey, and K.L. Summar, Medical update for children with Down syndrome for the pediatrician and family practitioner. *Advances in pediatrics*, 2012. **59**: p. 137-157.
13. Allanson, J.E., P. O'Hara, L.G. Farkas, and R.C. Nair, Anthropometric craniofacial pattern profiles in Down syndrome. *Am J Med Genet*, 1993. **47**(5): p. 748-52.
14. Brugmann, S.A., L.H. Goodnough, A. Gregorieff, P. Leucht, D. ten Berge, C. Fuerer, H. Clevers, R. Nusse, and J.A. Helms, Wnt signaling mediates regional specification in the vertebrate face. *Development*, 2007. **134**(18): p. 3283-95.
15. Lan, Y., R.C. Ryan, Z. Zhang, S.A. Bullard, J.O. Bush, K.M. Maltby, A.C. Lidral, and R. Jiang, Expression of Wnt9b and activation of canonical Wnt signaling during midfacial morphogenesis in mice. *Dev Dyn*, 2006. **235**(5): p. 1448-54.

Bibliography

16. Antonarakis, S.E., R. Lyle, E.T. Dermitzakis, A. Reymond, and S. Deutsch, Chromosome 21 and down syndrome: from genomics to pathophysiology. *Nature Reviews Genetics*, 2004. **5**: p. 725-738.
17. Maslen, C.L., Molecular genetics of atrioventricular septal defects. *Current opinion in cardiology*, 2004. **19**: p. 205-210.
18. Gessert, S. and M. Kuhl, The multiple phases and faces of wnt signaling during cardiac differentiation and development. *Circ Res*, 2010. **107**(2): p. 186-99.
19. Brade, T., J. Manner, and M. Kuhl, The role of Wnt signalling in cardiac development and tissue remodelling in the mature heart. *Cardiovasc Res*, 2006. **72**(2): p. 198-209.
20. Qyang, Y., S. Martin-Puig, M. Chiravuri, S. Chen, H. Xu, L. Bu, X. Jiang, L. Lin, A. Granger, A. Moretti, L. Caron, X. Wu, J. Clarke, M.M. Takeito, K.L. Laugwitz, R.T. Moon, P. Gruber, S.M. Evans, S. Ding, and K.R. Chien, The renewal and differentiation of Isl1+ cardiovascular progenitors are controlled by a Wnt/beta-catenin pathway. *Cell Stem Cell*, 2007. **1**(2): p. 165-79.
21. Sullivan, S.G., R. Hussain, E.J. Glasson, and A.H. Bittles, The profile and incidence of cancer in Down syndrome. *J Intellect Disabil Res*, 2007. **51**(Pt 3): p. 228-31.
22. Wend, P., J.D. Holland, U. Ziebold, and W. Birchmeier, Wnt signaling in stem and cancer stem cells *Semin Cell Dev Biol*, 21 (2010). pp. **855**.
23. Reya, T. and H. Clevers, Wnt signalling in stem cells and cancer. *Nature*, 2005. **434**(7035): p. 843-50.
24. Shackleton, M., F. Vaillant, K.J. Simpson, J. Stingl, G.K. Smyth, M.L. Asselin-Labat, and J.E. Visvader, Generation of a functional mammary gland from a single stem cell. *Nature*, 2006. **439**: p. 84-88.
25. McNeill, H. and J.R. Woodgett, When pathways collide: collaboration and connivance among signalling proteins in development. *Nat Rev Mol Cell Biol*, 2010. **11**(6): p. 404-13.
26. Malanchi, I., A. Santamaria-Martínez, E. Susanto, H. Peng, H.A. Lehr, J.F. Delaloye, and J. Huelsken, Interactions between cancer stem cells and their niche govern metastatic colonization. *Nature*, 2012. **481**: p. 85-89.
27. Holland, J.D., A. Klaus, A.N. Garratt, and W. Birchmeier, Wnt signaling in stem and cancer stem cells. *Current opinion in cell biology*, 2013. **25**: p. 254-264.
28. Stewart, D.J., Wnt signaling pathway in non-small cell lung cancer. *J Natl Cancer Inst*, 2014. **106**(1): p. djt356.
29. Malinge, S., M. Bliss-Moreau, G. Kirsammer, L. Diebold, T. Chlon, S. Gurbuxani, and J.D. Crispino, Increased dosage of the chromosome 21 ortholog Dyrk1a promotes megakaryoblastic leukemia in a murine model of Down syndrome. *The Journal of clinical investigation*, 2012. **122**: p. 948-962.
30. Nizetic, D. and J. Groet, Tumorigenesis in Down's syndrome: big lessons from a small chromosome. *Nat Rev Cancer*, 2012. **12**(10): p. 721-32.
31. Waaler, J., O. Machon, L. Tumova, H. Dinh, V. Korinek, S.R. Wilson, and S. Krauss, A novel tankyrase inhibitor decreases canonical Wnt signaling in colon carcinoma cells and reduces tumor growth in conditional APC mutant mice. *Cancer research*, 2012. **72**: p. 2822-2832.

Bibliography

- 32.** Cuadrado, E. and M.J. Barrena, Immune dysfunction in Down's syndrome: primary immune deficiency or early senescence of the immune system? *Clin Immunol Immunopathol*, 1996. **78**(3): p. 209-14.
- 33.** Kusters, M.A., R.H. Verstegen, E.F. Gemen, and E. de Vries, Intrinsic defect of the immune system in children with Down syndrome: a review. *Clin Exp Immunol*, 2009. **156**(2): p. 189-93.
- 34.** Cossarizza, A., D. Monti, G. Montagnani, C. Ortolani, M. Masi, M. Zannotti, and C. Franceschi, Precocious aging of the immune system in Down syndrome: alteration of B lymphocytes, T-lymphocyte subsets, and cells with natural killer markers. *Am J Med Genet Suppl*, 1990. **7**: p. 213-8.
- 35.** Bloemers, B.L., G.M. van Bleek, J.L. Kimpen, and L. Bont, Distinct abnormalities in the innate immune system of children with Down syndrome. *J Pediatr*, 2010. **156**(5): p. 804-9, 809 e1-809 e5.
- 36.** Perry, J.M., X.C. He, R. Sugimura, J.C. Grindley, J.S. Haug, S. Ding, and L. Li, Cooperation between both Wnt/ β -catenin and PTEN/PI3K/Akt signaling promotes primitive hematopoietic stem cell self-renewal and expansion. *Genes & development*, 2011. **25**: p. 1928-1942.
- 37.** Staal, F.J. and H.C. Clevers, WNT signalling and haematopoiesis: a WNT-WNT situation. *Nat Rev Immunol*, 2005. **5**(1): p. 21-30.
- 38.** Staal, F.J., T.C. Luis, and M.M. Tiemessen, WNT signalling in the immune system: WNT is spreading its wings. *Nat Rev Immunol*, 2008. **8**(8): p. 581-93.
- 39.** Alvarez, A.R., J.A. Godoy, K. Mullendorff, G.H. Olivares, M. Bronfman, and N.C. Inestrosa, Wnt-3a overcomes β -amyloid toxicity in rat hippocampal neurons. *Experimental cell research*, 2004. **297**: p. 186-196.
- 40.** Cerpa, W., G.G. Farias, J.A. Godoy, M. Fuenzalida, C. Bonansco, and N.C. Inestrosa, Wnt-5a occludes Abeta oligomer-induced depression of glutamatergic transmission in hippocampal neurons. *Mol Neurodegener*, 2010. **5**: p. 3.
- 41.** Toledo, E.M. and N.C. Inestrosa, Wnt signaling activation reduces neuropathological markers in a mouse model of Alzheimer's disease. *Mol Psychiatry*, 2010. **15**: p. 228.
- 42.** Harvey, K. and B. Marchetti, Regulating Wnt signaling: a strategy to prevent neurodegeneration and induce regeneration. *J Mol Cell Biol*, 2014. **6**(1): p. 1-2.
- 43.** Wan, W., S. Xia, B. Kalionis, L. Liu, and Y. Li, The role of Wnt signaling in the development of Alzheimer's disease: a potential therapeutic target? *Biomed Res Int*, 2014. **2014**: p. 301575.
- 44.** Quintanilla, R.A., F.J. Munoz, M.J. Metcalfe, M. Hitschfeld, G. Olivares, J.A. Godoy, and N.C. Inestrosa, Trolox and 17 β -estradiol protect against amyloid beta-peptide neurotoxicity by a mechanism that involves modulation of the Wnt signaling pathway. *J Biol Chem*, 2005. **280**(12): p. 11615-25.
- 45.** Cerpa, W., J.A. Godoy, I. Alfaro, G.G. Farias, M.J. Metcalfe, R. Fuentealba, and N.C. Inestrosa, Wnt-7a modulates the synaptic vesicle cycle and synaptic transmission in hippocampal neurons. *Journal of Biological Chemistry*, 2008. **283**: p. 5918-5927.
- 46.** Kawamoto, E.M., M. Gleichmann, L.M. Yshii, S. Lima Lde, M.P. Mattson, and C. Scavone, Effect of activation of canonical Wnt signaling by the Wnt-3a protein on the susceptibility of PC12 cells to oxidative and apoptotic insults. *Braz J Med Biol Res*, 2012. **45**(1): p. 58-67.

Bibliography

47. Wexler, E.M., D.H. Geschwind, and T.D. Palmer, Lithium regulates adult hippocampal progenitor development through canonical Wnt pathway activation. *Mol Psychiatry*, 2008. **13**(3): p. 285-92.
48. Fiorentini, A., M.C. Rosi, C. Grossi, I. Luccarini, and F. Casamenti, Lithium improves hippocampal neurogenesis, neuropathology and cognitive functions in APP mutant mice. *PLoS One*, 2010. **5**(12): p. e14382.
49. Zhang, X., W.K. Yin, X.D. Shi, and Y. Li, Curcumin activates Wnt/beta-catenin signaling pathway through inhibiting the activity of GSK-3beta in APPswe transfected SY5Y cells. *Eur J Pharm Sci*, 2011. **42**(5): p. 540-6.
50. Caccamo, A., S. Oddo, L.M. Billings, K.N. Green, H. Martinez-Coria, A. Fisher, and F.M. LaFerla, M1 receptors play a central role in modulating AD-like pathology in transgenic mice. *Neuron*, 2006. **49**(5): p. 671-82.
51. Farias, G.G., J.A. Godoy, F. Hernandez, J. Avila, A. Fisher, and N.C. Inestrosa, M1 muscarinic receptor activation protects neurons from beta-amyloid toxicity. A role for Wnt signaling pathway. *Neurobiol Dis*, 2004. **17**(2): p. 337-48.
52. Inestrosa, N.C., J.A. Godoy, J.Y. Vargas, M.S. Arrazola, J.A. Rios, F.J. Carvajal, F.G. Serrano, and G.G. Farias, Nicotine prevents synaptic impairment induced by amyloid-beta oligomers through alpha7-nicotinic acetylcholine receptor activation. *Neuromolecular Med*, 2013. **15**(3): p. 549-69.
53. Wang, C.Y., W. Zheng, T. Wang, J.W. Xie, S.L. Wang, B.L. Zhao, W.P. Teng, and Z.Y. Wang, Huperzine A activates Wnt/beta-catenin signaling and enhances the nonamyloidogenic pathway in an Alzheimer transgenic mouse model. *Neuropsychopharmacology*, 2011. **36**(5): p. 1073-89.
54. Mao, B., W. Wu, Y. Li, D. Hoppe, P. Stannek, A. Glinka, and C. Niehrs, LDL-receptor-related protein 6 is a receptor for Dickkopf proteins. *Nature*, 2001. **411**(6835): p. 321-5.
55. Zenzmaier, C., J. Marksteiner, A. Kiefer, P. Berger, and C. Humpel, Dkk3 is elevated in CSF and plasma of Alzheimer's disease patients. *J Neurochem*, 2009. **110**: p. 653-661.
56. Caricasole, A., A. Copani, F. Caraci, E. Aronica, A.J. Rozemuller, A. Caruso, and F. Nicoletti, Induction of Dickkopf-1, a negative modulator of the Wnt pathway, is associated with neuronal degeneration in Alzheimer's brain. *J Neurosci*, 2004. **24**: p. 6021-6027.
57. Caraci, F., C. Busceti, F. Biagioni, E. Aronica, F. Mastroiacovo, I. Cappuccio, G. Battaglia, V. Bruno, A. Caricasole, A. Copani, and F. Nicoletti, The Wnt antagonist, Dickkopf-1, as a target for the treatment of neurodegenerative disorders. *Neurochem Res*, 2008. **33**(12): p. 2401-6.
58. Iozzi, S., R. Remelli, B. Lelli, D. Diamanti, S. Pileri, L. Bracci, R. Roncarati, A. Caricasole, and S. Bernocco, Functional Characterization of a Small-Molecule Inhibitor of the DKK1-LRP6 Interaction. *ISRN Mol Biol*, 2012. **2012**: p. 823875.
59. Purro, S.A., E.M. Dickins, and P.C. Salinas, The secreted Wnt antagonist Dickkopf-1 is required for amyloid β -mediated synaptic loss. *J Neurosci*, 2012. **32**: p. 3492-3498.
60. Adayev, T., J. Wegiel, and Y.-W. Hwang, Harmine is an ATP-competitive inhibitor for dual-specificity tyrosine phosphorylation-regulated kinase 1A (Dyrk1A). *Arch Biochem Biophys*, 2011. **507**(2): p. 212-218.
61. Becker, W., U. Soppa, and F.J. Tejedor, DYRK1A: a potential drug target for multiple Down syndrome neuropathologies. *CNS Neurol Disord Drug Targets*, 2014. **13**(1): p. 26-33.

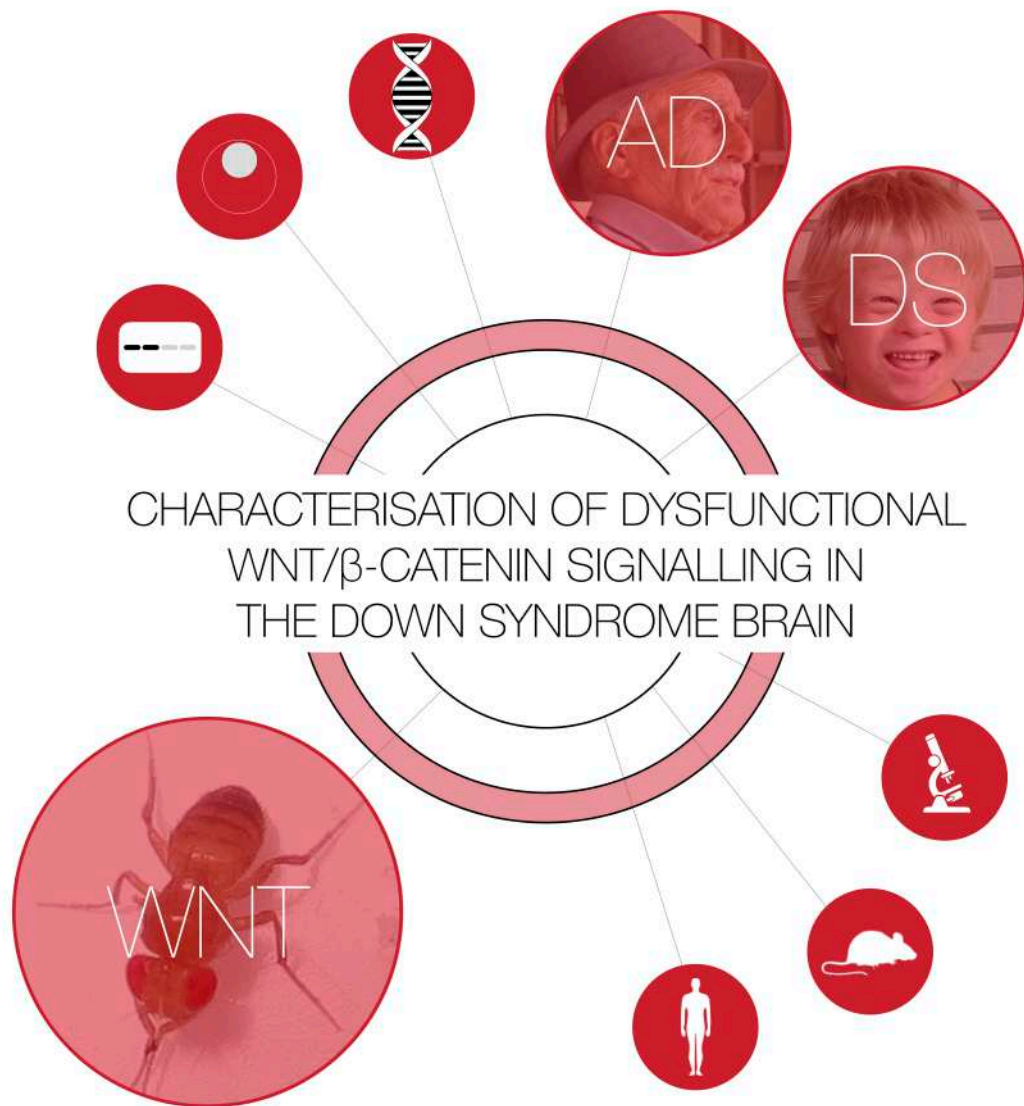
Bibliography

- 62.**Torre, R., S. Sola, M. Pons, A. Duchon, M.M. Lagran, M. Farré, M. Fitó, B. Benejam, K. Langohr, and J. Rodriguez, Epigallocatechin-3-gallate, a DYRK1A inhibitor, rescues cognitive deficits in Down syndrome mouse models and in humans. *Mol Nutr Food Res*, 2014. **58**(2): p. 278-288.
- 63.**Coutadeur, S., H. Benyamine, L. Delalonde, C. de Oliveira, B. Leblond, A. Foucourt, T. Besson, A.S. Casagrande, T. Taverne, A. Girard, M.P. Pando, and L. Desire, A novel DYRK1A (dual specificity tyrosine phosphorylation-regulated kinase 1A) inhibitor for the treatment of Alzheimer's disease: effect on Tau and amyloid pathologies in vitro. *J Neurochem*, 2015. **133**(3): p. 440-51.
- 64.**Stagni, F., A. Giacomini, M. Emili, S. Guidi, E. Ciani, and R. Bartesaghi, Epigallocatechin gallate: A useful therapy for cognitive disability in Down syndrome? *Neurogenesis (Austin)*, 2017. **4**(1): p. e1270383.
- 65.**Guedj, F., C. Sebrie, I. Rivals, A. Ledru, E. Paly, J.C. Bizot, D. Smith, E. Rubin, B. Gillet, M. Arbones, and J.M. Delabar, Green tea polyphenols rescue of brain defects induced by overexpression of DYRK1A. *PLoS One*, 2009. **4**(2): p. e4606.
- 66.**Ogawa, Y., Y. Nonaka, T. Goto, E. Ohnishi, T. Hiramatsu, I. Kii, M. Yoshida, T. Ikura, H. Onogi, H. Shibuya, T. Hosoya, N. Ito, and M. Hagiwara, Development of a novel selective inhibitor of the Down syndrome-related kinase Dyrk1A. *Nat Commun*, 2010. **1**: p. 86.
- 67.**Lin, L.C., M.N. Wang, T.Y. Tseng, J.S. Sung, and T.H. Tsai, Pharmacokinetics of (-)-epigallocatechin-3-gallate in conscious and freely moving rats and its brain regional distribution. *J Agric Food Chem*, 2007. **55**(4): p. 1517-24.
- 68.**Pons-Espinal, M., M. Martinez de Lagran, and M. Dierssen, Environmental enrichment rescues DYRK1A activity and hippocampal adult neurogenesis in TgDyrk1A. *Neurobiol Dis*, 2013. **60**: p. 18-31.
- 69.**Thomazeau, A., O. Lassalle, J. Iafrati, B. Souchet, F. Guedj, N. Janel, P. Chavis, J. Delabar, and O.J. Manzoni, Prefrontal deficits in a murine model overexpressing the down syndrome candidate gene *dyrk1a*. *J Neurosci*, 2014. **34**(4): p. 1138-47.
- 70.**Souchet, B., F. Guedj, Z. Penke-Verdier, F. Daubigney, A. Duchon, Y. Herault, J.C. Bizot, N. Janel, N. Creau, B. Delatour, and J.M. Delabar, Pharmacological correction of excitation/inhibition imbalance in Down syndrome mouse models. *Front Behav Neurosci*, 2015. **9**: p. 267.
- 71.**Xie, W., N. Ramakrishna, A. Wieraszko, and Y.W. Hwang, Promotion of neuronal plasticity by (-)-epigallocatechin-3-gallate. *Neurochem Res*, 2008. **33**(5): p. 776-83.
- 72.**De la Torre, R., S. De Sola, M. Pons, A. Duchon, M.M. de Lagran, M. Farre, M. Fito, B. Benejam, K. Langohr, J. Rodriguez, M. Pujadas, J.C. Bizot, A. Cuenca, N. Janel, S. Catuara, M.I. Covas, H. Blehaut, Y. Herault, J.M. Delabar, and M. Dierssen, Epigallocatechin-3-gallate, a DYRK1A inhibitor, rescues cognitive deficits in Down syndrome mouse models and in humans. *Mol Nutr Food Res*, 2014. **58**(2): p. 278-88.
- 73.**Stringer, M., I. Abeysekera, K.J. Dria, R.J. Roper, and C.R. Goodlett, Low dose EGCG treatment beginning in adolescence does not improve cognitive impairment in a Down syndrome mouse model. *Pharmacol Biochem Behav*, 2015. **138**: p. 70-9.
- 74.**Valenti, D., L. de Bari, D. de Rasmio, A. Signorile, A. Henrion-Caude, A. Contestabile, and R.A. Vacca, The polyphenols resveratrol and epigallocatechin-3-gallate restore the severe impairment of mitochondria in hippocampal progenitor cells from a Down syndrome mouse model. *Biochim Biophys Acta*, 2016. **1862**(6): p. 1093-104.

75. Stagni, F., A. Giacomini, M. Emili, S. Trazzi, S. Guidi, M. Sassi, E. Ciani, R. Rimondini, and R. Bartesaghi, Short- and long-term effects of neonatal pharmacotherapy with epigallocatechin-3-gallate on hippocampal development in the Ts65Dn mouse model of Down syndrome. *Neuroscience*, 2016. **333**: p. 277-301.
76. De la Torre, R., S. De Sola, G. Hernandez, M. Farre, J. Pujol, J. Rodriguez, J.M. Espadaler, K. Langohr, A. Cuenca-Royo, A. Principe, L. Xicota, N. Janel, S. Catuara-Solarz, G. Sanchez-Benavides, H. Blehaut, I. Duenas-Espin, L. Del Hoyo, B. Benejam, L. Blanco-Hinojo, S. Videla, M. Fito, J.M. Delabar, M. Dierssen, and T.s. group, Safety and efficacy of cognitive training plus epigallocatechin-3-gallate in young adults with Down's syndrome (TESDAD): a double-blind, randomised, placebo-controlled, phase 2 trial. *Lancet Neurol*, 2016. **15**(8): p. 801-10.
77. Valenti, D., D. De Rasmio, A. Signorile, L. Rossi, L. de Bari, I. Scala, B. Granese, S. Papa, and R.A. Vacca, Epigallocatechin-3-gallate prevents oxidative phosphorylation deficit and promotes mitochondrial biogenesis in human cells from subjects with Down's syndrome. *Biochim Biophys Acta*, 2013. **1832**(4): p. 542-52.
78. Sitz, J.H., K. Baumgartel, B. Hammerle, C. Papadopoulos, P. Hekerman, F.J. Tejedor, W. Becker, and B. Lutz, The Down syndrome candidate dual-specificity tyrosine phosphorylation-regulated kinase 1A phosphorylates the neurodegeneration-related septin 4. *Neuroscience*, 2008. **157**(3): p. 596-605.
79. Frost, D., B. Meechoovet, T. Wang, S. Gately, M. Giorgetti, I. Shcherbakova, and T. Dunckley, beta-carboline compounds, including harmine, inhibit DYRK1A and tau phosphorylation at multiple Alzheimer's disease-related sites. *PLoS One*, 2011. **6**(5): p. e19264.
80. Mazur-Kolecka, B., A. Golabek, E. Kida, A. Rabe, Y.W. Hwang, T. Adayev, J. Wegiel, M. Flory, W. Kaczmarek, E. Marchi, and J. Frackowiak, Effect of DYRK1A activity inhibition on development of neuronal progenitors isolated from Ts65Dn mice. *J Neurosci Res*, 2012. **90**(5): p. 999-1010.
81. Fotaki, V., M. Dierssen, S. Alcantara, S. Martinez, E. Marti, C. Casas, J. Visa, E. Soriano, X. Estivill, and M.L. Arbones, Dyrk1A haploinsufficiency affects viability and causes developmental delay and abnormal brain morphology in mice. *Mol Cell Biol*, 2002. **22**(18): p. 6636-47.
82. Benavides-Piccione, R., M. Dierssen, I. Ballesteros-Yanez, M. Martinez de Lagran, M.L. Arbones, V. Fotaki, J. DeFelipe, and G.N. Elston, Alterations in the phenotype of neocortical pyramidal cells in the Dyrk1A^{+/-} mouse. *Neurobiol Dis*, 2005. **20**(1): p. 115-22.
83. Moller, R.S., S. Kubart, M. Hoeltzenbein, B. Heye, I. Vogel, C.P. Hansen, C. Menzel, R. Ullmann, N. Tommerup, H.H. Ropers, Z. Tumer, and V.M. Kalscheuer, Truncation of the Down syndrome candidate gene DYRK1A in two unrelated patients with microcephaly. *Am J Hum Genet*, 2008. **82**(5): p. 1165-70.
84. Zhou, F., K. Gong, B. Song, T. Ma, T. van Laar, Y. Gong, and L. Zhang, The APP intracellular domain (AICD) inhibits Wnt signalling and promotes neurite outgrowth. *Biochim Biophys Acta*, 2012. **1823**: p. 1233-1241.
85. Ferrer, I., M. Barrachina, B. Puig, M. Martinez de Lagran, E. Marti, J. Avila, and M. Dierssen, Constitutive Dyrk1A is abnormally expressed in Alzheimer disease, Down syndrome, Pick disease, and related transgenic models. *Neurobiol Dis*, 2005. **20**(2): p. 392-400.
86. Janel, N., M. Sarazin, F. Corlier, H. Corne, L.C. de Souza, L. Hamelin, A. Aka, J. Lagarde, H. Blehaut, V. Hindie, J.C. Rain, M.L. Arbones, B. Dubois, M.C. Potier, M. Bottlaender, and J.M. Delabar, Plasma DYRK1A as a novel risk factor for Alzheimer's disease. *Transl Psychiatry*, 2014. **4**.

Bibliography

- 87.**Dierssen, M., Down syndrome: the brain in trisomic mode. *Nat Rev Neurosci*, 2012. **13**(12): p. 844-58.
- 88.**Tang, M., J.C. Villaescusa, S.X. Luo, C. Guitarte, S. Lei, Y. Miyamoto, and E.J. Huang, Interactions of Wnt/ β -catenin signaling and sonic hedgehog regulate the neurogenesis of ventral midbrain dopamine neurons. *The Journal of Neuroscience*, 2010. **30**: p. 9280-9291.
- 89.**Ribeiro, D., K. Ellwanger, D. Glasgow, S. Theofilopoulos, N.S. Corsini, A. Martin-Villalba, and E. Arenas, Dkk1 regulates ventral midbrain dopaminergic differentiation and morphogenesis. *PLoS one*, 2011. **6**: p. 2.
- 90.**Joksimovic, M., M. Patel, M.M. Taketo, R. Johnson, and R. Awatramani, Ectopic Wnt/Beta-Catenin Signaling Induces Neurogenesis in the Spinal Cord and Hindbrain Floor Plate. *PLoS one*, 2012. **7**: p. 1.
- 91.**Mazieres, J., B. He, L. You, Z. Xu, and D.M. Jablons, Wnt signaling in lung cancer. *Cancer Lett*, 2005. **222**(1): p. 1-10.
- 92.**Clevers, H., Wnt/beta-catenin signaling in development and disease. *Cell*, 2006. **127**(3): p. 469-80.
- 93.**Anastas, J.N. and R.T. Moon, WNT signalling pathways as therapeutic targets in cancer. *Nat Rev Cancer*, 2013. **13**(1): p. 11-26.
- 94.**Xue, G., E. Romano, D. Massi, and M. Mandala, Wnt/beta-catenin signaling in melanoma: Preclinical rationale and novel therapeutic insights. *Cancer Treat Rev*, 2016. **49**: p. 1-12.
- 95.**Yang, K., X. Wang, H.M. Zhang, Z.L. Wang, G.X. Nan, Y.S. Li, F.G. Zhang, M.K. Mohammed, R.C. Haydon, H.H. Luu, Y. Bi, and T.C. He, The evolving roles of canonical WNT signaling in stem cells and tumorigenesis: implications in targeted cancer therapies. *Lab Invest*, 2016. **96**(2): p. 116-136.



Photograph credits

Wnt - Copyright © 2011 John R. Maxwell

AD - Ahmet Demirel for National Geographic

DS - Vanellus Foto, Wikimedia Commons, GNU Free Documentation License

